Australian Government
Geoscience Australia

Australia's seismogenic neotectonic record

A case for heterogeneous intraplate deformation

Clark, D., McPherson, A. and Collins, C.D.N.

Record
2011/11

GeoCat #
70288

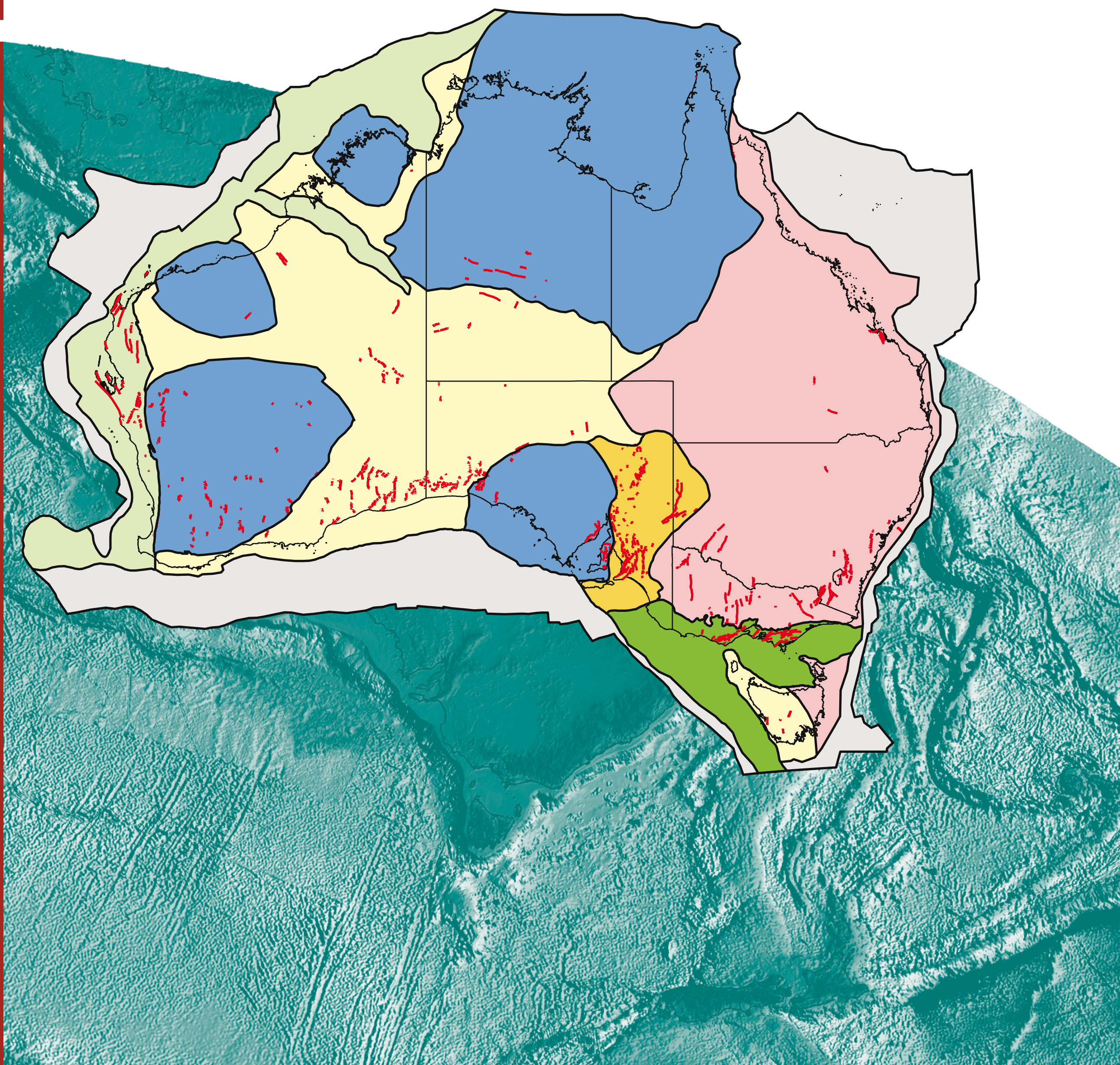

Australia's seismogenic neotectonic record: a case for heterogeneous intraplate deformation

GEOSCIENCE AUSTRALIA
RECORD 2011/11

by

Dan Clark, Andrew McPherson and Clive Collins

Australian Government
Geoscience Australia

Earthquake Hazard Project, Geospatial & Earth Monitoring Division, Geoscience Australia, GPO Box 378, Canberra, ACT, 2601.

Department of Resources, Energy and Tourism
Minister for Resources and Energy: The Hon. Martin Ferguson, AM MP
Secretary: Mr Drew Clarke

Geoscience Australia
Chief Executive Officer: Dr Chris Pigram

ISSN 1448-2177
ISBN 978-1-921781-92-6 Print
ISBN 978-1-921781-91-9 Web

GeoCat # 70288

Bibliographic reference: Clark, D., McPherson, A. and Collins, C.D.N. 2011. *Australia's seismogenic neotectonic record: a case for heterogeneous intraplate deformation*. Record 2011/11. Geoscience Australia, Canberra.

Contents

Executive Summary

Australia's rich neotectonic record provides an opportunity to better understand the characteristics of seismogenic intraplate deformation, both at the scale of a single fault and at the scale of the entire continent. Over the last decade knowledge of Australian intraplate faults has advanced significantly. Herein we review this knowledge and propose six preliminary seismicity source zones (domains) based upon neotectonic data. Each source zone contains faults that we contend share common recurrence and behavioural characteristics, in a similar way that source zones are defined using the historic record of seismicity. A seventh offshore domain is proposed based upon analogy with the eastern United States. The power of this domain approach lies in the ability to extrapolate characteristic behaviours from well-characterised faults (few) to faults about which little is known (many), both nationally and to analogous regions elsewhere in the world. These data, and conceptual and numerical models describing the nature of the seismicity in each source zone, have the potential to significantly enhance our understanding of seismic hazard in Australia at a longer time scale than the snapshot provided by the historic record of seismicity. This includes providing a means by which to estimate key parameters underpinning the next generation seismic hazard maps for Australia, such as maximum magnitude earthquake and seismic source zone *b* values.

Key Words:
Seismic hazard, intraplate, neotectonics, maximum magnitude earthquake

Introduction

Australia is considered to be a Stable Continental Region (SCR) in terms of its plate tectonic setting and seismicity (Johnston *et al.* 1994). While such settings produce only approximately 0.2% of the world's seismic moment release, large and potentially damaging earthquakes are not uncommon (e.g. Crone *et al.* 1997). Five earthquakes sufficiently large to rupture the Earth's surface are documented in Australia in the last four decades (Figure 1) - 1968 Meckering (Gordon & Lewis 1980); 1970 Calingiri (Gordon & Lewis 1980); 1979 Cadoux (Lewis *et al.* 1981); 1986 Marryat Creek (Machette *et al.* 1993; Crone *et al.* 1997); 1988 Tennant Creek (Crone *et al.* 1992, 1997). Low strain accumulation and release rates in SCRs relative to plate margin regions suggest that the recurrence of large earthquakes on individual faults is typically thousands to hundreds of thousands of years or more (e.g. Adams *et al.* 1991; Crone *et al.* 1997; Clark & Leonard 2003; Crone *et al.* 2003; Clark *et al.* 2008a; Clark *et al.* 2010) (Figure 2). A notable exception is the New Madrid Seismic Zone (NMSZ) in the central United States where the recurrence of M>7 events for the last three seismic cycles, reportedly on one of several faults responsible for the 1811-1812 earthquakes (the Reelfoot Fault, Van Arsdale *et al.* 1998; Guccione *et al.* 1999; Champion *et al.* 2001), has been five hundred years on average (e.g. Tuttle *et al.* 2002; Tuttle *et al.* 2005). While palaeo-liquefaction investigations of the Charleston seismic zone in South Carolina (Talwani & Schaeffer 2001) and Charlevoix (Tuttle & Atkinson 2010) seismic zone in southeastern Quebec also suggest a recurrence of large earthquakes on the order of several hundred to several thousand years, such studies are not fault-specific (e.g. Obermeier *et al.* 1992). Similarly, frequent recurrence of damaging ground shaking in the Kachchh rift region of northwest India has been attributed to earthquake activity on several faults (e.g. Bhatt *et al.* 2009), potentially strongly influenced by the ~400 km distant Eurasian/Indian plate margin (Stein *et al.* 2001; Shulte & Mooney 2005). An association was proposed between extended continental crust (failed rifts and passive margins) and the heightened intraplate earthquake activity that might give rise to this remarkable moment release (Johnston *et al.* 1994; Gangopadhyay & Talwani 2003), but analysis of an updated catalogue later showed this to lack statistical significance, at least for the historic period (Shulte & Mooney 2005). In the case of Peninsular India, Vita-Finzi (2004) proposes that lithospheric-wavelength buckles relating to stresses arising in the Himalayan Orogen influence the localisation of seismicity. A link with seismicity has not been demonstrated in other continents where similar lithospheric buckling is apparent (e.g. Cloetingh *et al.* 2005; Sandiford & Quigley 2009).

The few palaeoseismological studies of SCR faults suggest that periods of activity are often separated by much longer periods of quiescence (Crone & Luza 1990; Crone & Machette 1997; Crone *et al.* 2003; Clark *et al.* 2007; Clark *et al.* 2008a) (Figure 2). For example, the Hyden Fault in southwestern Australia has experienced three surface-rupturing earthquakes in the last 100 ka (Clark *et al.* 2008a), yet prior events are estimated to have occurred hundreds of thousands to a million years or more ago (Crone *et al.* 2003; Clark *et al.* 2008a). Data and modelling from elsewhere in the world identify similar behaviour on faults with low slip rates (e.g. Wallace 1987; Ritz *et al.* 1995; Marco *et al.* 1996; Friedrich *et al.* 2003) and suggest that the time between successive clusters of events is highly variable but significantly longer than the times between successive earthquakes within an active phase (e.g. Marco *et al.* 1996; Stein *et al.* 1997; Chéry *et al.* 2001; Chéry & Vernant 2006; Li *et al.* 2009). This behaviour poses particular problems for seismic hazard assessment in that it implies that recurrence of large earthquakes is not random (Poissonian) as is implicitly assumed in most probabilistic seismic hazard assessment methods (e.g. Frankel *et al.* 1996; Stirling *et al.* 2002b). In addition, it has been proposed that many of the earthquakes comprising the short historic record of plate interiors, which are used to assess seismic hazard for these regions, are aftershocks of large earthquakes that occurred hundreds of years previously (Stein & Liu 2009).

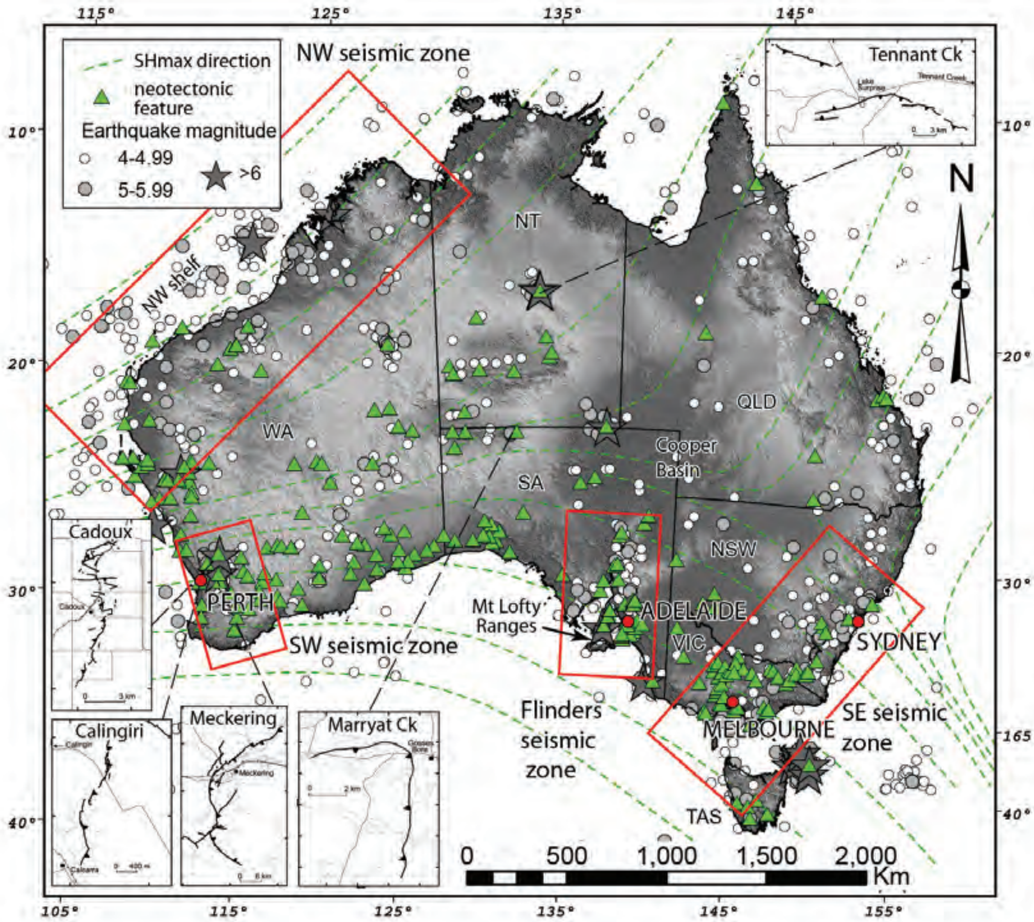

Figure 1 *– Shaded relief map of Australia showing locations and magnitudes of historic seismicity (M>4), locations of seismic zones (Hillis et al. 2008; Leonard 2008), traces for the five historic surface ruptures, (Gordon & Lewis 1980; Lewis et al. 1981; Crone et al. 1997), locations of known and suspected neotectonic features (Geoscience Australia, unpublished data), and maximum horizontal stress vectors (Hillis & Reynolds 2000; Hillis & Reynolds 2003). Red dots mark the major southern Australian population centres of Sydney, Melbourne, Adelaide and Perth.*

In general, Australia is under-explored in terms of its neotectonic and paleoseismic record (cf. Sandiford 2003b; Quigley *et al.* 2006; Hillis *et al.* 2008; Sandiford *et al.* 2009; Sandiford & Quigley 2009; Quigley *et al.* 2010). As a consequence, important conclusions regarding the level of earthquake hazard Australia-wide, and the earthquake activity of specific faults, are often based on comparisons with presumably similar crust or faults elsewhere in Australia and/or elsewhere in the world. However, over the last decade a significant body of new information has become available regarding seismogenic neotectonic faulting in Australia. In the sections of the manuscript that follow we describe the characteristics of seismogenic neotectonic faulting in Australia, and present a region by region compilation of such deformation. This report constitutes the most thorough characterisation of seismogenic neotectonic deformation available for Australia, and is a vital step towards assessing the validity of using fault data from one region to characterise fault behaviour in another. Furthermore, the data compiled here may be used to define earthquake source parameters, such as maximum magnitude earthquake, that are not accessible from the instrumental catalogue of seismicity. A comparison of the earthquake recurrence behaviour of seismogenic neotectonic faults in Australia with other SCR faults worldwide serves as a guide for analogue studies.

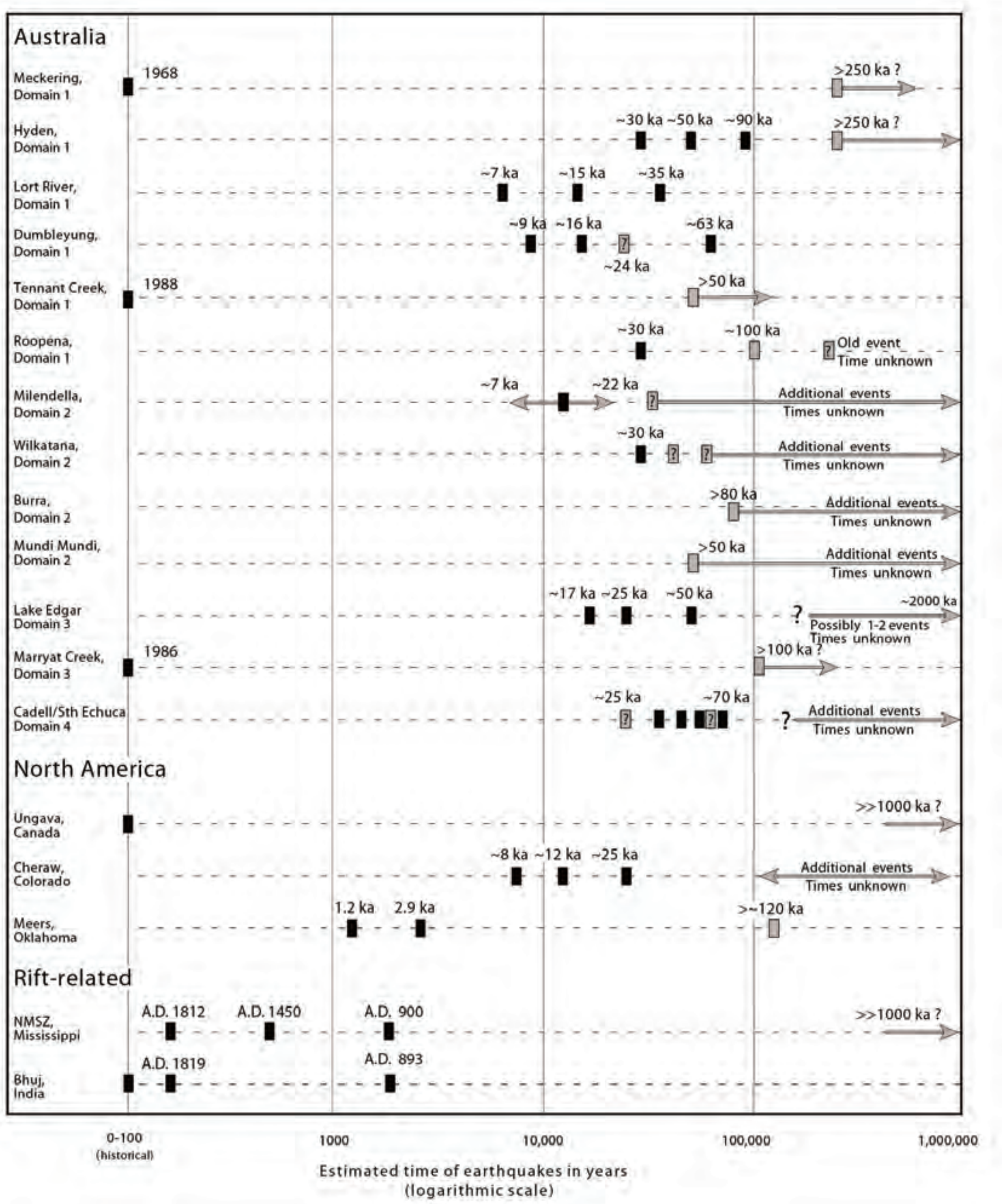

Figure 2 *– Compilation of surface-breaking earthquake recurrence data for SCR settings (expanded after Crone et al. (2003)). Lort River and Dumbleyung data from Estrada (2009), Wilkatana, Burra and Mundi Mundi data from Quigley et al. (2006), Lake Edgar data from Clark et al. (2011) and Cadell data from Clark et al. (2007). Domains are as presented in Figure 33.*

THE NEOTECTONIC ERA IN AUSTRALIA

In this contribution two terms that are used repeatedly require careful definition. A 'neotectonic fault' is defined as a fault that has hosted displacement under conditions imposed by the current Australian crustal stress regime, and hence may move again in the future. Similarly, 'neotectonic displacement/deformation' is defined as displacement/deformation under conditions imposed by the current crustal stress regime. These definitions recognise, after Machette (2000), that assigning an 'active/inactive' label to a fault in a slowly deforming area based upon the occurrence (or non-occurrence) of an event in the last few thousands to tens of thousands of years is not a useful indicator of future seismic potential.

There is structural and sedimentary evidence in southeast Australian basins which suggests that the current crustal stress regime was established during the interval 10-5 Ma (e.g. Dickinson *et al.* 2001; Dickinson *et al.* 2002; Sandiford 2003b, a; Sandiford *et al.* 2004; Hillis *et al.* 2008). This evidence includes a major unconformity related to substantial regional-scale tilting, uplifting, folding and reverse faulting of Late Miocene and older strata occurs in all southeast Australian basins (e.g. Gippsland and Otway Basins). Pliocene and Quaternary strata overlying the unconformity contain neotectonic structures yielding palaeo-stress indicators consistent with the current *in situ* stress field, as determined from seismicity and down-hole stress determination techniques (e.g. Hillis & Reynolds 2000; Hillis & Reynolds 2003; Hillis *et al.* 2008).

The most significant neotectonic deformation consistent with contemporary stress trends plate-wide is thought to have occurred during the Late Miocene (*ca.* 10-5 Ma) transitional period between stress regimes, followed by ongoing deformation, potentially at a lower bulk strain rate (Sandiford *et al.* 2004; Hillis *et al.* 2008). This Late Miocene reorganisation coincides temporally with significant changes at the Australian Plate margins (Dyksterhuis & Müller 2008; Hillis *et al.* 2008), including the onset of mountain building in the New Zealand Southern Alps (Sutherland 1996; Walcott 1998) and in Papua New Guinea (Packham 1996; Hill & Raza 1999; Hill & Hall 2003). Keep *et al.* (2002) recognise the same deformation event in the Timor Sea, correlating it to the main compression phase in Papua New Guinea (Hill & Raza 1999) and a proposed collision between a micro-continental fragment and the Banda Arc (Richardson & Blundell 1996). The authors relate this collision to reactivation of structures in the Carnarvon Basin on the North West Shelf and the Cooper-Eromanga Basin in central eastern Australia (c.f. Etheridge *et al.* 1991). A locally more intense event in the Timor Sea at *ca.* 3 Ma is proposed to reflect collision of the Australian and Eurasian plates (Packham 1996; Keep *et al.* 2002). Deformation structures relating to this Pliocene event have not been documented elsewhere in the Australian Plate.

Although local sources of stress cannot be everywhere precluded (e.g. Dentith & Featherstone 2003), the neotectonic data presented in this report suggest that ongoing deformation within the Australian Plate is primarily a response to distant plate boundary interactions (Sandiford *et al.* 2004; Hillis *et al.* 2008). Indeed, the current intraplate stress condition has been satisfactorily modelled in terms of plate boundary forces in combination with mantle basal tractions (Coblentz *et al.* 1995; Coblentz *et al.* 1998; Reynolds *et al.* 2003; Burbidge 2004; Dyksterhuis & Müller 2008).

SEISMOGENIC DEFORMATION OF THE AUSTRALIAN SCR CRUST

There is abundant evidence for ongoing deformation of the Australian crust in the catalogue of historic earthquakes maintained by Geoscience Australia (http://www.ga.gov.au/earthquakes/searchQuake.do). A simple visual examination of the spatial distribution of earthquake epicentres suggests that deformation of the Australian crust is markedly heterogeneous (Figure 1), at least over the short timeframe captured by the historic record (Hillis *et al.* 2008; Leonard 2008). There is a concentration of epicentres along a N-S axis in the Mt Lofty and Flinders Ranges in South Australia, and diffuse clusters in northwest Australia (NW seismic zone) and the southeast Australian highlands (SE seismic zone). Even more sparsely distributed epicentres in the west of Australia are punctuated by 'hotspots' of activity that closely correlate to the five historic surface rupturing earthquake events (i.e. those in the Southwest Seismic Zone (Doyle 1971b), Tennant Creek (Crone *et al.* 1992) and Marryat Creek (Machette *et al.* 1991)). Other hotspots may represent prolonged aftershock sequences relating to pre-historic large earthquake events (Li *et al.* 2009). In contrast, some areas, such as much of Queensland, are devoid of significant concentrations of historic seismicity.

The vast majority of earthquakes reported in the historic catalogue are of small magnitude (99.2% are $M_W < 5$) and so could be expected to contribute negligibly to the overall moment budget for the continent, especially if a number of concentrations relate to aftershock sequences. Hence, it is unclear how much this snapshot of deformation (i.e. seismicity) reveals about patterns of neotectonic deformation. For example, one of the highest historic concentrations of seismicity occurs in the Southwest Seismic Zone of Western Australia (Figure 1), in a region of low and subdued topography and very low erosion rates (e.g. Chappell 2006). Long term continuation of the moment release that has occurred in the last 40 years, estimated to correspond to E-W shortening at a strain rate of between 0.15-1.6 mm/yr (Leonard 2008), and which involved three surface rupturing earthquakes (Gordon & Lewis 1980; Lewis *et al.* 1981), is clearly inconsistent with the landscape. So, while the historic record of seismicity might provide a guide to the areas of the continent which are accommodating seismogenic deformation now, we must turn to the neotectonic record to learn how the Australian crust has accommodated strain over the neotectonic era. Fortunately, where environmental conditions are conducive to their preservation, the larger events that might be expected to contribute significantly to the moment budget appear to leave an enduring footprint in the landscape (e.g. Gordon & Lewis 1980; Lewis *et al.* 1981; Machette *et al.* 1991; Clark & McCue 2003; Crone *et al.* 2003; Sandiford 2003b, a; Quigley *et al.* 2006; Quigley *et al.* 2007a; Clark *et al.* 2008a; Clark 2009).

Australia's seismogenic neotectonic record

At least three distinct modes of neotectonic surface deformation are evident in the Australian landscape (Sandiford 2007; Sandiford et al. 2009; Sandiford & Quigley 2009). At long wavelengths (several 1000's of km), systematic variations in the extent of Neogene marine inundation imply the continent has tilted north-down, southwest-up (Sandiford 2007). This is most convincingly seen along the southern Australian margin, where Miocene limestone of the Nullarbor Plain has been uplifted and subjected to marine erosion to form iconic cliffs. At intermediate-wavelengths (several 100's of km) several undulations of ~100-200 m amplitude have developed on the 1-10 Ma timescale, consistent with the buckling amplitude of the lithosphere. In the most notable case, Celerier et al. (2005) report that the pattern of deformation of the Flinders Ranges and the surrounding basins such as the Torrens and Frome Basins includes an undulation of several hundred metres amplitude over about 200 km between the basins bounding the ranges. The absence of any marine sediment in the Torrens Basin, which is now separated from the sea by a sill only ~30 m above sea level, implies that this undulation must have developed in the late Neogene, and probably since the early Pliocene, and includes absolute subsidence of the basins (Quigley et al. 2007c). In two other prominent cases, the Lake Mackay palaeo-drainage is now internally draining in its northern reaches, and palaeo-lake Billa Kalina now sits high on a watershed (Sandiford & Quigley 2009). At still shorter wavelengths (several 10's of km), fault related motion has produced local relief at rates of up to ~100 m/Myr over a period of several million years (Sandiford & Quigley 2009). For example, Sandiford (2003b) and Quigley et al. (2006) suggest that 30-50% of the present-day elevation of the Flinders Ranges relative to adjacent piedmonts has developed in the last 5 Ma. Uplifted Pliocene strandlines on the western flank of the Otway Ranges suggest a similar proportion of neotectonic uplift (Sandiford 2003a).

Continental tilting is thought to operate at a wavelength larger than would induce bending stresses in the crust sufficient to result in seismicity (Mike Sandiford, personal communication, 2007). Furthermore, the orientation and compressive nature of the crustal stress field is inconsistent with any such relationship (Hillis & Reynolds 2003) (Figure 1). It is possible that the concentration of seismicity associated with the Flinders Ranges may be associated in some way with the Flinders Ranges “buckle” (Celerier et al. 2005). For example, Vita-Finzi (2004) proposes that lithospheric-wavelength buckles relating to stresses arising in the Himalayan Orogen influence the localisation of seismicity in Peninsula India, thousands of kilometres to the south. However, it is not clear if the buckle, or the abundance of neotectonic faults is the dominant driver for seismicity in this region. Contemporary seismicity does not appear to be associated with the other lithospheric-wavelength buckles known from Australia (Sandiford et al. 2009; Sandiford & Quigley 2009).

In contrast, there is very good evidence to suggest that the third mode of deformation (several 10’s of km wavelength or less) is associated with seismicity. Most compelling is that the majority of features catalogued in the neotectonics database (Appendix Table 1) share geomophological characteristics with the scarps generated during the five known historic surface breaking earthquakes (cf. Gordon & Lewis 1980; Lewis et al. 1981; Crone et al. 1997). In particular, neotectonic features assigned a confidence value of A and B are typically associated with significant drainage modifications, such as ponding, channel oversteepening, diversion or incision and terrace formation. While aseismic creep might plausible explain the formation of some features, and has been proposed to account for vertical changes in topographic levelling profiles across moderately active intraplate normal faults proximal to the European Cenozoic Rift System in Belgium (Demoulin 2004), such behaviour has not been reported from any other SCR setting. Where features in Australia and the United States have been trenched (confidence Level A in the respective databases), clean fault dislocations of fluvial and colluvial strata (e.g. Crone & Luza 1990; Crone et al. 1997; Crone et al. 2003; Quigley et al. 2006; Estrada 2009), gravity deposits in colluvial wedges indicative of the former existence of a free face (e.g. Crone et al. 2003; Clark et al. 2008a), and in one instance fluvial terrace deposits at different elevations but of the same age (Clark et al. 2011), suggest that scarps relate to geologically instantaneous events rather than aseismic creep. In regions of Australia where neotectonic folding is prevalent (e.g. the Carnarvon, Otway, Murray and Gippsland Basins), seismic data suggests that folds are underlain by faults at depth (e.g. Malcolm et al. 1991; Williamson et al. 1991; Hill et al. 1994; Perincek & Cockshell 1995; Clark et al. 2007). The folding deformation documented in the neotectonic database might therefore be reasonably associated with multiple discrete fault displacements, and hence earthquakes. Based upon this evidence, we propose that the features catalogued in the neotectonics database reflect a long-term seismogenic record that might be mined for magnitude and recurrence information related to the largest of Australia’s earthquakes.

Quantitative estimates of land-surface erosion, based upon a combination of apatite fission track and cosmogenic radionuclide methods, indicate that the notion of long-term (i.e. Era-scale) tectonic and geomorphic stability for the Australian SCR is not tenable (Belton et al. 2004). Erosion rates derived from cosmogenic 10Be abundances obtained in geographically dispersed sediments and resistant lithologies are ubiquitously non-zero: low relief regions of the western two thirds of Australia are characterised by erosion rates of 0.2-5 m/Ma (Bierman & Caffee 2002; Belton et al. 2004; Fujioka et al. 2005; Chappell 2006; Quigley et al. 2010), higher relief areas of eastern Australia by rates of up to 30-50 m/Ma (Weissel & Seidl 1998; Heimsath et al. 2000, 2001; Wilkinson et al. 2005; Tomkins et al. 2007), and those in the Flinders Ranges by rates locally up to 122 m/Ma, but averaging around 40 m/Ma (Bierman & Caffee 2002; Chappell 2006; Quigley et al. 2007a; Quigley et al. 2007b). In general, erosion rates appear to correlate primarily with regional relief, and at second order to local relief. In the case of the Flinders Ranges, anomalously high bedrock erosion rates have been linked to relief and to neotectonism, and correlate negatively with climate (Quigley et al. 2007a; Quigley et al. 2007b). The first order topographic control on erosion rates implies that fault scarps, the footprint of seismic events, might be recognisable in the landscape for hundreds of thousands of years or more in central and western Australia, but only for several tens of thousands of years to a hundred thousands years in the Flinders Ranges and eastern Australia. In regions with extremely low erosion rates, such as on the Nullarbor Plain, it has been claimed that a seismic record spanning the last 15 Ma has been preserved essentially intact (Hillis et al. 2008). Indirect evidence for tectonic uplift, such as enhanced rates of erosion (Quigley et al. 2007a), and deformation of fossil planation surfaces and bedrock-sediment interfaces (Celerier et al. 2005; Quigley et al. 2007c; Quigley et al. 2010) can be significantly more long-lived, sometimes surviving the entire neotectonic era.

The inventory of neotectonic features, especially where catalogued on the basis of visibility in remotely sensed datasets (e.g. Digital Elevation Models - DEMs) is hence heterogeneous in terms of completeness and biased to regions with better data coverage (e.g. Clark 2010). Despite being far from complete, the neotectonic record provides a longer, richer and more robust measure of long-term deformation of the Australian SCR crust than that presented by the historic record of seismicity. Below we present a compilation of potential and confirmed neotectonic features known from across Australia considered approximately in relation to the zones of historic seismicity defined by Hillis (2008) and Leonard (2008) (Figure 1). A summary table of this data, including confidence ratings is provided in Appendix Table 1.

WESTERN AND CENTRAL AUSTRALIA

The arid and semi-arid regions of western and central Australia are characterised by generally low relief and undulating topography. Inselbergs and typically low, rounded ranges of resistant rock locally punctuate the landscape (e.g. Mount Augustus in Western Australia, the MacDonnell Ranges in central Australia). Erosion rates determined from cosmogenically derived ^{10}Be abundances are often significantly less than 5 m/Ma (Bierman & Caffee 2002; Belton *et al.* 2004; Fujioka *et al.* 2005; Chappell 2006; Quigley *et al.* 2010). Hence, there is the potential for long-term preservation of seismic topography in the landscape. The longevity and/or discoverability of such relief is, however, diminished in regions where dunes have been active in glacial times (e.g. Rhodes *et al.* 2005; Fitzsimmons *et al.* 2009), and where thick, easily erodable regolith blankets the landscape.

A number of fault scarps have been the subject of palaeoseismological investigation in western and central Australia (Figures 2 and 3). These include Meckering (Geoscience Australia, unpublished data, Figures 4 and 5), Dumbleyung and Lort River (Estrada 2009), Hyden (Crone *et al.* 2003; Clark *et al.* 2008a), Tennant Creek (Crone *et al.* 1992, 1997) and Marryat Creek (Machette *et al.* 1991). A potentially historic pair of surface ruptures has been mapped in detail near Mt Narryer (Williams 1979), while surface deformation relating to a modern rupture has been documented near Katanning using interferometric synthetic aperture radar (Dawson *et al.* 2008). More than fifty additional features with topographic characteristics similar to the known fault scarps have been identified in digital elevation data (Clark 2010). Twenty one of these have been the subject of ground reconnaissance and were found to exhibit characteristics consistent with recent tectonic displacement (e.g. drainage diversion, disruption or impedance, disturbed Quaternary sedimentary deposits, enhanced local slope erosion, etc.).

Although this part of the continent has produced some of Australia's largest recorded earthquakes and the largest moment release (Leonard 2008; Braun *et al.* 2009), the only structural feature with appreciable relief is the Darling Fault scarp, which is historically aseismic and has no published evidence for Quaternary displacement (e.g. Wyrwoll 2003; Sandiford & Egholm 2008). Erosion rates determined from cosmogenically derived ^{10}Be abundances from the scarp face, summit surfaces and streams incising the scarp are inconsistent with significant Neogene tectonic activity (Jakica *et al.* 2010; Quigley *et al.* 2010). An east-facing, 1.5 m high and 19 km long scarp extending south from Serpentine along the foot of the Darling Range is evident in 10 m resolution DEM data

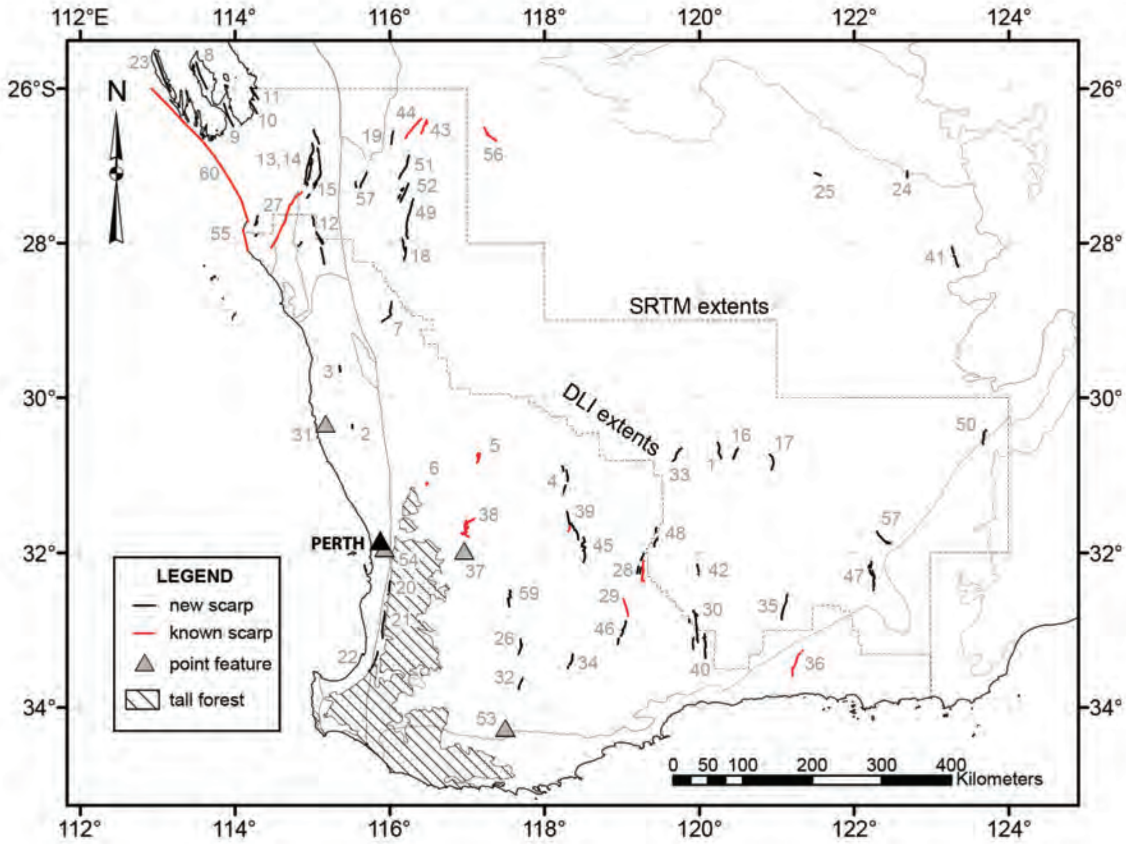

Figure 3 – Scarps identified in southwest western Australia using high resolution DEM data (after Clark 2010). Those scarps that have been visited in the field appear to be related to surface rupturing earthquakes. It might be expected that a similar density and distribution of scarps extends beyond the coverage of high resolution data.

(Clark 2010) and may represent a minor reactivation of the Darling Fault. However, a backhoe trench across the apparent scarp failed to identify discrete fault traces or any material suitable for dating the landform (Geoscience Australia, unpublished report).

Faults with demonstrated Quaternary displacement, including the Meckering, Calingiri, Cadoux, Hyden, Lort River, Dumbleyung and Mt Narryer faults, are associated with discrete scarps up to 40 km long and less than 5 m high (Williams 1979; Gordon & Lewis 1980; Lewis *et al.* 1981; Crone *et al.* 2003; Twidale & Bourne 2004; Clark *et al.* 2008a; Estrada 2009). In cases where early or pre-Neogene units were exposed in trench excavations (e.g. Meckering, Lort River, Hyden), the total vertical neotectonic displacement across these units appears to be significantly less than 10 m. Trench excavations across the recently discovered Dumbleyung Fault (Clark 2005; Clark 2010) and the Lort River Fault (Thom 1972; Clark & McCue 2003) reveal evidence for multiple surface ruptures in the last 100 ka (Estrada 2009), similar to that documented on the Hyden Fault scarp (Crone *et al.* 2003; Clark *et al.* 2008a). In apparent contrast, excavations of the 1968 Meckering Fault scarp identified evidence for only the 1968 event and no prior surface ruptures during the preceding several hundred thousand years (Geoscience Australia, unpublished data) (Figures 4 and 5). The Meckering rupture is complex and exploits basement geology structures with three major intersecting trends (Dentith *et al.* 2009). It may therefore be mechanically difficult to reactivate slip planes due to locking at intersections (cf. Talwani 1988), with the result that consecutive ruptures might use nearby faults. Trenches excavated in the Mortlock River floodplain at a site where Gordon & Lewis (1980) reported that liquefaction had occurred during the 1968 Meckering earthquake failed to find unequivocal evidence for liquefaction produced as the result of the 1968

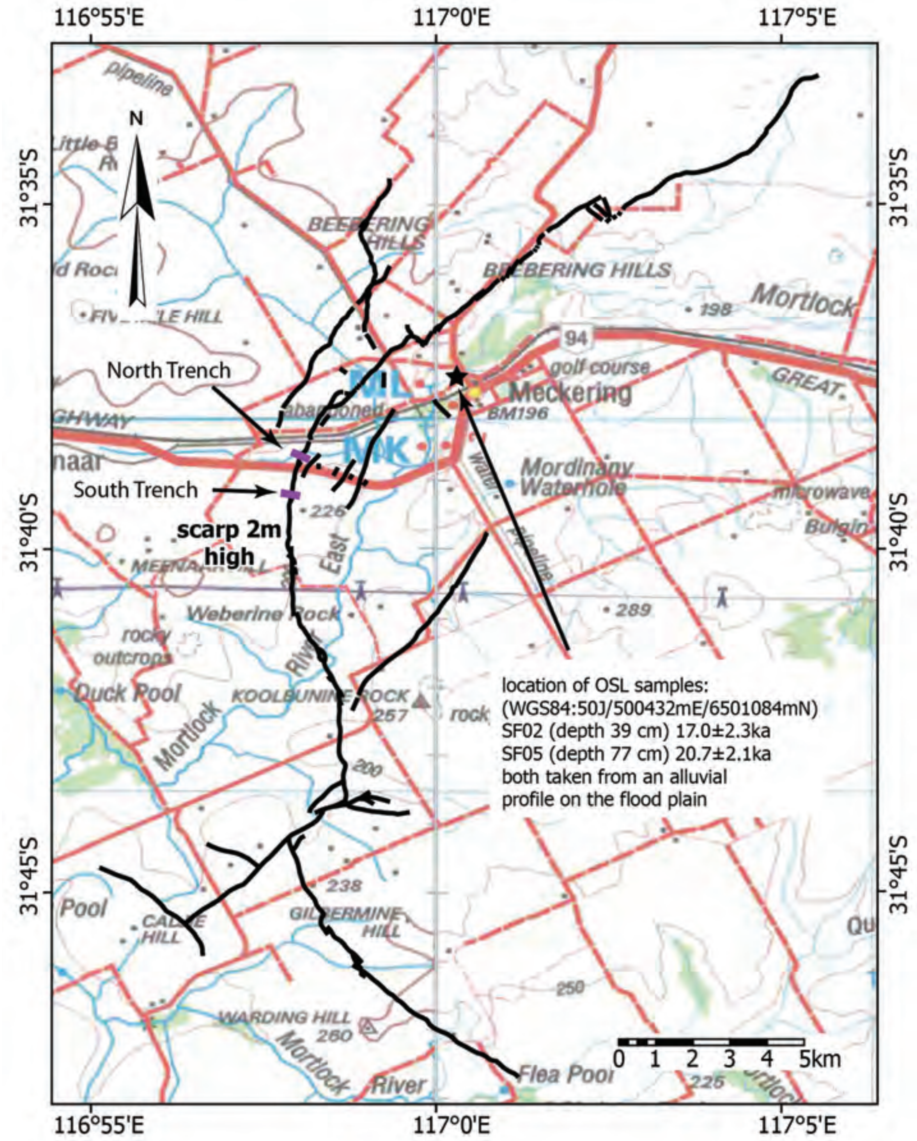

***Figure 4** – Arcuate surface trace of the scarp relating to the 1968 M_s6.8 Meckering Earthquake (Gordon & Lewis 1980) showing the location of trenches excavated in 2005 (logs presented in Figure 5). The scarp is 37 km long and up to 2 m high. See #38 on Figure 3 for scarp location. See Dentith et al. (2009) for relationship of scarp to underlying bedrock geology. OSL ages from Tuttle (2003) and unpublished Geoscience Australia data (see also Figure 6). Base map is 1:250,000 topography.*

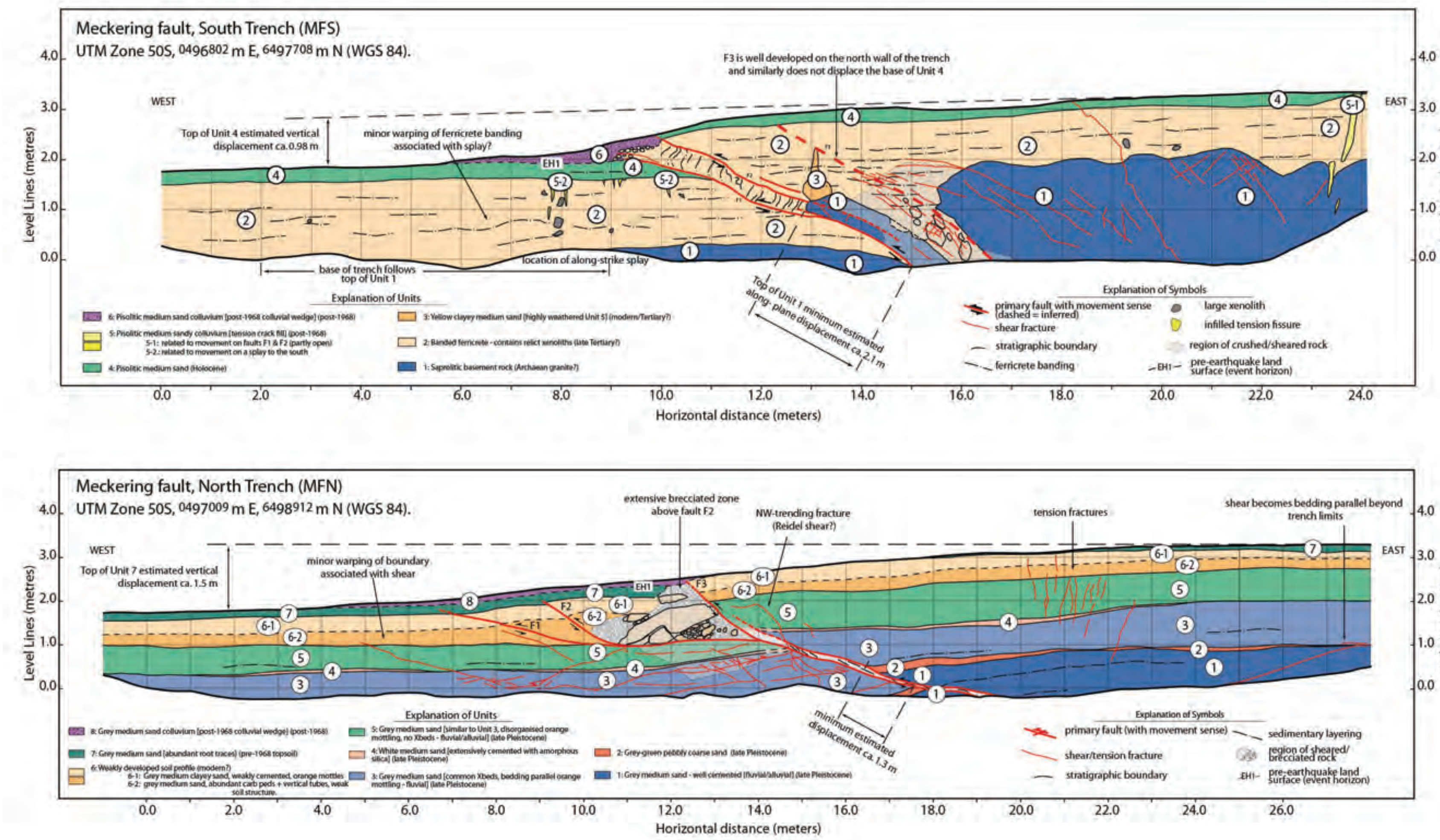

Figure 5 *– logs of trenches excavated through the Meckering scarp (Geoscience Australia, unpublished data). See Figure 4 for location relative to the scarp. The south trench was excavated on an upper slope exposing ferruginous duricrust, and the north trench on an alluvial flat. The northern trench strata record evidence for only the 1968 event. Sediments analogous to those exposed in the upper 1.0 m of the northern trench obtained OSL ages of ~17-20 ka (Figure 6, Tuttle (2003)). Duricrust in the southern trench bears evidence for a penultimate event for which all relief has been removed by erosion, suggestive of great antiquity (erosion rates are likely to be «5 m/Ma, Belton et al. (2004)).*

earthquake, but did find structures that may reflect prior nearby ruptures (Tuttle 2003) (Figure 6). Two generations of sand-filled features that superficially resemble root casts but share properties in common with liquefaction-induced sand dykes (e.g. fining of grainsize away from the "vent", and silt accumulations at "vent" margins) were present in the trenches. OSL dating of two soil samples collected in the trenches (sample SF02 and SF05, Figures 4 & 6) constrains the older sand sheet and "vent' to the interval *ca.* 17-20 ka, and the younger to *ca.* 0.15-17 ka (Olley 2004). Further research is required to prove an earthquake origin for these features.

Length and height data from 33 scarps identified in DEMs (Clark 2010) is consistent with the features studied in detail. Average scarp length is 26 km, with 90% of values less than 40 km in length. Average height (a proxy for vertical displacement) is 4 m with 90% of values less than 10 m. Relationships between scarp length and height (Wells & Coppersmith 1994) suggest single event displacements of up to 2 m for a rupture length of 40 km or less, with the implication that most of the scarps identified in DEM data are the result of more than one Quaternary surface rupturing event. Strain localisation is therefore a common characteristic of neotectonic faults in this part of the continent. However, the absence of evidence for ongoing fault-related relief generation on geological timescales implies that, while seismic events might be spaced only a few tens of thousands of years apart for a few seismic cycles (e.g. Crone *et al.* 2003; Clark *et al.* 2008a), average recurrence over the entire neotectonic era is in the order of half a million years or more. Consequently, while slip rates in active periods might approach several metres per hundred thousand years or more, long term slip rates might be expected to be several orders of magnitude less (e.g. Clark *et al.* 2008a).

The 'average' strike of the features in southwest Western Australia (as shown in Figure 3), defined as the trend of the dominant structural components, is plotted in Figure 7. A dominant northerly trend is clearly apparent in the data, which has a mean of 4 degrees east of north. More than 85% of orientations are within 30 degrees either side of north. Presumably, given favourable fluid conditions and welding, orientation with respect to the prevailing E-W crustal stress field (e.g. Hillis and Reynolds 2000) is paramount in determining which elements of the pre-existing structure are likely to be active. High resolution aeromagnetic data indicate that complex interactions between oblique elements of pre-existing structure serve to localise stress at a regional scale (Dentith *et al.* 2009; Estrada 2009).

Furthermore, the uniform distribution of northerly trending reverse fault scarps is consistent with scarp formation under conditions imposed by the contemporary E-W oriented compressive crustal stress regime, and suggests that strain is uniformly distributed over the Yilgarn Craton over the timescale recorded in the land surface (say *ca.* >100 ka). These observations, when combined with the above evidence, is consistent with a seismicity/crustal strain model whereby the ductile part of the lithosphere deforms uniformly in response to an imposed easterly-trending contractional strain, and the upper (seismogenic) layer accommodates this large-scale flow by localised, transient and recurrent brittle deformation along lines of pre-existing crustal weakness (c.f. Braun *et al.* 2009; Clark 2010).

With the exception of the two well documented historic surface ruptures at Tennant Creek (Crone *et al.* 1992, 1997) and Marryat Creek (Machette *et al.* 1993; Crone *et al.* 1997), which have similar characters to the southwest Western Australia scarps just described, little is known of the large earthquake characteristics in the arid centre of the continent. Despite extensive dune fields and widespread deep regolith, several prominent scarps are known (e.g. the Iragana scarps, Munro scarps). The Iragana scarps stretch discontinuously over ~ 230 km of the Gibson Desert, in part

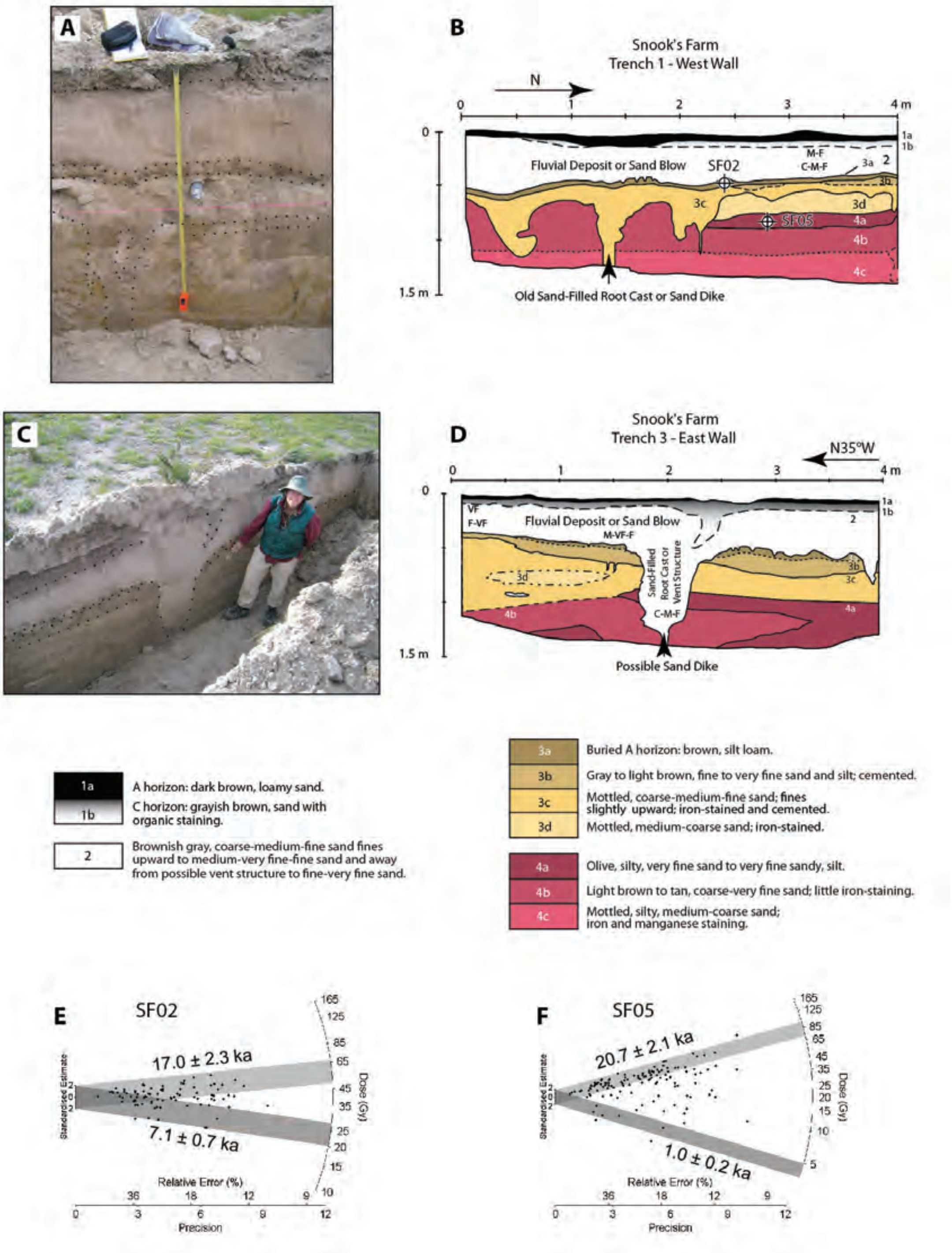

Figure 6 – Trenches excavated in the Mortlock River floodplain at a site where Gordon & Lewis (1980) reported that liquefaction occurred during the 1968 Meckering earthquake (modified from Tuttle 2003). Location in relation to Meckering surface rupture and dating results are shown on Figure 4. Two generations of sand-filled features that may be root casts or sand dykes are present. Parts E and F are single grain OSL results from samples SF02 and SF05, respectively (Olley 2004). OSL sample SF02 was taken from layer 3a on the east wall of the trench shown, and contained no ^{137}Cs or excess ^{210}Pb (Olley 2004).

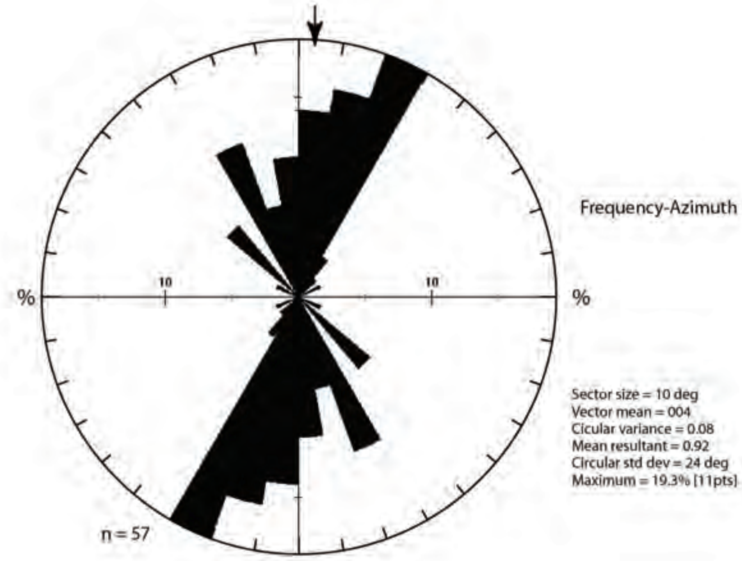

***Figure** 7 – Rose diagram of orientations of the scarps identified in southwest western Australia using high resolution DEM data (after Clark 2010).*

coinciding with the Iragana Fault which is mapped in Proterozoic orogenic basement (van de Graaff 1975). The central scarp section is over 70 km long and up to 5 m high where it crosses alluvial palaeo-channels (Figure 8). At the resolution of the 3 arc-second SRTM DEM, the deposition patterns of Pleistocene desert dunes do not appear to change across the scarp, consistent with the scarp postdating dune formation. Similarly, linear dunes show no change in pattern across the two bounding scarps of the Munro horst (Figure 9). The SRTM DEM suggests that these features rise up to 10 m above the surrounding sand and alluvial plains of the Great Sandy Desert, consistent with several causative seismic events. Palaeo-drainage lines are extensively affected where the scarps cross them, forming a series of small lakes.

In addition to scarps, several air photo lineaments defined predominantly by concentrations of vegetation are known (e.g. Kalga Hills, Mt Liesler and Mt Theo features). In most cases the lineaments are parallel to major Proterozoic basement structural trends (cf. Shaw *et al.* 1996). It is possible that these features might relate to surface rupturing earthquakes by analogy to similar lineaments identified in the Mt Narryer region (Williams 1979; Clark 2004).

THE NULLARBOR PLAIN

The Nullarbor Plain is a marine terrace capped with limestone which was exposed at *ca.* 15 Ma as the result of gentle long wavelength uplift of the southwestern part of the Australian continent (Sandiford *et al.* 2009; Sandiford & Quigley 2009). The plain surface slopes gently to the south at significantly less than 1% and is extremely flat, with local relief in the order of a few tens of metres at most. These characteristics have resulted in an almost total absence of fluvial and hill slope processes on the plain, and the consequent dominance of karst solution processes throughout the entire neotectonic era. Preliminary estimates of land surface lowering rates, determined using cosmogenic ^{36}Cl abundances in calcrete cappings, are in the order of ~ 5 m/Ma (Stone *et al.* 1994).

The Nullarbor Plain preserves an extraordinary neotectonic record that paradoxically reflects the long-term tectonic stability of the underlying Proterozoic basement terranes. Numerous linear fault scarps are visible in SRTM DEM data across the plain (Figure 10a). Assuming approximately uniform surface lowering of the limestone plain across faults, displacements in the last 15 Ma have

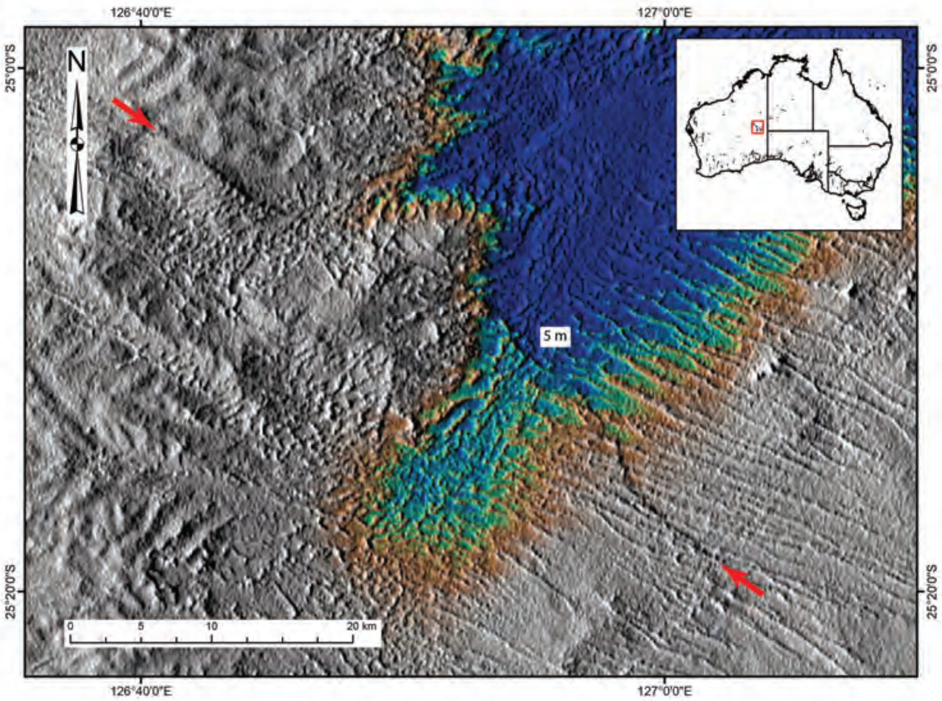

Figure 8 – *90m resolution SRTM DEM data over a 50 km long segment of the central part of the Iragana scarp, Central Australia. Note that palaeochannel is elevated to the SW of the scarp, indicating differential uplift of the landsurface. Aeolian dunes appear unaffected by this movement, suggesting that the faulting post-dates dune emplacement. Sun illumination is from the west.*

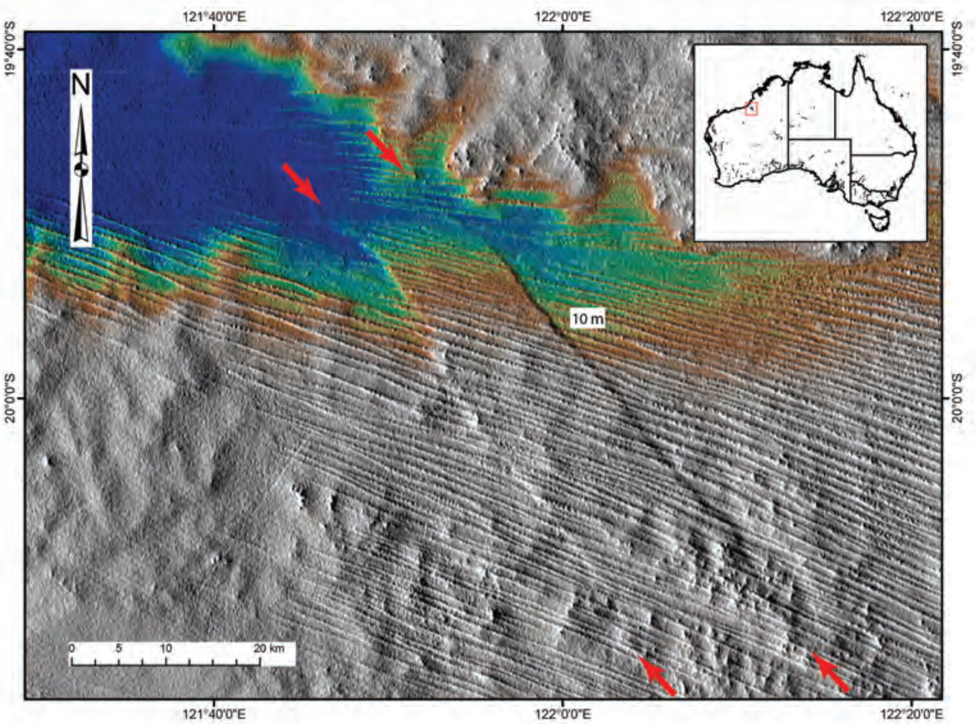

Figure 9 – *90m resolution SRTM DEM data over the 60 km long scarps of the Munro Horst, northwestern Australia. Note that palaeochannel is partly impeded by faulting, forming ephemeral lakes. Aeolian dunes appear unaffected by this movement, suggesting that the faulting post-dates dune emplacement. Sun illumination is from the west.*

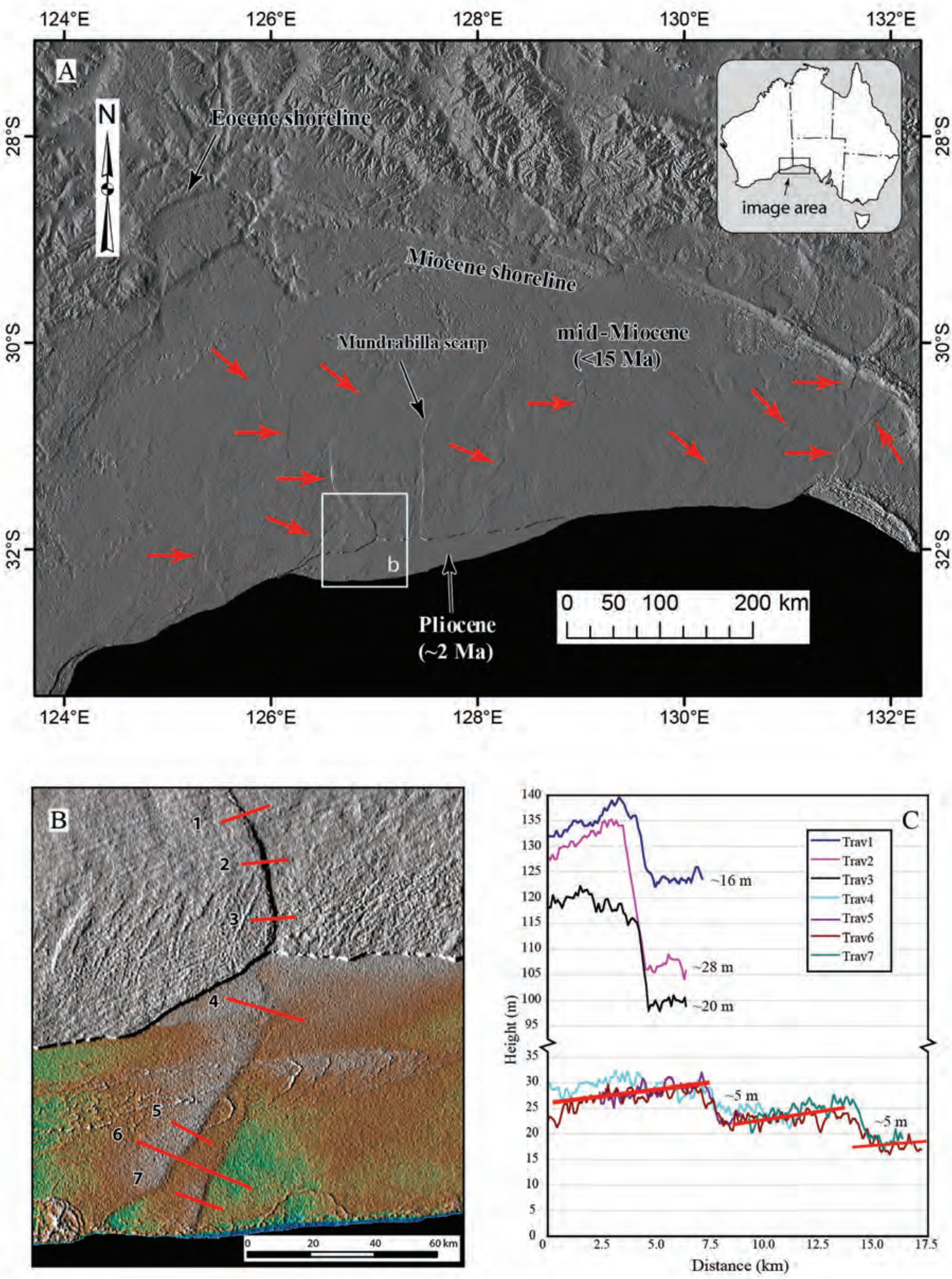

Figure 10 *– (a) 90m resolution SRTM DEM data over the Nullarbor Plain. (b) inset showing the Roe Plain Scarp where it crosses both the Nullarbor and Roe Plains, (c) topographic profiles across the Roe Plain Scarp.*

been in the order of a few tens of metres at most, and more commonly less than 10 m. Slip rates averaged over the neotectonic era are therefore everywhere in the range of 1-3 m/Ma or less. This conclusion is supported by the observation that several scarps do not continue from the Nullarbor Plain onto the *ca.* 2 Ma (James *et al.* 2006) Roe Plain surface. Two scarp traces do displace the Roe Plain surface vertically by ~ 5 m each (Figures 10b, c), and appear to link into a single scarp trace towards the Nullarbor Plain edge. A vertical slip rate estimate in the range of 2.5 m/Ma is obtained, or twice that number if it is assumed that the scarps link into a single fault at depth. This corresponds to dip-slip rates of ~ 3.5 – 7.0 m/Ma for a 45° dipping fault. The vertical displacement across the Roe Plain scarp where it cuts the Nullarbor Plain surface is in the range of 15-30 m (cf. 5 m, Figure 10c). Slip rates over the entire neotectonic era therefore appear to be consistent with those measured over the Pleistocene. Although there are no present-day stress data for this area, the orientation of these small displacement faults is consistent with the east–west orientation of the present-day stress field inferred for the area from plate-boundary force modelling and *in situ* data (Figure 1) (Coblentz *et al.* 1995; Coblentz *et al.* 1998; Hillis & Reynolds 2003; Hillis *et al.* 2008). It is therefore possible that the scarp record relates to the last 5-10 Ma only, rather than the last 15 Ma.

The Mundrabilla Scarp (Figure 10a) coincides exactly with a linear feature imaged in national scale aeromagnetic data which is interpreted to mark the boundary of a Proterozoic basement terrane (Shaw *et al.* 1996). This testifies to a strong basement influence in localising neotectonic strain release, similar to that seen elsewhere in Western Australia (Dentith *et al.* 2009; Estrada 2009). Consistent with observations in other parts of Western Australia, the scarps do not appear to show any strong spatial arrangement with respect to each other, although they appear to be longer than their counterparts in the southwest of the State.

SOUTHERN SOUTH AUSTRALIA

The Flinders and Mount Lofty Ranges of South Australia are bound on the east and the west by reverse faults that thrust Proterozoic and/or Cambrian basement rocks above Quaternary sediment (Sprigg 1946; Williams 1973; Sandiford 2003b; Quigley et al. 2006; Hillis et al. 2008). Faults in this region with documented Pliocene to Quaternary displacements include the Wilkatana/Depot Creek, Burra, Milendella, Para, Paralana, Willunga, Morgan, Gawler/Concordia, Ochre Cove-Clarendon, Eden-Burnside, Bremer, and Ediacara (Binks 1972; Williams 1973; Bourman & Lindsay 1989; Alley & Lindsay 1995; Sandiford 2003b; Quigley *et al.* 2006; Quigley *et al.* 2010) (Figure 11). Fault-propagation folding is well developed in Miocene strata proximal to the Willunga and Gawler faults (Lemon & McGowran 1989; Green 2007).

Celerier *et al*. (2005) show how variations in both absolute abundance and depth of heat-producing elements provide a plausible thermal control on lithospheric strength that helps localise deformation in the Flinders Ranges. The Flinders Ranges form part of a zone of anomalous surface heat flow (Neumann *et al.* 2000) with an average surface heat flow of 85 mW/m^2 reflecting unusually elevated heat production in the Proterozoic basement. Celerier *et al*. (2005) conclude that the upper-most mantle beneath the Flinders seismic zone may be 50-100°C hotter than surrounding zones because of the distribution of heat production within the crust. Neo-Proterozoic rift structures partially overprinted by Late Proterozoic to Palaeozoic compressional orogenic structures (Delamerian Orogeny) combine with this thermally weakened zone to create crust that is primed for focussing deformation. A similar mechanism has been proposed as a means of localising crustal deformation in the New Madrid Seismic Zone in the USA (Liu & Zoback 1997).

Summit surfaces in the central Flinders Ranges have been uplifted relative to flanking piedmonts by more than 12 m in the last 70 ka, equivalent to a rate of ~ 170 m/Ma, due to activity on the

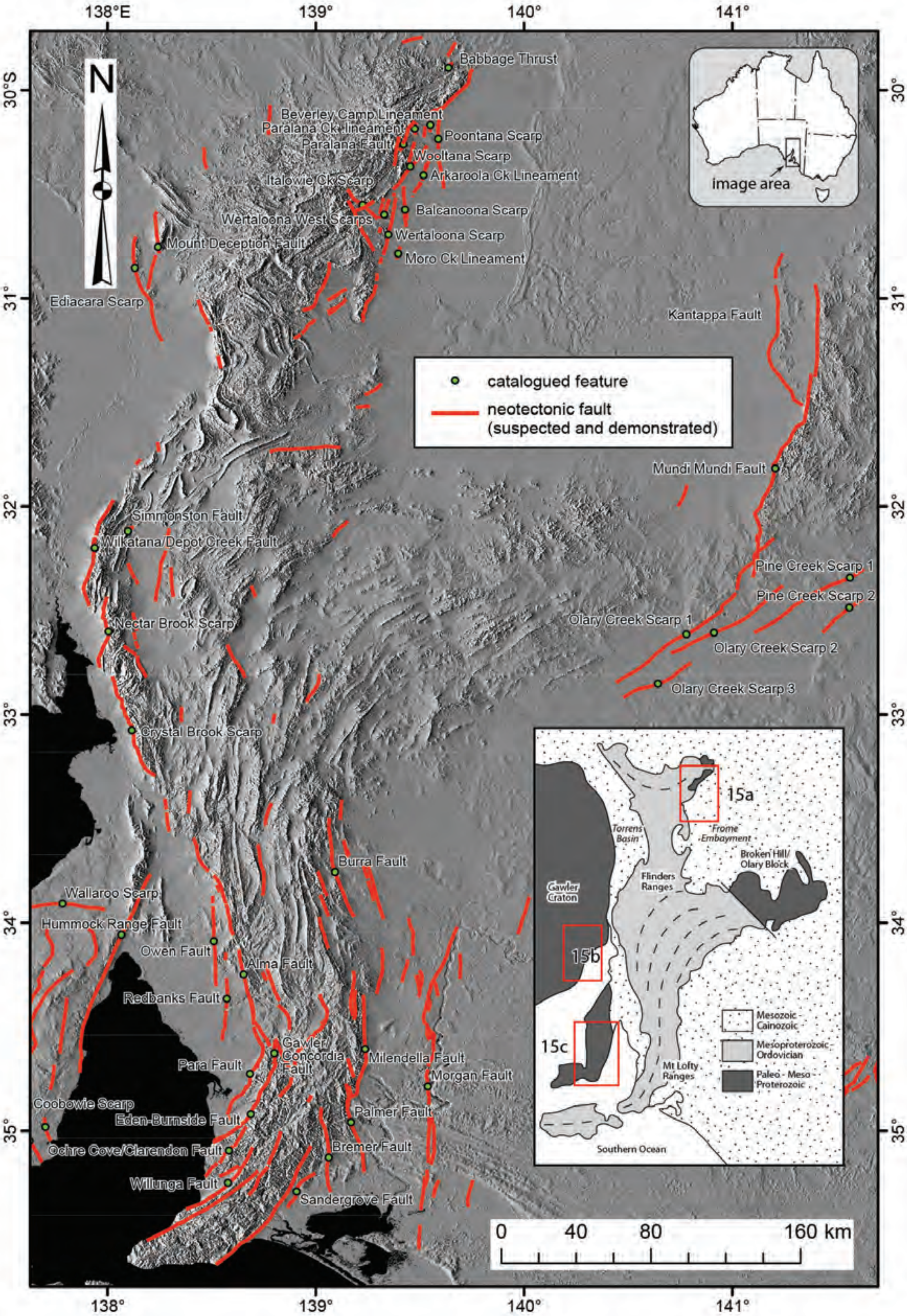

***Figure 11** – 90 m resolution SRTM DEM over the Mt Lofty and Flinders Ranges, which together are denoted the Sprigg Orogen. Red lines denote fault scarps with suspected or demonstrated neotectonic movement (extracted from the Geoscience Australia neotectonics database, January 2010). Inset shows major geological provinces (after Celerier et al. 2005). Location boxes for Figure 15 are marked.*

Wilkatana range bounding fault (Quigley *et al.* 2006) (Figure 12). Taking into account the intermittent nature of faulting in Australia (e.g. Crone *et al.* 2003), Quigley *et al*. (2006) and Sandiford (2003b) suggest that 30-50% of the present-day elevation of the Flinders Ranges relative to adjacent piedmonts has developed in the last 5 Ma. Cosmogenic ^{10}Be concentrations in exposed bedrock surfaces and alluvial sediment in the same area support ongoing relief generation (Quigley *et al.* 2006; Quigley *et al.* 2007b), which has been termed the Sprigg Orogeny (Sandiford 2003b).

Range bounding faults in the Flinders and Mt Lofty Ranges range from a few tens to almost 100 km long and tend to be spaced significantly less than a fault length apart, often linking or arranged in an *en echelon* pattern (e.g. Figure 11). In the few instances where the thickness of overthrust colluvium can be estimated, total neotectonic throws are in the order of 100-200 m (Williams 1973; Preiss & Faulkner 1984; Bourman & Lindsay 1989; Celerier *et al.* 2005; Quigley *et al.* 2006). Recurrence data exists for the Wilkatana Fault, which is believed to have hosted a minimum of three surface rupturing earthquakes in the last 67 ka, involving approximately 15 m of slip (Quigley *et al.* 2006) (Figure 12). A single event slip estimate by these authors in excess of 3.8 m implies earthquakes with magnitudes of greater than M_w 7.0. A detached Cambrian bedrock slab ~ 7 m long overlies Pleistocene Ochre Cove Formation colluvium on the footwall of the Milendella Fault near Cambrai (Figures 13 & 14). The coherence of the fabric in the slab suggests that it was tectonically emplaced in its current location, rather than being transported by hillslope processes. The high angle of the fabric in the slab (i.e. slope parallel) to the hanging wall bedrock fabric, and the observation that a successive rupture has detached the slab from the bedrock (Figures 13c & 14), suggests the slab came to be in its current setting as the result of a single large magnitude seismic event (Geoscience Australia, unpublished field data; Reid 2007). Slip rates on individual faults have been estimated to be in the order of 20-150 m/Ma (Sandiford 2003b). However, a slip rate estimate of over 700 m/Ma has been suggested for the Para Fault over the last 125 ka (Malcolm Sheard, PIRSA, pers. communication, 2009).

Along deeply dissected lines of drainage in the northeast Flinders Ranges, exposures of the Paralana Fault system show Proterozoic metamorphic rocks thrust over unmetamorphosed sediments of the Frome Embayment and Quaternary hillslope deposits (Belperio 1995; Sandiford 2003b; Celerier *et al.* 2005). Extensive alluvial fans associated with the Paralana Escarpment, dating from perhaps *ca.* 30-120 ka (Williams 1973; Bourman *et al.* 1998), are crossed by numerous low scarps and parallel lineaments (e.g. Harper 2002; Sandiford 2003b; Celerier *et al.* 2005) (Figures 11 & 15a). Rare stream exposures indicate that these features are underlain by low-angle west-dipping reverse faults, similar to the range front fault, with several metres of offset (Sandiford 2003b, Figure 9). Detailed geological mapping links these features with Delamerian basement structures (Dubieniecki & Hill 2007). Similar relationships are exposed along the Mt Babbage Thrust (Belperio 1995, Wolfgang Preiss, personal communication, 2006).

Neotectonic deformation is more subtle moving away from the topographic axis of the Flinders Ranges (Figures 11 & 15b, c). To the west, neotectonism is well documented on a number of faults on the northeast Eyre Peninsula (e.g. Miles 1952; Dunham 1992; Hutton *et al.* 1994; Crone *et al.* 2003; McCormack 2006; Weatherman 2006; Robert 2007) (Figure 15b), the Yorke Peninsula (Crawford 1965) (Figure 15c), and on the western margin of the Eyre Basin (Wopfner 1968; Waclawik *et al.* 2008; Quigley *et al.* 2010). To the east, the Mundi Mundi and Kantappa faults displace Quaternary strata (Hill & Kohn 1998; Quigley *et al.* 2006) (Figure 11). Additional scarps are apparent in 3 arc-second SRTM DEM data in the Pine Creek and Olary regions (Figure 11). These structures are similarly arranged to faults in the Flinders Ranges, tending to be spatially clustered, but typically appear to displace pre-Pliocene basement by less than a few tens of metres.

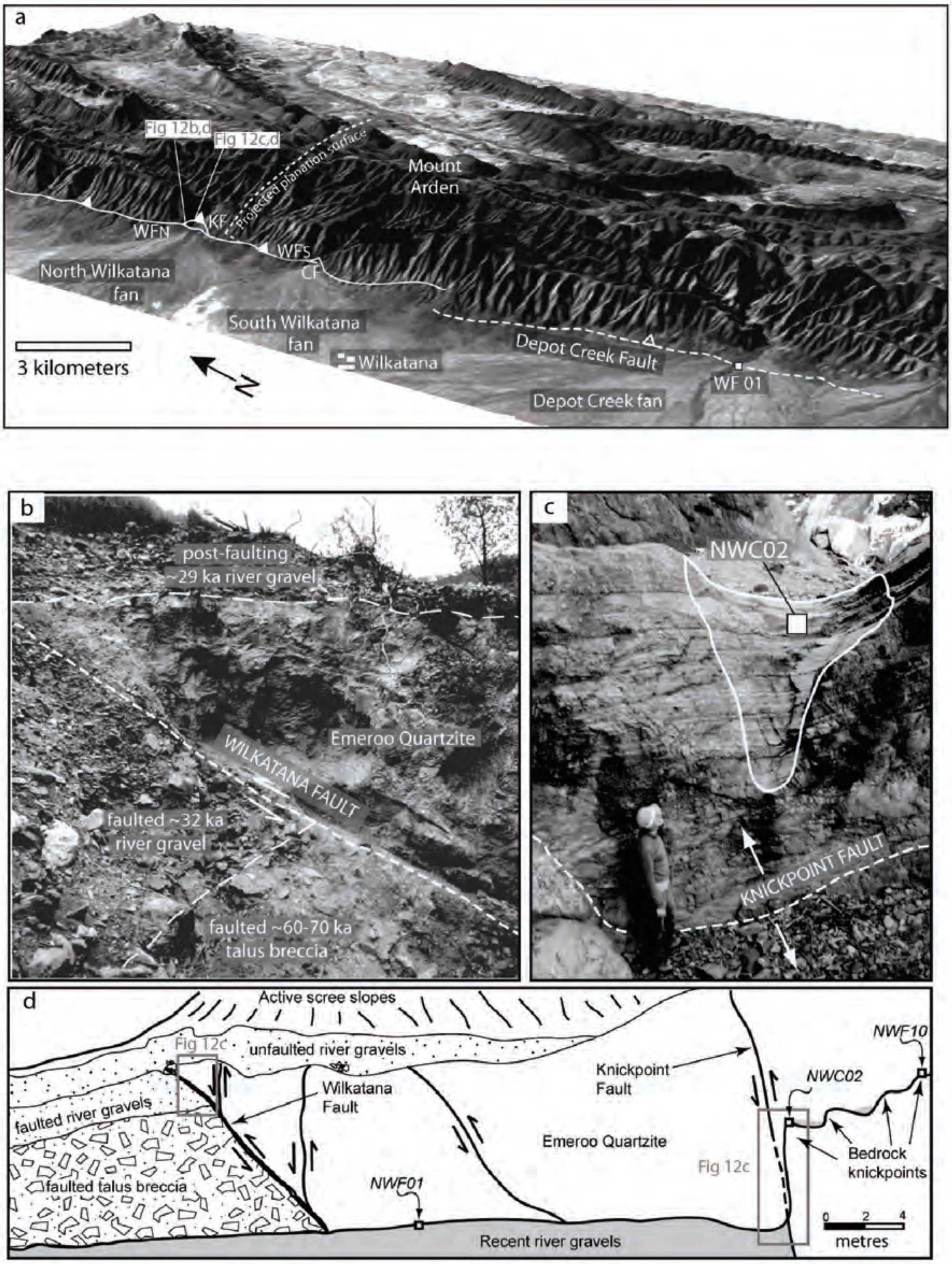

Figure 12 *– (a) ASTER mosaic over the Wilkatana/Depot Creek Fault in the central west Flinders Ranges, showing first order relationship to topography. (b) the Wilkatana fault as exposed near the apex of the North Wilkatana fan. OSL geochronology from (Quigley et al. 2006) shown. (c) the Knickpoint Fault where it intersects the creek at the head of the North Wilkatana fan. (d) cartoon showing faulting and relationship of faulting to the range front at the head of the North Wilkatana fan. Images adapted after Quigley et al. (2006) and Quigley et al. (2007a).*

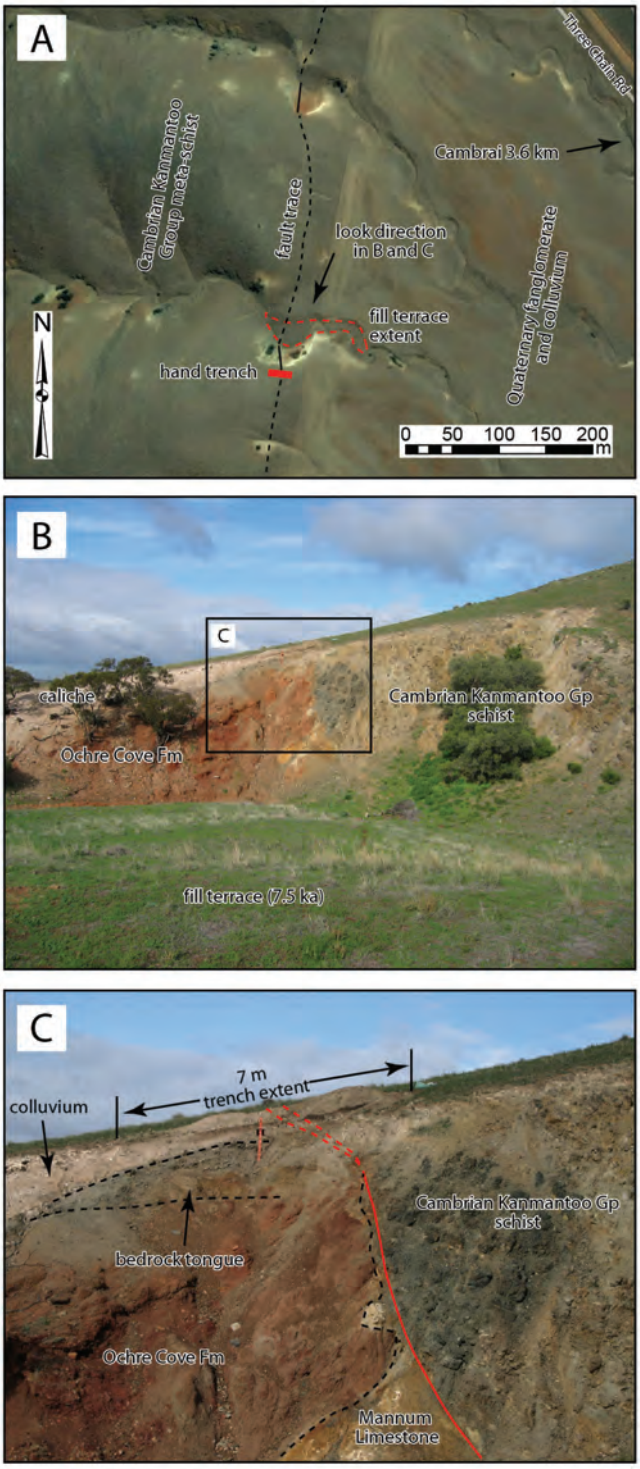

Figure 13 *– The Milendella Fault, eastern Mt Lofty Ranges. Location near Cambrai is marked by a green dot on the Milendella fault trace on Figure 11. (a) Aerial photograph showing exposures of the Milendella fault (see also Bourman & Lindsay 1989; Sandiford 2003b), location of hand trench, and unfaulted inset fill terrace. (b) field photo looking south towards the southern fault exposure in (a) from a position on an unfaulted inset fill terrace. Note bedrock over-riding mid Pleistocene Ochre Cove Formation. Pale yellow Miocene Mannum Limestone has been dragged up the fault plane. Groundwater circulation along the fault plane has resulted in significant calcification of colluvial deposits downslope of the trace. (c) enlargement of the region where the fault plane intersects the surface. Bedrock tongue contains a coherent schistose fabric parallel to the palaeo-slope surface represented by the top of the Ochre Cover Formation, and is 7 m long. Note hand trench extents.*

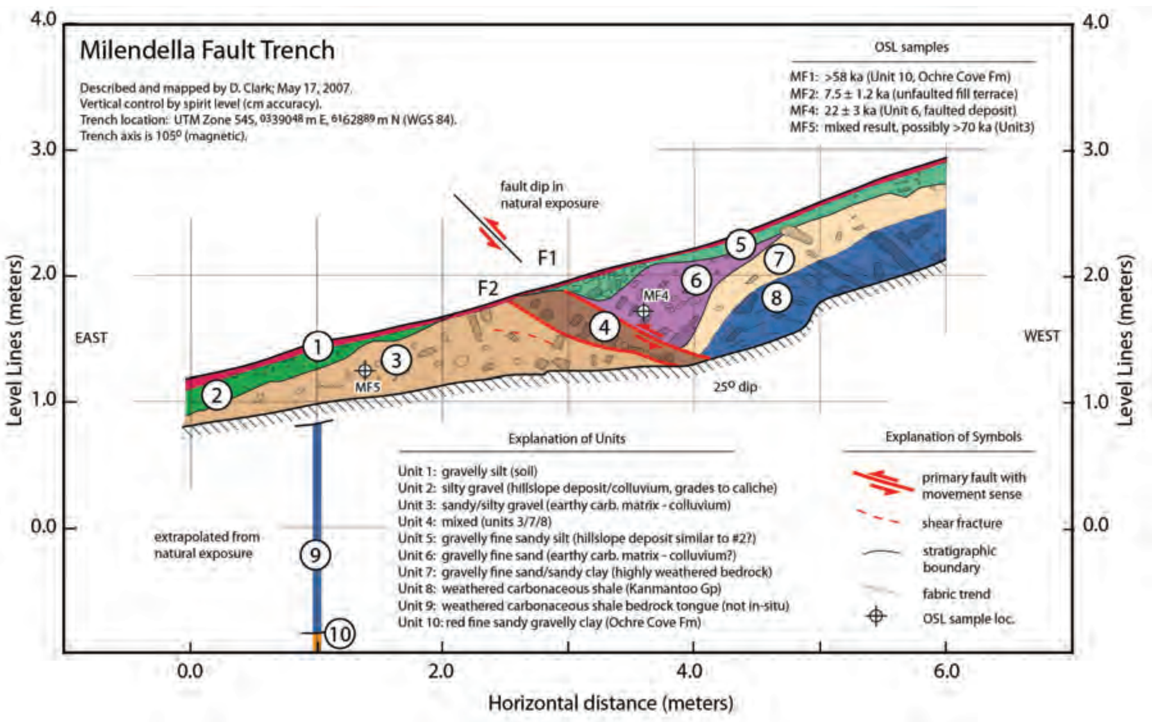

***Figure 14** – Log of hand trench excavated across the surface trace of the Milendella fault. Trench location is shown in Figure 10. Dating results suggest at least one surface rupture between ca. 22 ka and 7.5 ka. A penultimate event resulted in the emplacement of a 7 m long bedrock tongue over the Ochre Cove Formation in the footwall (age < 780 ka (Pillans 2003b)).*

EASTERN AUSTRALIA

Eastern Australia is characterised by some of the greatest relief on the continent, and some of the higher bedrock erosion rates. The Eastern Highlands have been the subject of numerous studies of bedrock erosion rates, values for which predominantly fall in the range of 20-50 m/Ma (e.g. Bishop *et al.* 1985; Weissel & Seidl 1998; Bishop & Goldrick 2000; Heimsath *et al.* 2000, 2001; Wilkinson *et al.* 2005; Tomkins *et al.* 2007). The bulk of the contemporary elevation of the highlands has been related to the late Mesozoic opening of the Tasman Sea (Vandenberg 2010), with relief being maintained by isostatic rebound (Bishop 1988; Bishop & Brown 1992; Bishop 1995; Bishop 2007). Holdgate *et al.* (2008) presented evidence from the southern Eastern Highlands that resurrected the idea of a punctuated post-Eocene Kosciuszko Uplift event (cf. Andrews 1910; Sprigg 1946; Browne 1967) that continued into the Late Pliocene and potentially into the Pleistocene. It is possible that this event might be responsible for adding several hundred metres of local relief to the highlands, and relate to the pulse of deformation seen in south-east Australian offshore basins in the interval 10-5 Ma associated with the reorganisation of the crustal stress field into its present configuration (Dickinson *et al.* 2001; Dickinson *et al.* 2002; Sandiford *et al.* 2004; Hillis *et al.* 2008). The Lake George Fault east of Canberra (Coventry 1976; Singh *et al.* 1981; Abel 1985) (Figure 16), and faults of the Lapstone Structural Complex (LSC) near Sydney (Branagan & Pedram 1990; Pickett & Bishop 1992), may also have accumulated much of their several hundred metres of neotectonic displacement in this event (Clark 2009). However, while palaeomagnetic data indicate that folding and uplift relating to the LSC had largely ceased by late Pliocene (Bishop *et al.* (1982) with age recalculated by Pillans (2003a)), the preliminary findings from a fault-bounded lake adjacent to the Kurrajong Fault in the northern LSC indicate that neotectonic displacement may be limited to less than 20 m on this major fault (Clark *et al.* 2009). The implication is that most relief at the eastern range front of the Blue Mountains relates to erosional exhumation of 'old' structures

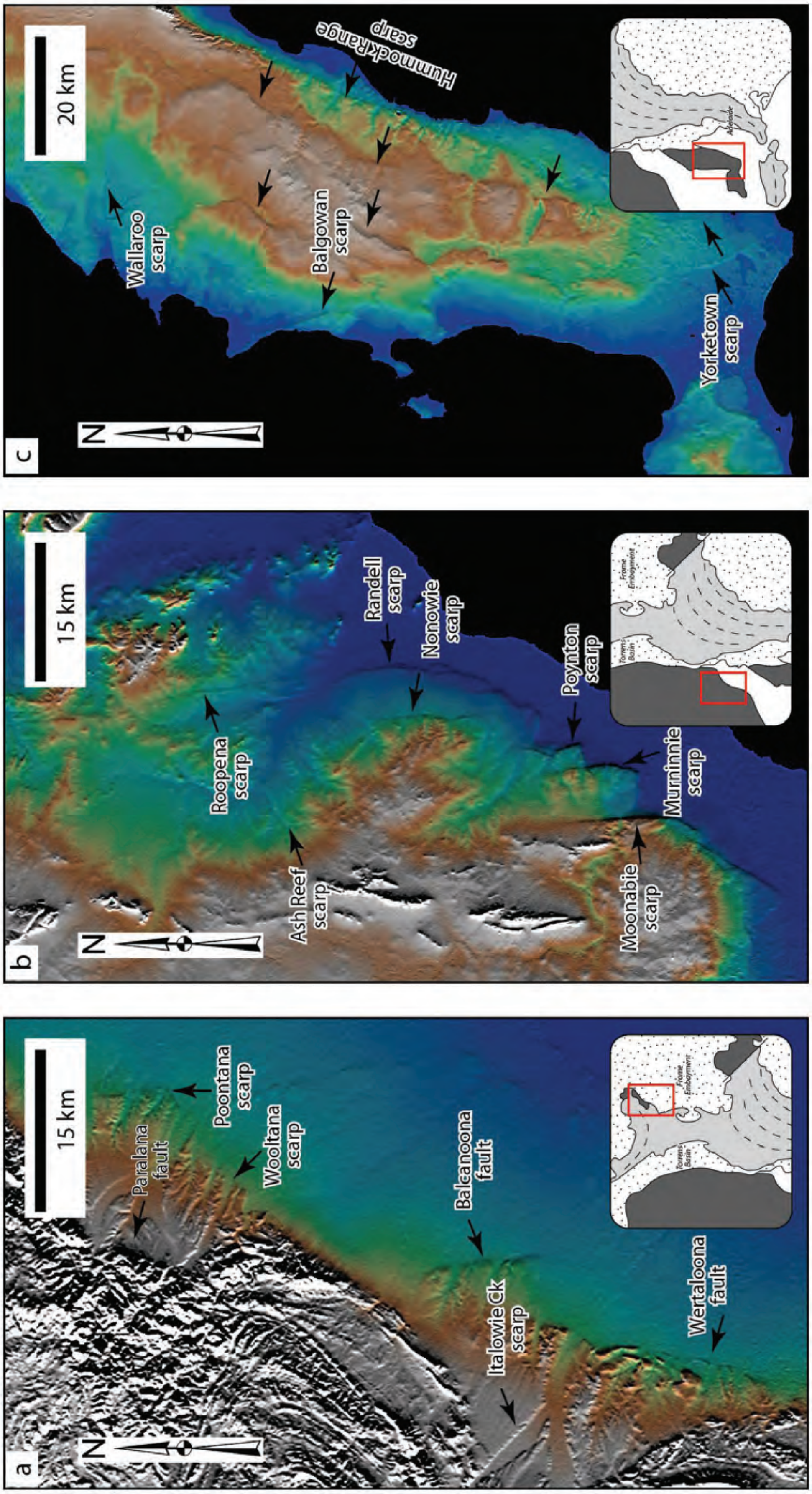

Figure 15 *– 90 m resolution SRTM DEM images. (a) scarps cutting alluvial fans east of the Paralana escarpment, (b) scarps on the eastern margin of the Eyre Peninsula, including the Roopena scarp (Crone et al. 2003), (c) scarps on the Yorke Peninsula. Refer to Figure 11 inset for more detailed location.*

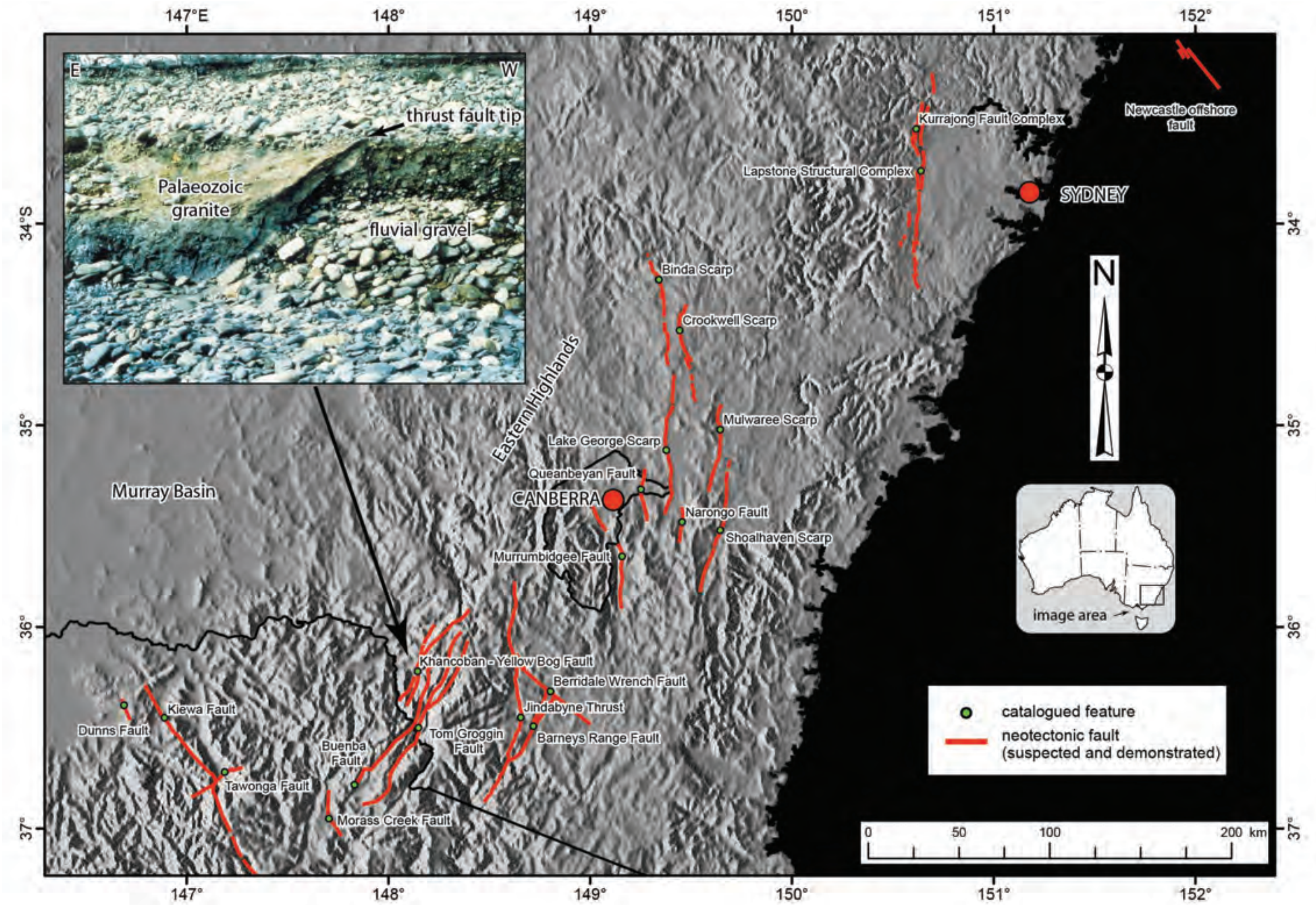

Figure 16 *– 90 m resolution SRTM DEM over the eastern highlands. Red lines denote fault scarps with suspected or demonstrated neotectonic movement (extracted from the Geoscience Australia neotectonics database, January 2010). Inset shows the Khancoban-Yellow Bog Fault as exposed in the bed of Khancoban Creek shortly after the Murray 1 power station was commissioned in the late 1960's. Inset image kindly provided by David Stapleton (formerly of Snowy Hydro).*

(Pickett & Bishop 1992; Clark *et al.* 2008b, 2009). Further north, at the boundary between the Lachlan and New England Fold Belts, warping of Miocene strata during the Pleistocene has resulted in the formation of a monocline of 30 m amplitude (Huftile *et al.* 1999). This ~ 30 km long northwest trending structure, the Newcastle offshore fault (Figure 16), occurs along strike of the Hunter Thrust system, and close to the epicentre of the 1989 M5.6 Newcastle earthquake.

Comparable bedrock erosion rates and tectonic relief production rates might be expected to result in low scarp survivability, bar exceptional circumstances. This general expectation is borne out by examples such as the Khancoban-Yellow Bog Fault, which superposes Mesozoic granite over up to 500 m of Cenozoic fluvial gravels (Moye *et al.* 1963; Sharp 2004), yet has little topographic expression. The Tawonga (Beavis 1960; Hills 1975; Beavis & Beavis 1976; Sharp 2004) and Kiewa Faults (Beavis & Beavis 1976) also fall into this category, with hundreds of metres of neotectonic displacement likely. Further south in the Victorian Goldfields active faulting is often known only from displacement of the bases of Pliocene and younger basalt flows capping palaeochannel fill sediments (i.e. deep leads) (e.g. Canavan 1988; Kotsonis & Joyce 2003a; Kotsonis & Joyce 2003b).

Significantly lower relief and the widespread preservation of retrogressive Pliocene marine strandline deposits in the Murray Basin to the west of the highlands suggests significantly lower erosion rates (Figure 17). Consequently, preservation of fault scarps might be expected to be greater than in the highlands. However, the materials in which scarps are developed within the basin are typically partially indurated Cenozoic sediments rather than bedrock, and so are highly susceptible to degradation resulting from fluvial and lacustrine processes. Examples are the Danyo, Iona and Neckarboo Ridges in the central Murray Basin (Sandiford 2003b), and the Cadell tilt block in the eastern Murray Basin (Harris 1938; Bowler & Harford 1966; Bowler 1978; Rutherfurd & Kenyon 2005). These features are the broad scale-expression within Cenozoic cover sediments of reactivated Lachlan Fold Belt basement faults (e.g. Figure 17 – inset) – the “resurgent tectonics” of Hills (1961). Similar features are evident in the upper catchments of the Murray-Darling Basin drainage system. For example, 90 m SRTM DEM data show that the Namoi River is diverted north around the < 6 m high and 35 km long Walgett Scarp (Figure 18a). Further north, neotectonic deformation of Mesozoic rocks of the Surat Basin has raised a ridge of overlying Cenozoic sediment which constricts the channel of the Balonne River (Figure 18b). The displacement profile across this ridge suggests that the northern margin of the ridge is underlain by a southwest dipping reverse fault.

The Cadell Fault is one of the best characterised neotectonic faults in eastern Australia in terms of its earthquake behaviour. It is situated in the Riverine Plain, a broad, topographically subdued region of the Murray-Darling Basin (Bowler & Harford 1966; Bowler 1978; Brown & Stephenson 1991) (Figures 17 & 19). West-side up displacements across the 80 km long fault have resulted in the formation of a scarp up to 15 m high which diverted the course of Australia’s largest river, the Murray River. (Bowler 1978). The 3-4 m height of a tectonic terrace riser bordering the channel of the palaeo-Murray River in Green Gully, now an air gap, is consistent with entire scarp-length rupture (~ M_w 7.2-7.3)(Clark *et al.* 2007) (Figure 20). At least four earthquakes of this magnitude are required to produce the observed 14-15 m relief across the scarp. Perhaps a further two events of similar magnitude are required to account for 6 m of aggradation of the Barmah Fan, which buries the foot of the scarp (Stone 2006). Optically stimulated luminescence dating of fluvial and lacustrine sediments that pre- and post-date the first and last recognised seismic events, respectively, indicate that the 4-6 events occurred over a *ca.* 60 ka time interval between 80-20 ka, and involved a total slip in the order of 25 m, suggesting an average slip rate over this interval of ~ 0.4 mm/yr (Stone 2006; Clark *et al.* 2007). Seismic reflection data obtained over the scarp (Geoscience Australia, unpublished data) (Figure 21) indicate only ~ 55 m of displacement of Neogene strata

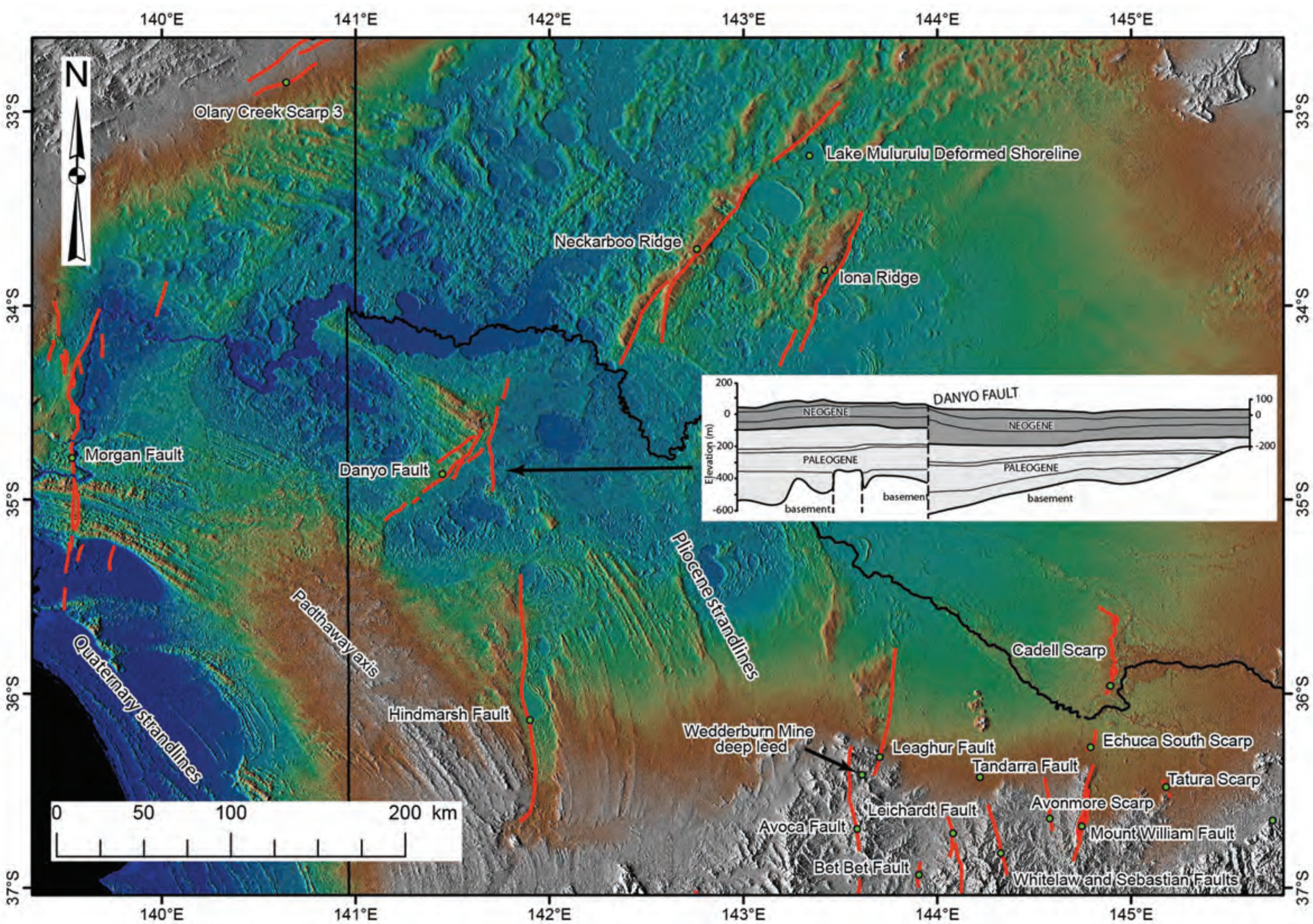

Figure 17 – *90 m resolution SRTM DEM over the central and lower Murray Basin. Red lines denote fault scarps with suspected or demonstrated neotectonic movement (extracted from the Geoscience Australia neotectonics database, January 2010). Inset shows a borehole-constrained geologic section across the Danyo Fault (adapted after Nott 1989). Note that base of Neogene is faulted, while upper Neogene is warped. This structure is likely to be mimicked beneath the Iona and Neckarboo Ridges.*

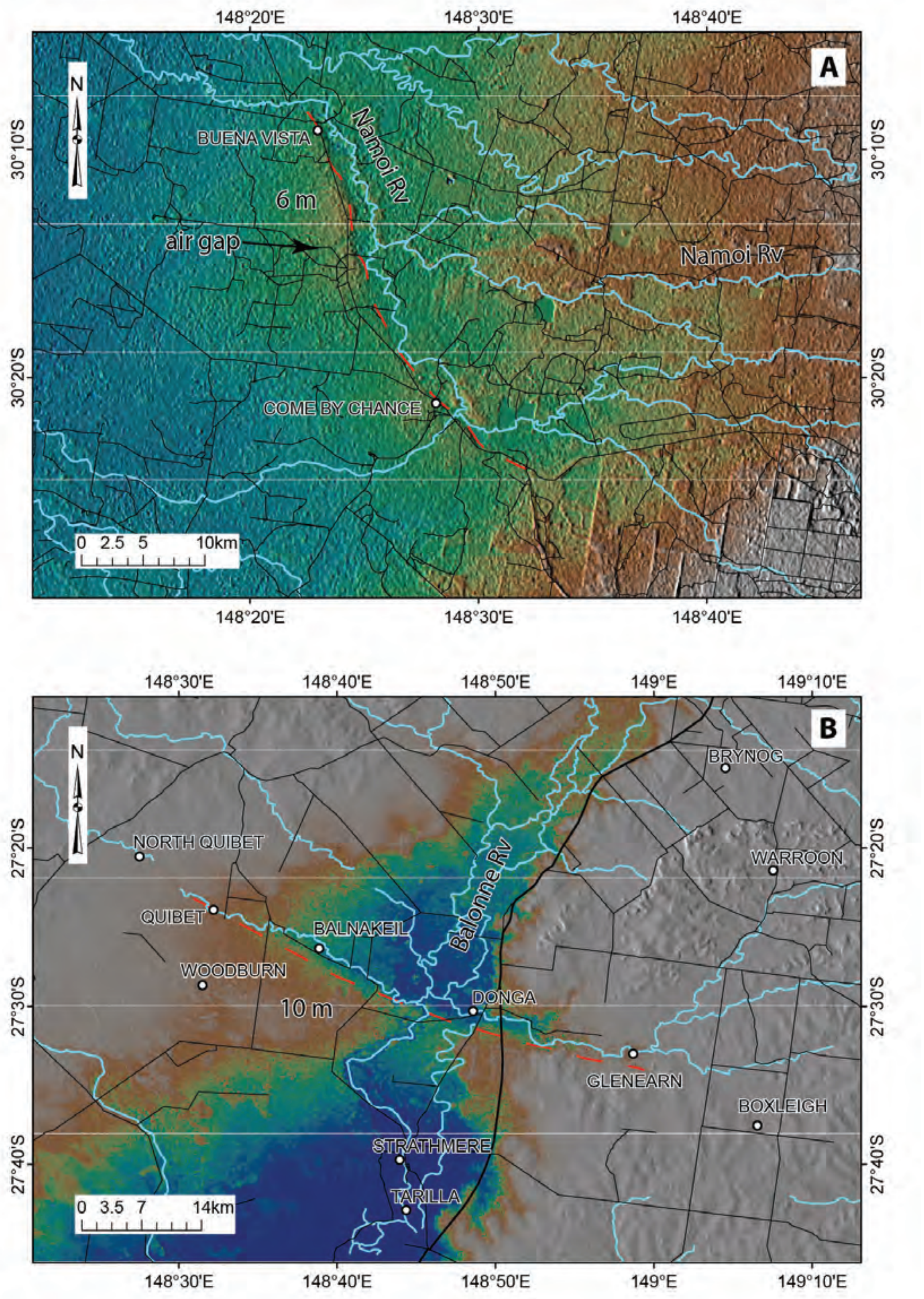

***Figure 18** – 90 m resolution SRTM DEM over two Murray Basin scarps. (a) Walgett scarp indicated by red dashed line. Note Namoi River diversion, air gap and that uplift height diminishes to the west away from the scarp (a triangular displacement profile). This suggests that the uplifted area is underlain by a southwest dipping reverse fault. (b) Balonne River scarp (Condamine Creek scarp) indicated by red dashed line. Uplifted ridge developed in Balonne River alluvium. Displacement profile is again suggestive of a southwest dipping reverse fault.*

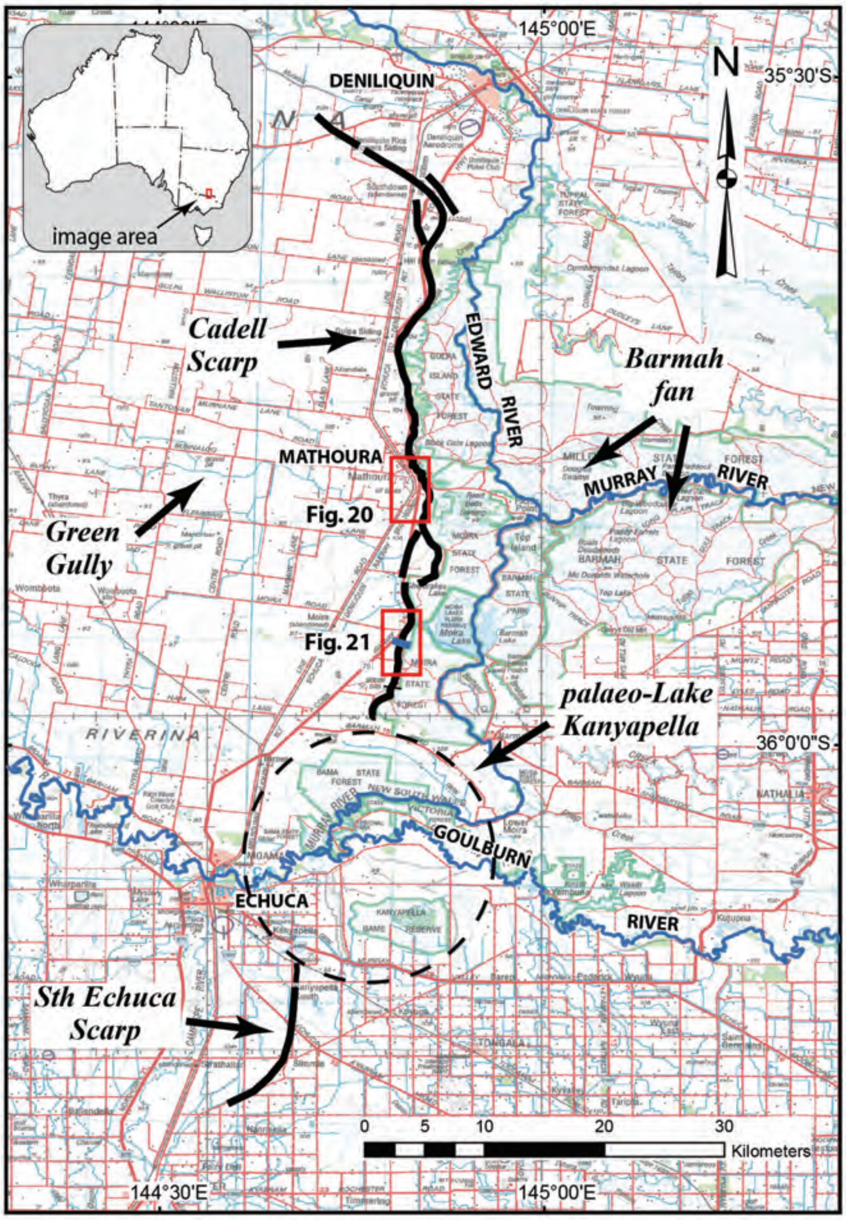

Figure 19 *– (inset) Location of the Cadell Fault in the Murray Darling Basin and (main) detailed scarp location map showing the current configuration of the major rivers. Prior to uplift of the western side of the Cadell Scarp the Murray River flowed westward across the scarp at Mathoura. After initial diversion, the Murray is thought to have occupied the course of the Edwards River. Perhaps as little as 500 years ago the course changed to its current location, probably as the result of non-seismic avulsion (Stone 2006).*

across a 50° west-dipping fault. This additional ~ 30 m of slip appears to have occurred largely in a discrete episode during the Pliocene sea-level high stand. Pronounced temporal clustering of events is implied, with long periods of inactivity separating short periods of scarp building (Clark *et al.* 2007). Borehole data across the scarp at the latitude of palaeo-Lake Kanyapella (approximately 15 km south of the seismic line, see Figure 19) indicate ~ 25 m of vertical displacement across the base of the late Pliocene – Quaternary Shepparton Formation (Tickell & Humphrys 1987).

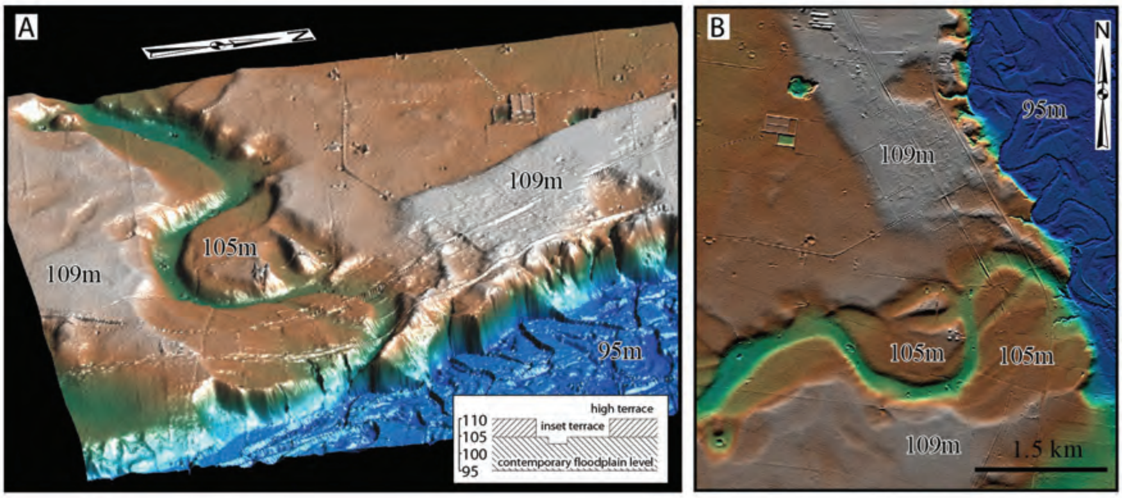

Figure 20 *– 2m resolution LIDAR DEM data over the Murray River palaeo-channel (Green Gully). Note inset terrace at an elevation 4 m lower than the highest terrace. This elevation change potentially reflects a large earthquake event. The contemporary floodplain is 10 m lower than the inset terrace, implying further seismic events. Mathoura township exists below the northern-most 109 m label.*

Neotectonic faults in the highlands of central Victoria, to the south of the Murray Basin, share similar characteristics to Murray Basin faults (Figure 17). For example, the Cadell Fault emerges from cover to the south as the Heathcote Fault Zone, which is expressed as a prominent ridgeline corresponding to the elevated hanging-wall of the west-dipping Mt Ida/Mt William thrust faults (Gray *et al.* 1991). Similarly, the Avonmore/Meadow Valley, Whitelaw, Sebastian, Leichardt and Leaghur Faults emerge from the Murray Basin as prominent scarps developed in Lachlan Fold Belt basement rocks (Canavan 1988; Kotsonis & Joyce 2003a; Kotsonis & Joyce 2003b; Holdgate *et al.* 2006).

In southwest Tasmania, the Miocene/Pliocene marine unconformity that marks the onset of the neotectonic era (Dickinson *et al.* 2002; Sandiford *et al.* 2004) is exposed onshore by virtue of the slow northward tilting of the continent (Sandiford 2007). This surface, denoted the Henty Peneplain (e.g. Colhoun 1985), is locally developed in Pliocene sediments which are displaced vertically by ~ 80 m across a ~ 45 km long section of the D'Aguilar Ranges Fault (Baillie *et al.* 1985; Houshold *et al.* 2008) (Figure 22a). Further east, the Lake Edgar Fault is associated with a prominent 30 km long and up to 8 m high scarp developed largely in periglacial alluvium and colluvium (Figure 22b). Three events of M_w 6.8-7.0, involving between 2.4 m and 3.1 m of vertical uplift per event, are constrained by OSL dating of uplifted river terraces to have occurred on this fault in the last 60 ka, with an average slip rate of 0.11-0.24 mm/yr (Clark *et al.* 2010). The little studied Lake Echo (Fairbridge 1948) and Gell River (McCue *et al.* 2003) scarps attest to the potential for large earthquake occurrence in central Tasmania.

Very few neotectonic features are known from the northeast of Australia, and most of these are less than convincing (Figure 23). The progressive depression of the northern margin (Sandiford 2007), often deep regolith cover, and in the far east relief combined with dense vegetation cover, may play a part in low scarp preservation and discoverability. However, shallow or exposed bedrock or duricrust is sufficiently common to suggest that the paucity of features may be an accurate reflection of the neotectonic environment.

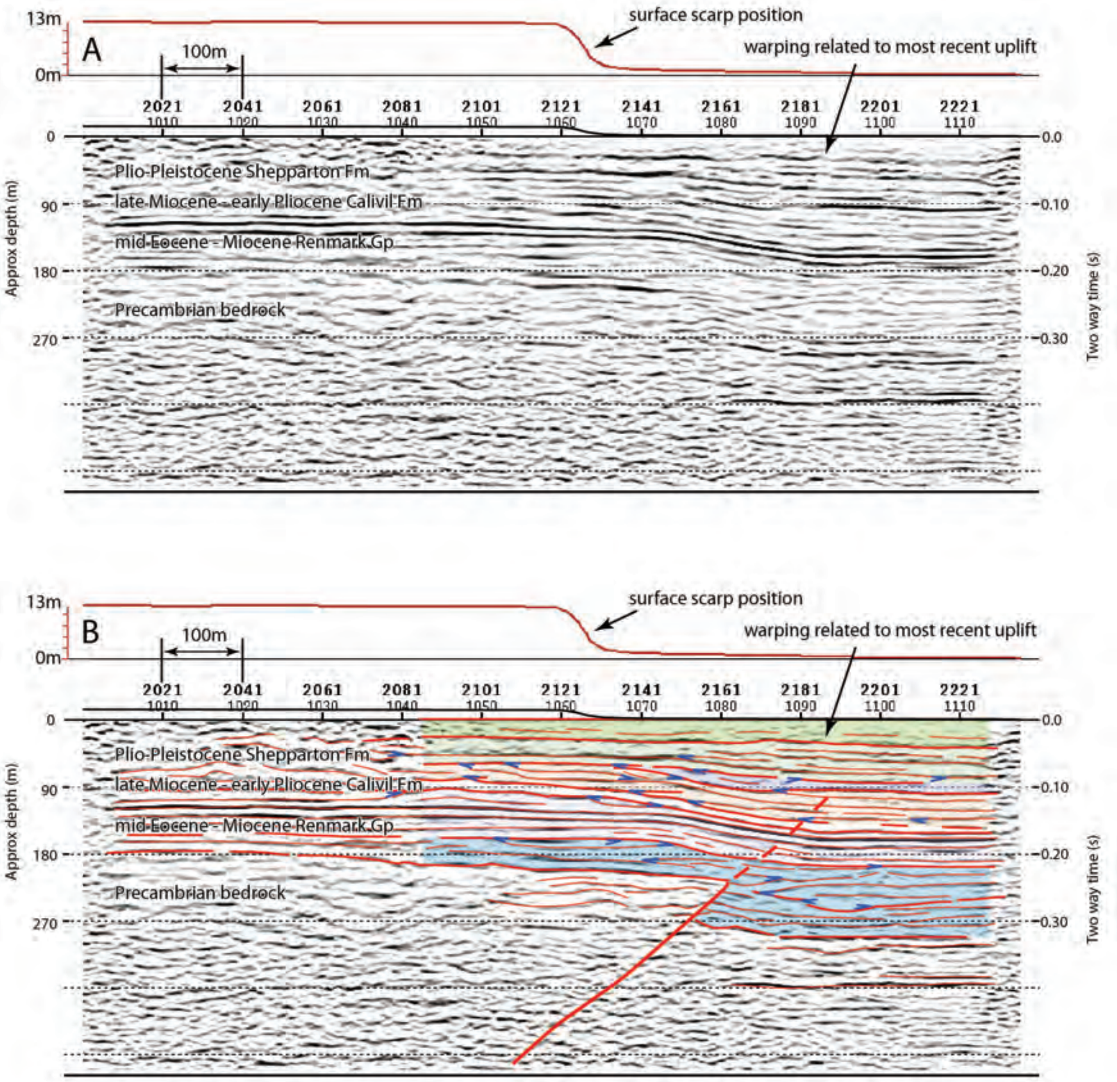

***Figure 21** – East-west seismic reflection profile over the central Cadell Scarp, shot with 10 m geophone spacing (Geoscience Australia, unpublished data). Note that scarp has retreated ~400m from the projection of the intersection of the fault tip with the surface as the result of fluvial erosion. Expression in the upper section is of a fault propagation fold. The Renmark Group/Calivil Formation boundary approximates the start of the neotectonic era.*

Two prominent scarps relating to the Palmerville Fault, arranged in an *en echelon* pattern, occur on the strandplain of Princess Charlotte Bay in northeast Queensland (Figure 24). The southernmost of these scarps is in the order of 40 km long and appears to displace Plio-Pleistocene residual sand deposits (Blewett & Wilford 1996) by 20 m vertically. The 36 km long northern scarp is also associated with 20 m of relief. However, Quaternary alluvial and coastal deposits have obscured residual sand deposits on the downthrown block at this location, so the displacement estimate may be treated as a minimum. Depositional discontinuities in Quaternary barrier dune ridges suggest that the transgressing seas of both Pleistocene and Holocene age encountered terraces relating to the Palmerville Fault zone (Burne & Graham 1995).

Near to the tip of Cape York, the inferred Vrilya Fault offsets a laterite developed in Cretaceous rocks (Figure 23). Laterite in the region of the Vrilya Fault has been mapped as Pliocene in age (Gibson & Smart 1973), but it is not known whether the laterite displaced by the fault is of this age (Colin Pain, pers. comm., 2006). A linear range front behind Rockhampton (Dee Range Fault) and an ENE-trending geophysical lineament at the mouth of the Fitzroy River (Fitzroy lineament) have

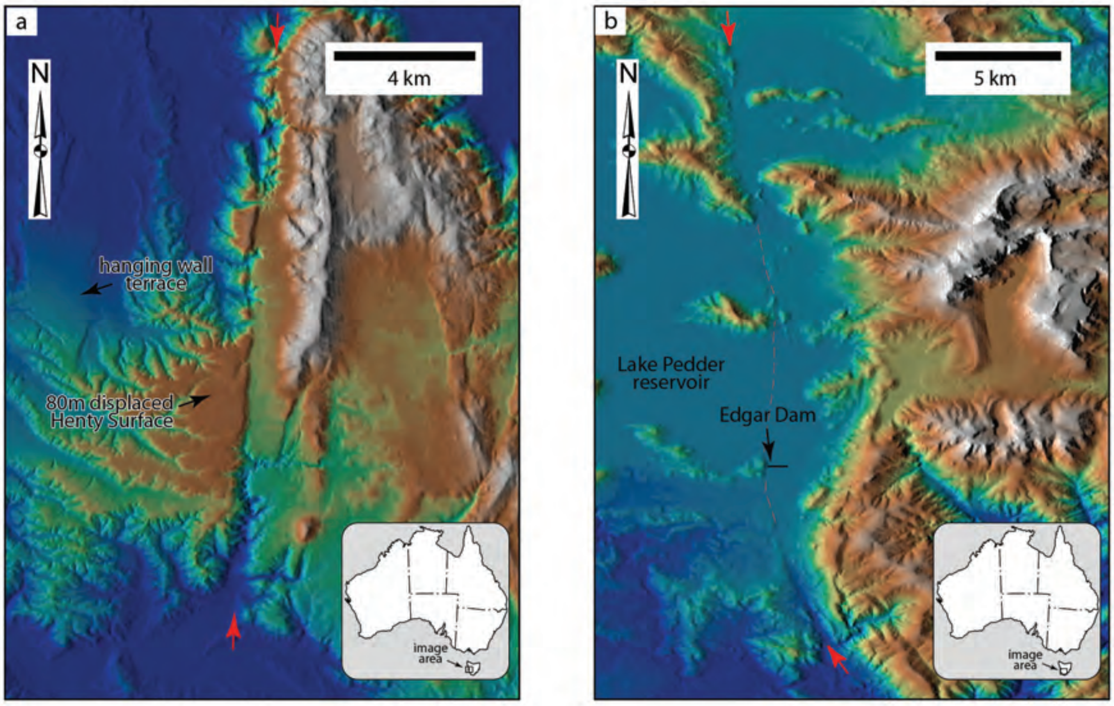

Figure 22 *– (a) SRTM 3 arc second DEM over the D'Aguilar Ranges scarp near Birches Inlet, SW Tasmania. Note that the southern part of the scarp displaces a planation surface developed in Pliocene sediments by up to 80 m. (b) 30 m DEM over the Lake Edgar Fault showing termination of bedrock ridges at the fault trace. The DEM is not of sufficient resolution to show the fine detail of the terraces dated by Clark et al. (2010), nor other subtle scarp features important for interpretation of its earthquake rupture behaviour.*

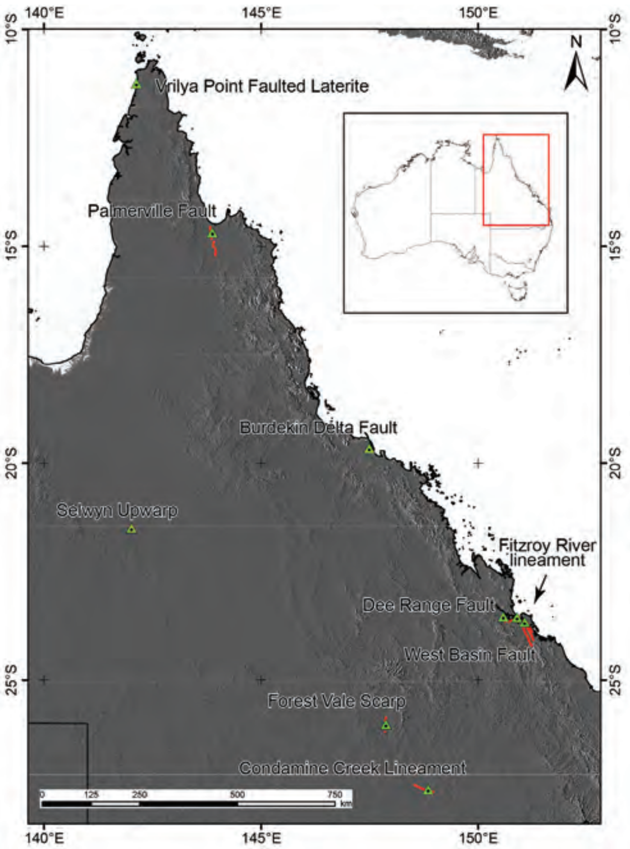

Figure 23 *– Potential neotectonic features in northeastern Australia. Background image is the 90 m SRTM DEM. See Figure 18b for a map of the Condamine creek lineament, and Figure 24 for a map of the Palmerville Fault.*

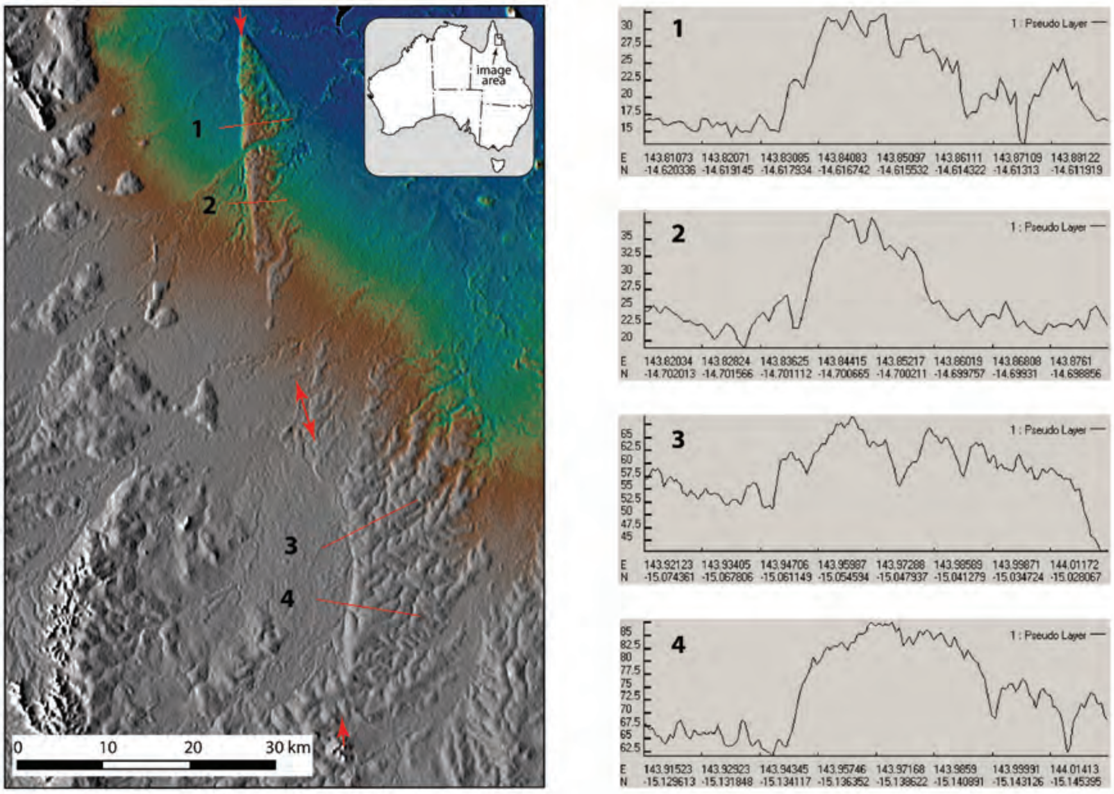

***Figure 24** – The Palmerville Fault scarp in northeast Queensland. Left: SRTM 3 arc second DEM over the northern Palmerville Fault where it goes offshore into Princess Charlotte Bay. The scarp here is developed in indurated residual sands of probable Pliocene age. The scarp strongly influences Holocene and Pleistocene dune patterns. Right: Topographic profiles across the Palmerville Fault scarp. Location of profiles shown in left panel.*

been interpreted to be underlain by active faults on the basis of an association with seismicity (McKavanagh *et al.* 1993; McKavanagh *et al.* 1994). The Western Basin Fault near Gladstone was identified as a fault of interest by virtue of an association with Quaternary sedimentation (Amy Brown, pers. comm., 2002). Twidale (1966) interpreted a Cenozoic change in stream morphology with time to the west of Mt Isa as reflecting broad scale northward tilting. This feature was denoted the Selwyn Warp. Further study is required to reconcile the potential for neotectonic movement with the northward tilting of the continent (Sandiford 2007).

The inventory of neotectonic faults in eastern Australia is likely to be highly incomplete as the result of relief reducing discoverability, and/or high erosion rates. However, of those known, spatial associations are locally apparent. Faults are arranged in north-south to northeast-southwest complexes up to 100-150 km long that are offset in an *en echelon* fashion from neighbouring complexes. Examples are provided by the Neckarboo, Danyo and Iona Ridges (Figure 17), the Khancoban-Yellow Bog and Lake George Faults, and the Lapstone Structural Complex (Figure 16). This style changes to reasonably closely spaced north-trending faults in central Victoria, and to highly interconnected, closely spaced networks of faults in the Mesozoic basins of southern Victoria.

MESOZOIC BASINS AND EXTENDED CONTINENTAL CRUST

Australia's passive margins are fringed by extended continental crust resulting from the Mesozoic break-up of the super-continent Gondwana (Veevers 2000). In most places this crust is submerged and so might not easily be examined in terms of palaeoseismic record. However, Mesozoic extensional basins which preserve rich neotectonic records are exposed onshore in the southeast (Gippsland and Otway Basins) and along the western margin (Perth and Carnarvon Basins) of the continent. Neogene inversion of Mesozoic to Tertiary basins in southeastern Australia has resulted in the formation of upland systems such as the Otway and Strzelecki Ranges which are defined at the surface by Pliocene to Quaternary broad anticlines, monoclines, synclines and rare reverse faults (e.g. Figure 25) (Hill *et al.* 1994). On the northern flanks of the Otway Range, in southern Victoria, the remnants of a Pliocene strandplain rise ~ 120 metres over a series of ENE trending faults and monoclines to elevations of ~ 250 metres (Sandiford 2003b, a; Sandiford *et al.* 2004; Wallace *et al.* 2005) (Figure 25). Along with its correlatives in the Murray and Gippsland Basins (Holdgate *et al.* 2003; Wallace *et al.* 2005), this strandplain developed during falling sea levels following a 6 Ma high stand at ~ 65 m above present day sea level (Brown & Stephenson 1991), implying almost 200 m of fault-related tectonic uplift. Displacement of Neogene strata in the Otway Ranges has accumulated in the last 5-6 Ma (Sandiford *et al.* 2004) giving time averaged displacement on bounding faults of ~ 40- 50 m/Ma (Perincek & Cockshell 1995; Quigley *et al.* 2010). However, it is possible that these rates are not representative of current displacement rates, given evidence for a major pulse of deformation in the Otway Ranges that is constrained to have occurred between *ca.* 2-1 Ma (Sandiford 2003a).

Given the above-mentioned potential for episodicity the following estimates of slip rate, based upon displacement of Miocene strata, Pliocene strandlines, or Newer Volcanic flows of Pliocene and younger age, must be treated with appropriate caution (Clark & McPherson 2009) (Figures 25 and 26): Avalon Fault (~ 6 m/Ma), Bambra Fault (~ 4 m/Ma) (Tickell *et al.* 1992), Barabool Fault (~ 20-30 m/Ma), Castle Cove Fault (> 6-12 m/Ma), Colac Fault (~ 10-25 m/Ma), Cooriejong Monocline (~ 5 m/Ma), Curdie Monocline (~ 10-20 m/Ma), Curlewis Monocline (~ 4 m/Ma), Fergusson Hill anticline (~ 23-58 m/Ma), Johanna Fault (> 7-13 m/Ma), Lovely Banks Monocline (~ 35 m/Ma), Pirron-Yallock Monocline (~ 5-13 m/Ma), Rowsley Fault (> 55 m/Ma), Selwyn Fault (~ 50 m/Ma) (Janssen 2001), Simpson Anticline (~ 5-13 m/Ma). It is also likely that the Torquay Fault has a significant neotectonic slip rate as it bounds the southern margin of the Otway Ranges. Numerous other structures are likely to have hosted neotectonic displacement in this complex region (e.g. Perincek & Cockshell 1995). However, no palaeoseismicity data exists for single earthquakes due in large part to a predominance of folding, as opposed to discrete faulting at the surface (e.g. Edwards *et al.* 1996) (Figure 25b & c), perhaps combined with relatively little deformation in the last 1-2 Ma (c.f. Sandiford 2003a). A handful of fault exposures are known, but these are observed to displace only Pliocene lithology at the surface and hence offer no insight into the Quaternary faulting history [e.g. Barabool Hills Fault (Gibson & Boston 2008, Day 5 Stop 6) (Figure 26 inset), unnamed fault near Aire Valley (Edwards *et al.* 1996, excursion Stop 38)].

Neotectonism in the Gippsland Basin has a similar expression to the Otway Basin, with folding being more common than faulting at the surface (Gloe 1960; Beavis 1975; Barton 1981; Dickinson *et al.* 2002; Sandiford 2003b). In the onshore basin, coal deposition ceased as a result of late Miocene compression (Holdgate *et al.* 2007). On structural highs, the uppermost coal seam (the Yallourn Seam) is overlain by the same Late Pliocene unconformity that denotes the onset of the neotectonic era offshore. The eroded subcrop surface of the coal seams was buried < 5 Ma ago by a series of 10–40 m thick outwash fan deposits known as the Haunted Hill Formation (HHF) (e.g. Bolger 1991; Holdgate *et al.* 2008). Slip rate estimates slightly in excess of those of Otway Basin

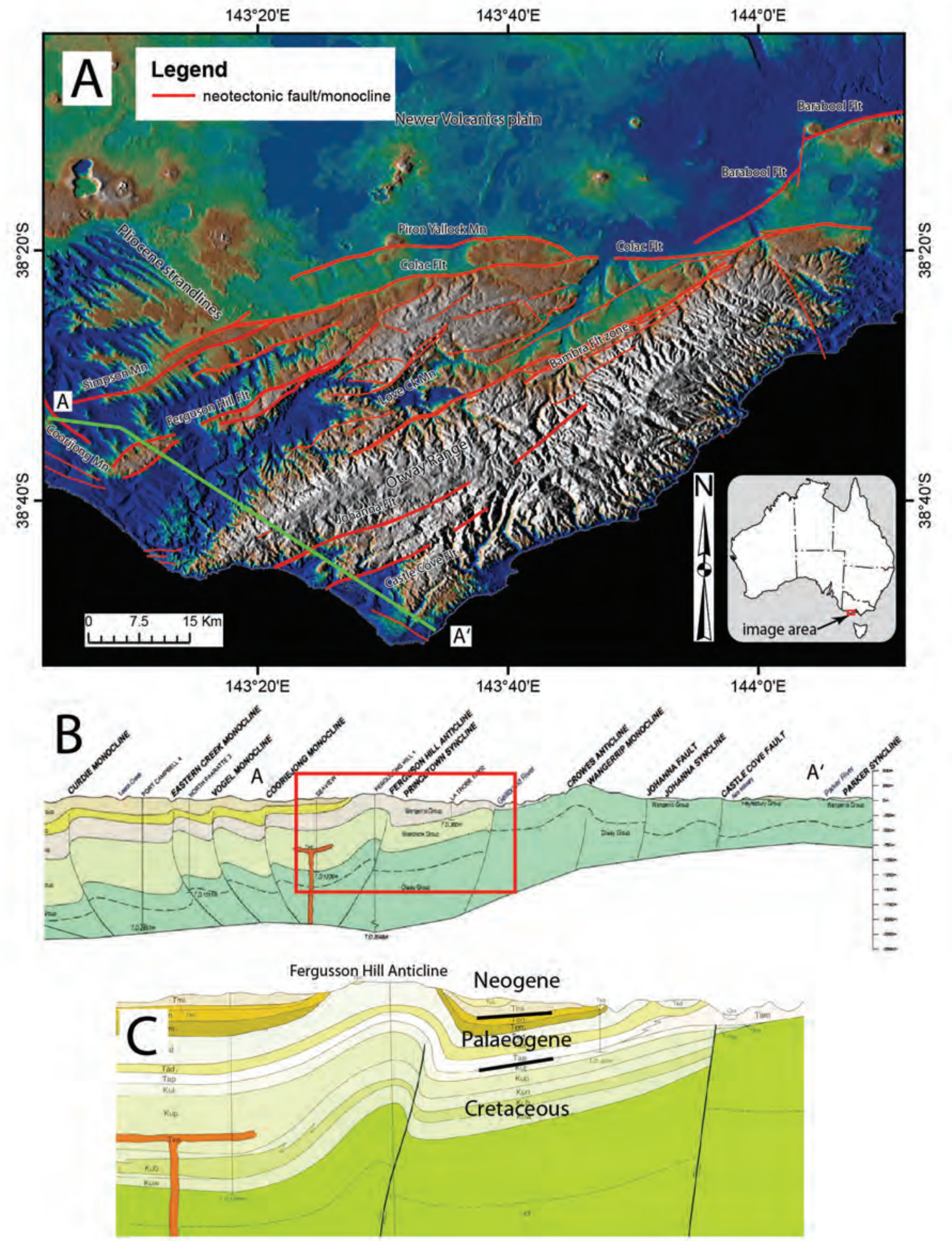

Figure 25 – Neotectonics of the Otway Ranges, southeast Otway Basin. (a) 90 m SRTM DEM over the Otway Ranges showing surface trace of major neotectonic faults and monoclines. Note Pliocene strandlines (Hanson Plain sand) are uplifted across the Simpson and Fergusson Hill monoclines, providing a datum for slip-rate estimation. Newer Volcanics flows provide a similar datum in the east of the ranges. (b) NW-SE cross section through the Otway Ranges showing inverted rift basin structure (after Edwards et al. 1996), (c) detail of stratigraphy folded over the Fergusson Hill Anticline (after Tickell et al. 1992). The base material in parts (b) and (c) is © State of Victoria, Department of Primary Industries, 1996 and 1992, respectively. Reproduced with permission. Note that while most Neogene units have eroded from the anticline crest there are remnants of originally flat-lying Pliocene Hanson Plains sand (Tpb) on the crest and within syncline to the southeast.

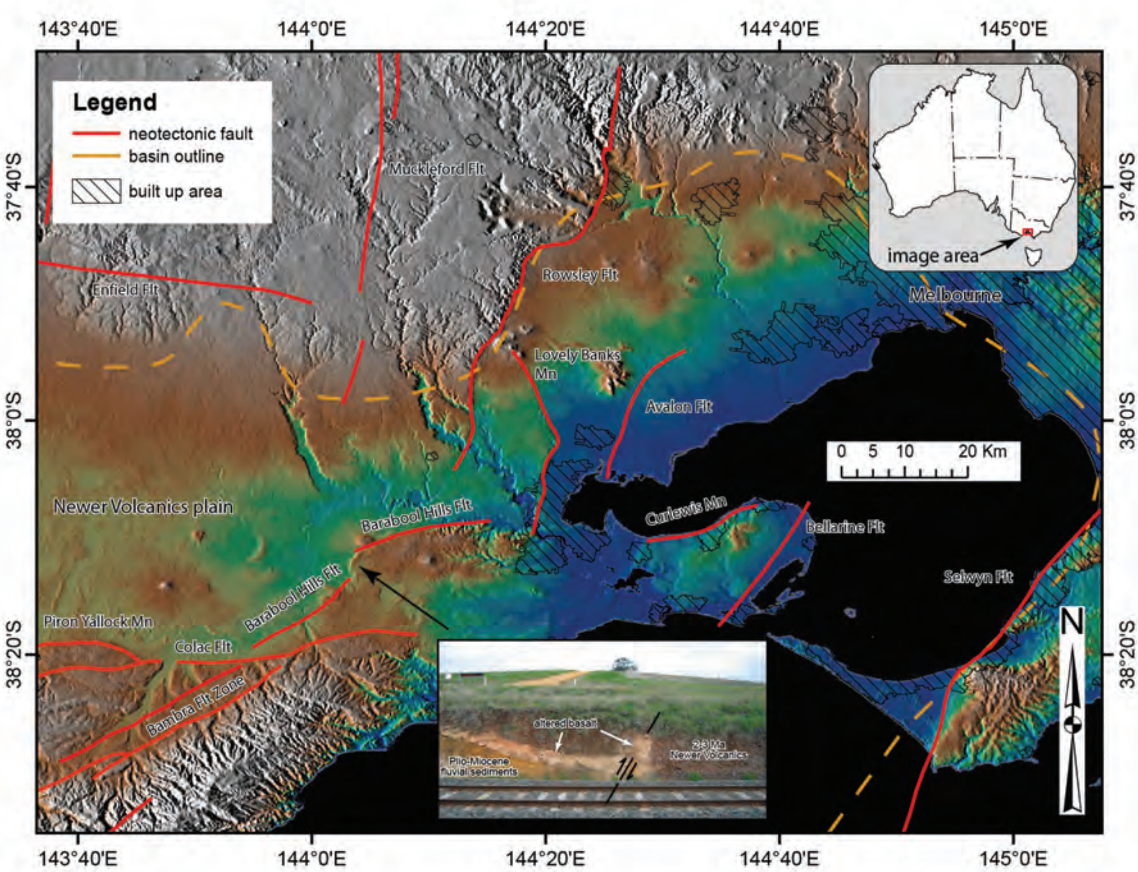

Figure 26 *– 90 m SRTM DEM showing neotectonic deformation of the eastern Otway Basin. Newer Volcanics flows, perhaps 2-3 Ma old (Gibson 2007), are extensively folded and faulted. Inset shows faulted Newer Volcanics associated with the Barabool Hills Monocline near Winchelsea (38°13'48.35"S, 144°03'5.53"E).*

faults (~ 65 m/Ma) have been obtained from the preliminary results of cosmogenic radionuclide burial and exposure dating of Haunted Hill Formation gravels folded over the Snake Ridge and Morwell Monoclines (Geoscience Australia, unpublished data, Figure 27, Figures 28a,b). The slip rate on the basin-bounding Yallourn Fault, also based upon CRN dating of uplifted HHF gravels, is > 63 m/Ma (Figure 28c). The base of the Haunted Hills Formation is seen to be vertically displaced by ~ 30 m across the Yallourn Monocline at the eastern end of the Yallourn North open cut mine (Dickinson *et al.* 2002) (see Figure 28b), although the age of the unit is not known at this locality precluding a slip rate estimate.

A northerly dipping thrust fault, superposing Jurassic sediments over the Latrobe coal seam by ~ 85 m, and perhaps also the HHF, was exposed briefly over a length of ~ 330 m during mining in the western end of the same pit (Gloe 1960, Figure 13). The Yallourn Monocline is again faulted near to where it is truncated by the Haunted Hills Fault (see Figure 27, 26b). Drilling beneath the site of the Yallourn power station identified a discrete fault trace relating to the Yallourn Fault that displaces the Oligocene Latrobe coal seam by 160 m (Beavis 1975). Based upon the drilling results, the Pliocene unconformity surface underlying the HHF at this location was not interpreted to be significantly displaced (Dickinson *et al.* 2002, Figure 15), suggesting that much of this deformation pre-dates the deposition of the HHF, and perhaps the neotectonic era. However, given the relatively young HHF ages obtained from the Morwell Monocline and Snake Ridge Monocline (630±63 - 1200±430 ka, Geoscience Australia, unpublished data, Figure 28a, b), significant deformation might have accrued on this fault in neotectonic times.

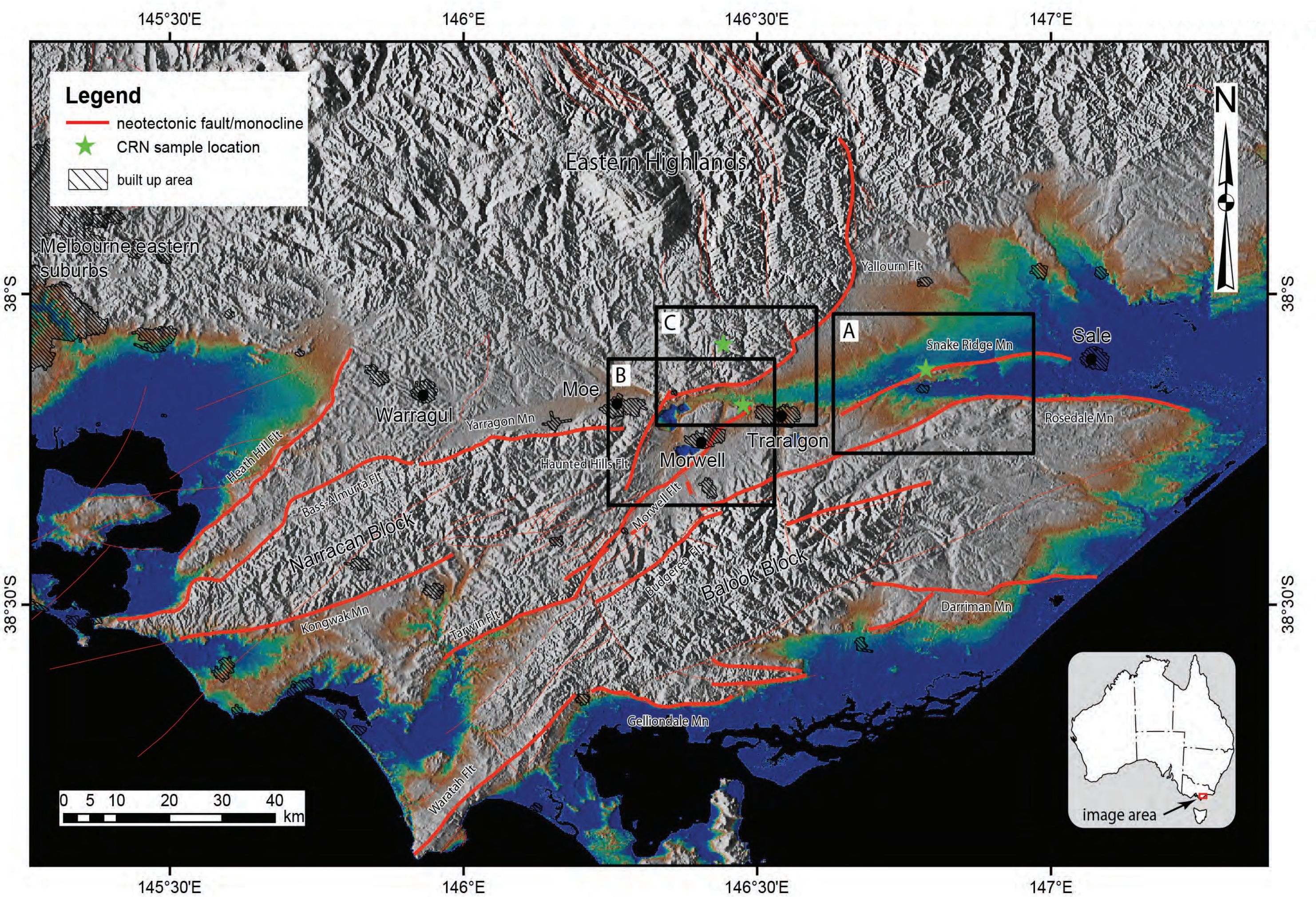

Figure 27 – 90 m SRTM DEM over the onshore Gippsland Basin showing major neotectonic faults and monoclines. The landscape is underlain by an inverting basin architecture similar to that in the Otway Basin (c.f. Figure 25b). CRN sample locations are shown with green stars. Frames marked A, B, & C refer to Figure 28. The three major open cut coal mines, Yallourn, Hazelwood and Loy Yang, appear as blue polygons in the DEM.

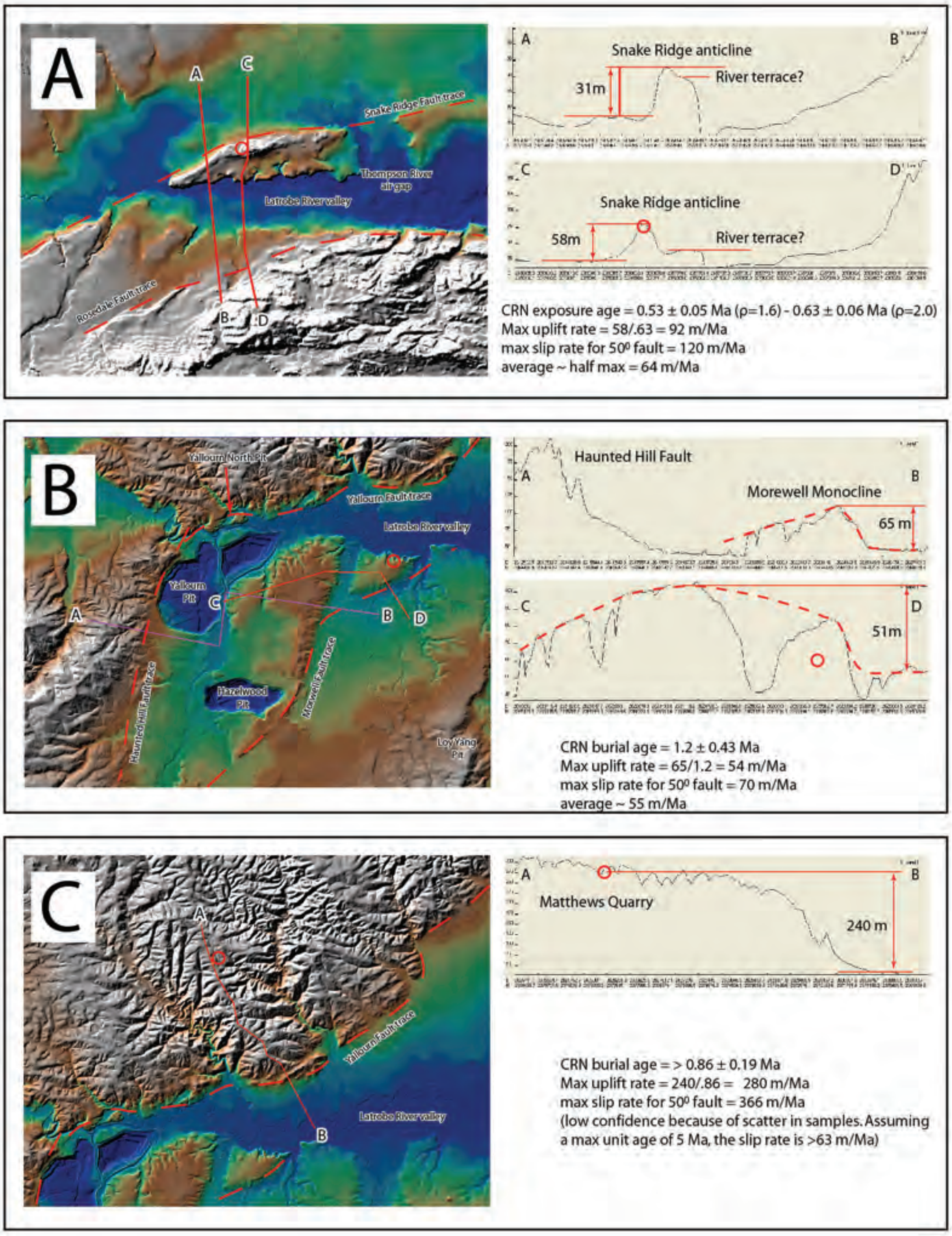

***Figure 28** – Context of onshore Gippsland Basin CRN samples (marked with open red circles). Locations of panels are shown in Figure 27. (a) 20 m DEM over the Snake Ridge Monocline. The Latrobe River cuts a shallow E-W oriented canyon through the uplifted block. A wind-gap relating to a former course of the Thomson River occurs near the eastern edge of the ridge. (b) 10 m DEM over the Morwell Monocline and Haunted Hills Fault. Morwell fault trace position is derived from SEC borehole data (Guy Holdgate, pers. comm., 2009). Note narrow canyon that the Latrobe River has cut through the uplifted block relating to the Haunted Hill Fault. Northern and southern pits relate to the Yallourn and Hazelwood open cut coal mines, respectively. (c) 10 m DEM over the Yallourn Fault trace. The geology on the north side of the Yallourn Fault is dominated by Lachlan Fold Belt basement rocks. However, remnants of Cretaceous Gippsland Basin rocks and Haunted Hill Gravels occur close to the fault trace (VandenBerg 1971).*

Extensive normal faulting of the HHF overburden is evident in the Loy Yang Dome region (Figure 29a, see Figure 28b for location – the Loy Yang Pit is excavated into the Loy Yang Dome), and is also reported from face of the Morwell Monocline (Gloe 1960; Barton 1981) and Yallourn North open cut (Gloe 1960). In the case of the Morwell Monocline, surface normal faulting is interpreted to relate to flexure on the crest of the monocline in response to reverse faulting at depth (Barton 1981) (Figure 29c). This hypothesis plausibly accounts for the normal faulting seen at Yallourn and Loy Yang, as reverse faulting is known from deeper in both sections (e.g. Beavis 1975) (e.g. Figure 29b).

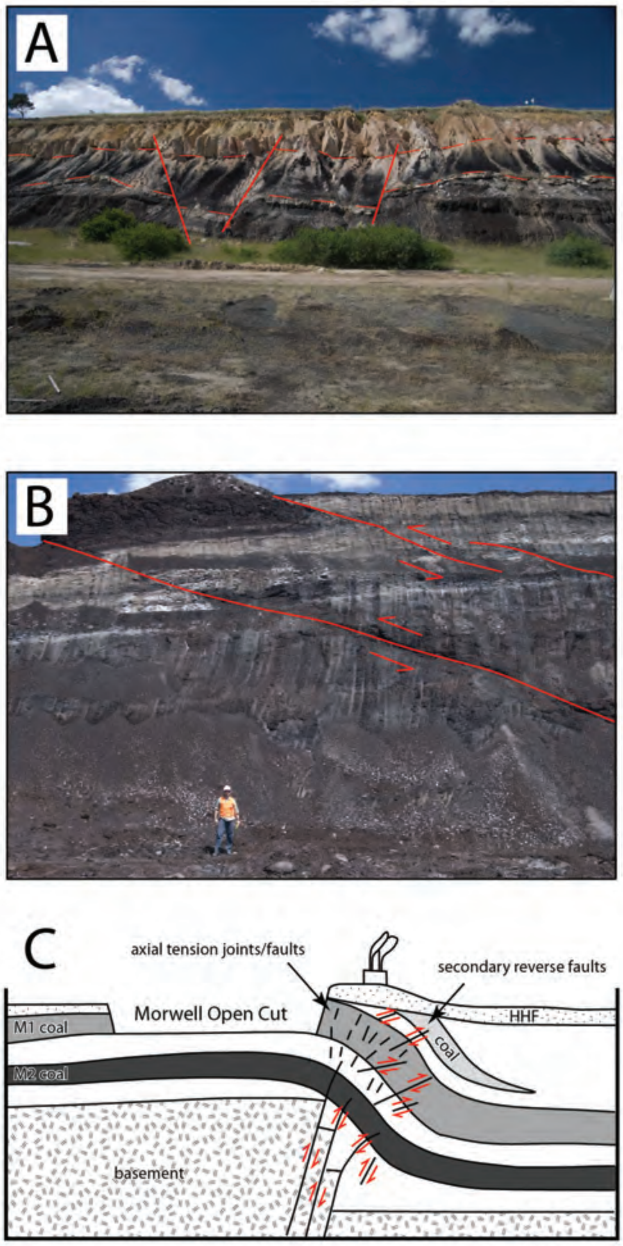

Figure 29 *– Style of Gippsland Basin neotectonic features. (a) southern batters of Loy Yang open cut mine showing normal faulting displacing the base of the HHF. (b) secondary reverse faulting within Loy Yang Open cut mine at a deeper structural level than (a). (c) schematic structural section based upon the Morwell open cut mine (after Barton 1981) tying together shallow and deep observations. It is proposed that this section is relevant to most monoclines in the Latrobe Valley.*

Long-term slip rate estimates for the Gippsland Basin are subject to the same uncertainty as those in the Otway Basin stemming from apparent episodic pulses of regional deformation. The parallelism and conformable nature of most Pliocene strandlines across Victoria has been taken as evidence for very little tectonism in the interval 6-3 Ma (Wallace *et al.* 2005). In the eastern onshore Gippsland Basin an angular unconformity between the Jemmy's Point formation (Pliocene) and the overlying Haunted Hill Formation (late Pliocene to Quaternary) suggests significant post 3 Ma deformation. Seismic reflection evidence combined with palynological age constraint suggests that a major episode of deformation involving folding ceased at 1.0 Ma in the offshore Gippsland Basin while continuing onshore until approximately 0.2-0.25 Ma (Holdgate *et al.* 2003). Based upon this chronology, the same authors estimated an uplift rate of 50-80 m/Ma for the Rosedale Fault over the interval 1.5-0.25 Ma, which equates to a slip rate of < 105 m/Ma for a 50° dipping fault. Assuming constant slip from 1.5 Ma to present, the rate becomes 88 m/Ma, comparable to that estimated for the Yallourn Fault. Gardner et al. (2009) obtained slip rates on the Waratah Fault (see Figure 27 for location) of 10-40 m/Ma for displacements across both 125 ka and Pliocene marine terraces, suggesting periodic rupture behaviour in contrast to the above-mentioned faults.

On the Western Australian margin, a series of asymmetric anticlines (e.g. Cape Range, Barrow Island, Rough Range, Giralia, Cape Cuvier, Cape Peron, Dirk Hartog Island anticlines) have developed as fault propagation folds above blind wrench and oblique reverse faults in the Carnarvon Basin (McWhae *et al.* 1956; Hocking 1988; Hillis *et al.* 2008) (Figure 30). The trend of the anticlines and their underlying faults changes from northwest in the southern basin through northerly in the central basin to northeast in the northern basin, in part mimicking the cratonic margin and the trends of underlying Mesozoic wrench structures (Malcolm *et al.* 1991; Keep *et al.* 2002) (Figure 30). The growth of fault propagation anticlines is generally dated as Miocene and younger (e.g. Barber 1988; Crostella & Iasky 1997; Keep *et al.* 2000; Hearty *et al.* 2002; Keep *et al.* 2002), and is typically not related to the major basin-bounding faults (as has also been demonstrated for the Darling Fault in the Perth Basin, Jakica et al. (2010)). Seismic reflection imaging suggests that the loci of reactivation are dominantly steep, flower-type structures, and that significant inversion and the formation of transpressional anticlines is restricted to one or two major faults within the flower (Malcolm *et al.* 1991; Keep *et al.* 2000; Keep *et al.* 2002).

Emerged Pleistocene marine terraces on the Cape Range Anticline (Figure 31), overlying the Learmonth Fault (Crostella & Iasky 1997, Figure 19), and anticlinal folds in offshore Plio-Quaternary sea floor sediments (van de Graaff *et al.* 1976; Wyrwoll *et al.* 1993), indicate that Neogene deformation has continued to at least the last interglacial. Faults in the entirely-offshore Browse Basin appear to be similar in character (Symonds *et al.* 1994; Keep *et al.* 2002). Evidence interpreted to suggest that the last interglacial terrace has been tectonically uplifted to the south to form the 'Cape Cuvier Anticline' (Denman & van de Graaff 1976; Veeh *et al.* 1979) has recently been challenged (O'Leary *et al.* 2008). Preliminary ^{36}Cl cosmogenic radionuclide dates from a terrace 10-15 m above present sea level on the Cape Range (the Jurabi Terrace of van de Graaf et al. (1976)) are consistent with a Marine Isotope Stage 7 (*ca.* 200 ka) age for formation of the surface

(Geoscience Australia, unpublished data). In contrast to the last interglacial (MIS Stage 5), where sea level may have reached up to 3-4 m higher than present (e.g. Zhu *et al.* 1993), sea level is not thought to have exceeded present levels during MIS Stage 7 (Siddall *et al.* 2003). This implies uplift rates on the underlying Learmonth Fault of a few tens of metres per million years, similar to faults in the eastern inverting basins. There is a suggestion in topographic profiles (Figure 31b) that this uplift is heterogeneously distributed along the western coastline of the Cape Range. A northerly dip on the cliff-base notch at the landward edge of the terraces is apparent and can be correlated for a

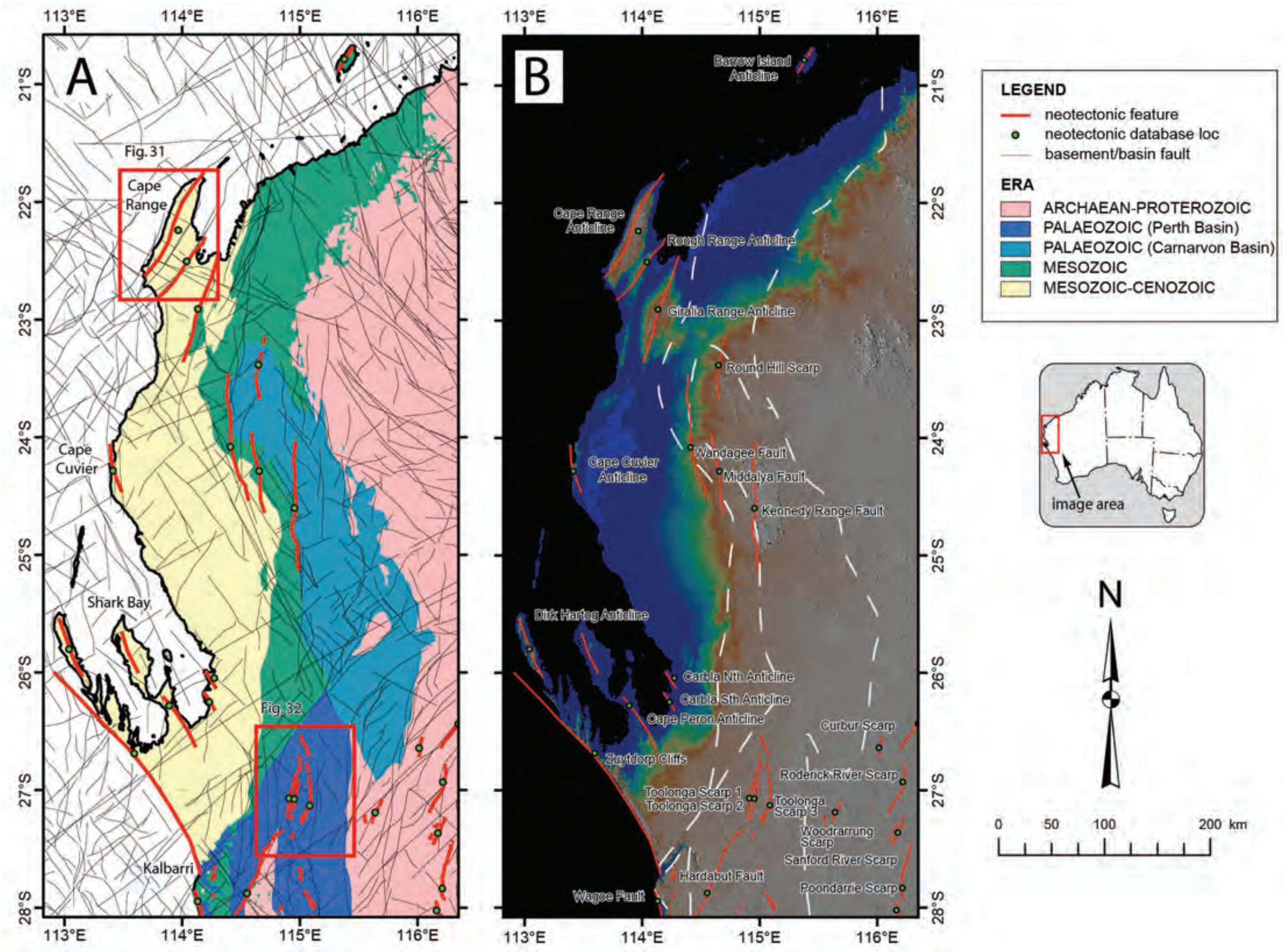

Figure 30 *– Carnarvon and northern Perth basins. (a) Surface geology age distribution, structure and neotectonics (adapted from GSWA 1:500 000 scale digital geology), and (b) 90 m SRTM DEM showing major topographic uplift relating to neotectonic inversion of Carnarvon Basin extensional structures, and general proportional elevation relationship with decreasing geologic age.*

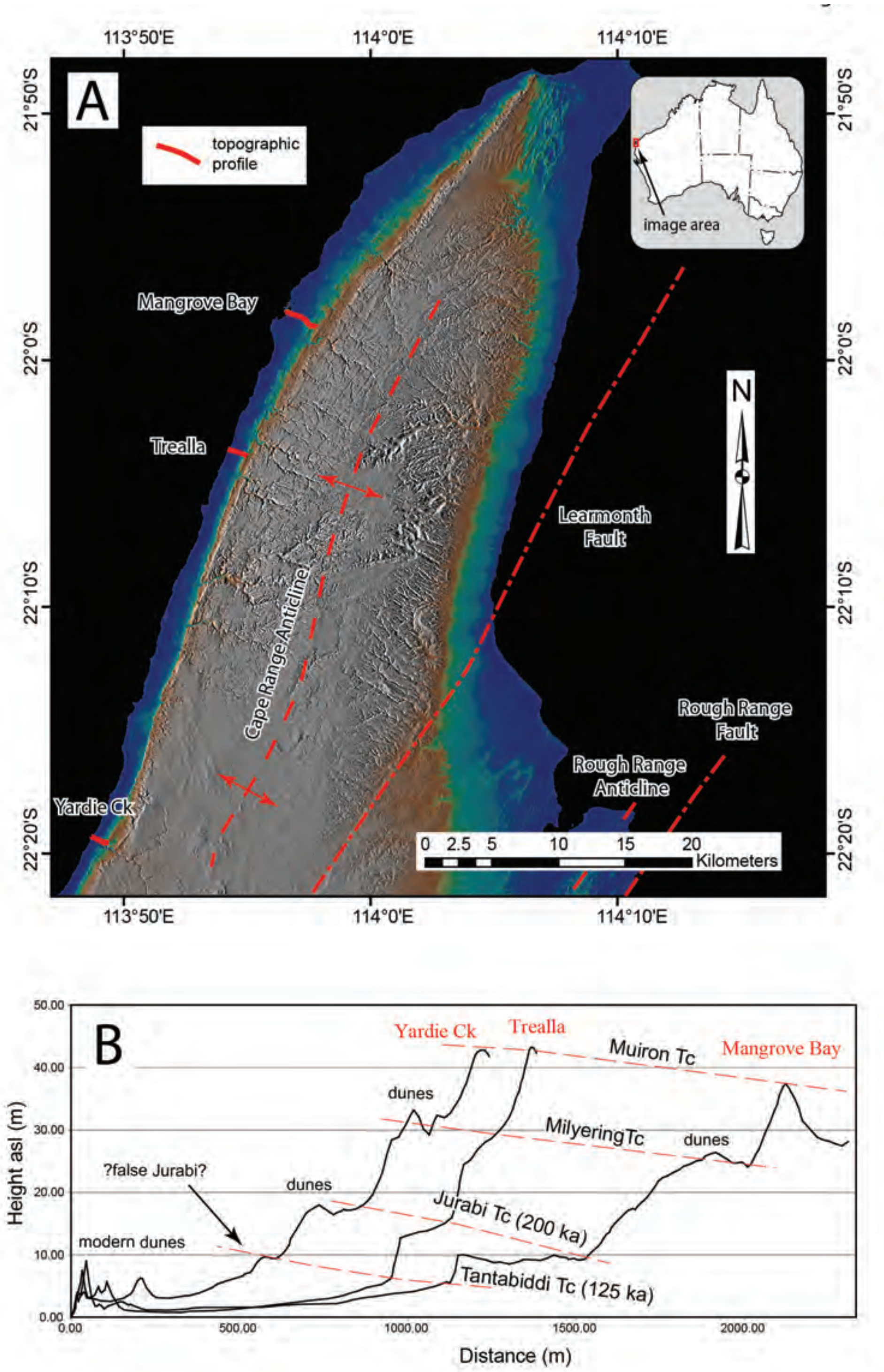

Figure 31 *– Topography and structure of the Cape Range Anticline. (a) 10 m DLI DEM data showing major structure, and position of elevation traverses. Note that anticline crest elevation decreases to the south. (b) Total station elevation traverses showing distinct wave cut terraces on the western flank of the anticline. Note apparent increase in elevation of correlative terrace surfaces to the south, consistent with anticline growth in this direction. Location of figure shown on Figure 30a.*

distance of ~ 25 km. The last interglacial surface (Tantabiddi terrace) also appears to follow this trend.

In parts of the Carnarvon and northern Perth Basins adjacent to the cratons, where structures relating to Palaeozoic extension dominate over those related to Mesozoic extension, and evidence for Neogene extension is sparse, neotectonic features appear to be intermediate in character between basin and craton features (see also Western and Central Australia section). Clusters of scarps, coinciding with mapped basement structure, occur in the Midalya/Kennedy Range area east of Cape Cuvier, and the Toolonga area east of Shark Bay (Figure 30). The Toolonga group of scarps include features greater than 60 km in length and with up to 30 m of vertical displacement (Figure 32). Regressive marine strandlines of unknown age have been uplifted across these features, with the total uplift across the fault group being in the order of 90 m (Figure 32, section A-B). If it were speculated that the ridges are early Pliocene in age (similar to the Murray Basin ridges in eastern Australia), modest surface uplift rates are obtained. The onshore Canning Basin (including the Fitzroy Trough), and the Bonaparte Basin might also be placed in this intermediate category, though only one feature is known (the Munro scarps).

The geometry of, and relationships between, neotectonic faults in the inverted basins around the margins of Australia is largely inherited from the original extensional basin architecture (e.g. Hocking 1988; Williamson *et al.* 1991; Keep *et al.* 2000; Keep *et al.* 2002) (e.g. Figure 25). Faults bound topography (e.g. the Otway, Strzelecki and Cape Ranges) (Figures 25, 27 & 31) and form interlinked anastomosing networks that extend in some cases for hundreds of kilometres. There is an indication that the level of neotectonic activity in a given inverting system bears a relationship to how long prior to compression the last major basin-structuring extensional event occurred. For example, there is a progression of increasing neotectonic activity from the parts of the Carnarvon Basin formed mainly in the Palaeozoic, to those where extension continued to the Mesozoic, and perhaps early Cenozoic (see Figure 30). Similarly, the Fitzroy Trough attained its major structural architecture in the Palaeozoic, was relatively little effected by Mesozoic Gondwana break-up, and is today less neotectonically active than parts of the Canning Basin that were involved in Mesozoic breakup (e.g. Keep *et al.* 2007, Figure 17). Similar conclusions may be drawn from extended margins around Australia (Blevin & Cathro 2008).

Australian Neotectonic domains

In the previous section the general characteristics of neotectonic features known from across Australia were explored. From this it is clear that there is regional variation in the response of the Australian continental crust to the imposed tectonic forces, and in the character of the neotectonic features that accommodate that response. For example, compare the isolated, low displacement faults of the Southwest Seismic Zone (Figure 3), the *en echelon* network of high-density, relatively high-displacement faults in the Mt Lofty and Flinders Ranges (Figure 11), the anastomosing network of highly interlinked, relatively high-displacement faults in the Carnarvon, Otway and Gippsland Basins (Figures 25, 27 & 30), and the relatively isolated, moderate to high displacement features arranged in belt-like patterns in the Murray Basin and Eastern Highlands (Figures 16 & 17). Clark & Van Dissen (2006) made a first attempt to discriminate between the characters of faults from different regions (see Table 1 for a modified version of their table). It is reasonable to assume that this variation arises as the result of the interaction between the crustal stress field (e.g. Hillis & Reynolds 2003) and continental crust of varying character. Hence, large earthquake occurrence behaviours might be extrapolated from regions rich in data to those poor in data by mapping regions of similar crustal properties, with the caveat that changing stress conditions (magnitude and

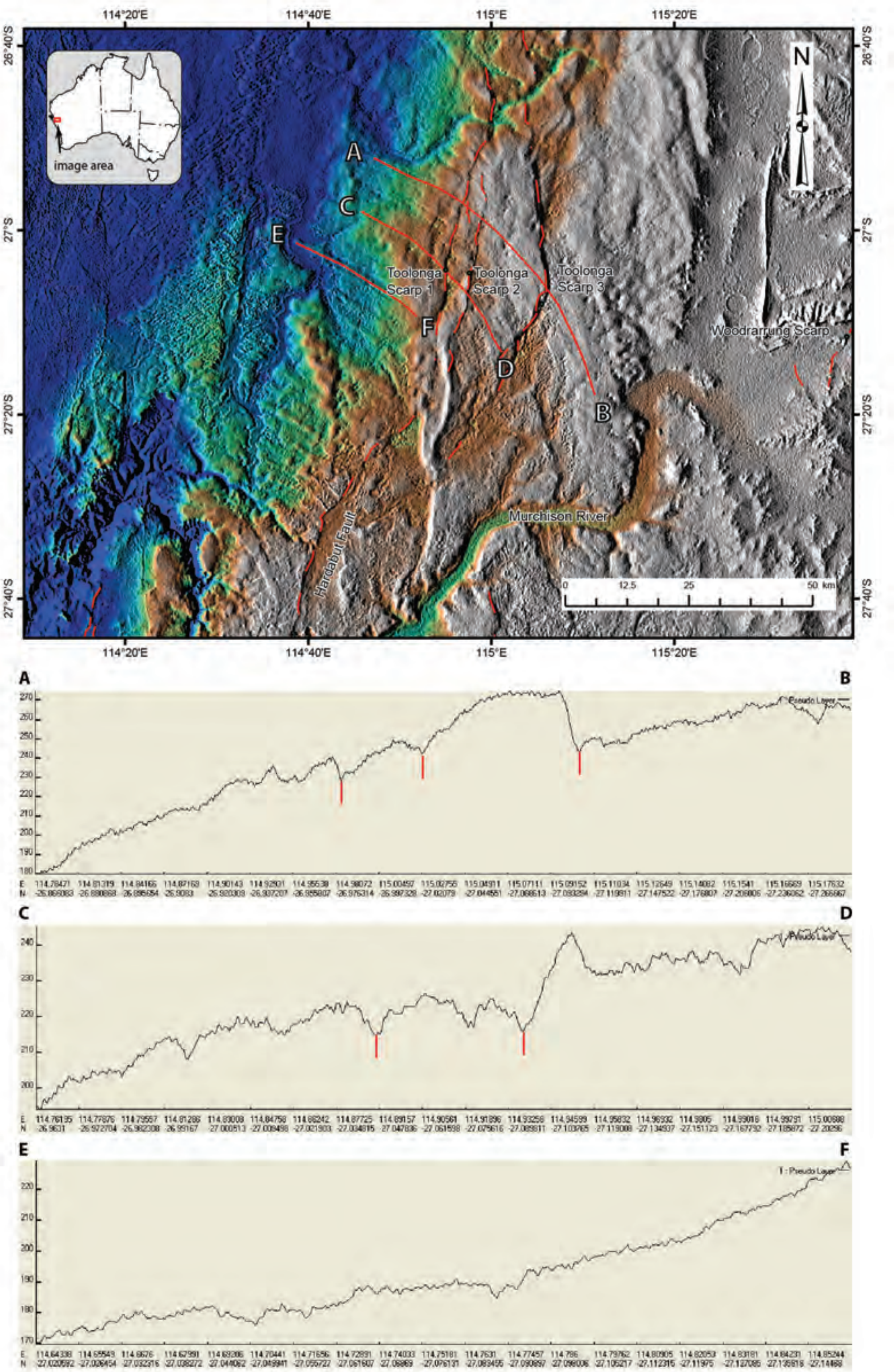

Figure 32 *– 90m SRTM DEM data over a cluster of scarps in the Toolonga region of the northernmost Perth Basin (Murchison District). Note prominent regressive strandline ridges are uplifted across the scarps. Note also that to the southwest of the image strandlines are uplifted on the up-thrown block of the Hardabut Fault, providing evidence for neotectonic movement on this feature. Location of figure shown on Figure 30a.*

***Table 1** – Subjective comparison of fault characteristics across Australia, which are used as the basis for a subjective discrimination of Neotectonic Domains.*

Neotectonic region	Western and central Australia[$]	Nullarbor	Flinders/Mt Lofty Ranges	Eastern Australia	Mesozoic extended crust
Completeness of active fault dataset	high in SW, low elsewhere	moderate to high	moderate in Mt Lofty and northern Flinders Ranges, low elsewhere	moderate to high in Victoria, moderate to low elsewhere	moderate to high in onshore settings
Number of known and suspected active faults*	~80-100	40-50	40-50 (a dozen more occur on the Eyre and Yorke peninsulas)	~40-50^	40-50
Relative density of known and suspected active faults	low	low to moderate	moderate to high	low to high (clustered)	moderate (high in Gippsland/Otway)
Relationship between active faults to building of ranges	no relation between active faults and large-scale topography, except perhaps in the Carnarvon Basin	no relation between active faults and subdued large-scale topography	ranges bound by active faults	typically no relation between active faults and large-scale topography, but locally some active faults do bound ranges	typically no relation between active faults and large-scale topography, but locally some active faults do bound ranges
Relative historic seismicity rate	moderate to high in SW, low elsewhere	very low	high	moderate (low in the north)	moderate to high in onshore settings
Relationship of historic seismicity to known active faults	concentrated where there have been historic surface ruptures, rarely associated with pre-historic fault scarps	no association with pre-historic scarps	well defined belt of high seismicity, locally associated with pre-historic fault scarps	no clear association with pre-historic fault scarps	local clear association with pre-historic fault scarps
Post ca. 10 Ma displacement on known active faults	10 m or less	10 m or less, rarely 30 m	many with displacements up to ~100-150 m	many less than 10 m, some up to 100-200 m	many less than 50 m, some up to 200 m
Number of post ca. 10 Ma ruptures on an individual fault	few (<5?)	no data (likely to be <5-10)	many (several tens or more)	few to many	many (several tens or more)
Examples	Hyden, Meckering, Lort River	Roe Plain, Mundrabilla	Wilkatana, Millendala, Burra, Para	Khancoban, Cadell, Lake George, Lake Edgar, D'Aguillar Range, Palmerville	Rosedale monocline, Fergusson Hill monocline, Rough Range Fault.

* most regions are under explored, and the level of study is not homogeneous within and between regions. For example, large areas of NW Western Australia are shown as having no active faults. This may largely be a consequence of the area having not been studied.

[$] relationships based upon the better-studied SW portion of this region

^ several features in Victoria are based upon subsurface mine records of faulted Late Tertiary (10-3 Ma) basalts, where faulting has no surface expression. Further records associate concentrations of small earthquakes with large scarps.

orientation) may modify the activity level. Clark (2006) developed these ideas and proposed a preliminary neotectonic domains model for continental Australia, in a similar way that seismicity source zones are defined upon the basis of the historic earthquake catalogue (Gaull *et al.* 1990; Brown & Gibson 2004). As part of the present study, an attempt was made to objectively derive domains by statistically analysing the data to test for geographic variance of characteristics (cluster analysis). This proved unsuccessful due to large uncertainties and spread in the data.

Below we present a revision of the Clark (2006) domain boundaries, refined through assessment of detailed geological and geophysical data (Figure 33). Essentially, we have extrapolated from areas rich in neotectonic data to areas relatively poor in data by assessing the properties of the crust (e.g. age, geologic history, geophysical signature, etc.) across the continent. For example, high resolution DEM data in the southwest corner of the Yilgarn Craton has revealed many neotectonic scarps (Figure 3). The relatively poorly exposed and poorly explored northern and eastern parts of the Yilgarn Craton, and perhaps the similarly ancient Pilbara and Gawler Cratons, might be expected to behave similarly. Following this logic, the next section details the revision of the boundaries for six onshore domains in an attempt to group the neotectonic fault data. We also present the results of a comparative analysis of three key variables (fault length, vertical displacement, and fault density), both at the key variable and domain levels. This permits us to explore an expanded neotectonics database (see Appendix Table 1) in terms of variations in parameters such as maximum magnitude earthquake (M_{max}). A seventh, entirely offshore domain is defined based upon analogue studies with the central and eastern USA (Wheeler 1995, 1996; Wheeler & Frankel 2000; Wheeler 2009b).

There remains an inherent bias in the database in that there is little data in existence for much of northern Australia. This is due to a combination of factors, relating mainly to preservation and discoverability, as detailed in previous sections. In southern Australia, bias may similarly have been introduced by not including all faults within a deforming system in the analysis, as some that have neotectonic expression are not well enough characterised to have been included (e.g. Kongwak Monocline), or were not active in the database at the time of access (blue features on Figure 33). It is important to note that all features within the database are assigned a level of uncertainty as to whether they are neotectonic faults (see Appendix Table 1). Future work will almost certainly demonstrate that some features have been misidentified and are not neotectonic. However, for the purpose of this analysis all structures in the database are assumed to have an equal probability of being neotectonic in the current stress regime.

GEOLOGICAL AND GEOPHYSICAL DEFINITION OF DOMAIN BOUNDARIES

Below, the characteristics of the seven domains are discussed, and justifications provided for the positioning of domain boundaries (see Figure 33). Continental scale geologic and geophysical datasets provided guidance in terms of the gross division of crustal units (Wellman 1976; Palfreyman 1984; Shaw *et al.* 1996; Murray 1997; Blake 2000; FrOGTech 2005), and a range of finer scale data sets were consulted to adjust domain boundaries (see below).

Precambrian Craton Domain

This domain comprises highly structured Archaean and non-reactivated Palaeoproterozoic crust that was largely cratonised prior to the Mesoproterozoic (e.g. Palfreyman 1984; Shaw *et al.* 1996). The central rift of the McArthur Basin (see Figure 33), which was cratonised in the early Mesoproterozoic (e.g. Scott *et al.* 2000), does not appear to be anomalous within this context (c.f. Johnston *et al.* 1994). The seismic character of this domain is considered to be typified by that observed for the south west of the Yilgarn Craton (Clark 2010). Scarps are typically isolated and less than 40 km long, with less than 10 m of neotectonic displacement (see Table 1, “Western and

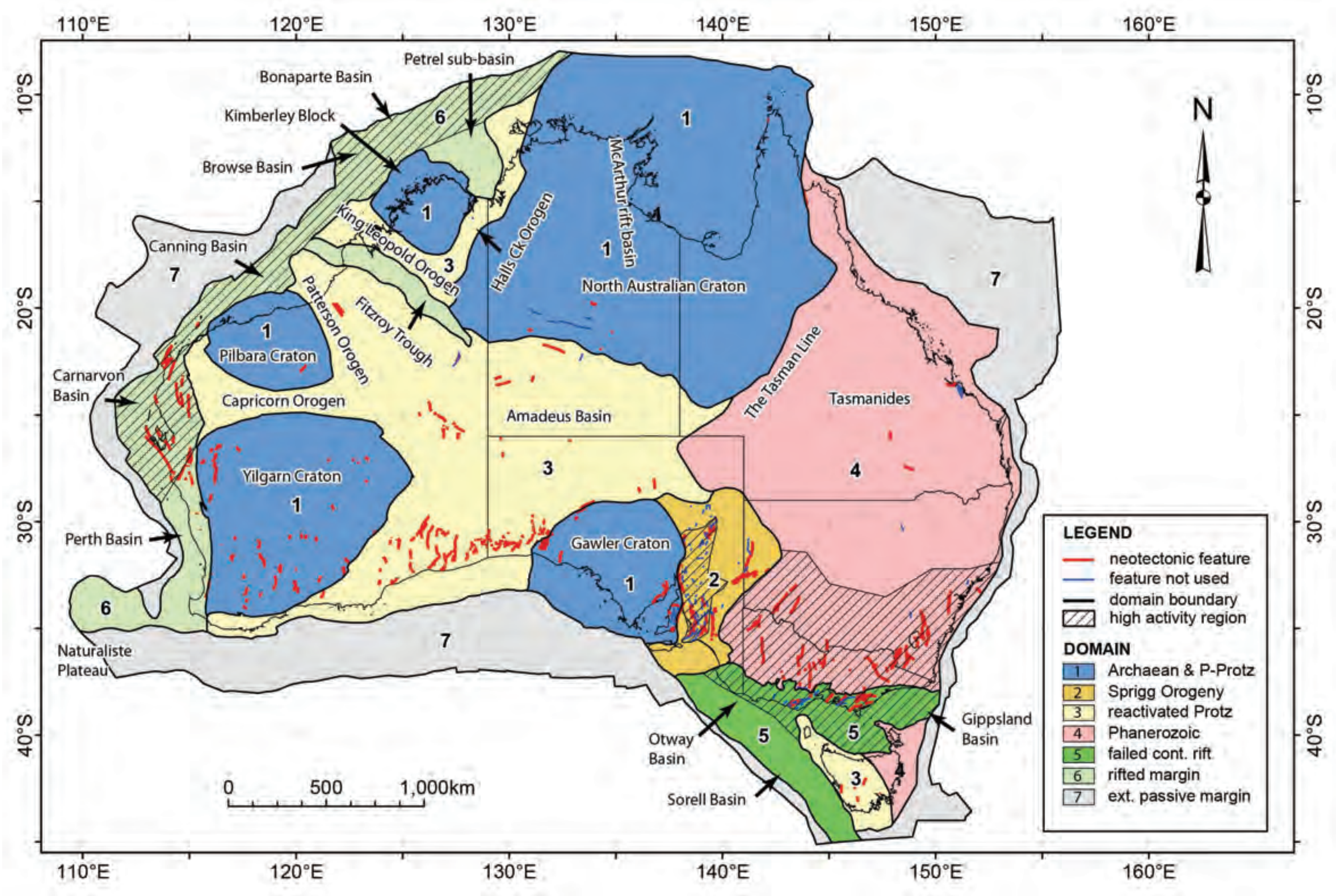

Figure 33 *– Map of neotectonic domains. Features marked in blue were not used in the analysis. Hatched polygons represent areas within domains of relatively higher activity, and should not be compared between domains. Note that the South West Seismic Zone does not appear as a zone of enhanced neotectonic activity. See text for justification of domain boundaries.*

central Australia"). However, there are exceptions in the northwest corner of the Yilgarn Craton where scarps tend to be longer and closer together (in the Mt Narryer region), and in eastern Gawler Craton where closely spaced scarps are arranged in an *en echelon* pattern (c.f. on the Eyre Peninsula). These may be related to stress concentration at the margins of the cratons.

It should be noted that there is no evidence in the neotectonic record (Clark 2010) to suggest that the region denoted the Southwest Seismic Zone (Doyle 1971a), so-called because of an anomalous concentration of epicentres in the last 50 years, is associated with a high level of neotectonic activity. Furthermore, models attempting to reproduce the pattern of historic epicentres concentrated in proximity to the Australian continental margin (Sandiford & Egholm 2008) do not predict the pattern of neotectonic scarps.

Sprigg Orogeny Domain

The margins of this domain mimic the extent of the sedimentary rocks that were deposited in the Neoproterozoic Adelaide Rift Complex, were later strongly affected by the Delamerian Orogeny (Preiss 1987; Drexel *et al.* 1993), and are now being affected by the Sprigg Orogeny (Sandiford 2003b). While it may be argued that the Mundi Mundi Fault system (Hill & Kohn 1998) should form part of the eastern boundary of the domain, and the Broken Hill Block part of Domain 3 (see below), for consistency the domain boundary follows the interpreted position of the Tasman Line over its full length (Wellman 1976; Direen & Crawford 2003) until the Otway Basin is encountered (c.f. Glen 2005). The western margin of the domain follows the interpreted position of the Torrens Hinge Zone (Preiss 1987; Drexel *et al.* 1993), which is believed to have been the western extent of rifting during the breakup of the supercontinent Rodinia (e.g. Glen 2005). The northwestern boundary is somewhat arbitrarily defined based upon the limit of significant concentrations of historic seismicity. The core of the domain encompasses the remarkable Sprigg Orogen (Sandiford 2003b), which continues to build in relief today along the axes of the Flinders and Mt Lofty Ranges, and is thus distinct from all other reactivated Proterozoic crust within the Australian continent (c.f. Domain 3). The seismic character of this domain is defined by the type-faults detailed in Sandiford (2003b), Celerier *et al.* (2005) and Quigley *et al.* (2006), being closely spaced, intimately connected to youthful topography, and hosting up to two hundred metres of neotectonic displacement. There is an excellent correlation between contemporary seismicity and broad neotectonic uplift in this domain, which may have built 50% of its modern relief within the neotectonic era (e.g. Braun *et al.* 2009).

While the pattern of faulting on the northeastern Eyre Peninsula is very similar to that seen in the Mt Lofty Ranges (compare Figures 11 and 15b), although with significantly smaller neotectonic displacements, the nature of the crust on the Eyre Peninsula is more akin to the Gawler Craton element of Domain 1. These faults have therefore been assigned to Domain 1, with the caveat that strain localisation across the domain boundary may explain their anomalous character.

Reactivated Proterozoic Crust Domain

The Australian continent (west of the Tasman Line) is criss-crossed by eroded orogenic belts that were active in the Proterozoic assembly of Australia. These orogenic belts, or mobile belts, encircle the Domain 1 cratonic nuclei (Figure 33) and tend to be reactivated time and again (e.g. Fitzsimons 2003; Betts & Giles 2006; Neumann & Fraser 2007). While there is much diversity in the timing and the pervasiveness of the last reactivation of each mobile belt (ranging from Mesoproterozoic to Devonian/Carboniferous) (e.g. Haines *et al.* 2001; Betts & Giles 2006), neotectonic features appear similar in character. Scarps tend to be longer than in Domain 1, and there is an indication of organisation, perhaps reflecting the strong and linear structural grain present in most mobile belts. An excellent long-term record of deformation of this type of crust is evidenced on the Nullarbor

Plain (Hillis *et al.* 2008), which is floored by the Proterozoic Albany-Fraser/Wilkes Orogen (Fitzsimons 2003). While little neotectonic data exists for the Capricorn, Patterson, King Leopold and Halls Creek Orogens they might be expected to behave in a similar fashion by virtue of their demonstrated susceptibility to reactivation throughout geologic time (e.g. Betts & Giles 2006; Neumann & Fraser 2007; Occhipinti & Reddy 2009).

Western Tasmania has been tentatively placed within this domain based upon the widespread exposure of Neoproterozoic rocks, metamorphism and deformation fabrics (e.g. Berry *et al.* 2008), and its pre-Delamerian Orogeny correlation with crust west of the Tasman Line (Glen 2005, Figure 1). Despite a long Palaeozoic deformation history, and the proposal that analogous Proterozoic basement floors the Selwyn Block in the Lachlan Fold Belt to the north (Cayley *et al.* 2002), we maintain that the character of the scarps is more akin to those of Domain 3 than those in Domain 4. Furthermore, there is little record of the rifting history that might align it with Domain 2, nor the strong organisation of scarps.

Eastern Australian Phanerozoic Accretionary Terranes Domain: the Tasmanides

This domain includes the five Phanerozoic Tasmanide orogens (Glen 2005), and excludes western Tasmania (part of Domain 3) and the Adelaide rift complex (Domain 2) (Figure 34). Following the breakup of the supercontinent Rodinia in the Late Neoproterozoic, and the formation of a passive margin along the east coast of Proterozoic Australia (the so-called Tasman Line), a series of five convergent margin orogenic belts formed (the Delamerian, Lachlan, Thomson, New England, and North Queensland Orogens, Figure 34) and accreted to the eastern seaboard from Middle Cambrian to Jurassic (Direen & Crawford 2003; Glen 2005).

The neotectonic record from this domain is restricted almost entirely to the Lachlan and Delamerian Orogens (approximated by the high neotectonic activity polygon marked on Figure 33, see also concentration of features in Figure 34). Given significant historic seismicity (Figure 34), it seems likely that further features remain to be discovered in the high-relief and relatively high-erosion regions of the New England and North Queensland Orogens. However, large changes in crustal stress orientation and possibly magnitude (Hillis & Reynolds 2003) centred on the New England Orogen may act to suppress neotectonic activity (cf. Figure 1). It is possible that the surface expression of earthquakes that nucleate in Thomson Orogen crust is subdued or suppressed by the cover rocks of the Cooper/Eromanga Basin. Alternatively, the low seismic activity rates recorded in historic times (Figure 34) may be a true indication of long term low levels of crustal deformation.

As palaeoseismic data within this domain are only available from the Cadell Fault, it is not yet possible to assign a seismic character to domain-wide faulting with confidence. However, it is not implausible that faults within this domain behave like the Cadell Fault, at least in terms of pronounced temporal clustering of surface rupture that might cumulatively amount to tens to a couple of hundreds of metres of displacement over the neotectonic era. The Kurrajong Fault within the Lapstone Structural Complex west of Sydney suggests caution in applying blanket rules within this domain. Only 15 m of the 130 m throw across this fault appears to be neotectonic (McPherson *et al.* 2009), whereas the Cadell Fault displaces Late Miocene and younger strata by more than 50-60 m (e.g. Clark *et al.* 2007), and the Lake George Fault impounds up to 200 m of late Miocene and younger sediment (Singh *et al.* 1981).

Eastern Extended Continental Crust Domain

Domain 5 comprises continental crust extended during the breakup of the supercontinent Gondwana in the late Mesozoic and overlain by thick sedimentary basin sequences (the Gippsland, Otway, Bass and Sorell Basins). The main regions of neotectonic activity centre on an aulocogen (a failed intra-

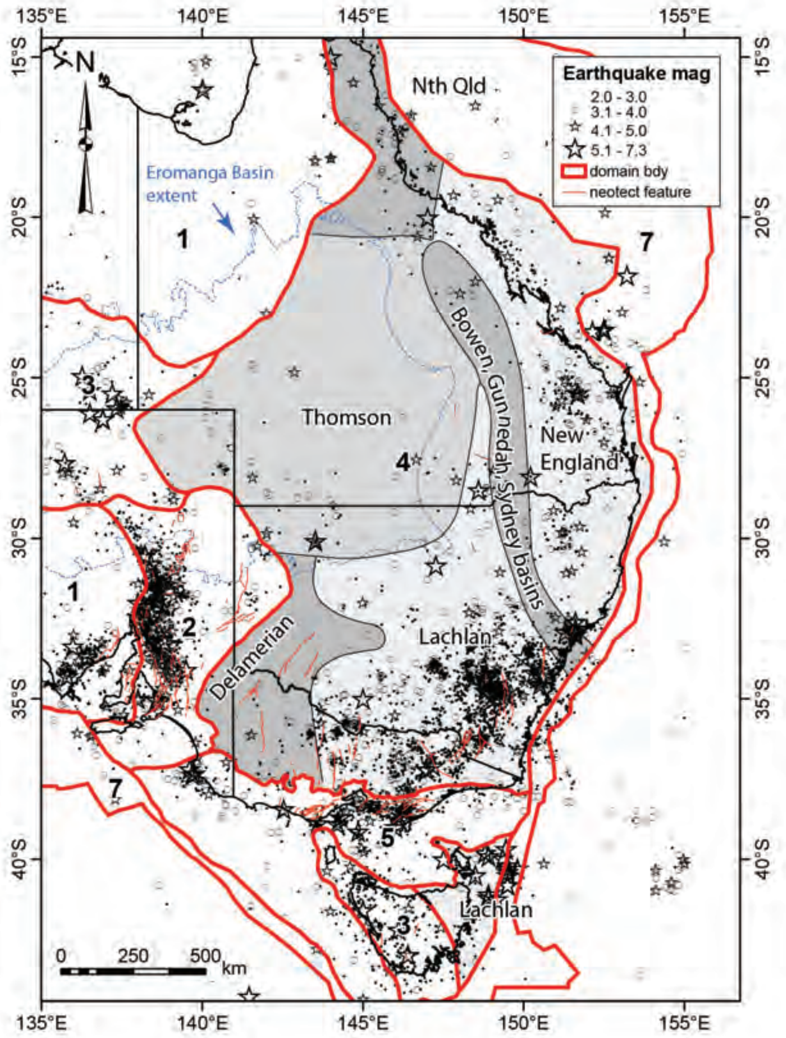

Figure 34 *– Internal structure of the Tasmanides Domain (after Glen 2005). Strong northerly structural grains are predominant in all bar the southern Thomson Orogen, where easterly trends are typical. The Thomson Orogen forms the basement to the Cooper/Eromanga Basins.*

cratonic rift - cf. Burke 1977) that developed between Tasmania and the mainland during the separation of Australian and Antarctica, and reactivated during the opening of the Tasman Sea (Veevers 2000). This aulocogen is overlain by the Gippsland, Bass and eastern Otway Basins. Seismic data clearly shows Neogene reverse reactivation of Mesozoic normal faults throughout these basins (Hill *et al.* 1994; Dickinson *et al.* 2002; Holdgate *et al.* 2003; Cummings *et al.* 2004; Blevin *et al.* 2005). Although palaeoseismic data is lacking, slip rate data, typically averaged over the last hundred thousand to a few million years, is available (e.g. Sandiford 2003a; Gardner *et al.* 2009).

The Sorell Basin (west of the Tasman Rise) is included in the domain as it is generally considered to be continuous with the western Otway Basin (Boreham *et al.* 2002; Krassay *et al.* 2004; Blevin & Cathro 2008). However, the prominent inversion structures that are characteristic of the Gippsland and Otway Basins, and to a lesser degree the Bass Basin (e.g. Blevin *et al.* 2005), appear to be much more subtle to absent in the Sorell Basin, suggesting lower activity (Boreham *et al.* 2002). This is perhaps analogous to the relationship between the active Carnarvon Basin and comparatively less active Perth Basin, as detailed in the following section. The D'Aguilar Ranges Fault, which occurs on the boundary of the Sorell Basin and Proterozoic Tasmanian basement rocks, may be more representative of minor inversion in the basin than typical activity in the Tasmanian Proterozoic crust.

Western Extended Continental Crust Domain

This domain comprises extended Precambrian and Palaeozoic crust flooring five marginal and offshore basins (Perth, Carnarvon, offshore Canning, Browse, and Bonaparte; see Figure 33) and their Mesozoic and Cenozoic (± late Palaeozoic) sedimentary fill rocks. Similar to Domain 5, most neotectonic activity focuses on the basins that primarily relate to Mesozoic fragmentation of Gondwana (Veevers 1972, 2000; Longley *et al.* 2002), and particularly those on the Northwest Shelf (i.e. Cape Range and north). However, 'subtle' Neogene reactivation of some basin segments, formed predominantly as the result of Palaeozoic rifting (e.g. Fitzroy Trough of the onshore Canning Basin, Petrel Trough of the Bonaparte Basin, Southern Carnarvon Basin, Northern Perth Basin), has been noted (Denman & van de Graaff 1976; Craig *et al.* 1984; Baillie & Jacobson 1995; Keep *et al.* 2007). The southern Perth Basin, which primarily developed in the Mesozoic, is also less active than basins further north, and may be considered to be similar to the Sorrell Basin in Domain 5. The onshore Canning Basin, excepting the Fitzroy Trough, is excluded from this domain as it is considered that the Precambrian basement dictates the seismic character rather than the thin cover sediments, in a similar fashion to faults cutting the Nullarbor Plain (cf. Domain 3). Future exploration may require revision of this assertion. Similarly, future data collection may identify the affinity of the Naturaliste Plateau as better aligned with Domain 3 rather than Domain 6 (e.g. Halpin *et al.* 2008), and parts of the Browse/Bonaparte Basins may require classification into a new non-intraplate domain given the affinity of deformation patterns found there with those further north associated with the Timor collision (Keep *et al.* 2007).

While no palaeoseismological information exists for single earthquake events, the neotectonic character of this domain is very similar to the Gippsland and Otway Basins, with large anticlines overlying inverting normal faults, here exemplified by the Cape Range and Rough Range Anticlines (Malcolm *et al.* 1991). In the case of the Fitzroy Trough, seismic reflection imaging shows that the major northern bounding fault has been reactivated to an extent during the Neogene (Keep *et al.* 2007), and is associated with a high level of historic seismicity (Figure 35, ~17°S 122°E). This subsidiary style of deformation may dominate in the Palaeozoic parts of the domain (e.g. the Perth Basin and southern Carnarvon Basin proximal to the shield).

Passive Margin Extended and Transitional Crust Domain

This domain contains extended, highly extended and transitional continental crust from the edge of the continental shelf (or adjacent neotectonic domain) out to the Continental/Oceanic Crust Boundary (Blake 2000; FrOGTech 2005). This "passive margin" domain formed as the result of the Mesozoic break-up of the supercontinent Gondwana (Veevers 2000). While there is no neotectonic data with which to characterise this domain, an appreciable number of Australian historic earthquakes of magnitude 5 and above are located either within this domain, or near the boundary of this domain and adjacent domains (Figure 35). Similar crust on the eastern seaboard of the United States hosted the M7+ Charleston earthquake sequence (Johnston 1996; Talwani & Schaeffer 2001), flagging this domain type as a potential source of damaging ground shaking (e.g. Wheeler 1995, 1996; Wheeler & Frankel 2000; Wheeler 2009b).

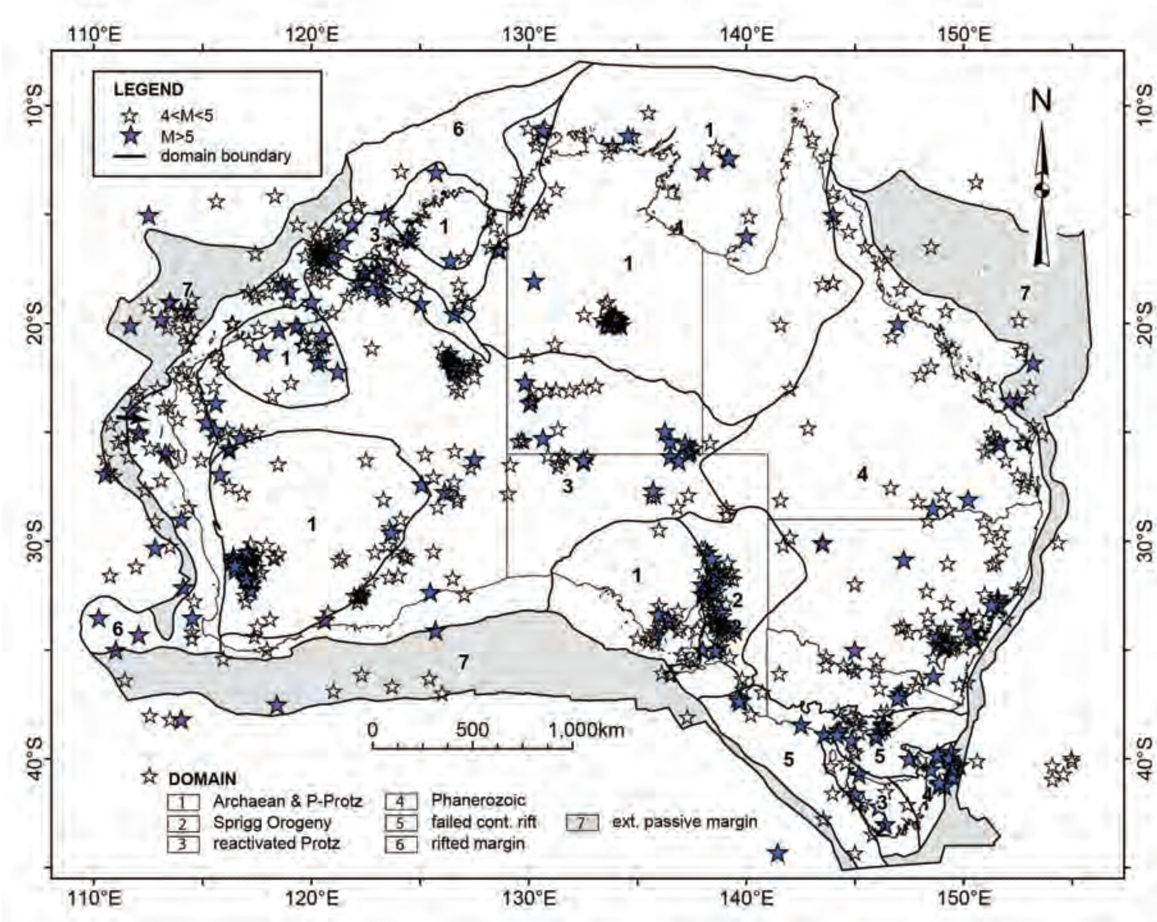

Figure 35 *– Relationship of historic earthquakes of M>4 to Neotectonic Domain boundaries.*

Comparative analysis of neotectonic domains data

The data from individual faults can be used to establish patterns (in space and time) of rupture, and provides a basis for deciding whether insights gained from neotectonic fault data in one region may be confidently extrapolated to faults occurring in a different region. The following section presents the characteristics of each of the neotectonic domains that we have defined for the Australian continent (Figure 33). The Australian Neotectonics Database (Geoscience Australia, unpublished data) houses the data used to test this domains hypothesis (accessed 31 July 2009, see Appendix Table 1). This data is derived from disparate sources which include the results of in-house DEM reconnaissance, published and unpublished reports, geological maps, and in a small number of cases, data from field investigations (e.g. Figure 2). Ideally, an active fault source should be characterised in terms of the geometry of its rupture plane, knowledge of the size and frequency of large earthquakes associated with that rupture (with an idea of variability), and perhaps an indication of whether the fault may be influenced by neighbouring active faults. However, in most cases the geometry of the rupture plane underlying a surface scarp, and the large earthquake recurrence behaviour on that rupture plane, are unknown or subjectively defined. The data currently compiled for Australia does, however, contain a small number of semi-quantitative key variables. As demonstrated below, these variable populations are subject to a level of uncertainty in their derivation, and also possess a common trait of non-normal distribution. Attempts to statistically normalise the data sets were unsuccessful, and accordingly multivariate statistical analysis of this data was not possible. Consequently the data have been treated and analysed as ordinal level data. Nonetheless, these three key variables – *fault length*, *vertical displacement* and *fault density* - still represent a semi-quantitative data set with which to test the neotectonic domains hypothesis. In addition, *fault length* and *vertical displacement* can be used to estimate maximum magnitude earthquake (M_{max}), while *fault density* has utility in assessing the potential for interaction between faults.

FAULT LENGTH

One of the most important physical characteristics of a fault rupture is its along-strike length, which can be related to the magnitude of the causative earthquake (e.g. Wells & Coppersmith 1994). Estimates of the maximum magnitude earthquake (M_{max}) that a structure is capable of producing can be determined from fault length data (e.g. Stirling *et al.* 2002a; Biasi & Weldon 2006; Wheeler 2009b) after careful consideration of the possibility of segmented rupture. In general, the fault lengths reported here might be expected to be underestimates as vertical displacement tapers towards the tails of ruptures, resulting in lower discoverability. This might be especially the case with those scarps identified in DEM data. For instance, features below 3 m high tend to be obscured by noise in 90 m SRTM DEM data. For a scarp built in only a small number of events, a proportion of the scarp may effectively be invisible.

The population distribution for fault length data is presented in Figure 36. It shows a positive skew (skewness = 1.63; 2 standard errors of skewness = 0.32) with 95% of data having values of less than 120 km, and 75% of data with values below 70 km. There is a vague suggestion of bi-modality, with a potential secondary peak at ~80-90 m. Summary statistics for the fault length data are presented in the inset table in Figure 36.

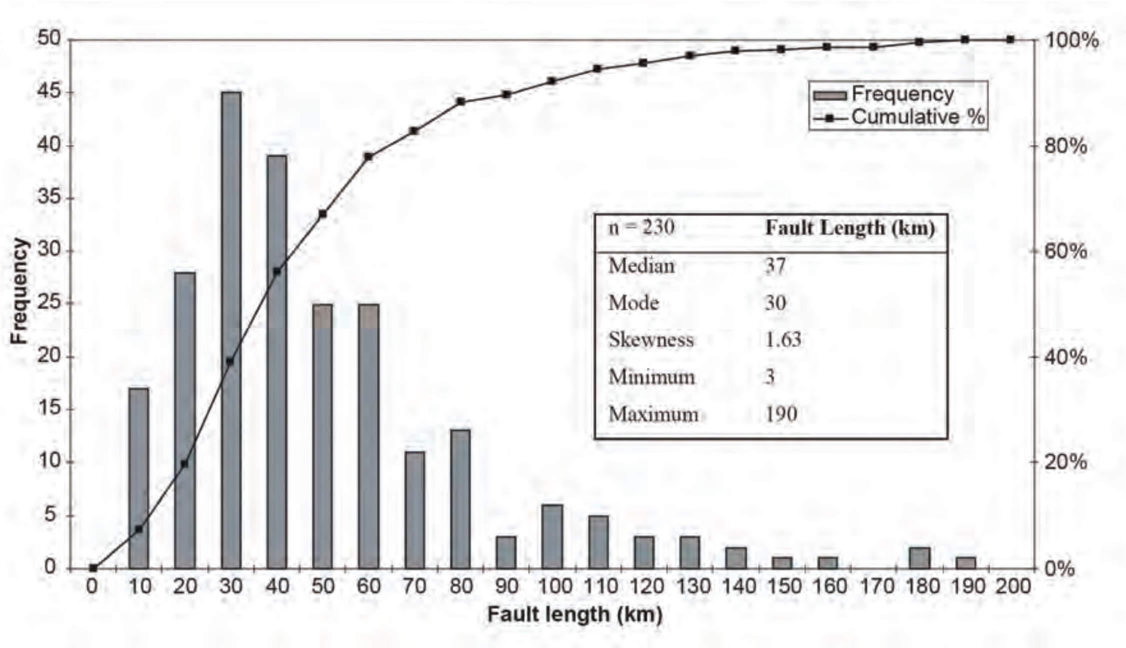

Figure 36 *– Cumulative frequency histogram showing a positively skewed distribution for fault length data. Inset table shows summary statistics.*

Fault length data for each defined domain are presented in Figure 37. While falling within the range of variability shown by Mesozoic Continental Rift domain (D5) the data suggest that the Archaean and Palaeoproterozoic Craton domain (D1) may be distinguished by virtue of having comparatively short fault lengths (90% less than 55 km long) and a small interquartile range (difference between the 75th and 25th percentiles) of less than 20 km. The Reactivated Proterozoic Craton domain (D3), Eastern Phanerozoic domain (D4) and Western Extended Phanerozoic domain (D6) display comparable median fault length values. Domains D3 and D4 also possess similar interquartile ranges, while D6 shows a larger range with generally higher values. This is not, however, reflected in the maximum value, which is lower than those for both D3 and D4. The Sprigg Orogeny (D2) exhibits slightly longer fault lengths than the D5, but both fall within approximately the same range of variability at the 10th and 90th percentiles. D2 does, however, have a maximum fault length more than twice as long as that in D5. With the exception of outlier values, these domains (D2 and D5) have fairly similar fault lengths, perhaps reflecting the rift-related structural architecture upon which they are founded. The Reactivated Proterozoic (D3) and Eastern Phanerozoic (D4) domains also have broadly similar fault lengths, which are furthermore consistent with those from the Western Extended Phanerozoic domain (D6), although faults in the latter are statistically slightly longer. The Archaean and Palaeoproterozoic Craton domain (D1) is characterised by faults with the shortest relative lengths.

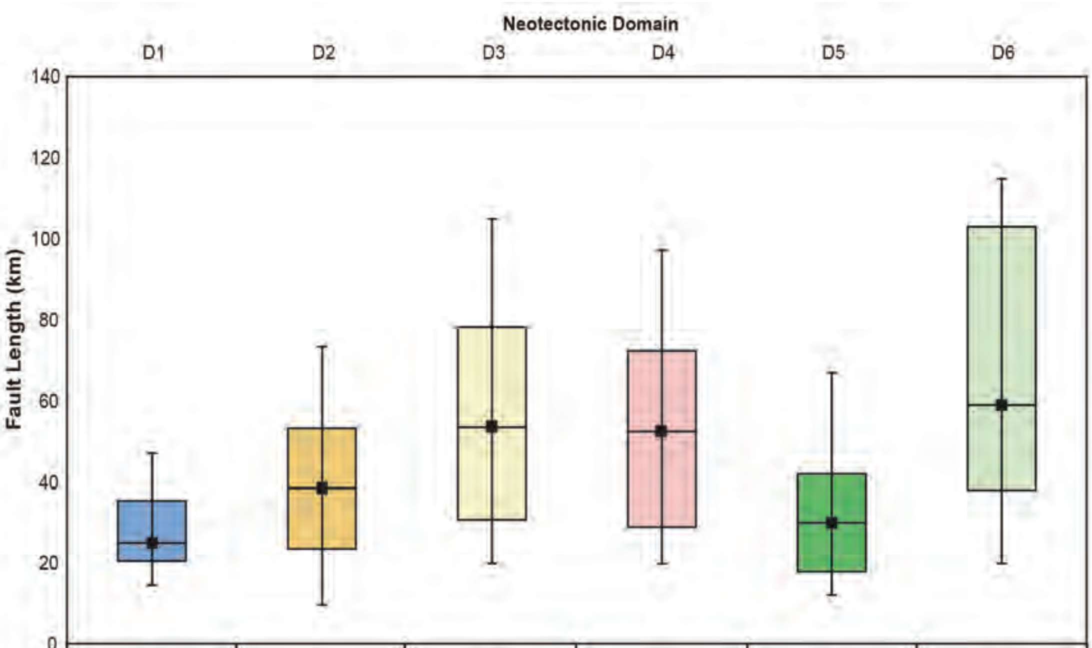

	D1	D2	D3	D4	D5	D6
min	8	4	4	10	3	6
max	57	172	155	190	80	124
med	25	38.5	53.5	52.5	30	59
n	64	40	50	38	21	17

Figure 37 *– Box and whisker plot of fault length data for each neotectonic domain. Boxes denote 75th and 25th percentiles, central point indicates median value, and whiskers define 90th and 10th percentiles. Data table shows minimum, maximum and number of data points for each domain. D1 - Archaean Craton and non-reactivated Palaeo-Proterozoic; D2 – Sprigg Orogeny; D3 - Reactivated Proterozoic; D4 - Eastern Australian Phanerozoic; D5 - SE Australian Rifted Crust; D6 - Extended Continental Crust; D7 – extended passive margin crust. Colours correspond to accompanying domain in Figure 33.*

VERTICAL DISPLACEMENT

Vertical displacement is a measure of the vertical separation between two sides of a fault as a result of movement on the structure. In general, this parameter is a measure of the highest displacement sustained on a kilometre-scale rather than an average or a maximum value. This measure has been adopted in lieu of fault slip due to the paucity of fault dip data and the dominance in the data set of features defined using DEMs. Uncertainty in the identification and measurement of scarp heights using DEM data might be expected to vary according to the resolution of the DEM, and the acquisition system. For example, DEMs derived from data acquired by airborne systems, such as Photogrammetry and LiDAR, generally have a higher resolution and a lower noise content than those derived from space borne acquisition platforms (e.g. SRTM etc.). However, while features might only become readily identifiable over the noise in SRTM data above 2-3 m relief (e.g. Clark 2010), the relief difference across a scarp can be estimated to greater precision by profiling the step in the noise.

In conjunction with temporal information on fault movement (if known), vertical displacement can be used to estimate slip rate (e.g. Murata *et al.* 2001; Philip *et al.* 2001). Estimates of neotectonic displacement also provide a first order indication of the number of earthquakes that a fault has generated in the current stress regime, given certain assumptions regarding single event slip and segmentation (Leonard & Clark 2006; Clark 2010; Leonard 2010; Leonard & Clark 2010).

Vertical displacement values in the Australian neotectonics database have, in most cases, been determined by measurement of the offset of topographic features (predominantly fault scarps) in digital elevation data, and as a result are subject to the limitations of the data (i.e. resolution and noise content). Spatial resolution issues can bias the displacement values, either through non-detection of smaller, more subdued surface displacements in the landscape, or by over- or under-estimation of observed displacements. It is also important to note that vertical displacements are typically minima, as erosion will usually act to reduce relief across a scarp with time. This might not be the case for fault-line scarps, where rocks with different resistances to erosion are brought alongside by movement on a fault. A small number of vertical displacement values found in the database are derived from published and unpublished reports in which measurements of displacement have been recorded. The timing and number of movements associated with a given displacement is usually unknown, but the latter can be estimated using standard relations (e.g. Wells & Coppersmith 1994).

The population distribution for vertical displacement data is presented in Figure 38. It shows a very strong positive skew (skewness = 4.23; two standard errors of skewness = 0.32) with 95% of data values below 150 m, and 75% of data with values less than 40 m. There is a weak suggestion of bi-modality in the data set, with a possible secondary peak at around 100 m. The extreme outlier value of 600 m relates to a single structure (Tawonga Fault) in D4. Summary statistics for vertical displacement data are presented in the inset table in Figure 38.

Figure 39 presents vertical displacement data for each defined domain. These data indicate that the D1, D3 and D6 domains have comparable median vertical displacement values of around 10 m and interquartile ranges less than 40 m. The D6 domain does, however, show higher variability (c.f. 10th and 90th percentiles) and a comparatively large range between the median and 75th percentile. The D2, D4 and D5 domains can similarly be grouped on the basis of their median values, which exceed 30 m, and a larger range of variability, particularly above their median values, as indicated by both percentile and interquartile ranges. In essence, this grouping distinguishes domains defining the

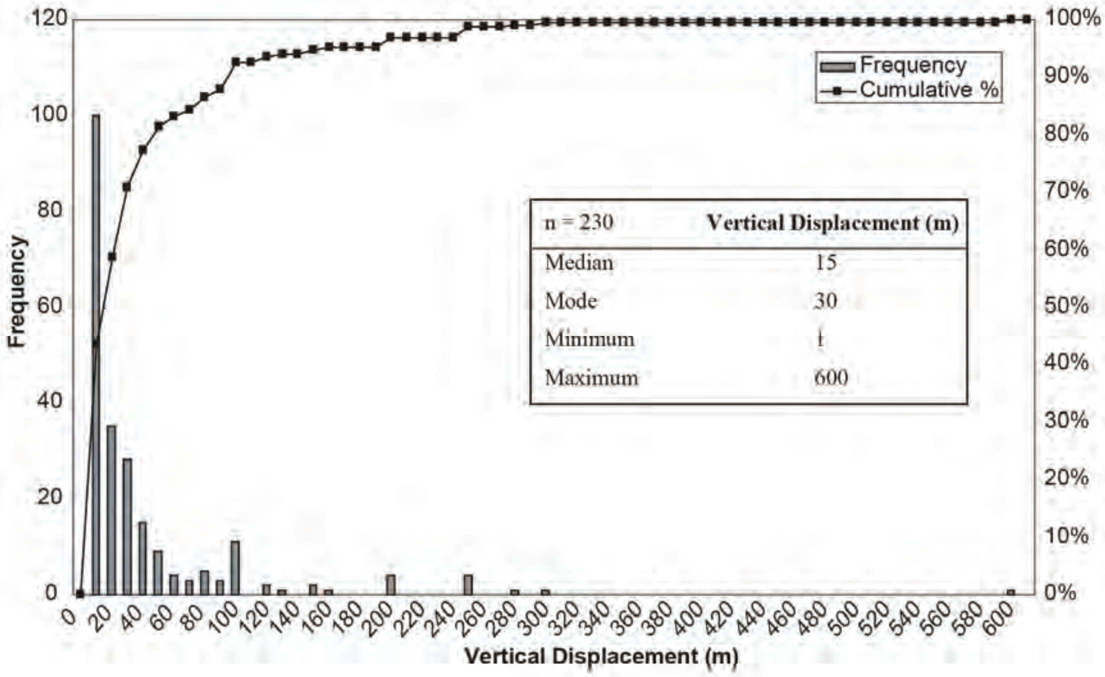

Figure 38 *– Cumulative frequency histogram showing a positively skewed distribution for vertical displacement data. Inset table shows summary statistics.*

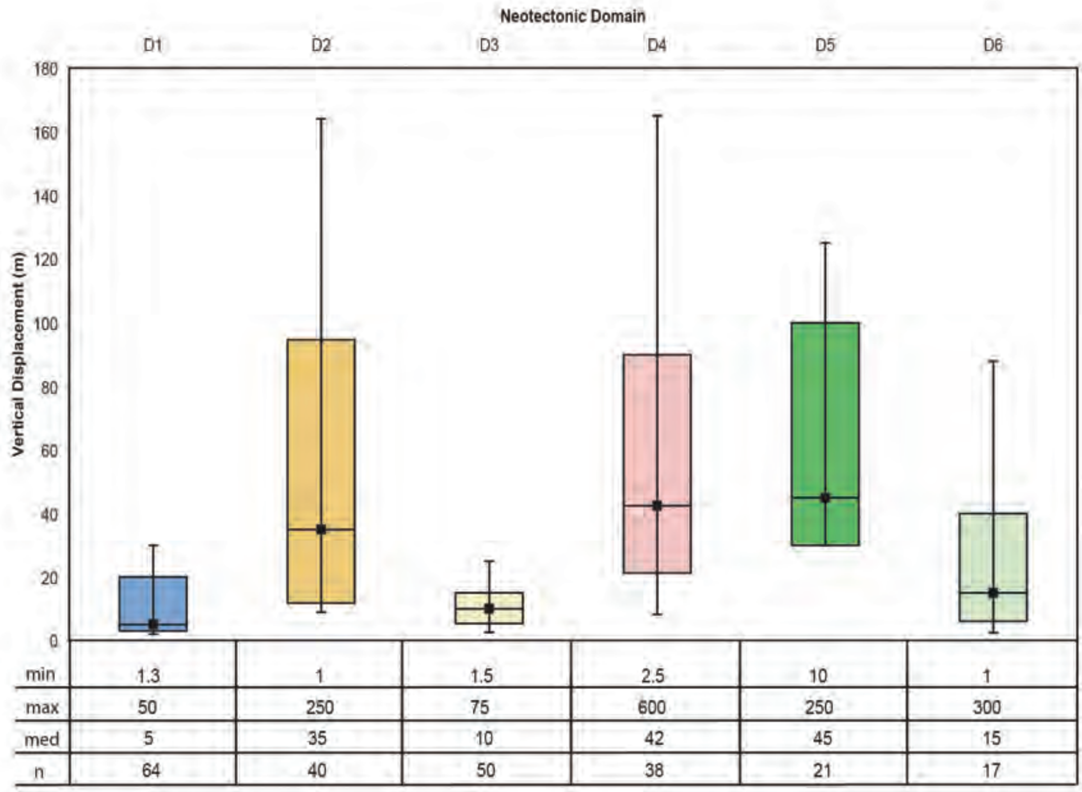

Figure 39 *– Box and whisker plot of vertical displacement data for each neotectonic domain. Explanation of symbols and tables as per Figure 37.*

central and western parts of the continent from those in the east, with the former showing overall lower displacements and less variability.

FAULT DENSITY

The density or relative spacing of neotectonic faults provides insights into the mechanism of neotectonic strain accommodation for a region (e.g. Cowie & Roberts 2001; Olson & Cooke 2005). This in turn can be related to crustal architecture and composition, and in certain cases, reflects mantle dynamics. In the Australian neotectonics database the relative density of faulting is expressed as the Euclidean distance between the centroid of a mapped fault and the centroid of the next closest fault (i.e. minimum separation distance). It is important to note that this measure may be somewhat misleading for non-parallel faults and faults arranged in along-strike or *en echelon* patterns. Data are presented in decimal degrees in order to account for curvature of the Earth, which can significantly impact estimates of linear distance for widely spaced faults.

The population distribution for data representing the minimum separation distance (MSD) between faults is presented in Figure 40. The distribution is highly positively skewed (skewness = 3.76; two standard errors of skewness = 0.32), with 95% of data values less than 1.5 decimal degrees (~167 km) and 75% with values below 0.6 (~66 km). There is a suggestion of poly-modality in the population, with potential secondary peaks around 0.6-0.7 and 1.4-1.7. However, a paucity of data, particularly at the upper end of the distribution, makes this difficult to test. Summary statistics for MSD data are presented in the inset table in Figure 40.

Figure 41 presents minimum separation distance (MSD) data for each domain. These data suggest that the MSD between faults is almost identical in the D1 and D6 domains, with median values of approximately 0.33-0.34 decimal degrees (~37 km). However, the range of values in D6 is larger. While not as closely matched as D1 and D6, the D2 and D5 domains have similar MSD values. However, D2 does show a far greater range in the 3rd quartile, indicating a slightly broader spacing between structures (larger MSD). The D4 domain has a median MSD value well within the range of the other domains. It also has a comparatively small interquartile range, and while its 90th and 10th percentile ranges generally exceed those for the D2, D3 and D5 domains, they fall within the bounds of those for the D1 and D6 domains. D3 exhibits the highest median MSD, although its 90th and 10th percentiles still fall within the range of those for D1, D4 and D6. Importantly, the domains characterising southern and eastern Australia (D2, D4 and D5) exhibit both the lowest interquartile ranges and median MSD values.

Discussion

DISCRIMINATION OF NEOTECTONIC DOMAINS

As the variation in neotectonic character across the continent is a result of differing crustal response to imposed stresses, the delineation of neotectonic domains according to crustal character seems justified. However, it is apparent that many of the domains are not statistically distinct with respect to the key neotectonic fault variables analysed. That is, for any given variable there is typically a significant degree of commonality in values between domains. In spite of the uncertainty implied by the large range in values, the central tendencies (in this case best described by the median) are instructive.

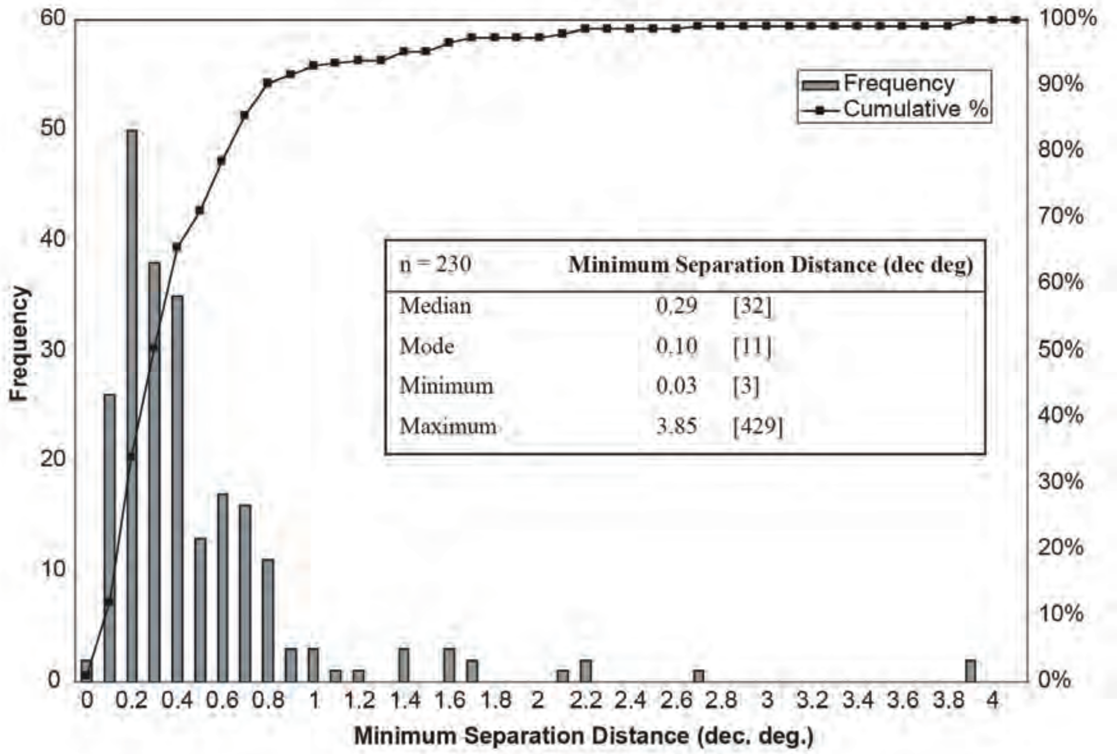

Figure 40 *– Cumulative frequency histogram showing a positively skewed distribution for minimum separation distance data. Inset table shows summary statistics for minimum separation distance between faults. Distance units are in decimal degrees with values in brackets denoting approximate distance in kilometres derived using x (km) = ((D*pi*d)/180)*0.001, where D = 6378137 [Earth's diameter: km]: d = distance [degrees].*

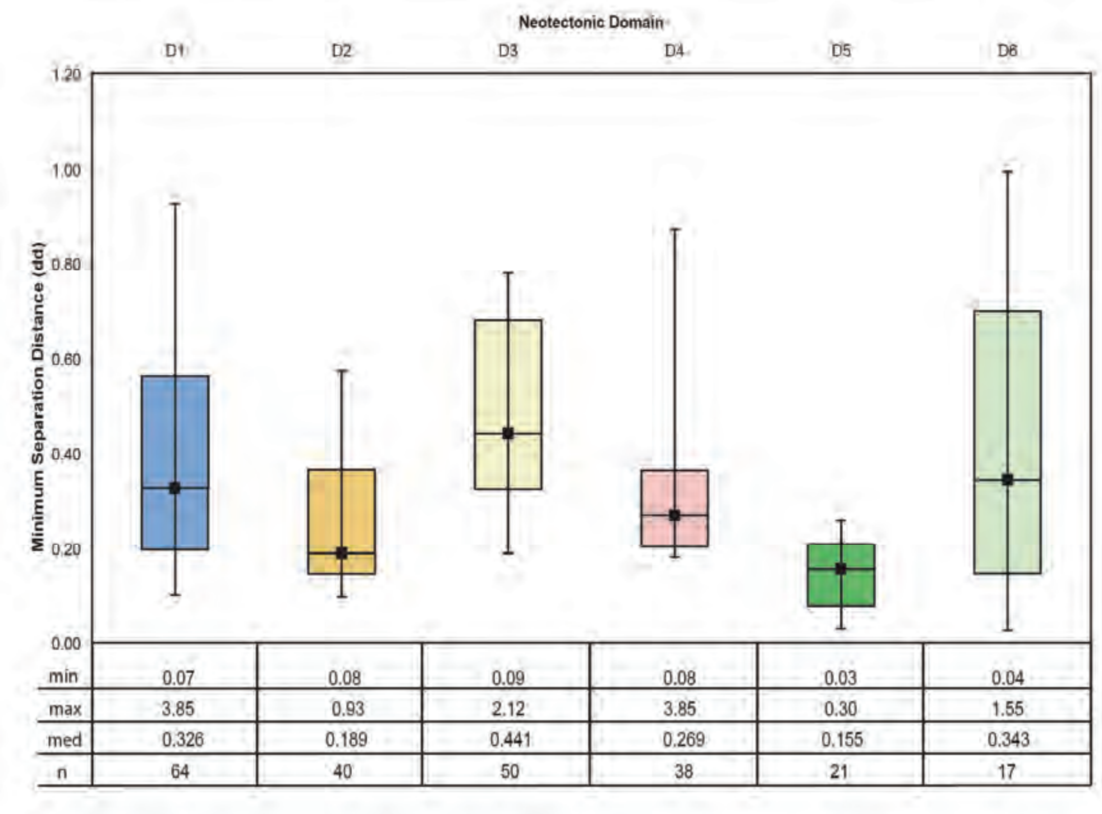

Figure 41 *– Box and whisker plot of minimum separation distance data for each neotectonic domain. Explanation of symbols and tables as per* *Figure 37*.

The shortest median fault lengths are evident in D1 and D5 (Figure 37). In the case of D1, this is very much likely to be a fundamental property of the highly structured cratonic crust which is being faulted (c.f. Hills 1961; Everingham & Gregson 1996; Dentith & Featherstone 2003; Pandey *et al.* 2008; Dentith *et al.* 2009). For example, Dentith *et al.* (2009) show the 1968 Meckering surface rupture to be strongly controlled by complex bedrock architecture, with individual rupture segments initiating and terminating at intersections between lithology and regional dyke and fault sets. Unpublished aeromagnetic data over the Hyden Scarp, also in southwest Western Australia, show a similar pattern (Geoscience Australia, unpublished data). In the case of D5 the result is counter-intuitive as several systems of apparently very long faults are evident (see Figure 27), and this trend appears to continue offshore, for at least the major depocentre-bounding faults (e.g. Williamson *et al.* 1991; Nelson & Hillis 2005). This latter observation may be the key, as intrabasin faults make up the bulk of database entries – it is often difficult to estimate neotectonic displacements on the larger faults (e.g. the Rosedale Fault in the Gippsland Basin) as dateable displaced strata have been eroded from highly uplifted blocks. In addition, detailed mapping reveals that the larger basin-bounding faults are typically segmented. For example, in the Gippsland Basin the Rosedale and Budgeree faults are continuous along strike and bound the northern margin of the Balook Block, and the Bass, Almurta and Yarragon Fault segments bound the northern margin of the Narracan Block (Figure 27). While not demonstrated by palaeoseismological data, this segmentation may well influence rupture extents. There is a possibility that longer fault lengths in D3, D4 and D6 may in part reflect incomplete characterisation of rupture segmentation. However, a single event displacement of ~ 7 m on the Milendella Fault (D2) and of ~ 5.2 m on the Cadell Fault (D4) suggests that very long scarp lengths are certainly real in some instances.

Median fault lengths from the D3, D4 and D6 domains are similar (Figure 37). This similarity potentially reflects the structural characteristics of the Proterozoic to Phanerozoic fold belts and mobile belts which constitute the basement of the domains (the Perth Basin and southern Carnarvon Basin are floored by the Proterozoic Pinjarra Orogen (Fitzsimons 2003)). The larger range and generally higher values for domain D6 perhaps relate to the reactivation of the mobile belt in extension during Gondwana break-up. However, the character of D6 might be modified substantially if more data were incorporated from the northern offshore part of the domain (i.e. on the Northwest Shelf).

Vertical displacement data distinguish the central and western parts (D1, D3 and D6) from the eastern parts (D2, D4 and D5) of the continent (Figure 39). The central and western domains are characterised by overall lower displacements with less variability, while the eastern domains show larger median displacements with much higher variability. The proportion of older, colder and thicker crust in the ancient cratons and mobile belts that dominate the central and western regions (e.g. Collins *et al.* 2003) may well contribute to the lower displacements. Enhanced heat flow, resulting in a mechanically weaker crust (Celerier *et al.* 2005), contributes to the large displacements, and high fault density (Figure 41), recorded in D2.

Fault density (minimum separation distance) data also broadly distinguish the domains characterising eastern Australia (D2, D4 and D5) from those in central and western Australia (D1, D3 and D6). However, the spatially biased nature of the data set combined with the broad areal extent of several of the domains leads to significant variability, and the generation of a small number of extreme values. This can be readily seen in the domains which extend into the less completely sampled northern parts of Australia (D1, D3, D4 and D6), which have significantly higher 90th percentile values than southerly domains (compare Figures 33 and 41). There is a weak indication in the data that fault density may be used to discriminate deformation styles between cratonic and non-cratonic domains. The interquartile ranges for cratonic domains (D1 and D3), for which little fault interaction in the upper crust might be expected (e.g. Braun *et al.* 2009; Clark 2010) are larger than for non-cratonic domains where scarps are ordered into *en echelon* or belt-like patterns (D2, D4 and D5 – see next section). D6 does not, however, fit this model. The ratio of median separation distance to median fault length provides an alternative measure of the ability of scarps to interact with each other (Table 2). For non-cratonic domains (D2, D4, D5 and D6) the median separation is consistently half the median fault length, implying significant potential for fault interaction and regional-scale strain localisation. The ratio is much closer to unity for the cratonic domains (D1 and D3), indicating a relatively reduced potential for interaction. The suggestion of bi- and poly-modality in all three variable data sets (Figures 36, 38 and 40) leaves open the possibility the populations harbour more discrete sub-populations that may be statistically discernible in a larger data set.

***Table 2** – Ratio of minimum fault separation (fault density – see Figure 41) to fault length (see Figure 37).*

	D1	D2	D3	D4	D5	D6
median separation (~km)	32.6	18.9	44.1	26.9	15.5	34.3
median length (km)	25	38.5	53.5	52.5	30	59
sep/length	1.3	0.5	0.8	0.5	0.5	0.6

PATTERNS IN LARGE INTRAPLATE EARTHQUAKE RECURRENCE

Both spatial and temporal patterns in large earthquake occurrence are suggested by the neotectonic data presented herein, and have in part guided the discrimination of domains. In most cases interpretation of patterning is speculative, as data is sparse.

Spatial patterning

Each domain is characterised by a unique spatial arrangement of scarps, reflecting the varying response of the crust to the imposed stresses (Figure 1). Scarps are predominantly randomly arranged in D1, and tend to be aligned close to perpendicular to the prevailing maximum compressive stress field trend (Clark 2010). In one case there is an apparent northerly arrangement of scarps (e.g. scarps 4, 39 and 45 in Figure 3), but it is not known if interaction between these faults occurs. Near to the D1 boundaries linear and belt-like spatial arrangement of scarps is more apparent (e.g. scarps 18, 49, 52, 51, 43 and 44 in Figure 3). This trend is apparent on the northwest and eastern boundaries of the Gawler Craton section of D1 also (Figure 33), and might reflect stress concentration associated with crustal rheology changes between cratons and marginal mobile belts.

Linear spatial arrangement is more common in D3, perhaps reflecting the strong structural grain common to orogenic and mobile belts (Figure 33). However, elements of randomly arranged rupture comparable to that found in D1 are apparent on the Nullarbor Plain, suggesting potential bi-modality in character. Similar to D1, scarps are again oriented more or less perpendicular to SH_{Max}. While scarp length in D4 is similar to D3 (Figure 37), linear arrangements dominate in D4. Linear scarps, or complexes of scarps, are arranged in an *en echelon* fashion relative to nearby complexes (e.g. Figure 16) in a belt-like arrangement (c.f. Caskey & Wesnousky 1997). A mix of scarp trends is apparent, from perpendicular to SH_{Max}, to more northerly oriented. These trends in part relate to the dominant structural grains in the different orogens that constitute D4 (c.f. Figure 34).

The western part of D4, within the Delamerian Orogen component of the Tasmanides (Figure 34) is similar in scarp character and arrangement to the eastern part of D2. However, as the axis of the Mt Lofty/Flinders Ranges is approached, the character changes dramatically to much shorter (Figure

37), more closely spaced (Figure 41), and higher displacement (Figure 39) faults arranged in linear and *en echelon* patterns with respect to one another (Figure 11). It is likely that many of these faults link, or at least interact strongly in the subsurface (e.g. Preiss & Faulkner 1984; Paul *et al.* 1999; Somerville *et al.* 2008). Along the axis of the ranges the predominant scarp trend is perpendicular to SH_{Max}.

Domain 5 and the Northwest Shelf region of D6 are characterised by well-linked anastomosing networks of faults. While the fault properties (length, displacement and spacing) are quite different between these domains (Figures 37, 39 & 41), the general characteristic of an inverted basin architecture is common. In the Perth Basin and Southern Carnarvon Basin the arrangement of faults is similar to the Sorell Basin.

Temporal patterning

Temporal patterns in large earthquake occurrence may be inferred at the scale of a single fault (Crone *et al.* 1997), of clusters of faults (Leonard & Clark 2006; Leonard & Clark 2010), and at the domain scale (Braun *et al.* 2009; Clark 2010). While the suite of active fault behaviours may vary across Australia, as implied by the domains model, one individual fault characteristic appears to be common to most Australian intraplate faults studied: active periods comprising a finite number of events are separated by typically much longer periods of quiescence (e.g. Crone *et al.* 2003; Clark & Van Dissen 2006; Clark *et al.* 2007).

Clark & Van Dissen (2006) and Clark *et al.* (2007) proposed a model to help conceptualise temporal clustering in long-term SCR fault behaviour, and the hazard posed by SCR faults, based largely upon data from the Cadell Fault (Figure 42). The sparse data set available suggests that an active period (T1 and T2 on Figure 42a) might constitute less than a half-dozen events, and perhaps as few as two or three in Western Australia (Figure 2), and the slip rate in an active period might be several orders of magnitude greater than in the long term (e.g. Clark *et al.* 2007; Clark *et al.* 2008a). Published data on faults in the west of Australia (Domain 1) suggest that the interseismic intervals between large events in an active period might be in the order of 20 - 40 ka (Crone *et al.* 1997; Crone *et al.* 2003; Clark *et al.* 2008a; Estrada 2009). Data on the Cadell Fault (Clark *et al.* 2007) indicate more frequent rupture in Domain 4; three times in the interval *ca.* 70 – 45 ka, and 3 times in the interval *ca.* 45 – 25 ka. It is inferred that three uplift events on the Cadell Fault had occurred prior to the diversion of the Murray and Goulburn Rivers, suggesting that these events are likely to have been spaced thousands of years apart, similar to the Meers and Cheraw faults in the western central United States (Crone & Luza 1990; Crone & Machette 1995). This contrasts with the New Madrid Seismic Zone in the intraplate central United States, where sequences of large earthquakes have occurred on average every ~ 500 years for at least the last two seismic cycles in the current active period (e.g. Tuttle *et al.* 2002). Quiescent intervals can be sufficiently prolonged, in the western and central parts of Australia in particular, that most or all relief relating to an active period might be removed by erosion prior to the next active period (Crone et al. 2003; Clark et al. 2007; Clark et al. 2008a).

The earthquake recurrence behaviour model presented in Figure 42a can also be used to express the relative probability for the occurrence of a future event on an SCR active fault (Figure 42b). If a "suspected" active fault has not experienced a surface-breaking earthquake for a very long time, say more than 100 kyr (or at least two mean seismic cycle intervals for an active period), our expectation of an event in the near future will be at some very low or "background" level. It is likely that most if not all of the relief relating to previous ruptures has been removed, either by erosion or depositional (e.g. aeolian) processes, for the majority of such faults (e.g. Meckering, Tennant Creek, Marryat Creek). These faults might not be recognised as active prior to the first event in a new active period.

Subsequent to the first event in a new active period our expectation of a future rupture, say within the following several tens of thousands of years, is greatly elevated (Figure 42b). This expectation will decay with successive ruptures until eventually reaching the "background" level again after the occurrence of only a finite number of events (fewer than ~6 based upon current data). The points critical to understanding the hazard posed by SCR faults, and modelling this hazard probabilistically, become: 1) is the fault in question about to enter an active period, in the midst of an active period, or in a quiescent period; 2) how many large events might constitute an active period, and how many ruptures has the fault generated so far in its current active period (should it be in one); and 3) what is the "mean" recurrence interval in an active period, and what is the variability around this mean? This "mean" can be incorporated statistically into probabilistic seismic hazard assessments (e.g. Stirling *et al.* 2011).

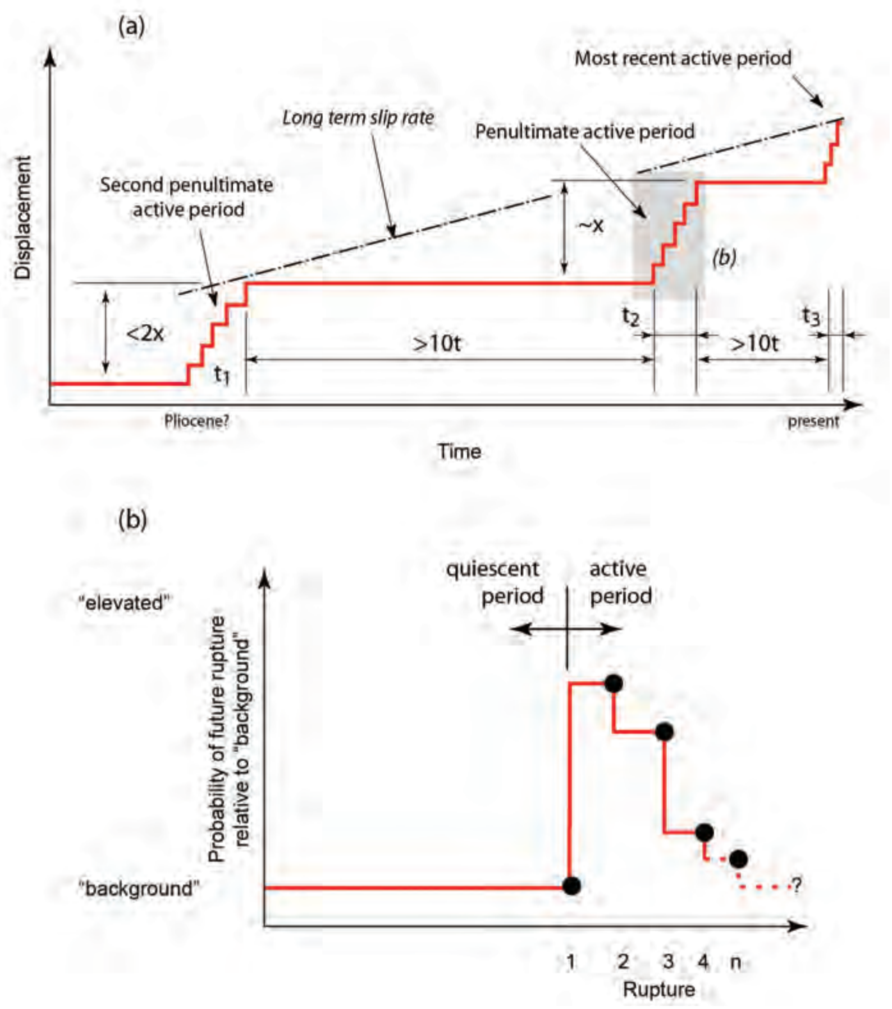

Figure 42 *– (a) Generalised fault slip diagram for Australian SCR faults based upon data from the Cadell Fault (Clark et al. 2007). Three active periods of fault growth (earthquake occurrence) are denoted by t1, t2, and t3. These active periods are relatively short lived, and are composed of only a few ruptures each (ca. < 6 events per active period). Inter-event times between successive ruptures within an active period may range up to several thousand to several tens of thousands of years. Long quiescent periods separate the active periods, and the length of the quiescent periods can range from many tens of thousands of years to greater than a million years. (b) detail of (a) expressed in terms of the expectance of a near future event.*

When considering the data presented in Figure 2, and the resulting fault behaviour model presented in Figure 42, it is important to be cognisant of the sampling bias inherent in the dataset. The majority of faults listed in Figure 2 are associated with significant and/or distinct topographic relief. In essence, they are the active SCR faults that are most discoverable, and because of this, they are the ones that have been the subject of study. The bias being that the dataset of active SCR faults is dominated by the faults that have been most recently the most active. Active SCR faults that are well into a quiescent phase may be nearly "invisible" in the landscape, are relatively unstudied, and are therefore underrepresented in Figure 2. Nevertheless, focused investigation on such SCR faults could yield data pertinent to testing the fault behaviour model depicted in Figure 42. Another limitation of the SCR fault dataset is that there are few active faults worldwide, like the Cadell Fault, were fault displacement behaviour over several active and quiescent phases has been determined.

There are a number of possible causes of episodic fault behaviour. If more than one active fault exists in a region, and the fault density is sufficiently high (e.g. a fault spacing that is one rupture length or less), then episodic behaviour might be the result of stress interactions between faults. The ratios of median separation to length presented in Table 2 suggest that it is plausible that such behaviour occurs in domains D2, D4, D5, D6 and perhaps D3. However, with the possible exception of faults in the Hyden region (e.g. Clark *et al.* 2008a), the much lower active fault density in domains D1 and D3 suggests an alternative mechanism. Chéry & Vernant (2006) were able to produce episodic slip behaviour in a single isolated fault embedded in an elastic lithosphere, in which fault stress fluctuations may occur, loaded by plate motion. In this case, deep post-seismic viscous strain can be the source of crustal transient strain that in turn allows earthquake clustering (e.g. Kenner & Segall 1999; Meade & Hager 2004). Possible causes for fault stress fluctuations include climatic change (e.g. crustal water content variation, erosion-depositional processes, Hertzel & Hampel 2005), or perhaps more importantly, self-induced fault weakening/healing (e.g. Ben-Zion *et al.* 1999). Chéry & Vernant (2006), assuming that weakening or strengthening processes are gradual and due to repeated earthquakes (e.g. Sleep & Blanpied 1992; Ben-Zion *et al.* 1999), found that if the fault weakening time is small enough (less than several tens of thousands of years), fast slip rate excursions occur, as well as a complete lack of activity.

Braun *et al.* (2009) suggest a model for the southwest of Western Australia whereby uniform contraction in the ductile lower crust and upper mantle is accommodated by essentially random brittle fracture in the upper crust. This model is supported by the generally non-clustered distribution of palaeoscarps within D1 (Clark 2010) (see also Table 2). However, the remarkable sequence of three surface breaking earthquakes east of Perth in 1968, 1970 and 1979 (Meckering, Calingiri and Cadoux, Gordon & Lewis 1980; Lewis *et al.* 1981) raises questions of how sections of upper crust "unload" in response to this uniform contractional strain, and at what scale. The Meckering, Calingiri and Cadoux scarps (scarps 38, 6 and 5 respectively on Figure 3) are 70-100 km apart; too distant for static stress changes to have promoted rupture (e.g. Caskey & Wesnousky 1997). Furthermore, the ruptures were sufficiently temporally separated that dynamic stress changes are unlikely to have promoted rupture. The observations are consistent with the postulate that blocks of upper crust on the scale of 10^4 kilometres can unload in the space of a decade. In the case of the southwest of Western Australia, this process may be facilitated by a mid- to upper-crustal architecture characterised by fundamental sub-horizontal structural discontinuities (most notably at ~10 km and ~25 km depth) (e.g. Everingham 1965; Drummond & Mohamed 1986; Goleby *et al.* 1993; Dentith *et al.* 2000) that are compartmentalised by major moderately-dipping fault systems, forming the "superterranes" of Wilde *et al.* (1996). With only one example of this phenomenon it is not possible to draw conclusions with any certainty. However, random brittle fracture might operate at larger than the scale of a single fault in some instances within D1.

If one compares a synthetic catalogue of large earthquakes derived from the neotectonic feature inventory presented in Figure 3 with the historic record of seismicity from the South West Seismic Zone it is clear that the last 40 years have been anomalously high in terms of moment release (Leonard & Clark 2006; Leonard & Clark 2010) (Figure 43a). This result is consistent with the low relief landscape in the southwest of Western Australia, and implies that seismicity is migratory, probably on the timescale of a few hundred years.

There is a compelling body of evidence emerging that the temporal clustering behaviour observed from individual fault studies in Australia may be symptomatic of a larger picture of the more or less continuous tectonic activity from late Miocene to recent being punctuated by "pulses" of activity in specific deforming regions (Quigley *et al.* 2010). For example, major deformation episodes are constrained to the interval 6-4 Ma in southwest Victoria (Paine *et al.* 2004) and 2-1 Ma in the Otway Ranges (Sandiford 2003a). A major episode of deformation ceased at 1.0 Ma in the offshore Gippsland Basin while continuing onshore until approximately 250 ka (Holdgate *et al.* 2003). Given the high sensitivity of the stress state in the Australian continent to distant boundary forcings (Coblentz *et al.* 1995; Coblentz *et al.* 1998; Sandiford *et al.* 2004; Hillis *et al.* 2008), it is possible that this behaviour relates to small changes at the plate margins, such as subduction of a sea mount, or processes such as the onset of extension episodes in the Taranaki Basin in New Zealand (e.g. King & Thrasher 1992). An alternative hypothesis is that the boundary conditions have remained essentially static and the locus of deformation has migrated across the Australian continent with time as stress changes in one piece of unloaded crust destabilise an adjacent piece of crust.

MAXIMUM MAGNITUDE EARTHQUAKE

Probabilistic seismic-hazard analyses (PSHAs) require an estimate of Mmax, the magnitude (M) of the largest earthquake that is thought possible within a specified area, and results are highly sensitive to the choice of Mmax (e.g. Mueller 2010). In seismically active areas such as some plate boundaries, large earthquakes occur frequently enough that Mmax might have been observed directly during historic times. In less active regions like Australia, and most of the Central and Eastern United States and adjacent Canada, large earthquakes are much less frequent and generally Mmax must be estimated indirectly. Indirect-estimation methods are many, their results vary widely, and opinions differ as to which methods are valid (Wheeler 2009b, a). Non-site specific earthquake hazard assessments for Australia, including those for the national seismic hazard maps, have typically taken the approach of assuming an Mmax value based upon adding a constant to the maximum earthquake magnitude observed (Mobs) in a zone of historic seismicity or continent-wide (Gaull & Michael-Leiba 1987; Gaull *et al.* 1990; Gibson 1995; McCue 1999; Brown & Gibson 2004; Hall *et al.* 2007). Values ranging from M3.6 to M8.0 are incorporated into the current national seismic hazard map (Gaull *et al.* 1990), while other studies have adopted values around M7.5 (e.g. Brown & Gibson 2004).

While Brown & Gibson (2004) defined seismicity source zones based upon geological and geophysical characteristics, only one attempt has been made to subdivide the Australian SCR crust on the basis of the expected influence of variation in geology (and by proxy, geophysical signature) on Mmax (Johnston *et al.* 1994). Kanter (1994) initially divided the continent on the basis of geology and geophysics, and the resulting domains were then assigned values of additional variables that "might be related to seismicity" (Kanter 1994, p. 2-8 - 2-16). These were then combined into "superdomains" on the basis of variables that might control Mmax (Cornell 1994). Principle amongst the variables that were thought to influence Mmax was whether the crust comprising the domain had been tectonically "extended" or not, and to a lesser degree the age and type of crust

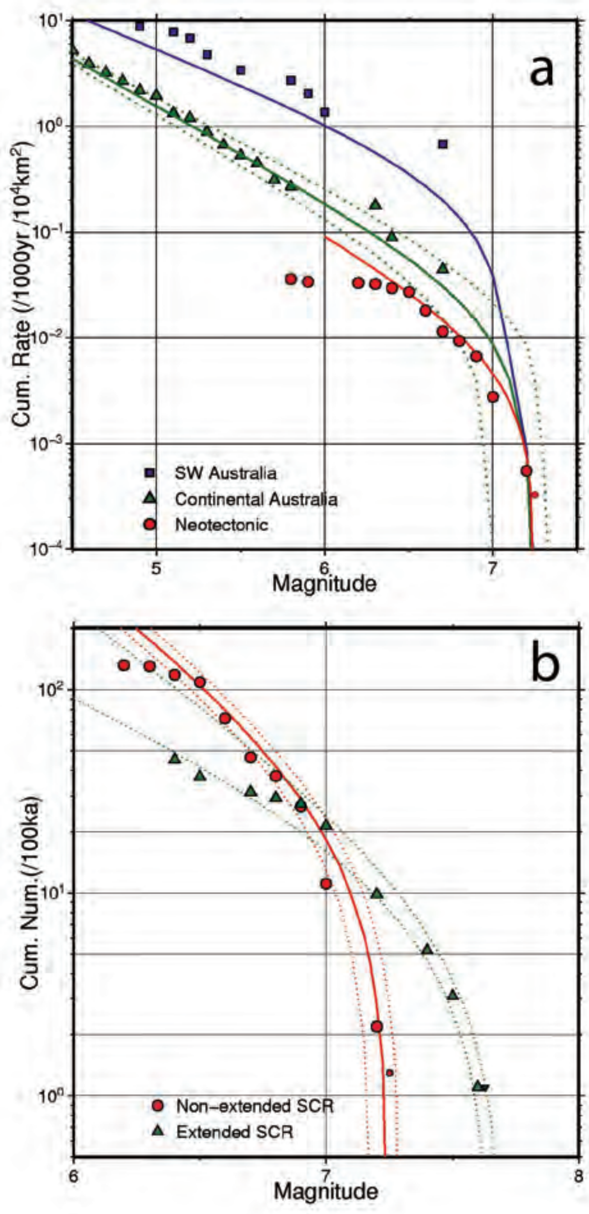

Figure 43 *– (a) Comparison of a subset of the neotectonic catalogue (Domain 1; see Figure 3 for location) with the catalogue of historic earthquakes in the Southwest Seismic Zone, and the whole Australian continent. The recurrence rate for Australian continent is the solid green line with the errors being the dotted green lines. The contemporary recurrence rate of the study area is ~10 times the implied neotectonic rate and the rate for the whole Australian continent is ~2 times the neotectonic rate. (b) The Magnitude – Frequency, or recurrence, statistics of the earthquake catalogue derived from a subset of neotectonic scarps from Domain 1 and Domain 6 (see Figure 3 for location). The small symbol represents the largest earthquake in each class (modified after Leonard & Clark 2011).*

(Coppersmith 1994; Johnston 1994b). No palaeoseismic studies had been published from Australia at the time of this research, so the Mmax estimates relied exclusively on the global SCR catalogue (Johnston 1994a, b, c). The results according to crustal type, expressed as maximum *observed* magnitude earthquake, were: M8.3±0.5, extended crust, intracontinental rift; M7.7±0.2 extended crust, passive margin; M6.8±0.3, non-extended crust, craton; M6.4±0.2, non-extended crust, Palaeozoic or Mesozoic fold belt (Johnston 1994b).

Where an active fault has been studied paleoseismically, single-event scarp lengths and single-event displacements can provide two independent estimates of the Mmax for that fault (e.g. Quigley *et al.* 2006; Somerville *et al.* 2008; Estrada 2009), with scarp length being considered the more reliable measure (e.g. Wells & Coppersmith 1994; Hemphill-Haley & Weldon 1999). This data is not known for the majority of features in the neotectonics database, and is difficult to estimate with confidence in the absence of detailed field investigation (see Figure 2 for features that have been studied). However, in regions where DEM data is of sufficient resolution that single event ruptures are visible, scaling relations may be used to discriminate between single and multiple event scarps, and a palaeo-earthquake catalogue constructed. A relatively large area of 10 m resolution DEM data in the southwest corner of the Yilgarn Craton section of D1 (Figures 3 & 33) has allowed for mapping of fault scarps in unprecedented detail (Clark 2010). It was estimated that most events above M_w6.5 that have occurred in the last ~ 100 ka were catalogued (Leonard & Clark 2010). The scaling relations of Leonard (2010) were then used to develop a palaeo-seismicity catalogue comprising 65 events (Figure 43) (Leonard & Clark 2006; Leonard & Clark 2010). The data has typical truncated Guttenberg-Richter recurrence characteristics with a slope (*b*) of 0.9-1.0 between M_w 6.5 and 6.9, and a rapid roll off in recurrence above M_w 6.9 towards an asymptote of M_w 7.2±0.1, which is considered to be the Mmax. A less well constrained Mmax result of Mw 7.6±0.1 was obtained for the southern Carnarvon Basin (Figure 43b).

The work in the southwest of Western Australia (Leonard & Clark 2006; Leonard & Clark 2010) supports the proposition that the longest fault scarps in the Yilgarn Craton section of D1 are attributable to single earthquake ruptures. Firstly, multiple smaller than full length ruptures would not fit the truncated Guttenberg Richter statistics as well (Figure 43b). Secondly, several smaller than full length rupture events generate significantly less than the observed scarp heights (cf. Leonard 2010), and many smaller than full length rupture events are inconsistent with the palaeoseismic data (e.g. Crone *et al.* 2003; Clark *et al.* 2008a). If it is assumed that the same is true beyond the Yilgarn Craton (with appropriate caveats), then the scarp lengths recorded in the neotectonic catalogue (Appendix Table 1) might be used to estimate Mmax in areas where the catalogue is not sufficiently complete to permit curve fitting.

An interpolated surface of scarp length variation implies variation in Mmax across the continent (Figure 44). The extents of these trends are consistent, within the limitations of the data, with the neotectonic domain boundaries. For example, scarp length is uniformly low in D1 regions (browns). In data-rich parts of D3 (e.g. the Nullarbor) and D6 (e.g. the Carnarvon Basin) scarp length is comparatively higher (greens). Although significant heterogeneity is apparent, there is also an indication that scarp lengths are in general greater in D4 than in D1, while scarp lengths in D5 appear to be comparable to D1. In some instances the relationship between scarp length and height requires segmented rupture (e.g. a very long scarp may not have the height expected of entire length rupture), and in some regions not all relief might be reasonably expected to be neotectonic. Mmax estimation for each domain obtained from scarp length assuming entire scarp-length rupture would therefore be non-conservative. As a conservative measure, we have based Mmax calculations on the 75% percentile scarp length for each domain and by averaging the maximum magnitudes predicted from a range of different published moment-area earthquake scaling relations appropriate for SCR reverse faulting (e.g. Somerville *et al.* 1999; Somerville 2001; Somerville *et al.* 2009; Leonard 2010). Results range between M_w 7.0–7.5±0.2 for a generic fault dip of 50°, a seismogenic depth of 15 km, and a fault aspect ratio as prescribed by Leonard (2010) until the seismogenic depth is reached (Table 3). This may be conservative for D1 and D3, where seismogenic depths may be as low as 10 km (Leonard 2008). Reduction of the seismogenic depth to 10 km for these domains results in a ~0.1 magnitude unit lowering in Mmax. At these magnitudes, choice of rupture aspect

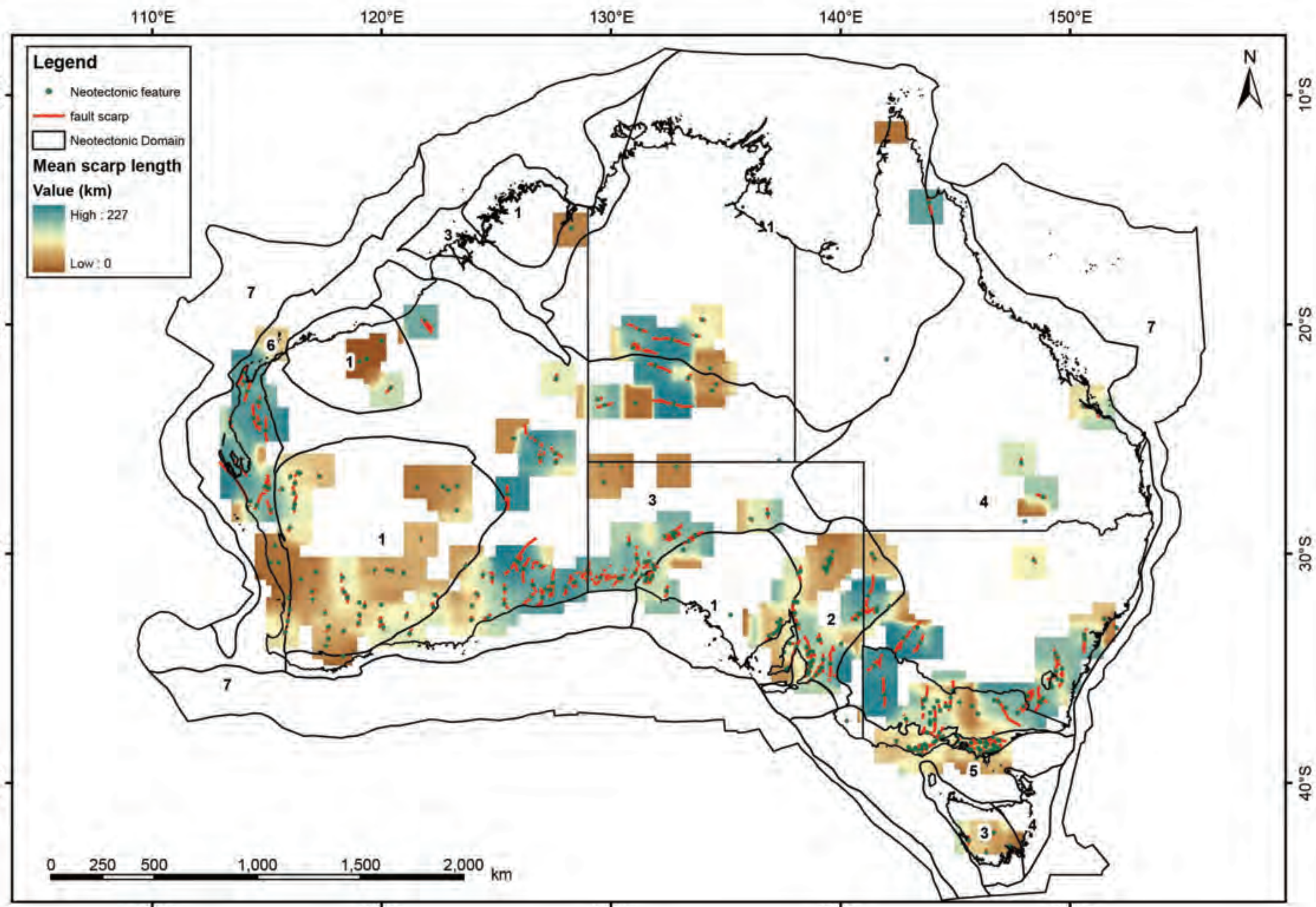

Figure 44 – *Mean scarp length surface interpolated using a natural neighbour model with a 0.5 degree cell size and a 0.5 degree search radius. Brown colours indicate relatively short scarp lengths while green colours indicate relatively higher scarp lengths. Note variation in scarp length between domains, with D1 and D5 regions generally low, and other regions comparatively higher.*

ratio (cf. Somerville *et al.* 2009; Leonard 2010) makes less than 0.1 magnitude unit of difference to the results.

The Mmax results appear to be reasonable where validating data is available. For example, the Mmax for D1 (M_w 7.0±0.2) and D5 (M_w 7.5±0.1) are within error of those estimated by Leonard & Clark (2010). Palaeoseismological investigations of the Cadell Fault in D4 indicate the largest events are of magnitude M_w7.3-7.4 (Clark *et al.* 2007), as compared to the 75th percentile estimate of M_w 7.3±0.1. Somerville et al. (2008) derive Mmax estimates of between M_w 7.3 – 7.5 from palaeoseismic data reported by Quigley et al. (2006) from several D2 faults. The upper boundary of this range is larger than our estimate for D2 (M_w 7.2±0.1), again highlighting the slightly conservative nature of calculations based upon remotely determined scarp length (i.e. 0.1-0.2 magnitude units).

The results indicate that the Australian historic catalogue of seismicity significantly underestimates Mmax in most regions (cf. Gaull *et al.* 1990). With the exceptions of intracontinental rifts (analogous to D5) and passive margin extended crust (analogous to D6), the global SCR catalogue of maximum observed earthquakes also underestimates Mmax, by up to one magnitude unit (cf. Johnston 1994b) (Table 3). Whereas the results for passive margin extended crust are statistically indistinguishable, there is a large discrepancy in Mmax for intracratonic rifts. Given the propensity for folding rather than discrete faulting at the surface within D5, the possibility of larger ruptures than mapped in the neotectonics database cannot be discounted. Based upon analogy with the eastern United States, an Mmax of M_w 7.7±0.2 may be assigned to D7 (Johnston 1994b; Wheeler & Frankel 2000).

***Table 3** – M_{max} estimates based upon 75th percentile fault length values (see Figure 37). Moment-area relations with applicability to intraplate settings were used in the calculations (Somerville et al. 1999; Somerville 2001; Somerville et al. 2009; Leonard 2010). Values reported are the average for these models, with uncertainties in M_{max} expressed as ±1 standard deviation from this average. A 15 km depth of seismogenic crust has been used for each domain, and a fault dip of 50 degrees. Mobs refers to maximum observed earthquakes in the Global SCR catalogue (Johnston 1994). At these magnitudes, choice of rupture aspect ratio (cf. Somerville et al. 2009; Leonard 2010) makes less than 0.1 magnitude unit of difference to the result.*

Domain	**Description**	**n**	**Fault Length (km)** ***[75th percentile value]*** **50 deg dip; 15 km depth**	***Mean Mmax*** **(SCR only)**	***SD***	***Mobs*** **GlobSCR**	***SD***
1	Archaean & P-Proterozoic	64	35.4	7.0	0.2	6.8	0.3
2	Sprigg Orogeny	40	53.25	7.2	0.1	6.8	0.3
3	Proterozoic Mobile Belt	50	78.15	7.4	0.1	6.8	0.3
4	Phanerozoic terrances	38	72.38	7.3	0.1	6.4	0.2
5	Failed continental rift	21	42	7.1	0.2	8.3	0.5
6	Inverting passive margin	17	103	7.5	0.1	7.7	0.2

IMPLICATIONS FOR STABLE CONTINENTAL REGION (SCR) ANALOGUE STUDIES

A fundamental implication of the domain model presented herein is that intraplate fault characters are not universal in their applicability in analogue studies. Careful choice of subject faults within analogous crust of similar stress field character is required to extrapolate meaningfully to imperfectly characterised areas. Johnston *et al.* (1994) identified continental crust that might be considered SCR worldwide (for analogue purposes), and proposed a fundamental distinction in the seismic activity levels between extended and non-extended parts of this crust. According to their definition, non-extended crust includes continental shields, platforms and Palaeozoic and Mesozoic fold belts, whereas extended crust includes intracontinental rifts of all ages and passive margins no younger than ~ 25 Ma. While it is not our intent to duplicate that work, the neotectonic inventory of scarps presented herein provides an opportunity to validate and refine the Johnston *et al*. (1994) model at a time-scale commensurate with the recurrence time of maximum magnitude earthquakes in the intraplate setting. The major tenet of the Johnston *et al.* (1994) model, that extended crust is more seismically active than non-extended crust, appears to hold true for the Australian neotectonic record (compare D2, D5 and D6 with D1, D3 and D4) (c.f. Shulte & Mooney 2005). Opportunities exist for the subdivision of both extended and non-extended crust based upon neotectonically-derived characters.

In extended crust domains (e.g. D5, D6), the age of major rifting appears to be important in terms of neotectonic activity level, and in terms of M_{max}. Palaeozoic intracratonic rifts and passive margin components are typically significantly less active than those rifted in the Mesozoic. For example, compare the level of activity in the Palaeozoic Fitzroy Trough and the Mesozoic Gippsland Basin aulocogens, or the Palaeozoic southern and Mesozoic northern Carnarvon passive margin basins (e.g. Figure 33). The distinction becomes more stark when one considers most Precambrian rifts. There is no evidence for neotectonic reactivation of the Mesoproterozoic rift in which sits the McArthur Basin (D1), nor extensional structures related to the Neoproterozoic Amadeus Basin (D3). However, in the latter case, there is evidence consistent with neotectonic reactivation of compressional structures formed at the northern and southern margins of the basin in the Peterman Ranges and Alice Springs orogenies (c.f. Korsch & Lindsay 1989).

D2 is anomalous within this framework. The domain formed as an intracratonic rift that developed into a marginal basin, similar to the Otway Basin, during the Neoproterozoic to Cambrian breakup of the supercontinent Rodinia (Preiss 1987; Drexel *et al.* 1993; Glen 2005). The interpretation of seismic imaging suggests that the fundamental structural architecture of the domain developed at this time; Cambrian platform and trough sequences overlying Adelaidean basement are normally displaced across major southeast-dipping normal faults that sole into a basal reflector at 12-13 km depth (Flottmann & Cockshell 1996, Figure 4). Reverse displacement during subsequent contractional orogenic events (i.e. the Delamerian, Alice Springs and Sprigg's orogenies) accrued on a spatially restricted subset of these faults corresponding to the topographic axes of Kangaroo Island, and the Mt Lofty and Flinders Ranges. Balanced cross sections derived from geological mapping suggest that a contractional architecture, developed during the Delamerian Orogeny, predominates at the surface, at least along the main topographic axes (Jenkins & Sandiford 1992; Paul *et al.* 1999). Smaller-scale, or less progressed, analogues of the Flinders and Mt Lofty Ranges can perhaps be seen in the Otway Ranges (Otway Basin) (Figure 25) and the Narracan and Balook Blocks (Gippsland Basin) (Figure 27). The fundamental differences that result in D2 accommodating up to one third of the seismic strain across the entire Australian continent (e.g. Braun *et al.* 2009) are the orientation of the Adelaidean palaeo-rift almost perpendicular to the contemporary SH_{max} (Figure 1), and perhaps enhanced heat flow resulting in a thermally and mechanically weakened crust (Neumann *et al.* 2000; Celerier *et al.* 2005). In these respects D2 may be unique amongst the world's SCR crust.

As we have shown in our analysis of data from domains D1, D3, and D4 there is a significant distinction to be made within the non-extended shield, platform and fold belt division of Johnston *et al.* (1994b). In particular, reactivated Proterozoic fold belts (D3) and Palaeozoic fold belts (D4) appear to be consistently more active than D1 cratonic (shield) crust. There is an indication that

Palaeozoic fold belts are more active than Proterozoic fold belts, at least in terms of the amount of slip that has accrued on the neotectonic faults. This assertion could be tested by summing the moment represented by each scarp in each domain.

Analogues between the Australian domains and SCR crust elsewhere in the world (see Johnston *et al.* 1994) are readily apparent. For example, poly-phase deformation of a compressional nature is a common feature in the post-rift evolution of many passive margins and rifts (D5/D6 analogues) (e.g. Gangopadhyay & Talwani 2003; Cloetingh *et al.* 2008). Archaean cratonic nuclei fringed by Palaeoproterozoic mobile belts (D1 analogues) comprise a large portion of the geology of Peninsula India (Balasubrahmanyan 2006) and North America (Hoffman 1989). Meso- and Neoproterozoic mobile belts involved in the accretion of the supercontinent Rodinia (D3 analogues) are found worldwide (e.g. Kroner & Cordani 2003), as are Phanerozoic accretionary terranes associated with the amalgamation of the supercontinent Gondwana (D4 analogues) (e.g. Collins & Pisarevsky 2005; Cawood & Buchan 2007). Below, we briefly discuss some analogous crust from the North American SCR as a detailed example of the power of the domains approach.

The Archaean and Palaeoproterozoic core of the North American continent (including the Superior, Wyoming, Hearne, Rae, Nain and Slave Provinces and interstitial Proterozoic orogenic belts) (Hoffman 1989) can be considered analogous in terms of crustal properties to D1. This core is fringed on the southern and eastern sides by reactivated Proterozoic mobile belts and orogenic crust analogous to D3 (e.g. the Yavapai-Mazatzal Province and Grenville Belt) (Davis & Bump 2009). Further to the southeast Palaeozoic fold belts similar to those in D4 extend to coastal plain east of the Appalachian Orogenic Belt (Wheeler & Frankel 2000). Mesozoic aulacogens extending through the Palaeozoic and into the Precambrian shield (e.g. the Reelfoot Rift, the Southern Oklahoma aulacogen, the Ottawa Rift, the Saguenay Graben) can be considered similar to D5. The main orientation of the aulacogen with respect to the prevailing stress field might be used to further refine the expectation of analogous crustal response. For instance, the small angle between the major structures of the Reelfoot Rift and the SH_{Max} is similar to the relationship expressed in the Gippsland Basin. The Reelfoot Fault (Van Arsdale *et al.* 1998) and faults such as the Haunted Hill Fault or Morwell Faults (Figure 27) are well suited for analogue studies.

The Mesozoic rifted passive margin of the eastern United States, containing the Charleston source zone (Johnston 1996; Wheeler & Frankel 2000; Talwani & Schaeffer 2001), might be considered analogous with parts of D6 (and perhaps the Sorell basin in D5), or perhaps D7. However, in contrast to our observations, Wheeler (1995) noted that Palaeozoic (Iapetan) passive margin crust to the west of and beneath Appalachian orogenic crust appears to be more active than Mesozoic rifted margin to the east, at least in terms of the historic seismic record.

Conclusions

Herein we have presented a review of knowledge pertaining to the neotectonic deformation of the Australian continent over the last 5-10 Ma (the Neotectonic Era). We propose by extrapolation from the five historic surface rupturing earthquakes, the small body of palaeoseismic data, and in the absence of compelling evidence to the contrary (cf. Demoulin 2004), that neotectonic deformation occurring at a scale of several tens of kilometres or less can be related to discrete seismogenic movements on faults. Based upon perceived differences in character of the seismogenic faults across the continent, and guided by variations in the geologic and geophysical makeup of the crust, we propose six onshore Neotectonic Domains (Figure 33). A seventh offshore domain is defined based upon analogy with the eastern United States. A simple statistical analysis of three semi-quantitative parameters of the neotectonic fault dataset (length, neotectonic slip, and fault density) reveals that, while the faults within each domain are not statistically distinguishable with respect to individual characters, combinations of the central tendencies of the data are sufficiently distinct so as to justify the domains model. For example, faults occurring within Proterozoic (D3) or Palaeozoic mobile (D4, D6) belts tend to be longer than faults elsewhere, and faults in central and western Australia (D1, D3) tend to have accumulated less neotectonic slip than those in eastern Australia (D2, D4, D5). Furthermore, faults in crust that has been rifted (D2, D6, D5) appear to be more closely spaced than those in non-extended crust. These characters relate to the fundamental properties of the crust that is being deformed, which might be seen as a consequence of deformation occurring on pre-existing faults in the intraplate setting (e.g. Hills 1961).

Variations in spatial and temporal patterns in large earthquake occurrence might therefore be inferred between domains. Scarps in D1 appear to be relatively short, randomly arranged, and spaced such that direct interactions between faults are unlikely (see also Table 2). However, the three historic surface ruptures at Meckering, Calingiri and Cadoux suggest that surface rupture occurs in response to unloading of hundred-kilometre scale sections of crust. Strain concentration at some margins of D1 cratons is evident in a more belt-like arrangement of scarps. Within Proterozoic and Palaeozoic mobile belt domains (D3, D4 and to some extent D6) linear arrangement of scarps is apparent, with the potential for direct interaction. Extended domains (D2, D5 and to some extent D6) are characterised by *en echelon* and anastomosing networks of faults where interaction between ruptures is highly likely. Episodic rupture behaviour has been noted in all domains where detailed palaeoseismic data is available (D1, D2, D4, D5) (see also Figure 42). Variations between domains can be seen in the number of ruptures and the interval between ruptures in an active period, and in the inter-active period intervals. This behaviour in individual faults seems to be mimicked at a larger scale in that punctuated episodes of deformation have been noted within deforming regions (e.g. Quigley *et al.* 2010), and perhaps relates to subtle changes in stress forcings at the plate margins (c.f. Sandiford *et al.* 2004; Sandiford & Quigley 2009).

Despite the difficulties presented by non-Poissonian rupture behaviour, neotectonic faults in the SCR context have the demonstrated potential to significantly impact probabilistic seismic hazard assessments at recurrence intervals relevant to engineered structures (Somerville *et al.* 2008). The points critical to understanding the hazard posed by SCR faults, and modelling this hazard probabilistically, can be summarised as: 1) is the fault in question about to enter an active period, in the midst of an active period, or in a quiescent period; 2) how many large events might constitute an active period, and how many ruptures has the fault generated so far in its current active period (should it be in one); and 3) what is the "mean" recurrence interval in an active period, and what is the variability around this mean? This "mean" can be incorporated statistically into probabilistic seismic hazard assessments (e.g. Stirling *et al.* 2011).

Our simple statistical analysis of fault length data allows for preliminary estimates of M_{max} to be assigned to each domain (Table 3). These are consistent with palaeoseismic data and with the more rigorous analysis of Leonard & Clark (2010). This is a powerful result applicable to future seismic hazard mapping in Australia, and also meets a need identified by the seismic hazard community for M_{max} estimates for analogous crustal regions elsewhere in the world (Wheeler 2009b). The results suggest that M_{max} values of less than $M_w = 7.0$ for any SCR region worldwide is non-conservative (cf. Gaull *et al.* 1990; Johnston 1994b; Wheeler 2009b).

Acknowledgements

Tish Tuttle (Tuttle and Associates), Paul Somerville (URSCorp) and Russell Wheeler (U.S.G.S.) are thanked for constructive reviews that have greatly improved this compilation. Matt Cupper of the University of Melbourne is thanks for many hours spent preparing and analysing samples used to produce the unpublished OSL data presented here. Tim Barrows of Exeter University is thanked for preparation and analysis of the Gippsland and Cape Range CRN samples.

References

ABEL R. S. 1985. Geology of the Lake George Basin, N.S.W. *Bureau of Mineral Resources, Geology and Geophysics Record 1985/4*, 57p.

ADAMS J., WETMILLER R., HASEGAWA H. & DRYSDALE J. 1991. The first surface faulting from a historical earthquake in North America. *Nature* **352**, 617619.

ALLEY N. F. & LINDSAY J. M. 1995. Chapter 10 - Tertiary. *In:* Drexel J. F. & Preiss W. V. eds. *The geology of South Australia, Volume 2 - The Phanerozoic* Geological Society of South Australia Bulletin 54, Adelaide.

ANDREWS E. C. 1910. Geographical unity of eastern Australia in late and post Tertiary time with applications to biological problems. *Journal and Proceedings of the Royal Society of New South Wales* **44**, 420-480.

BAILLIE P. W., CORBETT K. D. & GREEN G. R. 1985. Geological Atlas 1:50 000 series. Sheet 57(7913N). Strahan. . *Explanatory Report, Geological Survey of Tasmania*.

BAILLIE P. W. & JACOBSON E. 1995. Structural evolution of the Carnarvon Terrace, Western Australia. *Australian Petroleum Production and Exploration Journal* **35**, 321-331.

BALASUBRAHMANYAN M. N. 2006. Geology and tectonics of India: an overview. *International Association for Gondwana Research Memoir* **9**, 204pp.

BARBER P. 1988. The Exmouth Plateau deep water frontier: a case study. *In:* Purcell P. G. & Purcell R. R. eds. *The North West Shelf, Australia. Proceedings of the Petroleum Exploration Society of Australia Symposium*, pp. 173-187. Perth.

BARTON C. M. 1981. regional stress and structure in relation to brown coal open cuts of the Latrobe valley, Victoria. *Journal of the Geological Society of Australia* **28**, 333-339.

BEAVIS F. C. 1960. The Tawonga Fault, northeast Victoria. *Proceedings of the Royal Society of Victoria* **72**, 95-100.

BEAVIS F. C. 1975. Engineering geology of 'd' power station Yallourn, Australia. *Quarterly Journal of Engineering Geology and Hydrogeology* **8**, 103-117.

BEAVIS F. C. & BEAVIS J. C. 1976. Structural geology in the Kiewa region of the Metamorphic Complex, North-East Victoria. *Proceedings of the Royal Society of Victoria* **88**, 66-75.

BELPERIO A. P. 1995. Quaternary. In: Drexel J. F. & Preiss W. V. eds. The Geology of South Australia, Volume 2, The Phanerozoic. *Geological Survey of South Australia Bulletin* **54**, 219–281.

BELTON D. X., BROWN R. W., KOHN B. P., FINK D. & FARLEY K. A. 2004. Quantitative resolution of the debate over antiquity of the central Australian landscape: implications for the tectonic and geomorphic stability of cratonic interiors. *Earth and Planetary Science Letters* **219**, 21-34.

BEN-ZION Y., DAHMEN K., LYAKHOVSKY V., ERTAS D. & AGNON A. 1999. Self-driven mode switching of earthquake activity on a fault system. *Earth and Planetary Science Letters* **172**, 11-21.

BERRY R. F., STEELE D. A. & MEFFRE S. J. M. 2008. Proterozoic metamorphism in Tasmania: Implications for tectonic reconstructions. *Precambrian Research* **166**, 387-396.

BETTS P. G. & GILES D. 2006. The 1800–1100 Ma tectonic evolution of Australia. *Precambrian Research* **144**, 92-125.

BHATT K. M., HORDT A. & SANTOSH K. 2009. Seismicity analysis of the Kachchh aftershock zone and tectonic implication for 26 Jan 2001 Bhuj earthquake. *Tectonophysics* **465** 75-83.

BIASI G. P. & WELDON R. J., II 2006. Estimating Surface Rupture Length and Magnitude of Paleoearthquakes from Point Measurements of Rupture Displacement. *Bulletin of the Seismological Society of America* **96**, 1612-1623.

BIERMAN P. R. & CAFFEE M. 2002. Cosmogenic exposure and erosion history of Australian bedrock landforms. *GSA Bulletin* **114**, 787-803.

BINKS P. J. 1972. Late Cainozoic uplift of the Ediacara Range, South Australia. *Proceedings of the Australian Institute of Minerals and Metallurgy* **243**, 47-55.

BISHOP P. 1988. The eastern highlands of Australia; the evolution of an intraplate highland belt. *Progress in Physical Geography* **12**, 159-182.

BISHOP P. 1995. Landscape evolution and tectonics in southeastern Australia; discussion. *AGSO Journal of Australian Geology and Geophysics. 16; 3, Pages 315-317. 1995.: Australian Geological Survey Organization. Canberra, A.C.T., Australia. 1995.*

BISHOP P. 2007. Long-term landscape evolution: linking tectonics and surface processes. *Earth Surface Processes and Landforms* **32**, 329-365.

BISHOP P. & BROWN R. 1992. Denudational isostatic rebound of intraplate highlands; the Lachlan River valley, Australia. *Earth Surface Processes and Landforms. 17; 4, Pages 345-360. 1992.: Wiley & Sons. Chichester-New York, United Kingdom. 1992.*

BISHOP P. & GOLDRICK G. 2000. Geomorphological evolution of the East Australian continental margin. *In:* Summerfield M. A. ed. *Geomorphology and Global Tectonics*, pp. 227-255. Wiley, Chichester.

BISHOP P., HUNT P. & SCHMIDT P. W. 1982. Limits to the age of the Lapstone Monocline, N.S.W.; a palaeomagnetic study. *Journal of the Geological Society of Australia* **29**, 319-326.

BISHOP P., YOUNG R. W. & MCDOUGALL I. 1985. Stream profile change and longterm landscape evolution; early Miocene and modern rivers of the East Australian highland crest, central New South Wales, Australia. *Journal of Geology* **93**, 455-474.

BLAKE D. H. 2000. Geological Regions (National Geoscience Dataset). *Geoscience Australia, Canberra, Australia. ANZLIC ID ANZCW0703002397. Data set accessed November 2009 at https://www.ga.gov.au/products/servlet/controller?event=GEOCAT_DETAILS&catno=32366*.

BLEVIN J. & CATHRO D. 2008. Australian southern margin synthesis. *Internal Geoscience Australia report compiled by FrOGTech* **GA707**, 104.

BLEVIN J. E., TRIGG K. R., PARTRIDGE A. D., BOREHAM C. J. & LANG S. C. 2005. Tectonostratigraphy and potential source rocks of the Bass Basin. *APPEA Journal* **2005**, 601-622.

BLEWETT R. S. & WILFORD J. R. 1996. *Hann River Geology second edition (1:250 000 scale map): Sheet SD54/16.* . Australian Geological Survey Organisation.

BOLGER P. F. 1991. Lithofacies variations as a consequence of Late Cainozoic tectonic and palaeoclimatic events in the onshore Gippsland Basin. *Geological Society of Australia, Special Publication* **No. 18**, 158-180.

BOREHAM C. J., BLEVIN J. E., DUDDY I., NEWMAN J., LLU K., MIDDLETON H., MACPHAIL M. K. & COOK A. C. 2002. Exploring the potential for oil generation, migration and accumulation in Cape Sorell-1. Sorell Basin, offshore west Tasmania. *APPEA Journal* **2002**, 405-435.

BOURMAN R. P., BELPERIO A. P., MURRAY-WALLACE C. V. & CANN J. H. 1998. A last interglacial embayment fill at Normanville, South Australia, and its neotectonic implications. *Transactions of the Royal Society of South Australia* **122**, 63-67.

BOURMAN R. P. & LINDSAY J. M. 1989. Timing, extent and character of late Cainzoic faulting on the eastern margin of the Mt Lofty Ranges, South Australia. *Transactions of the Royal Society of South Australia.* **113**, 63-67.

BOWLER J. M. 1978. Quaternary climate an tectonics in the evolution of the Riverine Plain, south eastern Australia. *In:* Williams M. A. J. ed. *Landform Evolution in Australasia*, pp. 70-112. ANU Press, Canberra.

BOWLER J. M. & HARFORD L. B. 1966. Quaternary tectonics and the evolution of the Riverine Plain near Echuca, Victoria. *Geological Society of Australia Journal* **13**, 339-354.

BRANAGAN D. F. & PEDRAM H. 1990. The Lapstone Structural Complex, New South Wales. *Australian Journal of Earth Sciences* **37**, 23-36.

BRAUN J., BURBIDGE D., GESTO F., SANDIFORD M., GLEADOW A., KOHN B. & CUMMINS P. 2009. Constraints on the current rate of deformation and surface uplift of the Australian continent from a new seismic database and low-T thermochronological data. *Australian Journal of Earth Sciences* **56**, 99-110.

BROWN A. V. & GIBSON G. 2004. A multi-tiered earthquake hazard model for Australia. *Tectonophysics* **390**, 25-43.

BROWN C. M. & STEPHENSON A. E. 1991. Geology of the Murray Basin, southeastern Australia. *Bureau of MIneral Resources, Geology & Geophysics Australia Bulletin* **235**, 430p.

BROWNE W. R. 1967. Geomorphology of the Kosciusko block and its north and south extensions. *Proceedings of the Linnean Society of New South Wales* **92**, 117-144.

BURBIDGE D. R. 2004. Thin plate neotectonic models of the Australian plate. *Journal of geophysical Research* **109**, B10405, doi:10410.11029/12004JB003156.

BURKE K. 1977. Aulocogens and continental breakup. *Annual Review of Earth and Planetary Sciences* **5**, 371-396.

BURNE R. V. & GRAHAM T. L. 1995. Coastal Environment Geoscience of Cape York Peninsula. Final report on Project NR14 - Coastal Environment Geoscience Survey for Cape York.

CANAVAN F. 1988. Deep lead gold deposits of Victoria. *Geological Society of Victoria* **Bulletin 62**, 101p.

CASKEY S. J. & WESNOUSKY S. G. 1997. Static stress changes and earthquake triggering during the 1954 Fairview Peak and Dixie Valley earthquakes, central Nevada. *Bulletin of the Seismological Society of America* **87**, 521-527.

CAWOOD P. A. & BUCHAN C. 2007. Linking accretionary orogenesis with supercontinent assembly. *Earth Science Reviews* **82**, 217-256.

CAYLEY R. A., TAYLOR D. H., VANDENBERG A. H. M. & MOORE D. H. 2002. Proterozoic – Early Palaeozoic rocks and the Tyennan Orogeny in central Victoria: the Selwyn Block and its tectonic implications *Australian Journal of Earth Sciences* **49**, 225-254.

CELERIER J., SANDIFORD M., HANSEN D. L. & QUIGLEY M. 2005. Modes of active intraplate deformation, Flinders Ranges, Australia. *Tectonics* **24**, doi:10.029/2004&C001679.

CHAMPION J., MUELLER K., TATE A. & GUCCIONE M. J. 2001. Geometry, numerical models and revised slip rate for the Reelfoot Fault and trishear fault-propagation fold, New Madrid seismic zone. *Engineering Geology* **62**, 31-49.

CHAPPELL J. 2006. Australian landscape processes measured with cosmogenic nuclides. *In:* Pillans B. ed. *Regolith Geochronology and Landscape Evolution*, pp. 19-26. CRC LEME, Perth.

CHÉRY J., CARRETIER S. & RITZ J. F. 2001. Postseismic stress transfer explains time clustering of large earthquakes in Mongolia. *Earth and Planetary Science Letters* **194**, 277-286.

CHÉRY J. & VERNANT P. 2006. Lithospheric elasticity promotes episodic fault activity [rapid communication]. *Earth and Planetary Science Letters* **243**, 211-217.

CLARK D. 2005. A preliminary seismicity model for southwest Western Australia based on neotectonic data. *In: Earthquake Engineering in Australia Paper 22* Australian Earthquake Engineering Society Conference, Albury.

CLARK D. 2006. Neotectonics-based intraplate seismicity models and seismic hazard. Paper presented at Australian Earthquake Engineering Society Meeting, Albury, NSW (unpubl.).

CLARK D. 2009. Potential geologic sources of seismic hazard in the Sydney Basin: proceedings volume of a one day workshop, April 2005. *Geoscience Australia Record* **2009/011**, 115pp.

CLARK D. 2010. Identification of Quaternary scarps in southwest and central west Western Australia using DEM-based hill shading: application to seismic hazard assessment and neotectonics. *International Journal of Remote Sensing* **31**, 6297-6325.

CLARK D., DENTITH M., WYRWOLL K. H., YANCHOU L., DENT V. & FEATHERSTONE C. 2008a. The Hyden fault scarp, Western Australia: paleoseismic evidence for repeated Quaternary displacement in an intracratonic setting. *Australian Journal of Earth Sciences* **55**, 379-395.

CLARK D. & MCCUE K. 2003. Australian Palaeoseismology: towards a better basis for seismic hazard estimation. *Annals of Geophysics* **46**, 1087-1105.

CLARK D., MCPHERSON A. & TOMKINS K. 2008b. Re-evaluating the seismic hazard potential of the northern Lapstone Structural Complex. Paper presented at Australian Earthquake Engineering Society Conference, Ballarat, Victoria (unpubl.).

CLARK D., MCPHERSON A. & TOMKINS K. 2009. The role of neotectonism in the recent landscape evolution of the Eastern Blue Mountains, NSW. Paper presented at 7th international conference on geomorphology (ANZIAG), Melbourne, Australia (unpubl.).

CLARK D. & VAN DISSEN R. 2006. Characterisation of Australian intraplate active faulting with special mention of the Lake Edgar fault, Tasmania. *GNS Science Consultancy Report* **2006/099**, 66p.

CLARK D., VAN DISSEN R., CUPPER M., COLLINS C. & PRENDERGAST A. 2007. Temporal clustering of surface ruptures on stable continental region faults: a case study from the Cadell Fault scarp, south eastern Australia. Paper presented at Australian Earthquake Engineering Society Conference, Wollongong (unpubl.).

CLARK D. J. 2004. Reconnaissance of Recent fault scarps in the Mt Narryer region, Western Australia. *Geoscience Australia unpublished report*, 31p.

CLARK D. J., CUPPER M., SANDIFORD M. & KIERNAN K. 2010. Style and timing of late Quaternary faulting on the Lake Edgar Fault, southwest Tasmania, Australia: implications for hazard assessment in intracratonic areas. *Geological Society of America Special Publication "Palaeoseismology"* **in press**.

CLARK D. J., CUPPER M., SANDIFORD M. & KIERNAN K. 2011. Style and timing of late Quaternary faulting on the Lake Edgar Fault, southwest Tasmania, Australia: implications for hazard assessment in intracratonic areas. *Geological Society of America Special Publication 479: Geological Criteria for Evaluating Seismicity Revisited: Forty Years of Paleoseismic Investigations and the Natural Record of Past Earthquakes (edited by Franck A. Audemard M., Alessandro Michetti, and James P. McCalpin)* **Chapter 5**.

CLARK D. J. & LEONARD M. 2003. Principal stress orientations from multiple focal plane solutions: new insight in to the Australian intraplate stress field. *In:* Hillis R. R. & Muller D. eds. *Evolution and dynamics of the Australian Plate*, pp. 91-105. **22** Geol. Soc. Australia and Geol. Soc. America Joint Special Publication.

CLARK D. J. & MCPHERSON A. 2009. Potential sources of strong ground shaking within ~200 km of the Otways carbon capture and storage site. *Geoscience Australia unpublished report (prepared for GNS)*.

CLOETINGH S., BEEKMAN F., ZIEGLER P. A., VAN WEES J.-D. & SOKOUTIS D. 2008. Post-rift compressional reactivation potential of passive margins and extensional basins. *In:* Johnson H., Dore´ A. G., Gatliff R. W., Holdsworth R., Lundin E. R. & Ritchie J. D. eds. *The Nature and Origin of Compression in Passive Margins*, pp. 27-70. **306** Geological Society, London, Special Publications.

CLOETINGH S., ZIEGLER P. A., BEEKMAN F., ANDRIESSEN P. A. M., HARDEBOL N. & DEZES P. 2005. Intraplate deformation and 3D rheological structure of the Rhine Rift System and adjacent areas of the northern Alpine foreland. *International Journal of Earth Science* **94**, 758-778.

COBLENTZ D. D., SANDIFORD M., RICHARDSON R. M., SHAOHUA Z. & HILLIS R. 1995. The origins of the intraplate stress field in continental Australia. *Earth and Planetary Science Letters* **133**, 299-309.

COBLENTZ D. D., ZHOU S., HILLIS R. R., RICHARDSON R. M. & SANDIFORD M. 1998. Topography boundary forces and the Indo-Australian intraplate stress field. *Journal of Geophysical Research* **103**, 919-938.

COLHOUN E. A. 1985. Glaciations of the West Coast Range, Tasmania. *Quaternary Research* **24**, 39-59.

COLLINS A. S. & PISAREVSKY S. A. 2005. Amalgamating eastern Gondwana: The evolution of the Circum-Indian Orogens. *Earth Science Reviews* **71**, 229-270.

COLLINS C. D. N., DRUMMOND B. J. & NICOLL M. G. 2003. Crustal thickness patterns in the Australian continent. *ds Hillis R.R. & Muller D, Evolution and dynamics of the Australian Plate, Geological Society of Australia Special Publication.* **22**, 121-128.

COPPERSMITH K. J. 1994. Conclusions regarding maximum earthquake assessment. *In:* Johnston A. C., Coppersmith K. J., Kanter L. R. & Cornell C. A. eds. *The earthquakes of stable continental regions-v. 1, assessment of large earthquake potential*, pp. 6-1 - 6-24. Electric Power Research Institute, Palo Alto, California.

CORNELL C. A. 1994. Statistical analysis of maximum magnitudes. *In:* Johnston A. C., Coppersmith K. J., Kanter L. R. & Cornell C. A. eds. *The earthquakes of stable continental regions-v. 1,* *assessment of large earthquake potential*, pp. 5-1-5-27. Electric Power Research Institute, Palo Alto, California.

COVENTRY R. J. 1976. Abandoned shorelines and the late Quaternary history of Lake George, New South Wales. *Journal of the Geological Society of Australia* **23**, 249-273.

COWIE P. A. & ROBERTS G. P. 2001. Constraining slip rates and spacings for active normal faults. *Journal of Structural Geology* **23**, 1901-1915.

CRAIG J., DOWNEY J. W., GIBBS A. D. & RUSSELL J. R. 1984. The application of Landsat imagery in structural interpretation of the Canning Basin,WA. *in Purcell, P.G. (ed.), The Canning Basin,W.A.: Proceedings of the Petroleum Exploration Society of Australia Symposium, Perth*, 57-72.

CRAWFORD A. R. 1965. The geology of Yorke Peninsula. . *South Australia. Geological Survey Bulletin* **39**.

CRONE A. J., DE MARTINI P. M., MACHETTE M. N., OKUMURA K. & PRESCOTT J. R. 2003. Paleoseismicity of Two Historically Quiescent Faults in Australia: Implications for Fault Behavior in Stable Continental Regions. *Bulletin of the Seismological Society of America* **93**, 1913-1934.

CRONE A. J. & LUZA K. V. 1990. Style and timing of Holocene syrface faulting on the Meers Fault, southwestern Oklahoma. *Geological Society of America Bulletin* **102(1)**, 1-17.

CRONE A. J. & MACHETTE M. N. 1995. Holocene faulting on the Cheraw Fault, southeastern Colorado another hazardous late Quaternary fault in the stable continental interior. *EOS supplement (November 7, 1995)* **76**, F362.

CRONE A. J. & MACHETTE M. N. 1997. The temporal variability of surface-faulting earthquakes in stable continental regions; a challenge to seismic-hazard assessments. *Abstracts with Programs - Geological Society of America* **29**, 71.

CRONE A. J., MACHETTE M. N. & BOWMAN J. R. 1992. Geologic investigations of the 1988 Tennant Creek, Australia, earthquakes - implications for paleoseismicity in stable continental regions. *United States Geological Survey Bulletin* **2032-A**, 51p.

CRONE A. J., MACHETTE M. N. & BOWMAN J. R. 1997. Episodic nature of earthquake activity in stable continental regions revealed by palaeoseismicity studies of Australian and North American Quaternary faults. *Australian Journal of Earth Sciences* **44**, 203-214.

CROSTELLA A. & IASKY R. P. 1997. Structural interpretation and hydrocarbon potential of the Giralia area, Carnarvon Basin. *Western Australia Geological Survey* **Report 52**, 38p.

CUMMINGS A. M., HILLIS R. R. & TINGATE P. R. 2004. New perspectives on the structural evolution of the Bass Basin: implications for petroleum prospectivity. *Proceedings of the PESA Eastern Australasian Basins Symposium II, Adelaide, 19–22 September, 2004*, 133-149.

DAVIS G. H. & BUMP A. P. 2009. Structural geologic evolution of the Colorado Plateau. *In:* Kay S. M., Ramos V. A. & Dickinson W. R. eds. *Backbone of the Americas: Shallow Subduction, Plateau Uplift, and Ridge and Terrane Collision* pp. 99-124. **204** Geological Society of America Memoir.

DAWSON J., CUMMINS P., TREGONING P. & LEONARD M. 2008. Shallow intraplate earthquakes in Western Australia observed by Interferometric Synthetic Aperture Radar. *Journal of Geophysical Research* **113**, doi:10.1029/2008JB005807.

DEMOULIN A. 2004. Reconciling geodetic and geological rates of vertical crustal motion in intraplate regions. *Earth and Planetary Science Letters* **221**, 91-101.

DENMAN P. D. & VAN DE GRAAFF W. J. E. 1976. Emergent Quaternary marine deposits in the Lake Macleod area, W.A. Geological Survey of Western Australia, Perth.

DENTITH M. C., CLARK D. J. & FEATHERSTONE W. E. 2009. Aeromagnetic mapping of Precambrian geological structures that controlled the 1968 Meckering Earthquake (Ms 6.8): Implications for intraplate seismicity in Western Australia. *Tectonophysics* **475**, 544-553.

DENTITH M. C., DENT V. F. & DRUMMOND B. J. 2000. Deep crustal structure in the southwestern Yilgarn Craton, Western Australia. *Tectonophysics* **325**, 227-255.

DENTITH M. C. & FEATHERSTONE W. E. 2003. Controls on intra-plate seismicity in southwestern Australia. *Tectonophysics* **376**, 167-184.

DICKINSON J. A., WALLACE M. W., HOLDGATE G. R., DANIELS J., GALLAGHER S. J. & THOMAS L. 2001. Neogene tectonics in SE Australia: implications for petroleum systems. *The APPEA Journal* **41**, 37–52.

DICKINSON J. A., WALLACE M. W., HOLDGATE G. R., GALLAGHER S. J. & THOMAS L. 2002. Origin and timing of the Miocene-Pliocene unconformity in southeast Australia. *Journal of Sedimentary Research* **72**, 288-303.

DIREEN N. G. & CRAWFORD A. J. 2003. The Tasman Line: where is it, what is it, and is it Australia's Rodinian breakup boundary? *Australian Journal of Earth Sciences* **50**, 491-502.

DOYLE H. A. 1971a. Australian seismicity and plate boundaries. *Nature Physical Science* **234**, 174-175.

DOYLE H. A. 1971b. Seismicity and structure in Australia. *Bulletin of the Royal Society of New Zealand* **9**, 149-152.

DREXEL J. F., PREISS W. V. & PARKER A. J. 1993. The geology of South Australia. Vol. 1, The Precambrian. *South Australia. Geological Survey Bulletin* **54**, 249p.

DRUMMOND B. J. & MOHAMED R. E. 1986. Crustal structure in the Southwest Seismic Zone, Western Australia. *Abstracts - Geological Society of Australia. 15; Pages 59-60. 1986.: Geological Society of Australia. Sydney, N.S.W., Australia. 1986.*

DUBIENIECKI C. D. & HILL S. M. 2007. Constraints on the Four Mile Uranium Mineralisation, resulting from neotectonic activity in the northern Flinders Ranges, SA. Paper presented at 5th Sprigg Symposium, November 2007: Regolith Mineral Deposits and Environment, Geological Society of Australia Abstracts No.87, pp.15-18.(unpubl.).

DUNHAM M. H. R. 1992. The geomorphological nature and age of the linear escarpments of northeast Eyre Peninsula. University of Adelaide, SA. (unpubl.).

DYKSTERHUIS S. & MÜLLER R. D. 2008. Cause and evolution of intraplate orogeny in Australia. *Geology* **36**, 495-498.

EDWARDS J., LEONARD J. G., PETTIFER G. R. & MCDONALD P. A. 1996. Colac 1 : 250 000 map geological report. *Geological Survey of Victoria. Report* **98**, 170p.

ESTRADA B. 2009. Neotectonic and palaeoseismological studies in the southwest of Western Australia. The University of Western Australia, Perth (unpubl.).

ETHERIDGE M. A., MCQUEEN H. W. S. & LAMBECK K. 1991. The role of intraplate stress in Tertiary (and Mesozoic) deformation of the Australian continent and its margins: a key factor in petroleum trap formation. *Exploration Geophysics* **22**, 123-128.

EVERINGHAM I. B. 1965. The crustal structure of the southwest of Western Australia. *BMR Record* **1965/97**.

EVERINGHAM I. B. & GREGSON P. J. 1996. Magnetometer traverses across aeromagnetic anomalies near recent earthquake fault scarps in southwestern Australia. *AGSO Record* **1996/55**, 33p.

FAIRBRIDGE R. W. 1948. Geology of the country around Waddamana, Central Tasmania. *Papers & Proceedings of the Royal Society of Tasmania*, 111-149.

FITZSIMMONS K., RHODES E., MAGEE J. & BARROWS T. T. 2009. The timing of linear dune activity in the Strzelecki and Tirari Deserts , Australia. *Quaternary Science Reviews* **DOI: 10.1016/j.quascirev.2007.06.010.**, (in press)

FITZSIMONS I. C. W. 2003. Proterozoic basement provinces of southern and southwestern Australia, and their correlation with Antarctica. *In: Proterozoic East Gondwana: Supercontinent Assembly and Breakup (eds Yoshida, M., Windley, B. F. & Dasgupta, S.). Geological Society of London Special Publication* **206**, 93-130.

FLOTTMANN T. & COCKSHELL C. D. 1996. Palaeozoic basins of southern South Australia: New insights into their structural history from regional seismic data. *Australian Journal of Earth Sciences* **43**, 45-55.

FRANKEL A., MUELLER C., BARNHARD T., PERKINS D., LEYENDECKER E. V., DICKMAN N., HANSON S. & HOPPER M. 1996. National Seismic Hazard Maps, June 1996 Documentation. *U.S. geological Survey Open File Report 96532*.

FRIEDRICH A. M., WERNICKE B. P., NIEMI N. A., BENNETT R. A. & DAVIS J. L. 2003. Comparison of geodetic and geologic data from the Wasatch region, Utah, and implications for the spectral character of Earth deformation at periods of 10 to 10 million years. *Journal of Geophysical Research* **108 (B4)**, doi:10.1029/2001JB000682.

FROGTECH 2005. The OZ SEEBASE Project: A new view of Australia's Phanerozoic basins. *PESA News* **77**.

FUJIOKA T., CHAPPELL J., HONDA M., YATSEVICH I., FIFIELD K. & FABEL D. 2005. Global cooling initiated stony deserts in central Australia 2–4 Ma, dated by cosmogenic 21Ne-10Be. *Geology* **33**, 993-996.

GANGOPADHYAY A. & TALWANI P. 2003. Symptomatic features of intraplate earthquakes. *Seismological Research Letters* **74**, 863-883.

GARDNER T., WEBB J., PEZZIA C., AMBORN T., TUNNELL R., FLANAGAN S., MERRITTS D., MARSHALL J., FABEL D. & CUPPER M. L. 2009. Episodic intraplate deformation of stable continental margins: evidence from Late Neogene and Quaternary marine terraces, Cape Liptrap, Southeastern Australia. *Quaternary Science Reviews* **28**, 39-53.

GAULL B. A. & MICHAEL-LEIBA M. O. 1987. Probabilistic earthquake risk maps of southwest Western Australia. *BMR Journal of Australian Geology and Geophysics* **10**, 145-151.

GAULL B. A., MICHAEL-LEIBA M. O. & RYNN J. M. W. 1990. Probabilistic earthquake risk maps of Australia. *Australian Journal of Earth Sciences* **37**, 169-187.

GIBSON D. & BOSTON K. 2008. Neotectonics, salinity, palaeoclimates and volcanism. *CRC LEME Open File Report 235*, 71.

GIBSON D. L. 2007. Potassium-argon ages of Late Mesozoic and Cainozoic igneous rocks of Eastern Australia. CRC LEME, Perth.

GIBSON D. L. & SMART J. 1973. *Jardine River Geology first edition (1:250 000 scale map): Sheet SC54/15.* . Bureau of Mineral Resources Canberra.

GIBSON G. 1995. Earthquake hazard in Australia. *In:* Heinrichs P. & Fell R. eds. *Acceptable Risks for Major Infrastructure*, pp. 135- 144. A.A. Balkema, Sydney, NSW.

GLEN R. A. 2005. The Tasmanides of Eastern Australia. *In:* Vaughan A. P. M., Leat P. T. & Pankhurst R. J. eds. *Terrane Processes at the Margins of Gondwana*, pp. 23-96. **GSL Special Publications** The Geological Society of London.

GLOE C. S. 1960. The geology of the Latrobe Valley coal field. *Proceedings of the Australiasian Institute of Mining and Metallurgy* **194**, 57-125.

GOLEBY B. R., RATTENBURY M. S., SWAGER C. P., DRUMMOND B. J., WILLIAMS P. R., SHERATON J. W. & HEINRICH C. A. 1993. Archaean crustal structure from seismic reflection profiling, Eastern Goldfields, Western Australia. *Australian Geological Survey Organisation Record* **1993/15**.

GORDON F. R. & LEWIS J. D. 1980. The Meckering and Calingiri earthquakes October 1968 and March 1970. *Western Australia Geological Survey Bulletin* **126**, 229p.

GRAY D. R., WILSON C. J. L. & BARTON T. J. 1991. Intracrustal detachments and implication for crustal evolution within the Lachlan fold belt, southeastern Australia. *Geology* **19**, 574-577.

GREEN M. 2007. The Structure and Kinematics of the Concordia Fault: Constraining the age of the Indo-Australian Plate stress field. B.Sc. (Hons) thesis, The University of Melbourne, Melbourne (unpubl.).

GUCCIONE M. J., CHAMPION J. A. & MUELLER K. J. 1999. Dating deformation and slip rates along Reelfoot scarp, New Madrid Seismic Zone using radiocarbon dates from an abandoned Mississippi River meander. *Abstracts with Programs - Geological Society of America* **31**, 302.

HAINES P. W., HAND M. & SANDFORD M. 2001. Palaeozoic syn-orogenic sedimentation in central and northern Australia: a review of distribution and timing of intracontinental orogens. *Australian Journal of Earth Sciences* **48**, 911-928.

HALL L., DIMER F. & SOMERVILLE P. 2007. A Spatially Distributed Earthquake Source Model for Australia. Paper presented at 2007 Annual Meeting of the Australian Earthquake Engineering Society(unpubl.).

HALPIN J. A., CRAWFORD A. J., DIREEN N. G., COFFIN M. F., FORBES C. J. & BORISSOVA I. 2008. Naturaliste Plateau, offshore Western Australia: A submarine window into Gondwana assembly and breakup. *Geology* **36**, 807-810.

HARPER K. L. 2002. Geologic and geomorphic applications of aster satellite imagery, Northern Flinders Ranges, South Australia B.Sc. (Hons) thesis, The University of Melbourne Melbourne (unpubl.).

HARRIS W. M. J. 1938. The Physiography of the Echuca District. *Proceedings of the Royal Society of Victoria* **51(1)**, 45-60.

HEARTY D. J., ELLIS G. K. & WEBSTER K. A. 2002. Geological history of the western Barrow Sub-basin: implications for hydrocarbon entrapment at Woollybutt and surrounding oil and gas fields. *In:* Keep M. & Moss S. J. eds. *The Sedimentary Basins of Western Australia 3. Proceedings of the Petroleum Exploration Society of Australia Symposium*, pp. 577-598. Perth.

HEIMSATH A. M., CHAPPELL J., DIETRICH W. E., NISHIIZUMI K. & FINKEL R. C. 2000. Soil production on a retreating escarpment in southeastern Australia. *Geology* **28**, 787-790.

HEIMSATH A. M., CHAPPELL J., DIETRICH W. E., NISHIIZUMI K. & FINKEL R. C. 2001. Late Quaternary erosion in southeastern Australia: a field example using cosmogenic isotopes. *Quaternary International* **83-85**, 169-185.

HEMPHILL-HALEY M. A. & WELDON R. J. 1999. Estimating prehistoric earthquake magnitude from point measurements of surface rupture. *Bulletin of the Seismological Society of America* **89**, 1264-1279.

HERTZEL R. & HAMPEL A. 2005. Slip rate variations on normal faults during glacial-interglacial changes in surface loads. *Nature* **435**, 81-84.

HILL K. A., COOPER G. T., RICHARDSON M. J. & LAVIN C. J. 1994. Structural framework of the eastern Otway Basin: Inversion and interaction between two major structural provinces. *Exploration Geophysics* **25**, 79-87.

HILL K. C. & HALL R. 2003. Mezosoic-Cenozoic evolution of Australia's New Guinea margin in a West Pacific context. *Geological Society of America, Special Paper* **372**, 265-290.

HILL K. C. & RAZA A. 1999. Arc-continent collision in Papua New Guinea: constraints from fission track thermochronology. *Tectonics* **18**, 950-966.

HILL S. M. & KOHN B. P. 1998. Morphotectonic evolution of the Mundi Mundi range front, Broken Hill Region, Western N.S.W. Paper presented at Regolith '98: New Aproaches to an old continent., Kalgoorlie (unpubl.).

HILLIS R. & REYNOLDS S. 2003. In situ stress field of Australia. *In:* Hillis R. R. & Muller D. eds. *Evolution and dynamics of the Australian Plate* pp. 101-113. Geological Society of Australia Special Publication **22**.

HILLIS R. R. & REYNOLDS S. D. 2000. The Australian stress map. *Journal of the Geological Society of London* **157**, 915-921.

HILLIS R. R., SANDIFORD M., REYNOLDS S. D. & QUIGLEY M. C. 2008. Present-day stresses, seismicity and Neogene-to-Recent tectonics of Australia's 'passive' margins: intraplate deformation controlled by plate boundary forces. *In:* Johnson H., Dore´ A. G., Gatliff R. W., Holdsworth R., Lundin E. R. & Ritchie J. D. eds. *The Nature and Origin of Compression in Passive Margins*, pp. 71-90. **306** Geological Society, London, Special Publications.

HILLS E. S. 1961. Morphotectonics and the geomorphological sciences with special reference to Australia. *Quarterly Journal of the Geological Society of London* **117**, 77-90.

HILLS E. S. 1975. *Physiography of Victoria; an introduction to geomorphology*. Whitcombe & Tombs Pty. Ltd., Australia.

HOCKING R. M. 1988. Regional geology of the northern Carnarvon Basin. *In:* Purcell P. G. & Purcell R. R. eds. *North West Shelf symposium, Aug. 10-12, 1988*, pp. 97-114. PESA, Perth, Western Australia, Australia.

HOFFMAN P. F. 1989. Chapter 16 Precambrian geology and tectonic history of North America. *In:* Bally A. W. & Palmer A. R. eds. *The geology of North America - Vol. A, The geology of North America - An overview*, pp. 447-512. The Geological Society of America, Boulder, Colorado.

HOLDGATE G. R., CARTWRIGHT I., BLACKBURN D. T., WALLACE M. W., GALLAGHER S. J., WAGSTAFF B. E. & CHUNG L. 2007. The Middle Miocene Yallourn coal seam - the last coal in Australia. *International Journal of Coal Geology* **70**, 95-115.

HOLDGATE G. R., WALLACE M. W., GALLAGHER S. J., SMITH A. J., KEENE J. B., MOORE D. & SHAFIK S. 2003. Plio-Pleistocene tectonics and eustacy in the Gippsland Basin, southeast Australia: evidence from magnetic imagery and marine geological data. *Australian Journal of Earth Sciences* **50**, 403-426.

HOLDGATE G. R., WALLACE M. W., GALLAGHER S. J., WAGSTAFF B. E. & MOORE D. 2008. No mountains to snow on: major post-Eocene uplift of the East Victoria Highlands; evidence from Cenozoic deposits. *Australian Journal of Earth Sciences* **55**, 211-234.

HOLDGATE G. R., WALLACE M. W., GALLAGHER S. J., WITTEN R. B., STAS B. & WAGSTAFF B. E. 2006. Cenozoic fault control on 'deep lead' palaeoriver systems, Central Highlands, Victoria. *Australian Journal of Earth Sciences* **53**, 445-468.

HOUSHOLD I., CHAPPELL J. & FIFIELD K. 2008. Geomorphic response to intraplate neotectonics - Birch's Inlet, SW Tasmania. Paper presented at 13th ANZGG, Queenstown, Tasmania (unpubl.).

HUFTILE G. J., VAN ARSDALE R. & BOYD R. 1999. Pleistocene faulting offshore Newcastle, New South Wales. *Proceedings of the 1999 Conference, Earthquake Engineering Society, Sydney* **paper No. 17**.

HUTTON J. T., PRESCOTT J. R., BOWMAN J. R., DUNHAM M. N. E., CRONE A. J., MACHETTE M. N. & TWIDALE C. R. 1994. Thermoluminescence Dating of Australian PalaeoEarthquakes. *Quaternary Geochronology* **13**, 143-147.

JAKICA S., QUIGLEY M., SANDIFORD M., CLARK D., FIFIELD K. & ALIMANOVIC A. 2010. Geomorphic and cosmogenic nuclide constraints on escarpment evolution in an intraplate setting, Darling Escarpment, Western Australia. *Earth Surface Processes and Landforms* **DOI: 10.1002/esp.2058**.

JAMES N. P., BONE Y., CARTER R. M. & MURRAY-WALLACE C. V. 2006. Origin of the Late Neogene Roe Plains and their calcarenite veneer: implications for sedimentology and tectonics in the Great Australian Bight. *Australian Journal of Earth Sciences* **53**, 407-419.

JANSSEN D. 2001. The structure and tectonics of the Selwyn Fault, Mornington Peninsula, Victoria. Melbourne Univeristy, Melbourne (unpubl.).

JENKINS R. J. F. & SANDIFORD M. 1992. Observations on the tectonic evolution of the southern Adelaide Fold Belt. *Tectonophysics* **214(1-4) November. p27-36; 5 fig, 29 ref**.

JOHNSTON A. C. 1994a. Appendix C-summary tables, SCR seismicity database. *In:* Johnston A. C., Coppersmith K. J., Kanter L. R. & Cornell C. A. eds. *The earthquakes of stable continental regions-v. 2*, pp. C-1-C-46. Electric Power Research Institute, Palo Alto, California.

JOHNSTON A. C. 1994b. Seismotectonic interpretations and conclusions from the stable continental region seismicity database. *In:* Johnston A. C., Coppersmith K. J., Kanter L. R. & Cornell C. A. eds. *The earthquakes of stable continental regions-v. 1, Assessment of large earthquake potential*, pp. 4-1-4-103. Electric Power Research Institute, Palo Alto, California.

JOHNSTON A. C. 1994c. The stable continental region database. *In:* Johnston A. C., Coppersmith K. J., Kanter L. R. & Cornell C. A. eds. *The earthquakes of stable continental regions-v. 1, Assessment of large-earthquake potential*, pp. 3-1-3-80. Electric Power Research Institute, Palo Alto, California.

JOHNSTON A. C. 1996. Seismic moment assessment of stable continental earthquakes, Part 3 : 1811 1812 New Madrid, 1886 Charleston, and 1755 Lisbon. *Geophysical Journal International* **126**, 314-344.

JOHNSTON A. C., COPPERSMITH K. J., KANTER L. R. & CORNELL C. A. 1994. The earthquakes of stable continental regions. *Electric Power Research Institute Report.* **TR102261V1**.

KANTER L. R. 1994. Tectonic interpretation of stable continental crust. *In:* Johnston A. C., Coppersmith K. J., Kanter L. R. & Cornell C. A. eds. *The earthquakes of stable continental regions-v. 1, Assessment of large earthquake potential*, pp. 2-1-2-98. Electric Power Research Institute, Palo Alto, California.

KEEP M., BISHOP A. & LONGLEY I. 2000. Neogene wrench reactivation of the Barcoo sub-basin, northwest Australia: implications for Neogene tectonics of the northern Australia margin. *Petroleum Geoscience* **6**, 211-220.

KEEP M., CLOUGH M. & LANGHI L. 2002. Neogene tectonic and structural evolution of the Timor Sea region, NW Australia. *In:* Keep M. & Moss S. J. eds. *The Sedimentary Basins of Western Australia III, proceedings West Australian Basins Symposium, Perth, 2002*, pp. 341-353.

KEEP M., HARROWFIELD M. & CROWE W. 2007. The Neogene tectonic history of the North West Shelf, Australia. *Exploration Geophysics* **38**, 151-174.

KENNER S. & SEGALL P. 1999. Time-dependence of the stress shadowing effect and its relation to the structure of the lower crust. *Geology* **27**, 119-122.

KING P. R. & THRASHER G. P. 1992. Post-Eocene development of the Taranaki Basin, New Zealand: convergent overprint of a passive margin. *In:* Watkins J. S., Zhiqiang F. & McMillen K. J. eds. *Geology and geophysics of continental margins*, pp. 93-118. American Association of Petroleum Geologists, Tulsa, Oklahoma.

KORSCH R. J. & LINDSAY J. F. 1989. Relationships between deformation and basin evolution in the intracratonic Amadeus Basin, central Australia. *Tectonophysics* **158**, 5-22.

KOTSONIS A. & JOYCE E. B. 2003a. Regolith Mapping at Bendigo, and its relationship to gold in central Victoria, Australia. *In:* Roach I. C. ed. *Advances in regolith*, pp. 239-243. CRC LEME, Perth.

KOTSONIS A. & JOYCE E. B. 2003b. The regolith of the Bendigo 1:100,000 map area. *Victorian Initiative for Minerals and Petroleum Report* **77, Department of Primary Industries**, 62pp + map.

KRASSAY A. A., CATHRO D. L. & RYAN D. J. 2004. A regional tectonostratigraphic framework for the Otway Basin. *Proceedings of the PESA Eastern Australasian Basins Symposium II, Adelaide, 19–22 September, 2004* **2004**, 97-116.

KRONER A. & CORDANI U. 2003. African, southern Indian and South American cratons were not part of the Rodinia supercontinent: evidence from field relationships and geochronology *Tectonophysics* **375**, 325-352.

LEMON N. M. & MCGOWRAN B. 1989. Structural development of the Willunga embayment, St. Vincents basin, South Australia. *National Centre for Petroleum Geology and Geophysics, Adelaide, Field Guide (unpubl).*

LEONARD M. 2008. One hundred years of earthquake recording in Australia. *Bulletin of the Seismological Society of America* **98**, 1458-1470.

LEONARD M. 2010. Earthquake Fault Scaling: Relating Rupture Length, Width, Average Displacement, and Moment Release. *Bulletin of the Seismological Society of America* **100**, 1971-1988.

LEONARD M. & CLARK D. 2006. Reconciling neotectonic and seismic recurrence rates in SW WA. *In: Earthquake Engineering in Australia, 24 – 26 November 2006*, p. paper 19. Australian Earthquake Engineering Society, Canberra, ACT.

LEONARD M. & CLARK D. 2010. A 100 ka record of fault scarps: What can they tell us about contemporary earthquakes? *Journal of Geophysical Research - Solid Earth* **in review**.

LEWIS J. D., DAETWYLER N. A., BUNTING J. A. & MONCRIEFF J. S. 1981. The Cadoux earthquake. *Western Australia. Geological Survey Report* **1981/11**, 133 pages.

LI Q., LIU M. & STEIN S. 2009. Spatiotemporal Complexity of Continental Intraplate Seismicity: Insights from Geodynamic Modeling and Implications for Seismic Hazard Estimation. *Bulletin of the Seismological Society of America* **99**, 52-60.

LIU L. & ZOBACK M. D. 1997. Lithospheric strength and intraplate seismicity in the New Madrid seismic zone. *Tectonics* **16**, 585-595.

LONGLEY I. M., BUESSENSCHUETT C., CLYDSDALE L., CUBITT C. J., DAVIS R. C., JOHNSON M. K., MARSHALL N. M., MURRAY A. P., SOMERVILLE R., SPRY T. B. & THOMPSON N. B. 2002. The North West Shelf of Australia - a Woodside Perspective. *In:* Keep M. & Moss S. eds. *The Sedimentary Basins of Western Australia, Proceedings Western Australian Basins Symposium 3*, pp. 28-88. PESA, Perth.

MACHETTE M. N. 2000. Active, capable, and potentially active faults - a paleoseismic perspective. *Journal of Geodynamics* **29**, 387-392.

MACHETTE M. N., CRONE A. J. & BOWMAN J. R. 1993. Geologic investigations of the 1986 Marryat Creek, Australia, earthquake - implications for paleoseismicity in stable continental regions. *United States Geological Survey Bulletin* **2032-B**, 29p.

MACHETTE M. N., CRONE A. J., BOWMAN J. R. & PRESCOTT J. R. 1991. Surface ruptures and deformation associated with the 1988 Tennant Creek and 1986 Marryat Creek, Australia, intraplate earthquakes. *Open-File Report - U. S. Geological Survey* **OF 91-0582**, 27p.

MALCOLM R. J., POTT M. C. & DELFOS E. 1991. A new tectonostratigraphic synthesis of the North West Cape area. *The APEA Journal* **31**, 154-176.

MARCO S., STEIN M. & AGNON A. 1996. Long term earthquake clustering: a 50,000-year paleoseismic record in the Dead Sea Graben. *Journal of Geophysical Research* **101**.

MCCORMACK B. J. 2006. Quaternary Fault Scarps on the North-eastern Eyre Peninsula, South Australia; Geomorphic constraints on age and faulting history by investigation of knickpoint retreat. B.Sc. (Hons) thesis, The University of Melbourne, Melbourne (unpubl.).

MCCUE K. 1999. Seismic hazard mapping in Australia, the Southwest Pacific and Southeast Asia. *Annali di Geofisica.* **42**, 1191-1198.

MCCUE K., VAN DISSEN R., GIBSON G., JENSEN V. & BOREHAM B. 2003. The Lake Edgar Fault: an active fault in southwest Tasmania, Australia, with repeated displacement in the Quaternary. *Annals of Geophysics* **46**, 1107-1117.

MCKAVANAGH B. M., BOREHAM B. W., CUTHBERTSON R. J., MCCUE K. F. & COOPER W. V. 1993. The Bajool earthquake sequence of 1991, and implications for the seismicity of central Queensland. *Australian Journal of Earth Sciences* **40**, 455-460.

MCKAVANAGH B. M., BOREHAM B. W., HAFNER J. K., BUGDEN C. A. & WILKINSON J. E. 1994. Seismicity of central Queensland. *In: R.J. Holcombe, C.J. Stephens, C.R. Fielding (eds) Geological Society of Australia, Queensland Chapter 1994 Field Conference*, 122-136.

MCPHERSON A., CLARK D. & BARROWS T. 2009. Long-term slip rates for onshore faults in the Gippsland Basin, south-eastern Australia. Paper presented at 7th international conference on geomorphology (ANZIAG), Melbourne, Australia (unpubl.).

MCWHAE J. R. H., PLAYFORD P. E., LINDNER A. W., GLENISTER B. F. & BALME B. E. 1956. The stratigraphy of western Australia *Australian Journal of Earth Sciences* **4**, 1 - 153.

MEADE B. J. & HAGER B. H. 2004. Viscoelastic deformation for a clustered earthquake cycle. *Geophysical Research Letters* **31 (L 10610)**, doi:10.1029/2004GL019643.

MILES K. R. 1952. Tertiary Faulting in northeastern Eyre Peninsula. *Transactions of the Royal Society of South Australia* **75**, 89-96.

MOYE D. G., SHARP K. R. & STAPLEDON D. H. 1963. Geology of the Snowy Mountains Region. *Snowy Mountains Hydro-electric Authority, Cooma* **(unpubl.: held in Geological Survey of New South Wales Library).**

MUELLER C. S. 2010. The Influence of Maximum Magnitude on Seismic-Hazard Estimates in the Central and Eastern United States. *Bulletin of the Seismological Society of America* **100**, 699-711.

MURATA A., TAKEMURA K., MIYATA T. & LIN A. 2001. Quaternary vertical offset and average slip rate of the Nojima Fault on Awaji Island, Japan. *The Island Arc* **10**, 360-367.

MURRAY A. S. 1997. The Australian National Gravity Database. *Australian Geological Survey Organisation, Canberra* **17**, 145-155.

NELSON E. J. & HILLIS R. R. 2005. In situ stresses of the West Tuna area, Gippsland Basin. *Australian Journal of Earth Sciences* **52**, 299-313.

NEUMANN N. & FRASER G. 2007. Geochronological synthesis and time–space plots for Proterozoic Australia. *Geoscience Australia Record* **2007/06**.

NEUMANN N., SANDIFORD M. & FODEN J. 2000. Regional geochemistry and continental heat flow: Implications for the origin of the South Australian heat flow anomaly. *Earth and Planetary Science Letters* **183**, 107-120.

NOTT R. B. 1989. Preliminary hydrogeological assessment of the Mallee/Wimmera region of northern Victoria: summary of data from the deep drilling program 1986-1988. *groundwater*

Assessment and Policy Branch, Water Resources Management Division, Victorian Department of Water Resources, 53p.

O'Leary M. J., Hearty P. J. & McCulloch M. T. 2008. Geomorphic evidence of major sea-level fluctuations during marine isotope substage-5e, Cape Cuvier, Western Australia. *Geomorphology* **102**, 595-602.

Obermeier S. F., Munson P. J., Munson C. A., Martin J. R., Frankel A. D., Youd T. L. & Pond E. C. 1992. Liquefaction evidence for strong Holocene earthquake(s) in the Wabash Valley of Indiana, Illinois. *In: Johnston A.C., Shedlock, K.M., Herrmann, R.B. & Hopper, M.G. (eds) New Madrid special issue. Seismological Research Letters* **63**, 321-335.

Occhipinti S. A. & Reddy S. M. 2009. Neoproterozoic reworking of the Palaeoproterozoic Capricorn Orogen of Western Australia and implications for the amalgamation of Rodinia. *Geological Society of London Special Publication* **327**, 445-456.

Olley J. 2004. Report on the optical dating of sediments samples from Swan River and Meckering. *CSIRO Land and Water Report to Geoscience Australia*, 7p.

Olson E. L. & Cooke M. L. 2005. Application of three fault growth criteria to the Puente Hills thrust system, Los Angeles, California, USA. *Journal of Structural Geology* **27**, 1765-1777.

Packham G. 1996. Cenozoic SE Asia; reconstructing its aggregation and reorganisation. *In:* Hall R. & Blundell D. J. eds. *Tectonic evolution of Southeast Asia*, pp. 123-152. **106** Geological Society of London, Special Publications.

Paine M. D., Bennetts D. A., Webb J. A. & Morand V. J. 2004. Nature and extent of Pliocene strandlines in southwestern Victoria and their application to Late Neogene tectonics. *Australian Journal of Earth Sciences* **51**, 407-422.

Palfreyman W. D. 1984. Guide to the geology of Australia. *[Australia] Bureau of Mineral Resources, geology & Geophysics Bulletin* **181**, 111p.

Pandey O. P., Chandrakala K., Parthasarathy G., Reddy P. R. & Reddy G. K. 2008. Upwarped high velocity mafic crust, Subsurface Tectonics and causes of intra plate Latur-Killari (M 6.2) and Koyna (M 6.3) earthquakes, India - A comparative study. *Journal of Asian Earth Sciences* **doi: 10.1016/j.jseaes.2008.11.014**.

Paul E., Flottmann T. & Sandiford M. 1999. Structural geometry and controls on basement-involved deformation in the northern Flinders Ranges, Adelaide Fold Belt, South Australia. *Australian Journal of Earth Sciences* **46**, 343-354.

Perincek C. & Cockshell C. D. 1995. The Otway Basin: Early Cretaceous rifitng to Neogene inversion. *The APEA Journal* **35**, 451-466.

Philip H., Avagyan A., Karakhanian A., Ritz J.-F. & Rebai S. 2001. Estimating slip rates and recurrence intervals for strong earthquakes along an intracontinental fault: example of the Pambak-Sevan-Sunik fault (Armenia). *Tectonophysics* **343**, 205-232.

Pickett J. W. & Bishop P. 1992. Aspects of landscape evolution in the Lapstone Monocline area, New South Wales. *Australian Journal of Earth Sciences* **39**, 21-28.

Pillans B. 2003a. Dating ferruginous regolith to determine seismic hazard at Lucas Heights, Sydney. . *In: Ian C. Roach, (ed) Advances in Regolith: Proceedings of the CRC LEME Regional Regolith Symposia, 2003 CRC LEME* 324-327.

Pillans B. 2003b. Subdividing the Pleistocene using the Matuyama–Brunhes boundary (MBB): an Australasian perspective. *Quaternary Science Reviews* **22**, 1569-1577.

Preiss W. V. 1987. The Adelaide Geosyncline - late Proterozoic stratigraphy, sedimentation, palaeontology and tectonics. *Geological Survey of South Australia Bulletin* **53**.

Preiss W. V. & Faulkner P. 1984. Geology, geophysics and stratigraphic drilling at Depot Creek, Southern Flinders Ranges. *Geological Survey of South Australia Quarterly Geological Notes* **89**, 10-19.

Quigley M., Clark D. & Sandiford M. 2010. Late Cenozoic tectonic geomorphology of Australia. *Geological Society of London Special Publication* **346**, 243-265.

Quigley M., Sandiford M., Alimanovic A. & Fifield L. K. 2007a. Landscape responses to intraplate tectonism: quantitative constraints from 10Be abundances. *Earth and Planetary Science Letters* **261**, 120-133.

QUIGLEY M., SANDIFORD M., FIFIELD K. & ALIMANOVIC A. 2007b. Bedrock erosion and relief production in the northern Flinders Ranges, Australia. *Earth Surface Processes and Landforms* **32**, 929-944.

QUIGLEY M. C., CUPPER M. L. & SANDIFORD M. 2006. Quaternary faults of southern Australia: palaeoseismicity, slip rates and origin. *Australian Journal of Earth Sciences* **53**, 285-301.

QUIGLEY M. C., SANDIFORD M. & CUPPER M. L. 2007c. Distinguishing tectonic from climatic controls on range-front sedimentation, Flinders Ranges, South Australia. *Basin Research* **doi: 10.1111/j.1365-2117.2007.00336.x**.

REYNOLDS S. D., COBLENTZ D. D. & HILLIS R. R. 2003. Influences of plate-boundary forces on the regional intraplate stress field of continental Australia. *In:* Hillis R. R. & Muller D. eds. *Evolution and dynamics of the Australian Plate*, pp. 101-113. **22** Geological Society of Australia Special Publication

RHODES E., CHAPPELL J., FUJIOKA T., FITZSIMMONS K., MAGEE J., AUBERT M. & HEWITT D. 2005. The history of aridity in Australia : Chronological developments. *In:* Roach I. C. ed. *Regolith 2005. Ten years of CRC LEME* pp. 265-268. CRC LEME, Perth.

RICHARDSON A. N. & BLUNDELL D. J. 1996. Continental collision in the Banda Arc. *In:* hall R. & Blundell D. J. eds. *Tectonic evolution of Southeast Asia*, pp. 47-60. **106** Geological Society of London, Special Publication.

RITZ J. F., BROWN E. T., BOURLES D. L., PHILIP H., SCHLUPP A., RAISBECK G. M., YIOU F. & ENKHTUVSHIN B. 1995. Slip rates along active faults estimated with cosmic-ray-exposure dates; application to the Bogd Fault, Gobi-Altai, Mongolia *Geology* **23**, 1019-1022.

ROBERT A. 2007. Tectonic Geomorphology studies in South Australia : Whyalla's Scarps and Billa Kalina Basin. Masters thesis, The University of Melbourne, Melbourne (unpubl.).

RUTHERFURD I. D. & KENYON C. 2005. Geomorphology of the Barmah-Millewa forest. *Proceedings of the Royal Society of Victoria* **117**, 23-39.

SANDIFORD M. 2003a. Geomorphic constraints on the late Neogene tectonics of the Otway Ranges. *Australian Journal of Earth Sciences* **50**, 69-80.

SANDIFORD M. 2003b. Neotectonics of southeastern Australia: linking the Quaternary faulting record with seismicity and in situ stress. *eds Hillis R.R. & Muller D, Evolution and dynamics of the Australian Plate, Geological Society of Australia Special Publication.* **22**, 101-113.

SANDIFORD M. 2007. The tilting continent: a new constraint on the dynamic topographic field from Australia. *Earth and Planetary Science Letters* **261**, 152-163.

SANDIFORD M. & EGHOLM D. L. 2008. Enhanced intraplate seismicity along continental margins: Some causes and consequences. *Tectonophysics* **457**, 197-208.

SANDIFORD M., QUIGLEY M., DE BROEKERT P. & JAKICA S. 2009. Tectonic framework for the Cainozoic cratonic basins of Australia. *Australian Journal of Earth Sciences* **56**, s5-s18.

SANDIFORD M. & QUIGLEY M. C. 2009. Topo-Oz: insights into the various modes of intraplate deformation in the Australian continent. *Tectonophysics* **474**, 405-416.

SANDIFORD M., WALLACE M. & COBLENTZ D. 2004. Origin of the in situ stress field in southeastern Australia. *Basin Research* **16**, 325-338.

SCOTT D. L., RAWLINGS D. J., PAGE R. W., TARLOWSKI C. Z., IDNURM M., JACKSON M. J. & SOUTHGATE P. N. 2000. Basement framework and geodynamic evolution of the Palaeoproterozoic superbasins of north-central Australia: an integrated review of geochemical, geochronological and geophysical data. *Australian Journal of Earth Sciences* **47**, 341-380.

SHARP K. R. 2004. Cenozoic volcanism, tectonism and stream derangement in the Snowy Mountains and northern Monaro of New South Wales. *Australian Journal of Earth Sciences* **51**, 67-83.

SHAW R. D., WELLMAN P., GUNN P. J., WHITAKER A. J., TARLOWSKI C. & MORSE M. 1996. Guide to using the Australian crustal elements map. *Australian Geological Survey Organisation. Record* **1996/30**, 93p.

SHULTE S. M. & MOONEY W. D. 2005. An updated global earthquake catalogue for stable continental regions: reassessing the correlation with ancient rifts. *Geophysical Journal International* **161**, 707-721.

SIDDALL M., ROHLING E. J., ALMOGI-LABIN A., HEMLEBEN C., MEISCHNER D., SCHMELZER I. & SMEED D. A. 2003. Sea level fluctuations during the last glacial cycle. *Nature* **423**, 853-858.

SINGH G., OPDYKE N. D. & BOWLER J. M. 1981. Late Cainozoic stratigraphy, magnetic chronology and vegetational history from Lake George, N.S.W. . *Journal of the Geological Society of Australia* **28**, 435-452.

SLEEP N. H. & BLANPIED M. L. 1992. Creep, compaction, and the weak rheology of major faults. *Nature* **359**, 687-692.

SOMERVILLE P., GRAVES R. W., COLLINS N. F., SONG S. G. & NI S. 2009. Ground motion models for Australian earthquakes. *Report to Geoscience Australia* **29 June 2009**.

SOMERVILLE P., QUIJADA P., THIO H. K., SANDIFORD M. & QUIGLEY M. 2008. Contribution of Identified Active Faults to Near Fault Seismic Hazard in the Flinders Ranges. *In: Australian Earthquake Engineering Society Meeting*, p. Paper 45. Australian Earthquake Engineering Society, Ballarat, Victoria.

SOMERVILLE P. G. 2001. Earthquake source scaling and ground motion attenuation relations for the central and eastern United States *Final Report to the U.S. Geological Survey Contract No.* **99HQGR0098**.

SOMERVILLE P. G., IRIKURA K., GRAVES R., SAWADA S., WALD D., ABRAHAMSON N., IWASAKI Y., KAGAWA T., SMITH N. & KOWADA A. 1999. Characterizing earthquake slip models for the prediction of strong ground motion. *Seismological Research Letters* **70**, 59-80.

SPRIGG R. C. 1946. Reconnaissance geological survey of portion of the western escarpment of the Mt Lofty ranges. *Transactions of the Royal Society of South Australia* **70**, 313-347.

STEIN R. S., BARKA A. A. & DIETERICH J. H. 1997. Progressive failure on the North Anatolian fault since 1939 by earthquake stress triggering. *Geophysical Journal International* **128**, 594-604.

STEIN S. & LIU M. 2009. Long aftershock sequences within continents and implications for earthquake hazard assessment. *Nature* **462**, 87-89.

STEIN S., SCHOONOVER M., SELLA G. & OKAL E. 2001. Bhuj: A diffuse plate boundary zone earthquake? *In: GSA Annual Meeting, Session No. 162, Tectonics III: Wrench Systems - Oceanic and Global Tectonics, Geological Society of America, Boulder, CO*, (available at http://gsa.confex.com/gsa/2001AM/finalprogram/abstract_24251.htm).

STIRLING M., LITCHFIELD N., GERSTENBERGER M., CLARK D., BRADLEY B., BEAVAN J., MCVERRY G., DISSEN R. V., NICOL A., WALLACE L. & BUXTON R. 2011. Probabilistic Tectonic Hazard Analysis of the Otway Basin, Australia: Groundwork for the CO2CRC Otway Project. *Bulletin of the Seismological Society of America* **in review**.

STIRLING M., RHOADES D. & BERRYMAN K. 2002a. Comparison of Earthquake Scaling Relations Derived from Data of the Instrumental and Preinstrumental Era. *Bulletin of the Seismological Society of America* **92**, 812-830.

STIRLING M. W., MCVERRY G. H. & BERRYMAN K. R. 2002b. A new seismic hazard model for New Zealand. *Bulletin of the Seismological Society of America* **92(5)**, 1878-1903.

STONE J., ALLAN G. & FIFIELD L. K. 1994. Limestone erosion measurements with cosmogenic Cl-36 in Calcite - preliminary results from Australia. *Nuclear instruments and methods in physics research, section B - beam interactions with materials and atoms* **92**, 311-316.

STONE T. 2006. Late Quaternary rivers and lakes of the Cadell Tilt Block region, Murray Basin, southeastern Australia. PhD thesis, The University of Melbourne, Melbourne (unpubl.).

SUTHERLAND R. 1996. Transpressional development of the Australia-Pacific plate boundary through southern South Island New Zealand: constraints from Miocene-Pliocene sediments, Waiho-1 borehole, South Westland. . *New Zealand Journal of Geology and Geophysics* **39**, 251-264.

SYMONDS P. A., COLLINS C. D. N. & BRADSHAW J. 1994. Deep structure of the Browse Basin: implications for basin development and petroleum exploration. *In:* Purcell P. G. & Purcell

R. R. eds. *The sedimentary basins of Western Australia*, pp. 315-332. Proceedings of the Petroleum Exploration Society of Australia, Perth.

TALWANI P. 1988. The intersection model for intraplate earthquakes. *Seismological Research Letters* **59**, 305- 310.

TALWANI P. & SCHAEFFER W. T. 2001. Recurrence rates of large earthquakes in the South Carolina coastal plain based on paleoliquefaction data. *Journal of Geophysical Research* **106**, 6621-6642.

THOM R. 1972. A recent fault scarp in the Lort River area, Ravensthorpe 1:250,000 sheet. *Report of the Department of Mines, Western Australia, for the year 1971*, 102-103.

TICKELL S. J., EDWARDS J. & ABELE C. 1992. Port Campbell Embayment 1:100 000 map geological report (and map). *Geological Survey of Victoria Report* **95**.

TICKELL S. J. & HUMPHRYS W. G. 1987. Groundwater resources and associated salinity problems of the Victorian part of the riverine plain. *Victoria Geological Survey Report 84*.

TOMKINS K. M., HUMPHREYS G. S., WILKINSON M. T., FINK D., HESSE P. P., DOERR S. H., SHAKESBY R. A., WALLBRINK P. J. & BLAKE W. H. 2007. Contemporary versus long-term denudation along a passive plate margin: the role of extreme events. *Earth Surface Processes and Landforms* **32**, 1013-1031.

TUTTLE M. P. 2003. Paleoliquefaction Reconnaissance in Western Australia. Geoscience Australia, unpublished report.

TUTTLE M. P. & ATKINSON G. M. 2010. Localization of Large Earthquakes in the Charlevoix Seismic Zone, Quebec, Canada, during the Past 10,000 Years. *Seisomologucal Research Letters* **81**, 140-147.

TUTTLE M. P., SCHWEIG E., CAMPBELL J., THOMAS P. M., SIMS J. D. & LAFFERTY R. H. 2005. Evidence for New Madrid earthquakes in A.D. 300 and 2350 B.C. *Seismological Research Letters* **76**, 489-501.

TUTTLE M. P., SCHWEIG E. S., SIMS J. D., LAFFERTY R. H., WOLF L. W. & HAYNES M. L. 2002. The earthquake potential of the New Madrid seismic zone. *Bulletin of the Seismological Society of America* **92**, 2080-2089.

TWIDALE C. R. & BOURNE J. A. 2004. Neotectonism in Australia: its expressions and implications. *Geomorphologie* **3**, 179-194.

VAN ARSDALE R., PURSER J., STEPHENSON W. J. & ODUM J. K. 1998. Faulting along the southern margin of Reelfoot Lake, Tennessee. *Bulletin of the Seismological Society of America* **88**, 131-139.

VAN DE GRAAFF W. J. E. 1975. Cobb, Western Australia. *Geological Society of Western Australia Geological Sheet SG 52-1 explanatory notes*, 16p.

VAN DE GRAAFF W. J. E., DENMAN P. D. & HOCKING R. M. 1976. Emerged Pleistocene marine terraces on Cape Range, Western Australia. *Western Australia Geological Survey Annual Report 1975*, 62-70.

VANDENBERG A. H. M. 1971. Warragul [map] : Australia 1:250 000 geological series. Sheet Sj 55-10. *Geological Survey of Victoria* **1st edition**.

VANDENBERG A. H. M. 2010. Paleogene basalts prove early uplift of Victoria's Eastern Uplands. *Australian Journal of Earth Sciences* **57**, 291 - 315.

VEEH H. H., SCHWEBEL D., VAN DE GRAAFF W. J. E. & DENMAN P. D. 1979. Uranium-series ages of coralline terrace deposits in Western Australia. *Journal of the Geological Society of Australia* **26**, 285-292.

VEEVERS J. J. 1972. Evolution of the Perth and Carnarvon basins. *The APEA Journal. 12; 2, Pages 52-54. 1972.: Australian Petroleum Exploration Association. Sydney, N.S.W., Australia. 1972.*

VEEVERS J. J. 2000. *Billion-year earth history of Australia and neighbours in Gondwanaland*. GEMOC Press, Sydney, Australia.

VITA-FINZI C. 2004. Buckle-controlled seismogenic faulting in peninsular India. *Quaternary Science Reviews* **23**, 2405-2412.

WACLAWIK V. G., LANG S. C. & KRAPF C. B. E. 2008. Fluvial response to tectonic activity in an intra-continental dryland setting: The Neales River, Lake Eyre, Central Australia. *Geomorphology* **102**.

WALCOTT R. I. 1998. Modes of oblique compression: late Cainozoic tectonics of the South Island of New Zealand. *Reviews of Geophysics* **36**, 1-26.

WALLACE M. W., DICKINSON J. A., MOORE D. H. & SANDIFORD M. 2005. Late Neogene strandlines of southern Victoria: a unique record of eustasy and tectonics in southeast Australia. *Australian Journal of Earth Sciences* **52**, 279-297.

WALLACE R. E. 1987. Grouping and migration of surface faulting and variations in slip rates on faults in the Great Basin province. *Bulletin of the Seismological Society of America* **77**, 868-876.

WEATHERMAN M. 2006. Basement Control on Distribution of Active Faults on North-eastern Eyre Peninsula, and some Seismic Implications. B. Sc. (Hons) thesis, The University of Melbourne, Melbourne (unpubl.).

WEISSEL J. K. & SEIDL M. A. 1998. Inland propagation of erosional escarpments and river profile evolution across the southeast Australian passive continental margin. *In:* Tinkler K. J. & Wohl E. E. eds. *Geophysical Monograph*, pp. 189-206. **107** American Geophysical Union.

WELLMAN P. 1976. Gravity trends and the growth of Australia: A tentative correlation. *Australian Journal of Earth Sciences* **23**, 10-14.

WELLS D. L. & COPPERSMITH K. J. 1994. New empirical relationships among magnitude, rupture length, rupture width, rupture area, and surface displacement. *Bulletin of the Seismological Society of America* **84**, 974-1002.

WHEELER R. L. 1995. Earthquakes and the cratonward limit of Iapetan faulting in eastern North America. *Geology* **23**, 105-108.

WHEELER R. L. 1996. Earthquakes and the southeastern boundary of the intact Iapetan margin in Eastern North America. *Seismological Research Letters* **67**, 77-83.

WHEELER R. L. 2009a. Methods of Mmax Estimation East of the Rocky Mountains. *U.S. Geological Survey Open-File Report 2009–1018*, 48p.

WHEELER R. L. 2009b. Sizes of the largest possible earthquakes in the Central and Eastern United States-Summary of a workshop, September 8-9, 2008, Golden, Colorado. *U.S. Geological Survey Open-File Report* **2009-1263**, 308 p.

WHEELER R. L. & FRANKEL A. 2000. Geology in the 1996 USGS Seismic-hazard Maps, Central and eastern United States. *Seismological Research Letters* **71**, 273-282.

WILDE S. A., MIDDLETON M. F. & EVANS B. J. 1996. Terrane accretion in the southwest Yilgarn craton: evidence from a deep seismic crustal profile. *Precambrian Research* **78**, 179-196.

WILKINSON M. T., CHAPPELL J., HUMPHREYS G. S., FIFIELD K., SMITH B. & HESSE P. 2005. Soil production in heath and forest, Blue Mountains, Australia: influence of lithology and palaeoclimate. *Earth Surface Processes and Landforms* **30**, 923-934.

WILLIAMS G. E. 1973. Late Quaternary piedmont sedimentation, soil formation and palaeoclimates in arid South Australia. *Zeitschrift fur Geomorphologie* **17**, 102-123.

WILLIAMS I. R. 1979. Recent fault scarps in the Mount Narryer area, Byro 1:250 000 sheet. *Western Australia. Geological Survey. Annual Report 1978* **51-55**.

WILLIAMSON P. E., WILLCOX J. B., COLWELL J. B. & COLLINS C. D. N. 1991. The Gippsland Basin Deep Seismic Reflection/Refraction Grid. *Exploration Geophysics* **22**, 497-502.

WOPFNER H. 1968. Cretaceous sediments on the Mt. Margaret Plateau and evidence for neo-tectonism. *Quarterly geological notes, Geological Survey of South Australia* **28**, 7-11.

WYRWOLL K.-H., KENDRICK G. W. & LONG J. A. 1993. The geomorphology and Late cenozoic geomorphological evolution of the Cape Range - Exmouth Gulf region. *In:* Humphreys W. F. ed. *The biogeography of Cape Range, Western Australia* (Supplement No. 45, 1993 edition), pp. 1-23. Records of the Western Australian Museum Museum of Western Australia, Perth.

WYRWOLL K. H. 2003. The geomorphology of the Perth region, Western Australia. *Australian Geomechanics* **38**, 17-31.

ZHU Z. R., WYRWOLL K.-H., COLLINS L. B., CHEN J., WASSERBURG G. J. & EISENHAUER A. 1993. High precision U-series dating of Last Interglacial events by mass spectrometry: Houtman Abrolhos Islands,Western Australia. *Earth and Planetary Science Letters* **118**, 281- 293.

Appendix Table 1

The neotectonic data used in the analysis presented in this study is presented in the following table. The data are sourced from the Australian Neotectonics database, accessed March 2010. In some instances, values in the online database have been updated as new evidence comes to light. An up to date listing might be obtained from the authors on request. A dip value of "0" indicates that dip is unknown.

database #	Feature_Name	Domain ID	Lat	Long	Length km	Avg Strike deg	Dip deg	Dip Direction	Movement	Vert Displ m	Confidence	Dist to Nearest Feature dec deg	Shmax Orientation	Max Single Event Slip m	Max Prob M	Arcs source	Height source	Main Reference
442841	Mount Narryer East Scarp	1	116.443	-26.476	20.7	46	0	Northwest	Reverse	2.20	A	0.09481631136	44	1.54	6.7	Google earth imagery	CLARK D. J. 2004. Reconnaissance of Recent fault scarps in the Mt Narryer region, Western Australia. Geoscience Australia unpublished report, 31p.	WILLIAMS I. R. 1979. Recent fault scarps in the Mount Narryer area, Byro 1:250 000 sheet. Western Australia. Geological Survey. Annual Report 1978 51-55.
442842	Tennant Creek Scarps	1	134.000	-19.833	32.0	115	35	Southwest	Reverse	2.00	A	2.09414878210	97	2.00	6.8	Figure from main reference	main reference	CRONE A. J., MACHETTE M. N. & BOWMAN J. R. 1992. Geologic investigations of the 1988 Tennant Creek, Australia, earthquakes - implications for paleoseismicity in stable continental regions. United States Geological Survey Bulletin 2032-A, 51p.
442845	Cadoux Scarp	1	117.150	-30.750	15.0	13	0		Reverse	1.30	A	0.76817795331	71	1.28	6.5	Figure from main reference	main reference	LEWIS J. D., DAETWYLER N. A., BUNTING J. A. & MONCRIEFF J. S. 1981. The Cadoux earthquake. Western Australia. Geological Survey Report 1981/11, 133 pages.
442846	Meckering Scarp	1	117.000	-31.670	37.0	20	30	East	Dextral reverse	1.98	A	0.32999992000	67	2.18	6.9	Figure from main reference	main reference	GORDON F. R. & LEWIS J. D. 1980. The Meckering and Calingiri earthquakes October 1968 and March 1970. Western Australia Geological Survey Bulletin 126, 229p.
442847	Merredin Scarps	1	118.333	-31.667	43.0	157	0	West	Reverse	5.00	B	0.31392128276	71	2.39	7.0	Land Monitor 10 m DEM	DEM profile	CHIN R. J. 1985. Kellerberrin 1:250 000 scale geological series sheet explanatory notes. Geological Survey of Western Australia, 30p.
442848	Hyden North Scarps	1	119.250	-32.250	32.0	4	40	West	Reverse	2.50	A	0.25161077476	82	2.00	6.9	Land Monitor 10 m DEM	field investigation	CLARK D., DENTITH M., WYRWOLL K. H., YANCHOU L., DENT V. & FEATHERSTONE C. 2008. The Hyden fault scarp, Western Australia: paleoseismic evidence for repeated Quaternary displacement in an intracratonic setting. Australian Journal of Earth Sciences 55, 379-395.
442849	Lort River Scarp	3	121.220	-33.480	40.0	24	0	East	Reverse	2.60	A	0.77927305183	65	2.29	6.9	Land Monitor 10 m DEM	field investigation	ESTRADA B. 2009. Neotectonic and palaeoseismological studies in the southwest of Western Australia. Unpublished PhD thesis, The University of Western Australia, Perth.
442850	Roopena Scarp	1	137.378	-32.897	29.5	168	30	West	Reverse	3.80	A	0.18192826914	54	1.80	6.8	3 arc-second Shuttle Radar Tomography Mission DEM	main reference	CRONE A. J., DE MARTINI P. M., MACHETTE M. N., OKUMURA K. & PRESCOTT J. R. 2003. Paleoseismicity of Two Historically Quiescent Faults in Australia: Implications for Fault Behavior in Stable Continental Regions. Bulletin of the Seismological Society of America 93, 1913-1934.
442851	Lake Edgar Scarp	3	146.400	-43.000	30.0	171	0	West	Reverse	8.00	A	0.55878135365	58	2.26	7.0	Tasmap 1:25 000 colour aerial photogrpahy (1988)	main reference	CLARK D. J., CUPPER M., SANDIFORD M. & KIERNAN K. 2010. Style and timing of late Quaternary faulting on the Lake Edgar Fault, southwest Tasmania, Australia: implications for hazard assessment in intracratonic areas. Geological Society of America Special Publication "Palaeoseismology" in press.
442852	Gell River Fault	3	146.200	-42.500	10.0	34	0			1.00	B	0.55878135365	78	1.21	6.5	Figure from main reference	K. McCue per comm, 2003.	MCCUE K., VAN DISSEN R., GIBSON G., JENSEN V. & BOREHAM B. 2003. The Lake Edgar Fault: an active fault in southwest Tasmania, Australia, with repeated displacement in the Quaternary. Annals of Geophysics 46, 1107-1117.
442853	Cadell Scarp	4	144.750	-36.000	50.0	4	50	West	Reverse	100.00	A	0.33177557845	83	3.07	7.2	Murray Darling Basin Authority 1 m LIDAR DEM	main reference	CLARK D., VAN DISSEN R., CUPPER M., COLLINS C. & PRENDERGAST A. 2007. Temporal clustering of surface ruptures on stable continental region faults: a case study from the Cadell Fault scarp, south eastern Australia. Paper presented at Australian Earthquake Engineering Society Conference, Wollongong (unpubl.).
442855	Tatura Scarp	4	145.250	-36.500	10.0	162	0			2.50	C	0.50483475240	68	1.21	6.5	Figure from main reference	main reference	TICKELL S. J. & HUMPHREYS W. G. 1979. The Geology of the Riverine Plain in Victoria. Geological Survey of Victoria Report 1979/135, 57p.
442856	Ash Reef Scarp	1	137.243	-33.003	22.6	13	0	East	Reverse	4.00	A	0.14229401468	103	1.62	6.7	3 arc-second Shuttle Radar Tomography Mission DEM	main reference	MILES K. R. 1952. Tertiary Faulting in northeastern Eyre Peninsula. Transactions of the Royal Society of South Australia 75, 89-96.
442857	Avonmore Scarp (Meadow Valley Fault)	4	144.750	-36.500	25.0	178	0			3.00	B	0.20271719237	79	2.03	6.9	3 arc-second Shuttle Radar Tomography Mission DEM	DEM profile	
442858	Hyden South Scarp	1	119.040	-32.670	30.0	160	0	West	Reverse	10.00	B	0.35827645245	74	1.92	6.8	3 arc-second Shuttle Radar Tomography Mission DEM	DEM profile	CHIN R. J., HICKMAN A. H. & THOM R. 1984. Hyden 1:250 000 scale geological series sheet explanatory notes. Geological Survey of Western Australia, 21p.
442859	Mount Ragged Scarp	3	123.919	-32.874	35.0	16	0			3.00	C	0.60119894995	0	2.11	6.9	3 arc-second Shuttle Radar Tomography Mission DEM	DEM profile	
442861	Palmerville Fault	4	143.859	-14.682	77.0	151	0			15.00	B	3.84947080619	110	4.01	7.4	3 arc-second Shuttle Radar Tomography Mission DEM	DEM profile	SHAW R. D., FAWCKNER J. F. & BULTITUDE R. J. 1987. The Palmerville fault system: a major imbricate thrust system in the Northern Tasmanides, North Queensland (Australia). Australian-Journal-of-Earth-Sciences 34(1), 69-93.
442862	Kinchega Scarp	2	142.107	-32.268	21.9	0	0			20.00	C	0.55471409143	0	1.88	6.9	3 arc-second Shuttle Radar Tomography Mission DEM	DEM profile	
442864	Khancoban - Yellow Bog Fault	4	148.146	-36.199	59.5	35	45	East	Reverse	200.00	A	0.27996278281	66	3.41	7.3	Figure from main reference	main reference	MOYE D. G., SHARP K. R. & STAPLEDON D. H. 1963. Geology of the Snowy Mountains Region. Snowy Mountains Hydro-electric Authority, Cooma (unpubl.; held in Geological Survey of New South Wales Library).
442865	Mundi Mundi Fault	2	141.210	-31.823	150.0	23	0		Reverse	100.00	A	0.63584137704	75	6.15	7.7	3 arc-second Shuttle Radar Tomography Mission DEM	DEM profile	HILL S. M. & KOHN B. P. 1998. Morphotectonic evolution of the Mundi Mundi range front, Broken Hill Region, Western N.S.W. Paper presented at Regolith '98: New Aproaches to an old continent., Kalgoorlie (unpubl.).
442866	Rowsley Fault	4	144.297	-37.794	43.0	30	0			90.00	C	0.37397125973	90	2.80	7.2	3 arc-second Shuttle Radar Tomography Mission DEM	DEM profile	VANDENBERG, A.H.M. 1997. Queenscliff 1:250,000 Geological Map. Geological Survey of Victoria. 2nd Edition.
442867	Moorooduc Scarp	5	145.097	-38.204	5.8	26	0			30.00	C	0.25824684334	91	0.88	6.3	3 arc-second Shuttle Radar Tomography Mission DEM	DEM profile	VANDENBERG, A.H.M. 1997. Queenscliff 1:250,000 Geological Map. Geological Survey of Victoria. 2nd Edition.
442868	Muckleford Fault	4	144.113	-37.250	80.0	10	0		Reverse	50.00	A	0.28252470255	98	4.10	7.4	Melbourne 1:250000 geological map sheet	main reference	KOTSONIS A. & JOYCE E. B. 2003. The regolith of the Bendigo 1:100,000 map area. Victorian Initiative for Minerals and Petroleum Report 77, Department of Primary Industries, 62pp + map.
442869	Leichardt Fault	4	144.082	-36.719	39.0	155	0			45.00	A	0.26888404607	52	2.64	7.1	Bendigo 1:250000 geological map sheet	main reference	KOTSONIS A. & JOYCE E. B. 2003. The regolith of the Bendigo 1:100,000 map area. Victorian Initiative for Minerals and Petroleum Report 77, Department of Primary Industries, 62pp + map.
442870	Whitelaw Fault	4	144.329	-36.822	50.0	164	0			14.00	C	0.26888404607	61	3.07	7.2	Bendigo 1:250000 geological map sheet	main reference	KOTSONIS A. & JOYCE E. B. 2003. The regolith of the Bendigo 1:100,000 map area. Victorian Initiative for Minerals and Petroleum Report 77, Department of Primary Industries, 62pp + map.
442871	Leaghur Fault	4	143.807	-36.293	72.0	5	0			25.00	B	0.23139588015	91	3.84	7.4	St Arnaud 1:250000 geological map sheet	main reference	TICKELL S. J. & HUMPHREYS W. G. 1979. The Geology of the Riverine Plain in Victoria. Geological Survey of Victoria report 1979/135, 57p.
442872	Spring Hill Lead Fault	4	143.900	-37.300	31.0	0	0		Sinistral	3.00	B	0.14128976870	0	2.31	7.0	Martin Hughes pers comm (2002)	main reference	DUNN E. J. 1912. Geological notes on deep leads in the Loddon Valley. Record of the Geological Survey of Victoria 3, 160-162.
442873	Rosedale Monocline	5	146.909	-38.163	78.0	82	0	North	Reverse	100.00	A	0.07770338875	32	4.04	7.4	3 arc-second Shuttle Radar Tomography Mission DEM	main reference	HOLDGATE G. R., WALLACE M. W., GALLAGHER S. J., SMITH A. J., KEENE J. B., MOORE D. & SHAFIK S. 2003. Plio-Pleistocene tectonics and eustacy in the Gippsland Basin, southeast Australia: evidence from magnetic imagery and marine geological data. Australian Journal of Earth Sciences 50, 403-426.
442874	Yallourn Monocline	5	146.654	-37.998	67.0	33	0	West	Reverse	250.00	A	0.22747299818	80	3.67	7.3	3 arc-second Shuttle Radar Tomography Mission DEM	DEM profile	BEAVIS F. C. 1975. Engineering geology of 'd' power station Yallourn, Australia. Quarterly Journal of Engineering Geology and Hydrogeology 8, 103-117.
442875	Hindmarsh Fault	4	141.901	-36.136	178.0	158	0			30.00	C	1.34207473320	68	6.90	7.8	Horsham & Ouyen 1:250000 geological map sheets	JOHNS M. W. & LAWRENCE C. R. 1964. Aspects fo the geological Structure of the Murray Basin in North-western Victoria. Department of Mines, Victoria Geological Survey, Underground Water Investigation Report 10, 18p.	DOUGLAS J. G. & FERGUSON J. A. 1976. Geology of Victoria. Geological Survey of Victoria special publication 5, 528p.
442876	Tawonga Fault	4	147.190	-36.720	35.0	53	15	Southeast	Reverse	600.00	C	0.40295060296	56	2.48	7.1	Figure from main reference	main reference	BEAVIS F. C. 1960. The Tawonga Fault, northeast Victoria. Proceedings of the Royal Society of Victoria 72, 95-100
442877	Barjarg Fault	4	145.979	-36.953	20.0	16	0	West	Reverse	20.00	B	0.38848576612	84	1.79	6.8	Wangaratta 1:250000 geological map sheet	main reference	Michael Jorganson, confidential URS report.
442878	Buenba Fault	4	147.833	-36.783	80.0	36	0			50.00	C	0.23941851038	77	4.10	7.4	Tallangatta 1:250000 geological map sheet	main reference	BEAVIS F. C. & BEAVIS J. C. 1976. Structural geology in the Kiewa region of the Metamorphic Complex, North-East Victoria. Proceedings of the Royal Society of Victoria 88, 66-75.
442879	Tom Groggin Fault	4	148.150	-36.500	115.0	27	0			100.00	C	0.27996278281	80	5.17	7.6	Tallangatta 1:250000 geological map sheet	DEM profile	BOCK G. & DENHAM D. 1983. Recent earthquake activity in the Snowy Mountains region and its relationship to major faults. Journal of the Geological Society of Australia 30, 423-429.
442888	Berridale Wrench Fault	4	148.805	-36.320	70.0	135	0			30.00	C	0.19302016942	35	3.77	7.4	Bega 1:250000 geological map sheet	DEM profile	BOCK G. & DENHAM D. 1983. Recent earthquake activity in the Snowy Mountains region and its relationship to major faults. Journal of the Geological Society of Australia 30, 423-429.
442889	Barney's Range Fault	4	148.718	-36.493	22.0	16	0	Northwest		30.00	C	0.07602263462	89	1.89	6.9	Bega 1:250000 geological map sheet	DEM profile	BOCK G. & DENHAM D. 1983. Recent earthquake activity in the Snowy Mountains region and its relationship to major faults. Journal of the Geological Society of Australia 30, 423-429.
442890	Jindabyne Thrust	4	148.657	-36.449	100.0	10	0			100.00	C	0.07602263462	94	4.73	7.5	Bega 1:250000 geological map sheet	DEM profile	BOCK G. & DENHAM D. 1983. Recent earthquake activity in the Snowy Mountains region and its relationship to major faults. Journal of the Geological Society of Australia 30, 423-429.
442892	Dee Range Fault	4	150.560	-23.540	28.9	134	0	Northeast		40.00	C	0.31742212777	112	2.21	7.0	Figure from main reference	DEM profile	MCKAVANAGH B. M., BOREHAM B. W., CUTHBERTSON R. J., MCCUE K. F. & COOPER W. V. 1993. The Bajool earthquake sequence of 1991, and implications for the seismicity of central Queensland. Australian Journal of Earth Sciences 40, 455-460.
442893	Vrilya Point Faulted Laterite	1	142.115	-11.250	8.0	43	0			30.00	B	3.84947080619	4	1.07	6.4	Jardine River 1:250 000 geological map sheet	main reference	GIBSON D. L. & SMART J. 1973. Jardine River Geology first edition (1:250 000 scale map): Sheet SC54/15. . Bureau of Mineral Resources Canberra.
442894	Gibb Rock Scarp	1	119.030	-32.127	14.2	0	0			5.00	C	0.25161077476	0	1.24	6.5	Land Monitor 10 m DEM	DEM profile	
442895	Simmonston Fault	2	138.100	-32.120	4.0	73	0			20.00	C	0.17888956598	35	0.73	6.1	Orroroo 1:250 000 geological map sheet	DEM profile	Wolfgang Preiss, PIRSA, Pers Comm.
442896	Ediacara Scarp	2	138.143	-30.849	15.0	176	0			12.00	C	0.18439266011	69	1.52	6.7	Figure from main reference	DEM profile	Binks, P.J. 1972. Late Cainozoic uplift of the Ediacara Range, South Australia. Proc AusIMM No. 243, 47-55.
442897	Mount Deception Fault	2	138.259	-30.700	39.0	179	0			40.00	C	0.18439266011	73	2.64	7.1	Figure from main reference	DEM profile	Binks, P.J. 1972. Late Cainozoic uplift of the Ediacara Range, South Australia. Proc AusIMM No. 243, 47-55.
442898	Mount Margaret Fault	3	136.075	-28.484	20.0	158	0		Normal	75.00	B	0.77929882044	68	1.51	6.6	Figure from main reference	DEM profile	WOPFNER H. 1968. Cretaceous sediments on the Mt. Margaret Plateau and evidence for neo-tectonism. Quarterly geological notes, Geological Survey of South Australia 28, 7-11.
442900	Mann Fault	3	130.250	-26.170	10.0	110	0	South	Normal	15.00	C	0.64414143453	41	1.01	6.3	Google earth imagery	DEM profile	THOMSON B. P. 1966. Report on rifts and major shear faults, SA. Questionnaire for Working Group on Tectonics Upper Mantle Committee. South Australia Department Mines Report Book 62/00093.
442902	Alcoota Homestead Fault	3	134.408	-22.869	7.5	68	89	South		1.67	C	0.30733991292	52	0.86	6.2	Google earth imagery	main reference	WOODBURNE M. O. 1967. The Alcoota fauna, central Australia. An integrated palaeontological and geological study. Bureau of Mineral Resources, Australia. Bulletin 87, 211.

database #	Feature_Name	Domain ID	Lat	Long	Length km	Avg Strike deg	Dip deg	Dip Direction	Movement	Vert Displ m	Confidence	Dist to Nearest Feature dec deg	Shmax Orientation	Max Single Event Slip m	Max Prob M	Arcs source	Height source	Main Reference
442904	Lake Johnston Scarp	1	121.091	-32.716	37.0	13	0	West		7.00	B	0.77927305183	76	2.18	6.9	3 arc-second Shuttle Radar Tomography Mission DEM	DEM profile	CLARK D. 2010. Identification of Quaternary scarps in southwest and central west Western Australia using DEM-based hill shading: application to seismic hazard assessment and neotectonics. International Journal of Remote Sensing in press.
442905	Mount Black Lineament	1	123.285	-28.097	30.5	167	0	East		2.00	B	0.95445468147	76	1.94	6.8	Rason 1:250 000 geological map	max estimate from DEM profile	GOWER C. F. & BOEGLI J. C. 1977. Rason, Western Australia, . 1:250 000 geological series explanatory notes. Bureau of Mineral Resources, Australia & Geological Survey of WA Sheet SH/51-03., 17p.
442907	D'Aguilar Ranges Fault	2	145.583	-42.494	45.0	3	45	West	Sinistral reverse	80.00	C	0.60090995555	115	2.46	7.0	TASMAP 30 m DEM	main reference	HOUSHOLD I., CHAPPELL J. & FIFIELD K. 2008. Geomorphic response to intraplate neotectonics - Birch's Inlet, SW Tasmania. Paper presented at 13th ANZGG, Queenstown, Tasmania (unpubl.).
442909	Mount Theo Scarp	1	130.944	-21.024	30.0	117	0	Northeast	Reverse	3.00	C	1.55267320643	100	1.92	6.8	Mt Theo/Mt Solitaire 1:250000 geological map sheet	main reference	Andrew Crispe, NTGS, pers. Comm. 2002
442910	Milendella Fault	2	139.238	-34.609	54.0	240	44	West	Reverse	90.00	A	0.35039145042	46	3.22	7.3	3 arc-second Shuttle Radar Tomography Mission DEM	main reference	SANDIFORD M. 2003. Neotectonics of southeastern Australia: linking the Quaternary faulting record with seismicity and in situ stress. eds Hillis R.R. & Muller D, Evolution and dynamics of the Australian Plate, Geological Society of Australia Special Publication. 22, 101-113.
442911	Burra Fault	2	139.094	-33.758	53.0	343	0	West	Reverse	200.00	A	0.65893748582	0	3.18	7.2	3 arc-second Shuttle Radar Tomography Mission DEM	main reference	QUIGLEY M. C., CUPPER M. L. & SANDIFORD M. 2006. Quaternary faults of southern Australia: palaeoseismicity, slip rates and origin. Australian Journal of Earth Sciences 53, 285-301.
442915	Kiewa Fault/Sawpit Gully Fault	4	146.891	-36.450	62.0	161	0			150.00	C	0.19728641424	60	3.50	7.3	Tallangatta 1:250000 geological map sheet	main reference	BEAVIS F. C. & BEAVIS J. C. 1976. Structural geology in the Kiewa region of the Metamorphic Complex, North-East Victoria. Proceedings of the Royal Society of Victoria 88, 66-75.
442924	Selwyn Fault	5	144.908	-38.380	80.0	30	0			10.00	C	0.25824684334	91	4.10	7.4	Figure from main reference	Mallett, C. W. & Holdgate, G. R. 1985. Subsurface Neogene stratigraphy of Nepean Peninsula, Victoria, In: Murray, L. J. (ed.), Stratigraphy, Palaeontology, Malacology, papers in honour of Dr. Nell Ludbrook, Special Publication - South Australia, Department of Mines and Energy 5, 233 - 245.	HOLDGATE G. R., GALLAGHER S. J. & WALLACE M. W. 2002. Tertiary coal geology and stratigraphy of the Port Phillip Basin, Victoria. Australian Journal of Earth Sciences 49, 437-453.
442925	Leisler Lineament	3	129.567	-23.170	23.0	70	0			1.50	A	0.39670185823	31	1.64	6.7	Google earth imagery	main reference	Christine Edgoose, NTGS, Pers Comm. 2002
442926	Liebig Scarp	3	131.040	-23.361	4.0	19	0			2.00	B	0.39670185823	21	0.61	5.9	Google earth imagery	max estimate from DEM profile	Christine Edgoose, NTGS, Pers Comm. 2002
442927	Barrabool Fault	5	144.158	-38.155	17.8	80	0			30.00	C	0.15461709598	45	1.67	6.8	3 arc-second Shuttle Radar Tomography Mission DEM	DEM profile	CLARK D. J. & MCPHERSON A. 2009. Potential sources of strong ground shaking within ~200 km of the Otways carbon capture and storage site. Geoscience Australia unpublished report (prepared for GNS).
442928	Balfour Downs Scarp	1	120.392	-22.766	44.0	45	0	Northwest	Reverse	3.00	B	1.64209095160	25	2.43	7.0	Google earth imagery	DEM profile	Ian Williams, GSWA, pers. Comm. 2002
442929	Duketon Lineament	1	121.555	-27.114	8.5	111	0	Northeast		2.00	B	1.13678897344	25	0.92	6.3	Google earth imagery	main reference	David Champion, Geoscience Australia, pers comm. 2002
442930	Para Fault	2	138.685	-34.728	43.0	27	45	East	Reverse	160.00	A	0.15251074293	82	2.80	7.2	3 arc-second Shuttle Radar Tomography Mission DEM	SHEARD M. J. & BOWMAN G. M. 1996. Soils, stratigraphy and engineering geology of near surface materials of the Adelaide Plains. South Australia. Department of Mines and Energy. Report Book 94/9	FINLAYSON B. 1978. Para Fault gravity survey - West Adelaide. Department of mines and energy, South Australia Report Book 78/125, 14p.
442931	Eden-Burnside Fault	2	138.690	-34.920	53.0	34	0	Southeast	Reverse	250.00	B	0.19295717897	76	3.18	7.2	3 arc-second Shuttle Radar Tomography Mission DEM	DEM profile	BELPERIO A. P. 1995. Quaternary. In: Drexel J. F. & Preiss W. V. eds. The Geology of South Australia, Volume 2, The Phanerozoic. Geological Survey of South Australia Bulletin 54, 219–281
442932	Ochre Cove/Clarendon Fault	2	138.584	-35.095	33.0	43	0	Southeast	Reverse	100.00	B	0.15462003514	69	2.39	7.0	3 arc-second Shuttle Radar Tomography Mission DEM	DEM profile	GIBSON A. A. 1963. Final geological report on the Happy Valley Tunnels Project. South Australia. Department of Mines. Report Book 57/00092 41p.
442933	Willunga Fault	2	138.580	-35.252	45.0	49	50	Southeast	Reverse	70.00	A	0.15462003514	64	2.88	7.2	3 arc-second Shuttle Radar Tomography Mission DEM	BELPERIO A. P. 1992. Offshore extension of the Eden-Burnside Fault. Department of mines and energy, South Australia Report Book DME 142/83, 10.	DREXEL J. F. & PREISS W. V. 1995. The Geology of South Australia, Volume 2. The Phanerozoic. Geological Survey of South Australia Bulletin 54, 357p.
442934	Bremer Fault	2	139.064	-35.129	46.0	174	0			75.00	B	0.19921435769	65	2.82	7.2	3 arc-second Shuttle Radar Tomography Mission DEM	main reference	GIBSON D. & BOSTON K. 2008. Neotectonics, salinity, palaeoclimates and volcanism. CRC LEME Open File Report 235, 71.
442935	Palmer Fault	2	139.170	-34.960	42.0	163	0	West	Reverse	120.00	C	0.19921435769	55	2.76	7.1	3 arc-second Shuttle Radar Tomography Mission DEM	DEM profile	BELPERIO A. P. 1995. Quaternary. In: Drexel J. F. & Preiss W. V. eds. The Geology of South Australia, Volume 2, The Phanerozoic. Geological Survey of South Australia Bulletin 54, 219–281
442936	Wilkatana/Depot Creek Fault	2	137.956	-32.116	59.0	10	46	East	Reverse	93.00	A	0.17888956598	99	3.40	7.3	3 arc-second Shuttle Radar Tomography Mission DEM	main reference	QUIGLEY M. C., CUPPER M. L. & SANDIFORD M. 2006. Quaternary faults of southern Australia: palaeoseismicity, slip rates and origin. Australian Journal of Earth Sciences 53, 285-301.
442937	Paralana Fault	2	139.423	-30.262	15.7	24	0	West	Reverse	150.00	A	0.09275288712	82	1.56	6.7	3 arc-second Shuttle Radar Tomography Mission DEM	DEM profile	SANDIFORD M. 2003. Neotectonics of southeastern Australia: linking the Quaternary faulting record with seismicity and in situ stress. eds Hillis R.R. & Muller D, Evolution and dynamics of the Australian Plate, Geological Society of Australia Special Publication. 22, 101-113.
442938	Neckarboo Ridge	4	142.760	-33.710	190.0	38	0	West	Reverse	30.00	A	0.66910762827	50	7.20	7.8	3 arc-second Shuttle Radar Tomography Mission DEM	Pooncarie 1:250 000 geological map	SANDIFORD M. 2003. Neotectonics of southeastern Australia: linking the Quaternary faulting record with seismicity and in situ stress. eds Hillis R.R. & Muller D, Evolution and dynamics of the Australian Plate, Geological Society of Australia Special Publication. 22, 101-113.
442939	Fergusson Hill Structure	5	143.330	-38.560	32.0	65	0	West	Reverse	250.00	A	0.12041725376	71	2.35	7.0	3 arc-second Shuttle Radar Tomography Mission DEM	main reference	SANDIFORD M. 2003. Geomorphic constraints on the late Neogene tectonics of the Otway Ranges. Australian Journal of Earth Sciences 50, 69-80.
442940	Simpson Structure	5	143.250	-38.470	50.1	70	0			40.00	A	0.12041725376	65	3.07	7.2	3 arc-second Shuttle Radar Tomography Mission DEM	DEM profile	SANDIFORD M. 2003. Geomorphic constraints on the late Neogene tectonics of the Otway Ranges. Australian Journal of Earth Sciences 50, 69-80.
442944	Echuca South Scarp	4	144.792	-36.276	13.0	10	0	West	Reverse	4.00	A	0.33177557845	81	1.40	6.6	3 arc-second Shuttle Radar Tomography Mission DEM	DEM profile	CLARK D., VAN DISSEN R., CUPPER M., COLLINS C. & PRENDERGAST A. 2007. Temporal clustering of surface ruptures on stable continental region faults: a case study from the Cadell Fault scarp, south eastern Australia. Paper presented at Australian Earthquake Engineering Society Conference, Wollongong (unpubl.).
442945	Roderick River Scarp	1	116.224	-26.935	49.0	27	0	Northwest	Reverse	5.50	A	0.35391633035	65	2.59	7.0	3 arc-second Shuttle Radar Tomography Mission DEM	DEM profile	CLARK D. J. 2004. Reconnaissance of Recent fault scarps in the Mt Narryer region, Western Australia. Geoscience Australia unpublished report, 31p.
442946	Morass Creek Fault	4	147.674	-36.962	26.7	341	0			10.00	C	0.23941851038	0	2.11	6.9	3 arc-second Shuttle Radar Tomography Mission DEM	DEM profile	HILLS E. S. 1975. Physiography of Victoria; an introduction to geomorphology. Whitcombe & Tombs Pty. Ltd., Australia.
442949	Sandergrove Fault	2	138.914	-35.293	24.0	36	0			40.00	B	0.22525875010	75	1.99	6.9	Figure from main reference	main reference	GIBSON D. & BOSTON K. 2008. Neotectonics, salinity, palaeoclimates and volcanism. CRC LEME Open File Report 235, 71.
442951	Maruwa Scarp	3	127.608	-22.362	40.0	67	0			6.00	C	2.11883393483	2	2.29	6.9	3 arc-second Shuttle Radar Tomography Mission DEM	DEM profile	
442952	Iona Ridge	4	143.420	-33.820	93.0	21	0	West	Reverse	30.00	C	0.59539942980	66	4.51	7.5	3 arc-second Shuttle Radar Tomography Mission DEM	Pooncarie 1:250 000 geological map	SANDIFORD M. 2003. Neotectonics of southeastern Australia: linking the Quaternary faulting record with seismicity and in situ stress. eds Hillis R.R. & Muller D, Evolution and dynamics of the Australian Plate, Geological Society of Australia Special Publication. 22, 101-113.
442953	Danyo Fault	4	141.450	-34.870	96.0	37	0			30.00	C	1.34425915967	54	4.61	7.5	3 arc-second Shuttle Radar Tomography Mission DEM	DEM profile	SANDIFORD M. 2003. Neotectonics of southeastern Australia: linking the Quaternary faulting record with seismicity and in situ stress. eds Hillis R.R. & Muller D, Evolution and dynamics of the Australian Plate, Geological Society of Australia Special Publication. 22, 101-113.
442954	Mount Narryer West Scarp	1	116.355	-26.440	35.2	40	0	West	Reverse	1.50	B	0.09481631136	50	2.12	6.9	Google earth imagery	main reference	WILLIAMS I. R. 1979. Recent fault scarps in the Mount Narryer area, Byro 1:250 000 sheet. Western Australia. Geological Survey. Annual Report 1978 51-55.
442957	Kurrajong Fault Complex	4	150.617	-33.532	28.0	19	80	East	Reverse	15.00	B	0.20888926921	40	2.17	7.0	3 arc-second Shuttle Radar Tomography Mission DEM	main reference	CLARK D., MCPHERSON A. & TOMKINS K. 2009. The role of neotectonism in the recent landscape evolution of the Eastern Blue Mountains, NSW. Paper presented at 7th international conference on geomorphology (ANZIAG), Melbourne, Australia (unpubl.).
442958	Serpentine Scarp (Darling Fault)	1	115.989	-32.452	19.0	3	0	West	Reverse	1.50	C	0.53355013800	81	1.46	6.6	Land Monitor 10 m DEM	DEM profile	CLARK D. 2006. Field investigation of linear scarps south of Perth, Western Australia: relationships to faulting. Geoscience Australia, Earthquake Hazard Project unpublished report, 30p.
442960	Hardabut Fault	6	114.560	-27.880	96.0	22	0	West	Reverse	15.00	C	0.39222884268	71	3.99	7.3	3 arc-second Shuttle Radar Tomography Mission DEM	DEM profile	CLARK D. 2010. Identification of Quaternary scarps in southwest and central west Western Australia using DEM-based hill shading: application to seismic hazard assessment and neotectonics. International Journal of Remote Sensing in press.
442962	Sanford River Scarp	1	116.182	-27.365	28.1	24	0			3.20	A	0.43397118588	69	1.84	6.8	3 arc-second Shuttle Radar Tomography Mission DEM	DEM profile	CLARK D. 2010. Identification of Quaternary scarps in southwest and central west Western Australia using DEM-based hill shading: application to seismic hazard assessment and neotectonics. International Journal of Remote Sensing in press.
442963	Dunns Fault	4	146.700	-36.400	12.7	160	0			30.00	C	0.19728641424	62	1.38	6.6	Martin Hughes pers comm (2002)	main reference	DUNN E. J. 1917. A post-Tertiary fault at Beechworth. Record of the Geological Survey of Victoria 4, 77-78.
442964	Iragana Scarp 4	3	127.571	-25.614	73.0	126	0	Northeast		3.00	B	0.38133654213	46	3.34	7.2	3 arc-second Shuttle Radar Tomography Mission DEM	DEM profile	JORGENSEN D. C. 2006. Investigating Quaternary tectonic activity in Australia: geomorphic features relating to intraplate tectonics. Geoscience Australia, Earthquake Hazard Project unpublished graduate rotation report, 23p.
442965	Mount William Fault	4	144.750	-36.680	56.0	17	0			100.00	C	0.20271719237	82	3.29	7.3	3 arc-second Shuttle Radar Tomography Mission DEM	DEM profile	EDWARDS, J. and SLATER, K.R. (compilers). 2001. Bendigo 1:250,000 Geological Map. Geological Survey of Victoria, Melbourne.
442966	Iragana Fault	3	126.837	-25.123	135.0	131	0	Northeast	Reverse	4.00	B	0.74359705279	50	5.01	7.5	3 arc-second Shuttle Radar Tomography Mission DEM	DEM profile	JORGENSEN D. C. 2006. Investigating Quaternary tectonic activity in Australia: geomorphic features relating to intraplate tectonics. Geoscience Australia, Earthquake Hazard Project unpublished graduate rotation report, 23p.
442968	Leisler Lineament 2	3	129.734	-23.523	75.6	78	0			2.00	C	1.30377607731	54	3.42	7.2	3 arc-second Shuttle Radar Tomography Mission DEM	max estimate from DEM profile	
442970	Babbage Thrust	2	139.638	-29.892	4.3	25	60	Southeast	Reverse	10.00	A	0.28796973354	81	0.76	6.2	Wolfgang Preiss, PIRSA, pers. Comm. 2005	SANDIFORD M. 2003. Neotectonics of southeastern Australia: linking the Quaternary faulting record with seismicity and in situ stress. eds Hillis R.R. & Muller D, Evolution and dynamics of the Australian Plate, Geological Society of Australia Special Publication. 22, 101-113.	DREXEL J. F. & PREISS W. V. 1995. The Geology of South Australia, Volume 2. The Phanerozoic. Geological Survey of South Australia Bulletin 54, 357p.
442971	Morgan Fault	2	139.539	-34.785	172.0	6	0			30.00	B	0.35039145042	100	6.74	7.8	3 arc-second Shuttle Radar Tomography Mission DEM	DEM profile	

database #	Feature_Name	Domain ID	Lat	Long	Length km	Avg Strike deg	Dip deg	Dip Direction	Movement	Vert Displ m	Confidence	Dist to Nearest Feature dec deg	Shmax Orientation	Max Single Event Slip m	Max Prob M	Arcs source	Height source	Main Reference
442972	Iron Cap Scarp	1	119.967	-32.958	53.0	174	0			8.00	B	0.26204909231	87	2.72	7.1	Land Monitor 10 m DEM/3 arc-second SRTM DEM	DEM profile	CLARK D. 2010. Identification of Quaternary scarps in southwest and central west Western Australia using DEM-based hill shading: application to seismic hazard assessment and neotectonics. International Journal of Remote Sensing in press.
442974	Narembeen Scarp	1	118.515	-31.921	35.7	0	0	East	Normal	6.00	B	0.31392128276	0	2.13	6.9	Land Monitor 10 m DEM	DEM profile	CLARK D. 2010. Identification of Quaternary scarps in southwest and central west Western Australia using DEM-based hill shading: application to seismic hazard assessment and neotectonics. International Journal of Remote Sensing in press.
442975	Newdegate Scarp	1	119.010	-33.030	34.6	21	0	West	Reverse	2.00	B	0.35827645245	64	2.09	6.9	Land Monitor 10 m DEM	DEM profile	CLARK D. 2010. Identification of Quaternary scarps in southwest and central west Western Australia using DEM-based hill shading: application to seismic hazard assessment and neotectonics. International Journal of Remote Sensing in press.
442976	Katanning Scarp	1	117.679	-33.699	16.0	25	0	West	Normal	1.50	B	0.32244009564	57	1.32	6.5	Land Monitor 10 m DEM	DEM profile	CLARK D. 2010. Identification of Quaternary scarps in southwest and central west Western Australia using DEM-based hill shading: application to seismic hazard assessment and neotectonics. International Journal of Remote Sensing in press.
442977	Kuringup Scarp	1	118.357	-33.379	21.0	23	0	East	Normal	1.50	B	0.69310728265	61	1.55	6.7	Land Monitor 10 m DEM	DEM profile	CLARK D. 2010. Identification of Quaternary scarps in southwest and central west Western Australia using DEM-based hill shading: application to seismic hazard assessment and neotectonics. International Journal of Remote Sensing in press.
442978	Dumbleyung Scarp	1	117.692	-33.184	22.0	19	0	East	Normal	4.00	B	0.51497166066	64	1.60	6.7	Land Monitor 10 m DEM	ESTRADA B. 2009. Neotectonic and palaeoseismological studies in the southwest of Western Australia. The University of Western Australia, Perth (unpubl.).	CLARK D. 2010. Identification of Quaternary scarps in southwest and central west Western Australia using DEM-based hill shading: application to seismic hazard assessment and neotectonics. International Journal of Remote Sensing in press.
442979	Yealering Scarp	1	117.539	-32.596	23.5	0	0			6.00	B	0.61746233322	0	1.66	6.7	Land Monitor 10 m DEM	DEM profile	CLARK D. 2010. Identification of Quaternary scarps in southwest and central west Western Australia using DEM-based hill shading: application to seismic hazard assessment and neotectonics. International Journal of Remote Sensing in press.
442980	Bulyeranging Scarp	1	118.299	-31.035	39.0	7	0			3.75	B	0.63067780650	78	2.25	6.9	Land Monitor 10 m DEM	DEM profile	CLARK D. 2010. Identification of Quaternary scarps in southwest and central west Western Australia using DEM-based hill shading: application to seismic hazard assessment and neotectonics. International Journal of Remote Sensing in press.
442981	Moolyal Scarp	1	120.084	-33.193	35.3	176	0	West	Reverse	2.30	B	0.26204909231	89	2.12	6.9	Land Monitor 10 m DEM	DEM profile	CLARK D. 2010. Identification of Quaternary scarps in southwest and central west Western Australia using DEM-based hill shading: application to seismic hazard assessment and neotectonics. International Journal of Remote Sensing in press.
442982	Badgingarra Scarp	6	115.510	-30.374	6.0	2	0	West		3.00	B	0.34341712395	85	0.76	6.1	Land Monitor 10 m DEM	DEM profile	CLARK D. 2010. Identification of Quaternary scarps in southwest and central west Western Australia using DEM-based hill shading: application to seismic hazard assessment and neotectonics. International Journal of Remote Sensing in press.
442983	Bishop Hill Scarp	6	115.353	-29.644	9.0	174	0	West	Reverse	1.40	C	0.74494165576	90	0.95	6.3	Land Monitor 10 m DEM	DEM profile	CLARK D. 2010. Identification of Quaternary scarps in southwest and central west Western Australia using DEM-based hill shading: application to seismic hazard assessment and neotectonics. International Journal of Remote Sensing in press.
442984	Canna Scarp	1	116.001	-28.852	33.0	26	0	East		3.00	C	0.84379131937	71	2.03	6.9	Land Monitor 10 m DEM	DEM profile	CLARK D. 2010. Identification of Quaternary scarps in southwest and central west Western Australia using DEM-based hill shading: application to seismic hazard assessment and neotectonics. International Journal of Remote Sensing in press.
442985	Poondarrie Scarp	1	116.220	-27.837	57.0	14	0	West	Reverse	5.00	C	0.19438091559	81	2.85	7.1	3 arc-second Shuttle Radar Tomography Mission DEM	DEM profile	CLARK D. 2010. Identification of Quaternary scarps in southwest and central west Western Australia using DEM-based hill shading: application to seismic hazard assessment and neotectonics. International Journal of Remote Sensing in press.
442986	Culgatharra Scarp	1	116.171	-28.025	30.5	0	0			4.00	C	0.19438091559	0	1.94	6.8	3 arc-second Shuttle Radar Tomography Mission DEM	DEM profile	CLARK D. 2010. Identification of Quaternary scarps in southwest and central west Western Australia using DEM-based hill shading: application to seismic hazard assessment and neotectonics. International Journal of Remote Sensing in press.
442987	Woodrarrung Scarp	1	115.648	-27.192	24.0	22	0	Southeast	Normal	5.00	C	0.55868865825	71	1.68	6.7	3 arc-second Shuttle Radar Tomography Mission DEM	DEM profile	CLARK D. 2010. Identification of Quaternary scarps in southwest and central west Western Australia using DEM-based hill shading: application to seismic hazard assessment and neotectonics. International Journal of Remote Sensing in press.
442988	Lake George Scarp	4	149.378	-35.124	87.5	5	0	West	Reverse	280.00	A	0.23116050186	75	3.69	7.4	3 arc-second Shuttle Radar Tomography Mission DEM	main reference	SINGH G., OPDYKE N. D. & BOWLER J. M. 1981. Late Cainozoic stratigraphy, magnetic chronology and vegetational history from Lake George, N.S.W. . Journal of the Geological Society of Australia 28, 435-452.
442989	Norseman Scarp	1	122.262	-32.339	42.0	176	0			5.00	C	0.56190319541	85	2.36	7.0	3 arc-second Shuttle Radar Tomography Mission DEM	DEM profile	CLARK D. 2010. Identification of Quaternary scarps in southwest and central west Western Australia using DEM-based hill shading: application to seismic hazard assessment and neotectonics. International Journal of Remote Sensing in press.
442990	Woodcutters Camp Scarp	1	122.337	-31.782	24.0	136	0	Northeast		5.00	C	0.56190319541	45	1.68	6.7	3 arc-second Shuttle Radar Tomography Mission DEM	DEM profile	CLARK D. 2010. Identification of Quaternary scarps in southwest and central west Western Australia using DEM-based hill shading: application to seismic hazard assessment and neotectonics. International Journal of Remote Sensing in press.
442991	Queen Victoria Springs Scarp	1	123.683	-30.511	20.7	12	0	East	Normal	10.00	C	0.84673401931	81	1.54	6.7	3 arc-second Shuttle Radar Tomography Mission DEM	DEM profile	CLARK D. 2010. Identification of Quaternary scarps in southwest and central west Western Australia using DEM-based hill shading: application to seismic hazard assessment and neotectonics. International Journal of Remote Sensing in press.
442992	71 Mile Rock Scarp	1	120.253	-30.688	22.5	169	0	West	Reverse	7.00	C	0.21083795452	81	1.62	6.7	3 arc-second Shuttle Radar Tomography Mission DEM	DEM profile	CLARK D. 2010. Identification of Quaternary scarps in southwest and central west Western Australia using DEM-based hill shading: application to seismic hazard assessment and neotectonics. International Journal of Remote Sensing in press.
442993	Clive's Fantasy	1	120.458	-30.736	17.0	24	0	West	Reverse	6.00	C	0.21083795452	64	1.37	6.6	3 arc-second Shuttle Radar Tomography Mission DEM	DEM profile	CLARK D. 2010. Identification of Quaternary scarps in southwest and central west Western Australia using DEM-based hill shading: application to seismic hazard assessment and neotectonics. International Journal of Remote Sensing in press.
442994	Koolyanobbing Scarp	1	119.701	-30.729	21.3	35	0	East	Normal	4.00	C	0.55349787206	52	1.57	6.7	3 arc-second Shuttle Radar Tomography Mission DEM	DEM profile	CLARK D. 2010. Identification of Quaternary scarps in southwest and central west Western Australia using DEM-based hill shading: application to seismic hazard assessment and neotectonics. International Journal of Remote Sensing in press.
442995	Curbur Scarp	1	116.022	-26.642	19.4	10	0	West	Reverse	5.00	C	0.35391633035	82	1.48	6.6	3 arc-second Shuttle Radar Tomography Mission DEM	DEM profile	CLARK D. 2010. Identification of Quaternary scarps in southwest and central west Western Australia using DEM-based hill shading: application to seismic hazard assessment and neotectonics. International Journal of Remote Sensing in press.
442996	Coondarrie Scarp	1	120.962	-30.842	22.5	175	0	West		2.00	C	0.51494315143	86	1.62	6.7	3 arc-second Shuttle Radar Tomography Mission DEM	DEM profile	CLARK D. 2010. Identification of Quaternary scarps in southwest and central west Western Australia using DEM-based hill shading: application to seismic hazard assessment and neotectonics. International Journal of Remote Sensing in press.
442997	Toolonga Scarp 1	6	114.917	-27.074	61.5	39	0	West	Reverse	15.00	C	0.04304546491	54	2.99	7.1	3 arc-second Shuttle Radar Tomography Mission DEM	DEM profile	CLARK D. 2010. Identification of Quaternary scarps in southwest and central west Western Australia using DEM-based hill shading: application to seismic hazard assessment and neotectonics. International Journal of Remote Sensing in press.
442998	Lake Echo Scarp	3	146.663	-42.172	36.0	18	0			30.00	B	0.56948785769	89	2.14	6.9	3 arc-second Shuttle Radar Tomography Mission DEM	main reference	FAIRBRIDGE R. W. 1948. Geology of the country around Waddamana, Central Tasmania. Papers & Proceedings of the Royal Society of Tasmania, 111-149.
442999	Richmond Fault	2	147.410	-42.750	5.0	63	0			10.00	C	0.93201085397	49	0.69	6.0	TASMAP 30 m DEM	DEM profile	Colin Mazengarb pers. Comm. (MRTAS)
443000	Iragana Scarp 2	3	126.911	-25.793	65.0	174	0	East	Reverse	7.00	A	0.68354410071	88	3.10	7.2	3 arc-second Shuttle Radar Tomography Mission DEM	DEM profile	
443001	Iragana Scarp 3	3	127.602	-25.994	33.4	3	0	West	Reverse	9.00	A	0.38133654213	79	2.05	6.9	3 arc-second Shuttle Radar Tomography Mission DEM	DEM profile	
443002	Warri Scarp	3	125.788	-24.962	13.5	143	0	West	Reverse	2.00	A	0.74359705279	59	1.20	6.5	3 arc-second Shuttle Radar Tomography Mission DEM	DEM profile	
443003	Harcus Scarp	3	129.691	-26.859	21.0	174	0	East	Reverse	9.00	A	0.72466462157	97	1.55	6.7	3 arc-second Shuttle Radar Tomography Mission DEM	DEM profile	JORGENSEN D. C. 2006. Investigating Quaternary tectonic activity in Australia: geomorphic features relating to intraplate tectonics. Geoscience Australia, Earthquake Hazard Project unpublished graduate rotation report, 23p.
443004	Mann Range Scarp	3	129.607	-26.139	20.0	176	0	East	Reverse	9.00	A	0.64414143453	105	1.51	6.6	3 arc-second Shuttle Radar Tomography Mission DEM	DEM profile	
443005	Tallaringa Scarp	1	133.133	-29.843	18.0	26	0	East	Reverse	30.00	A	0.45665465346	75	1.42	6.6	3 arc-second Shuttle Radar Tomography Mission DEM	DEM profile	JORGENSEN D. C. 2006. Investigating Quaternary tectonic activity in Australia: geomorphic features relating to intraplate tectonics. Geoscience Australia, Earthquake Hazard Project unpublished graduate rotation report, 23p.
443006	Fowler Scarp	1	132.396	-31.627	57.0	14	0	East	Reverse	50.00	A	0.85976438720	101	2.85	7.1	3 arc-second Shuttle Radar Tomography Mission DEM	DEM profile	JORGENSEN D. C. 2006. Investigating Quaternary tectonic activity in Australia: geomorphic features relating to intraplate tectonics. Geoscience Australia, Earthquake Hazard Project unpublished graduate rotation report, 23p.
443007	Yalata Scarp	1	131.701	-31.121	45.0	9	0	East	Reverse	30.00	A	0.19330958363	99	2.46	7.0	3 arc-second Shuttle Radar Tomography Mission DEM	DEM profile	JORGENSEN D. C. 2006. Investigating Quaternary tectonic activity in Australia: geomorphic features relating to intraplate tectonics. Geoscience Australia, Earthquake Hazard Project unpublished graduate rotation report, 23p.
443008	Ivy Tank Scarp	1	131.479	-31.190	26.0	19	0	West	Reverse	40.00	A	0.17333291598	88	1.76	6.8	3 arc-second Shuttle Radar Tomography Mission DEM	DEM profile	JORGENSEN D. C. 2006. Investigating Quaternary tectonic activity in Australia: geomorphic features relating to intraplate tectonics. Geoscience Australia, Earthquake Hazard Project unpublished graduate rotation report, 23p.
443009	Karri Scarp	1	131.532	-31.025	56.0	17	0	W	Reverse	30.00	A	0.17333291598	90	2.82	7.1	3 arc-second Shuttle Radar Tomography Mission DEM	DEM profile	JORGENSEN D. C. 2006. Investigating Quaternary tectonic activity in Australia: geomorphic features relating to intraplate tectonics. Geoscience Australia, Earthquake Hazard Project unpublished graduate rotation report, 23p.
443010	Knottmi Scarp	1	131.798	-30.953	42.0	3	0	West	Reverse	30.00	A	0.19330958363	105	2.36	7.0	3 arc-second Shuttle Radar Tomography Mission DEM	DEM profile	JORGENSEN D. C. 2006. Investigating Quaternary tectonic activity in Australia: geomorphic features relating to intraplate tectonics. Geoscience Australia, Earthquake Hazard Project unpublished graduate rotation report, 23p.
443011	Maralinga Scarp	3	131.645	-30.330	81.0	11	0	East	Reverse	25.00	A	0.18815376932	91	3.57	7.3	3 arc-second Shuttle Radar Tomography Mission DEM	DEM profile	JORGENSEN D. C. 2006. Investigating Quaternary tectonic activity in Australia: geomorphic features relating to intraplate tectonics. Geoscience Australia, Earthquake Hazard Project unpublished graduate rotation report, 23p.

database #	Feature_Name	Domain ID	Lat	Long	Length km	Avg Strike deg	Dip deg	Dip Direction	Movement	Vert Displ m	Confidence	Dist to Nearest Feature dec deg	Shmax Orientation	Max Single Event Slip m	Max Prob M	Arcs source	Height source	Main Reference
443012	Ooldea Scarp	3	131.870	-30.676	37.0	44	0	East	Reverse	20.00	A	0.19245238502	62	2.18	6.9	3 arc-second Shuttle Radar Tomography Mission DEM	DEM profile	JORGENSEN D. C. 2006. Investigating Quaternary tectonic activity in Australia: geomorphic features relating to intraplate tectonics. Geoscience Australia, Earthquake Hazard Project unpublished graduate rotation report, 23p.
443013	Orp Scarp	3	131.814	-30.492	24.0	42	0	North	Reverse	25.00	A	0.19245238502	62	1.68	6.7	3 arc-second Shuttle Radar Tomography Mission DEM	DEM profile	JORGENSEN D. C. 2006. Investigating Quaternary tectonic activity in Australia: geomorphic features relating to intraplate tectonics. Geoscience Australia, Earthquake Hazard Project unpublished graduate rotation report, 23p.
443014	Yarle Scarp	3	131.462	-30.371	27.0	171	0	East	Reverse	15.00	A	0.18815376932	69	1.80	6.8	3 arc-second Shuttle Radar Tomography Mission DEM	DEM profile	JORGENSEN D. C. 2006. Investigating Quaternary tectonic activity in Australia: geomorphic features relating to intraplate tectonics. Geoscience Australia, Earthquake Hazard Project unpublished graduate rotation report, 23p.
443015	Watson Scarp	3	131.348	-30.909	59.0	38	0	West	Reverse	8.00	A	0.21729741916	67	2.92	7.1	3 arc-second Shuttle Radar Tomography Mission DEM	DEM profile	JORGENSEN D. C. 2006. Investigating Quaternary tectonic activity in Australia: geomorphic features relating to intraplate tectonics. Geoscience Australia, Earthquake Hazard Project unpublished graduate rotation report, 23p.
443016	O'Malley Scarp	3	131.031	-30.851	57.0	33	0	East	Reverse	8.00	A	0.32281856140	72	2.85	7.1	3 arc-second Shuttle Radar Tomography Mission DEM	DEM profile	JORGENSEN D. C. 2006. Investigating Quaternary tectonic activity in Australia: geomorphic features relating to intraplate tectonics. Geoscience Australia, Earthquake Hazard Project unpublished graduate rotation report, 23p.
443017	Cook Scarp	3	130.358	-31.078	97.0	41	0	East	Reverse	15.00	A	0.12354429361	62	4.02	7.3	3 arc-second Shuttle Radar Tomography Mission DEM	DEM profile	JORGENSEN D. C. 2006. Investigating Quaternary tectonic activity in Australia: geomorphic features relating to intraplate tectonics. Geoscience Australia, Earthquake Hazard Project unpublished graduate rotation report, 23p.
443018	Deakin Scarp	3	128.968	-30.726	85.0	28	0	East	Reverse	30.00	A	0.63590894227	72	3.69	7.3	3 arc-second Shuttle Radar Tomography Mission DEM	DEM profile	JORGENSEN D. C. 2006. Investigating Quaternary tectonic activity in Australia: geomorphic features relating to intraplate tectonics. Geoscience Australia, Earthquake Hazard Project unpublished graduate rotation report, 23p.
443019	Mundrabilla Scarp	3	127.468	-31.273	140.0	2	0	West	Reverse	10.00	A	0.32516519206	97	5.14	7.5	3 arc-second Shuttle Radar Tomography Mission DEM	DEM profile	JORGENSEN D. C. 2006. Investigating Quaternary tectonic activity in Australia: geomorphic features relating to intraplate tectonics. Geoscience Australia, Earthquake Hazard Project unpublished graduate rotation report, 23p.
443020	Madura Scarp	3	127.017	-31.885	91.0	14	0	East	Reverse	10.00	A	0.35434111108	85	3.86	7.3	3 arc-second Shuttle Radar Tomography Mission DEM	DEM profile	JORGENSEN D. C. 2006. Investigating Quaternary tectonic activity in Australia: geomorphic features relating to intraplate tectonics. Geoscience Australia, Earthquake Hazard Project unpublished graduate rotation report, 23p.
443021	Horseshoe Scarp	3	127.381	-31.587	70.0	8	0	East	Reverse	10.00	A	0.21318219746	91	3.25	7.2	3 arc-second Shuttle Radar Tomography Mission DEM	DEM profile	JORGENSEN D. C. 2006. Investigating Quaternary tectonic activity in Australia: geomorphic features relating to intraplate tectonics. Geoscience Australia, Earthquake Hazard Project unpublished graduate rotation report, 23p.
443022	Forrest Scarp	3	128.037	-31.449	104.0	19	0	East	Reverse	9.00	A	0.44130369452	81	4.21	7.4	3 arc-second Shuttle Radar Tomography Mission DEM	DEM profile	JORGENSEN D. C. 2006. Investigating Quaternary tectonic activity in Australia: geomorphic features relating to intraplate tectonics. Geoscience Australia, Earthquake Hazard Project unpublished graduate rotation report, 23p.
443023	Irish Well Scarp	3	131.119	-30.198	103.0	175	0	East	Reverse	15.00	A	0.38355376168	78	4.18	7.4	3 arc-second Shuttle Radar Tomography Mission DEM	DEM profile	JORGENSEN D. C. 2006. Investigating Quaternary tectonic activity in Australia: geomorphic features relating to intraplate tectonics. Geoscience Australia, Earthquake Hazard Project unpublished graduate rotation report, 23p.
443024	Talganna Scarp	3	127.169	-31.565	47.0	39	0	East	Reverse	12.00	A	0.21318219746	60	2.53	7.0	3 arc-second Shuttle Radar Tomography Mission DEM	DEM profile	JORGENSEN D. C. 2006. Investigating Quaternary tectonic activity in Australia: geomorphic features relating to intraplate tectonics. Geoscience Australia, Earthquake Hazard Project unpublished graduate rotation report, 23p.
443025	Knardna Scarp	3	130.481	-31.061	34.0	17	0	West	Reverse	8.00	A	0.12354429361	87	2.07	6.9	3 arc-second Shuttle Radar Tomography Mission DEM	DEM profile	JORGENSEN D. C. 2006. Investigating Quaternary tectonic activity in Australia: geomorphic features relating to intraplate tectonics. Geoscience Australia, Earthquake Hazard Project unpublished graduate rotation report, 23p.
443026	Coompana Scarps	3	129.538	-31.055	30.0	158	0	West	Reverse	5.00	A	0.63590894227	57	1.92	6.8	3 arc-second Shuttle Radar Tomography Mission DEM	DEM profile	JORGENSEN D. C. 2006. Investigating Quaternary tectonic activity in Australia: geomorphic features relating to intraplate tectonics. Geoscience Australia, Earthquake Hazard Project unpublished graduate rotation report, 23p.
443027	Moonera Scarp	3	126.496	-31.887	85.0	43	0	East	Reverse	12.00	A	0.52017913347	55	3.69	7.3	3 arc-second Shuttle Radar Tomography Mission DEM	DEM profile	JORGENSEN D. C. 2006. Investigating Quaternary tectonic activity in Australia: geomorphic features relating to intraplate tectonics. Geoscience Australia, Earthquake Hazard Project unpublished graduate rotation report, 23p.
443028	Bultanna Scarp	3	128.430	-31.248	53.0	171	0	East	Reverse	10.00	A	0.44130369452	71	2.72	7.1	3 arc-second Shuttle Radar Tomography Mission DEM	DEM profile	JORGENSEN D. C. 2006. Investigating Quaternary tectonic activity in Australia: geomorphic features relating to intraplate tectonics. Geoscience Australia, Earthquake Hazard Project unpublished graduate rotation report, 23p.
443029	Nurina Scarp	3	126.598	-31.352	54.0	164	0	West	Reverse	20.00	A	0.54488941105	68	2.76	7.1	3 arc-second Shuttle Radar Tomography Mission DEM	DEM profile	JORGENSEN D. C. 2006. Investigating Quaternary tectonic activity in Australia: geomorphic features relating to intraplate tectonics. Geoscience Australia, Earthquake Hazard Project unpublished graduate rotation report, 23p.
443030	Haig Scarp	3	126.202	-30.654	123.0	10	0	East	Reverse	10.00	A	0.37195709889	87	4.71	7.4	3 arc-second Shuttle Radar Tomography Mission DEM	DEM profile	JORGENSEN D. C. 2006. Investigating Quaternary tectonic activity in Australia: geomorphic features relating to intraplate tectonics. Geoscience Australia, Earthquake Hazard Project unpublished graduate rotation report, 23p.
443031	Gunnadorrah Scarp	3	125.959	-30.372	79.0	12	0	West	Reverse	15.00	A	0.09136761718	84	3.52	7.2	3 arc-second Shuttle Radar Tomography Mission DEM	DEM profile	JORGENSEN D. C. 2006. Investigating Quaternary tectonic activity in Australia: geomorphic features relating to intraplate tectonics. Geoscience Australia, Earthquake Hazard Project unpublished graduate rotation report, 23p.
443032	Endeavour Scarp	3	125.879	-30.329	155.0	37	0	West	Reverse	4.00	A	0.09136761718	59	5.51	7.5	3 arc-second Shuttle Radar Tomography Mission DEM	DEM profile	JORGENSEN D. C. 2006. Investigating Quaternary tectonic activity in Australia: geomorphic features relating to intraplate tectonics. Geoscience Australia, Earthquake Hazard Project unpublished graduate rotation report, 23p.
443033	Loongana Scarp	3	126.916	-30.516	30.0	39	0	East	Reverse	10.00	A	0.72701569456	58	1.92	6.8	3 arc-second Shuttle Radar Tomography Mission DEM	DEM profile	JORGENSEN D. C. 2006. Investigating Quaternary tectonic activity in Australia: geomorphic features relating to intraplate tectonics. Geoscience Australia, Earthquake Hazard Project unpublished graduate rotation report, 23p.
443034	Neales Lineament	3	136.812	-28.231	55.0	174	0	West	Reverse	3.00	A	0.77929882044	84	2.79	7.1	Figure from main reference	main reference	WACLAWIK V. G., LANG S. C. & KRAPF C. B. E. 2008. Fluvial response to tectonic activity in an intra-continental dryland setting: The Neales River, Lake Eyre, Central Australia. Geomorphology 102.
443035	Naretha Scarp	3	124.817	-31.026	57.0	4	0	East	Reverse	40.00	A	0.40495425118	91	2.85	7.1	3 arc-second Shuttle Radar Tomography Mission DEM	DEM profile	JORGENSEN D. C. 2006. Investigating Quaternary tectonic activity in Australia: geomorphic features relating to intraplate tectonics. Geoscience Australia, Earthquake Hazard Project unpublished graduate rotation report, 23p.
443036	Caiguna Scarp	3	125.364	-32.174	56.0	161	0	West	Reverse	17.00	A	0.66546452750	65	2.82	7.1	3 arc-second Shuttle Radar Tomography Mission DEM	DEM profile	JORGENSEN D. C. 2006. Investigating Quaternary tectonic activity in Australia: geomorphic features relating to intraplate tectonics. Geoscience Australia, Earthquake Hazard Project unpublished graduate rotation report, 23p.
443037	Culver Scarp	3	124.641	-32.774	43.0	38	0	East	Reverse	20.00	A	0.72934708220	57	2.39	7.0	3 arc-second Shuttle Radar Tomography Mission DEM	DEM profile	JORGENSEN D. C. 2006. Investigating Quaternary tectonic activity in Australia: geomorphic features relating to intraplate tectonics. Geoscience Australia, Earthquake Hazard Project unpublished graduate rotation report, 23p.
443038	Rawlinna Scarp	3	125.373	-31.509	53.0	176	0	West	Reverse	10.00	A	0.66546452750	80	2.72	7.1	3 arc-second Shuttle Radar Tomography Mission DEM	DEM profile	JORGENSEN D. C. 2006. Investigating Quaternary tectonic activity in Australia: geomorphic features relating to intraplate tectonics. Geoscience Australia, Earthquake Hazard Project unpublished graduate rotation report, 23p.
443039	Kitchener Scarp	3	124.182	-31.761	33.0	152	0	East	Reverse	15.00	A	0.56338267368	58	2.03	6.9	3 arc-second Shuttle Radar Tomography Mission DEM	DEM profile	JORGENSEN D. C. 2006. Investigating Quaternary tectonic activity in Australia: geomorphic features relating to intraplate tectonics. Geoscience Australia, Earthquake Hazard Project unpublished graduate rotation report, 23p.
443040	Woorlba Scarp	3	123.949	-32.274	18.0	157	0	East	Reverse	20.00	A	0.56338267368	63	1.42	6.6	3 arc-second Shuttle Radar Tomography Mission DEM	DEM profile	JORGENSEN D. C. 2006. Investigating Quaternary tectonic activity in Australia: geomorphic features relating to intraplate tectonics. Geoscience Australia, Earthquake Hazard Project unpublished graduate rotation report, 23p.
443041	Cundeelee Scarp	3	124.426	-30.921	38.0	12	0	East	Reverse	8.00	A	0.40495425118	82	2.22	6.9	3 arc-second Shuttle Radar Tomography Mission DEM	DEM profile	JORGENSEN D. C. 2006. Investigating Quaternary tectonic activity in Australia: geomorphic features relating to intraplate tectonics. Geoscience Australia, Earthquake Hazard Project unpublished graduate rotation report, 23p.
443042	Edjudina Scarp	1	121.719	-29.327	23.0	156	0	West	Reverse	4.00	A	1.69518572186	67	1.64	6.7	3 arc-second Shuttle Radar Tomography Mission DEM	DEM profile	JORGENSEN D. C. 2006. Investigating Quaternary tectonic activity in Australia: geomorphic features relating to intraplate tectonics. Geoscience Australia, Earthquake Hazard Project unpublished graduate rotation report, 23p.
443043	Gerard Scarp	1	122.692	-27.096	16.0	1	0	East	Reverse	10.00	A	0.26760318522	87	1.32	6.5	3 arc-second Shuttle Radar Tomography Mission DEM	DEM profile	JORGENSEN D. C. 2006. Investigating Quaternary tectonic activity in Australia: geomorphic features relating to intraplate tectonics. Geoscience Australia, Earthquake Hazard Project unpublished graduate rotation report, 23p.
443044	Lake Wells Scarp	1	122.934	-27.211	8.0	169	0	East	Reverse	8.00	A	0.26760318522	81	0.89	6.2	3 arc-second Shuttle Radar Tomography Mission DEM	DEM profile	JORGENSEN D. C. 2006. Investigating Quaternary tectonic activity in Australia: geomorphic features relating to intraplate tectonics. Geoscience Australia, Earthquake Hazard Project unpublished graduate rotation report, 23p.
443045	Lake Wells Scarp 2	1	123.321	-27.031	22.0	139	0	East	Reverse	18.00	C	0.42730077215	50	1.60	6.7	3 arc-second Shuttle Radar Tomography Mission DEM	DEM profile	JORGENSEN D. C. 2006. Investigating Quaternary tectonic activity in Australia: geomorphic features relating to intraplate tectonics. Geoscience Australia, Earthquake Hazard Project unpublished graduate rotation report, 23p.
443046	Boolarra Fault	5	146.300	-38.376	3.0	52	0	Northwest		30.00	B	0.06073679769	54	0.63	6.0	Warragul 1:250000 geological map sheet	SRTM DEM profile	
443047	Bass Fault	5	145.523	-38.501	56.0	63	0	North	Normal	45.00	B	0.30101201608	49	3.29	7.3	3 arc-second Shuttle Radar Tomography Mission DEM	DEM profile	
443048	Budgeree Fault	5	146.342	-38.420	25.0	49	0			100.00	A	0.06073679769	57	2.03	6.9	Warragul 1:250000 geological map sheet	DEM profile	
443049	Currajung Monocline	5	146.651	-38.341	23.0	80	0	North		125.00	A	0.20756116571	30	1.94	6.9	Warragul 1:250000 geological map sheet	DEM profile	
443050	Darriman Monocline	5	146.906	-38.455	34.0	87	0	South		30.00	A	0.16973139589	23	2.44	7.1	Warragul 1:250000 geological map sheet	DEM profile	
443051	Napier Monocline	5	146.744	-38.526	12.0	64	0	Southeast		50.00	B	0.16973139589	45	1.34	6.6	Warragul 1:250000 geological map sheet	DEM profile	
443053	Gelliondale Monocline	5	146.344	-38.664	24.3	92	0	South		120.00	C	0.17090626238	12	2.00	6.9	VICMAP 20m DTM 2000	DEM profile	
443054	Haunted Hills Fault	5	146.323	-38.209	21.0	15	0	Northwest	Reverse	80.00	A	0.09092223157	93	1.84	6.8	VICMAP 20m DTM 2000	DEM profile	
443055	Heath Hill Fault	5	145.690	-38.251	42.0	39	0	North		40.00	A	0.30101201608	70	2.76	7.1	3 arc-second Shuttle Radar Tomography Mission DEM	DEM profile	
443056	Morwell Monocline	5	146.374	-38.284	30.0	46	0	East	Reverse	70.00	A	0.02966641984	61	2.26	7.0	VICMAP 20m DTM 2000	DEM profile	MCPHERSON A., CLARK D. & BARROWS T. 2009. Long-term slip rates for onshore faults in the Gippsland Basin, south-eastern Australia. Paper presented at 7th international conference on geomorphology (ANZIAG), Melbourne, Australia (unpubl.).
443057	Waratah Fault	5	146.056	-38.770	37.0	40	0	Northwest	Dextral	20.00	C	0.19132883961	59	2.56	7.1	3 arc-second Shuttle Radar Tomography Mission DEM	main reference	GARDNER T., WEBB J., PEZZIA C., AMBORN T., TUNNELL R., FLANAGAN S., MERRITTS D., MARSHALL J., FABEL D. & CUPPER M. L. 2009. Episodic intraplate deformation of stable continental margins: evidence from Late Neogene and Quaternary marine terraces, Cape Liptrap, Southeastern Australia. Quaternary Science Reviews 28, 39-53.
443058	Snake Ridge Monocline	5	146.851	-38.111	37.0	82	0	North		45.00	A	0.07770338875	32	2.56	7.1	VICMAP 20m DTM 2000	main reference	MCPHERSON A., CLARK D. & BARROWS T. 2009. Long-term slip rates for onshore faults in the Gippsland Basin, south-eastern Australia. Paper presented at 7th international conference on geomorphology (ANZIAG), Melbourne, Australia (unpubl.).
443059	Tap Tap Fault	5	146.502	-38.800	13.5	96	0	North		40.00	A	0.02797778828	10	1.43	6.7	3 arc-second Shuttle Radar Tomography Mission DEM	DEM profile	
443060	Toora Fault	5	146.518	-38.623	14.0	83	0	South		40.00	A	0.02797778828	23	1.46	6.7	3 arc-second Shuttle Radar Tomography Mission DEM	DEM profile	
443062	Karari Scarp	1	133.387	-29.463	49.0	62	0	South	Reverse	40.00	A	0.37326875874	34	2.69	7.0	3 arc-second Shuttle Radar Tomography Mission DEM	DEM profile	
443063	Coober Pedy Scarp	3	133.651	-29.199	74.0	61	0	North	Reverse	30.00	C	0.37326875874	32	3.37	7.2	3 arc-second Shuttle Radar Tomography Mission DEM	DEM profile	
443065	Kalga Hills Scarp	3	131.900	-21.790	113.0	120	0			3.00	C	1.55267320643	0	4.45	7.4	3 arc-second Shuttle Radar Tomography Mission DEM	max estimate from DEM profile	
443066	Munro Scarps	3	121.890	-19.820	70.0	322	0			10.00	C	2.10183413887	0	3.25	7.2	3 arc-second Shuttle Radar Tomography Mission DEM	DEM profile	Jon Clarke, Geoscience Australia, pers. comm. 2008

database #	Feature_Name	Domain ID	Lat	Long	Length km	Avg Strike deg	Dip deg	Dip Direction	Movement	Vert Displ m	Confidence	Dist to Nearest Feature dec deg	Shmax Orientation	Max Single Event Slip m	Max Prob M	Arcs source	Height source	Main Reference
443067	Forest Vale Scarp	4	147.860	-26.030	42.0	6	0			10.00	C	2.60960203843	0	2.76	7.1	3 arc-second Shuttle Radar Tomography Mission DEM	DEM profile	
447731	Tambellup Scarp	1	117.597	-34.011	19.5	118	0			4.00	C	0.32244009564	37	1.49	6.6	Land Monitor 10 m DEM	DEM profile	
456419	Shoalhaven Scarp	4	149.645	-35.523	72.5	17	0			30.00	C	0.19218005982	65	3.86	7.4	3 arc-second Shuttle Radar Tomography Mission DEM	DEM profile	HILL S. M., ROACH I. C. & LEWIS A. 2004. Krawaree West, Upper Shoalhaven River Catchment, NSW. CRC LEME 1:25 000 Regolith Landform Map Explanatory Notes, 6p.
456499	Olary Creek Scarp 1	2	140.782	-32.614	73.0	65	0			9.00	C	0.13226154482	32	3.87	7.4	3 arc-second Shuttle Radar Tomography Mission DEM	DEM profile	
456500	Olary Creek Scarp 2	2	140.912	-32.608	62.0	60	0			10.00	C	0.13226154482	36	3.50	7.3	3 arc-second Shuttle Radar Tomography Mission DEM	DEM profile	
456501	Olary Creek Scarp 3	2	140.645	-32.852	36.0	65	0			4.00	C	0.27437781597	31	2.52	7.1	3 arc-second Shuttle Radar Tomography Mission DEM	DEM profile	
456502	Pine Creek Scarp 1	2	141.563	-32.346	60.0	60	0			10.00	C	0.14338643629	35	3.43	7.3	3 arc-second Shuttle Radar Tomography Mission DEM	DEM profile	
456510	Pine Creek Scarp 2	2	141.561	-32.488	25.0	45	0			8.00	C	0.14338643629	50	2.03	6.9	3 arc-second Shuttle Radar Tomography Mission DEM	DEM profile	
456797	Crystal Brook Scarp	2	138.119	-33.076	64.0	337	0	East	Reverse	250.00	B	0.48710004068	48	3.57	7.3	3 arc-second Shuttle Radar Tomography Mission DEM	DEM profile	SOMERVILLE P., QUIJADA P., THIO H. K., SANDIFORD M. & QUIGLEY M. 2008. Contribution of Identified Active Faults to Near Fault Seismic Hazard in the Flinders Ranges. In: Australian Earthquake Engineering Society Meeting, p. Paper 45. Australian Earthquake Engineering Society, Ballarat, Victoria.
456798	Nectar Brook Scarp	2	138.007	-32.602	38.0	5	0	East	Reverse	200.00	B	0.40752645442	104	2.60	7.1	3 arc-second Shuttle Radar Tomography Mission DEM	DEM profile	SOMERVILLE P., QUIJADA P., THIO H. K., SANDIFORD M. & QUIGLEY M. 2008. Contribution of Identified Active Faults to Near Fault Seismic Hazard in the Flinders Ranges. In: Australian Earthquake Engineering Society Meeting, p. Paper 45. Australian Earthquake Engineering Society, Ballarat, Victoria.
456940	Toolonga Scarp 2	6	114.960	-27.080	45.0	39	0	West	Reverse	10.00	C	0.04304546491	54	2.88	7.2	3 arc-second Shuttle Radar Tomography Mission DEM	DEM profile	CLARK D. 2010. Identification of Quaternary scarps in southwest and central west Western Australia using DEM-based hill shading: application to seismic hazard assessment and neotectonics. International Journal of Remote Sensing in press.
456941	Toolonga Scarp 3	6	115.092	-27.136	103.0	0	0	West	Reverse	25.00	C	0.14338721144	0	4.82	7.5	3 arc-second Shuttle Radar Tomography Mission DEM	DEM profile	CLARK D. 2010. Identification of Quaternary scarps in southwest and central west Western Australia using DEM-based hill shading: application to seismic hazard assessment and neotectonics. International Journal of Remote Sensing in press.
457301	Cape Range Anticline	6	113.974	-22.222	109.0	30	0	Northwest	Dextral reverse	60.00	A	0.27388278484	67	5.00	7.6	3 arc-second Shuttle Radar Tomography Mission DEM	DEM profile	VAN DE GRAAFF W. J. E., DENMAN P. D. & HOCKING R. M. 1976. Emerged Pleistocene marine terraces on Cape Range, Western Australia. Western Australia Geological Survey Annual Report 1975, 62-70.
457305	Cape Cuvier Anticline	6	113.421	-24.287	47.2	164	0		Reverse	5.00	B	1.01781519628	71	2.96	7.2	3 arc-second Shuttle Radar Tomography Mission DEM	DEM profile	DENMAN P. D. & VAN DE GRAAFF W. J. E. 1976. Emergent Quaternary marine deposits in the Lake Macleod area, W.A. Geological Survey of Western Australia, Perth.
457307	Concordia Fault	2	138.802	-34.629	14.0	22	0	East	Reverse	30.00	A	0.15251074293	86	1.46	6.7	Google earth imagery	main reference	GREEN M. 2007. The Structure and Kinematics of the Concordia Fault: Constraining the age of the Indo-Australian Plate stress field. B.Sc. (Hons) thesis, The University of Melbourne, Melbourne (unpubl.).
457566	Giralia Range Fault & Anticline	6	114.142	-22.913	106.0	17	0			300.00	B	0.41680198892	0	4.91	7.5	3 arc-second Shuttle Radar Tomography Mission DEM	DEM profile	CROSTELLA A. & IASKY R. P. 1997. Structural interpretation and hydrocarbon potential of the Giralia area, Carnarvon Basin. Western Australia Geological Survey Report 52, 38p.
457567	Rough Range Fault and Anticline	6	114.047	-22.507	40.0	37	0			80.00	B	0.27388278484	0	2.68	7.1	3 arc-second Shuttle Radar Tomography Mission DEM	main reference	MALCOLM R. J., POTT M. C. & DELFOS E. 1991. A new tectonostratigraphic synthesis of the North West Cape area. The APEA Journal 31, 154-176.
457568	Barrow Island Anticline	6	115.387	-20.789	27.0	32	0		Normal	100.00	B	1.54692856237	0	2.13	7.0	3 arc-second Shuttle Radar Tomography Mission DEM	main reference	BAILLIE P. W. & JACOBSON E. P. 1997. Prospectivity and exploration history of the Barrow sub-basin, Western Australia. APPEA Journal 37, 117-135.
457569	Dirk Hartog Anticline	6	113.047	-25.804	59.0	335	0			40.00	B	0.97707297014	0	3.40	7.3	3 arc-second Shuttle Radar Tomography Mission DEM	main reference	PLAYFORD P. E. 2003. Quaternary tectonism in the Carnarvon Basin, Western Australia. Geological Society of Australia, Abstracts 72, 89.
457574	Kennedy Range Fault	6	114.960	-24.603	124.0	359	0			40.00	C	0.43421517572	0	5.43	7.6	3 arc-second Shuttle Radar Tomography Mission DEM	DEM profile	MORY A. J., IASKY R. P. & GHORI K. A. R. 2003. A summary of the geological evolution and petroleum potential of the southern Carnarvon Basin, Western Australia. Geological Survey of Western Australia Report 86, 31p.
457575	Round Hill Scarp	6	114.656	-23.387	60.0	9	0			6.00	C	0.69924321906	0	3.43	7.3	3 arc-second Shuttle Radar Tomography Mission DEM	DEM profile	
457576	Wandagee Fault	6	114.418	-24.085	123.3	349	0			6.00	B	0.31910737859	0	5.40	7.6	3 arc-second Shuttle Radar Tomography Mission DEM	DEM profile	MORY A. J., IASKY R. P. & GHORI K. A. R. 2003. A summary of the geological evolution and petroleum potential of the southern Carnarvon Basin, Western Australia. Geological Survey of Western Australia Report 86, 31p.
457580	Alma Fault	2	138.655	-34.251	76.0	340	0			100.00	A	0.14146725806	54	7.40	4.0	3 arc-second Shuttle Radar Tomography Mission DEM	DEM profile	
457581	Redbanks Fault	2	138.575	-34.368	47.0	5	0			12.00	C	0.14146725806	0	2.96	7.2	3 arc-second Shuttle Radar Tomography Mission DEM	DEM profile	BELPERIO A. P. 1995. Quaternary. In: Drexel J. F. & Preiss W. V. eds. The Geology of South Australia, Volume 2, The Phanerozoic. Geological Survey of South Australia Bulletin 54, 219–281
457582	Owen Fault	2	138.512	-34.090	48.1	175	0			20.00	C	0.21443434125	68	3.00	7.2	3 arc-second Shuttle Radar Tomography Mission DEM	DEM profile	THOMSON B. P. 1969. Adelaide 1:250 000 geological series map sheet (SI 54-9). Department of MIneral REsources, South Australia.
457583	Crookwell Scarp	4	149.442	-34.532	55.0	349	0			60.00	C	0.27129247214	0	3.25	7.3	3 arc-second Shuttle Radar Tomography Mission DEM	DEM profile	Martin Scott, NSWGS, pers comm, 2002
457584	Binda Scarp	4	149.491	-34.282	64.0	349	0			50.00	C	0.27129247214	0	3.57	7.3	3 arc-second Shuttle Radar Tomography Mission DEM	DEM profile	Martin Scott, NSWGS, pers comm, 2002
457585	Mulwaree Scarp	4	149.644	-35.021	49.0	9	0			70.00	C	0.28636547479	0	3.03	7.2	3 arc-second Shuttle Radar Tomography Mission DEM	DEM profile	
457586	Queanbeyan Fault	4	149.250	-35.320	29.0	358	0			90.00	C	0.23116050186	0	2.22	7.0	3 arc-second Shuttle Radar Tomography Mission DEM	DEM profile	
457587	Narongo Fault	4	149.457	-35.481	19.0	5	0			60.00	C	0.19218005982	0	1.74	6.8	3 arc-second Shuttle Radar Tomography Mission DEM	DEM profile	
457588	Murrumbidgee Fault	4	149.159	-35.651	60.0	358	0			60.00	C	0.15412742298	0	3.43	7.3	3 arc-second Shuttle Radar Tomography Mission DEM	DEM profile	
457589	Nonowie Scarp	1	137.352	-33.095	23.0	355	0			10.00	C	0.10086529589	0	1.64	6.7	3 arc-second Shuttle Radar Tomography Mission DEM	DEM profile	MCCORMACK B. J. 2006. Quaternary Fault Scarps on the North-eastern Eyre Peninsula, South Australia; Geomorphic constraints on age and faulting history by investigation of knickpoint retreat. B.Sc. (Hons) thesis, The University of Melbourne, Melbourne (unpubl.).
457590	Randell Scarp	1	137.382	-33.190	34.0	19	0			20.00	C	0.09166980401	0	2.07	6.9	3 arc-second Shuttle Radar Tomography Mission DEM	DEM profile	MCCORMACK B. J. 2006. Quaternary Fault Scarps on the North-eastern Eyre Peninsula, South Australia; Geomorphic constraints on age and faulting history by investigation of knickpoint retreat. B.Sc. (Hons) thesis, The University of Melbourne, Melbourne (unpubl.).
457591	Poynton Scarp	1	137.308	-33.246	8.0	347	0			25.00	C	0.06897324965	0	0.89	6.2	3 arc-second Shuttle Radar Tomography Mission DEM	DEM profile	MCCORMACK B. J. 2006. Quaternary Fault Scarps on the North-eastern Eyre Peninsula, South Australia; Geomorphic constraints on age and faulting history by investigation of knickpoint retreat. B.Sc. (Hons) thesis, The University of Melbourne, Melbourne (unpubl.).
457592	Muminnie Scarp	1	137.295	-33.313	12.0	1	0			35.00	C	0.06897324965	0	1.12	6.4	3 arc-second Shuttle Radar Tomography Mission DEM	DEM profile	MCCORMACK B. J. 2006. Quaternary Fault Scarps on the North-eastern Eyre Peninsula, South Australia; Geomorphic constraints on age and faulting history by investigation of knickpoint retreat. B.Sc. (Hons) thesis, The University of Melbourne, Melbourne (unpubl.).
457593	Moonabie Scarp	1	137.235	-33.381	30.0	19	0			20.00	C	0.09086344425	0	1.92	6.8	3 arc-second Shuttle Radar Tomography Mission DEM	DEM profile	MCCORMACK B. J. 2006. Quaternary Fault Scarps on the North-eastern Eyre Peninsula, South Australia; Geomorphic constraints on age and faulting history by investigation of knickpoint retreat. B.Sc. (Hons) thesis, The University of Melbourne, Melbourne (unpubl.).
457595	Beverley Camp Lineament	2	139.552	-30.170	5.8	7	0			11.00	C	0.07700753300	0	0.80	6.3	3 arc-second Shuttle Radar Tomography Mission DEM	DEM profile	
457596	Poontana Scarp	2	139.588	-30.236	37.0	352	0			15.00	C	0.07734189564	0	2.56	7.1	3 arc-second Shuttle Radar Tomography Mission DEM	DEM profile	HARPER K. L. 2002. Geologic and geomorphic applications of aster satellite imagery, Northern Flinders Ranges, South Australia. B.Sc. (Hons) thesis, The University of Melbourne Melbourne (unpubl.).
457597	Wooltana Scarp	2	139.454	-30.369	28.0	33	0			50.00	C	0.07608045914	0	2.17	7.0	3 arc-second Shuttle Radar Tomography Mission DEM	DEM profile	HARPER K. L. 2002. Geologic and geomorphic applications of aster satellite imagery, Northern Flinders Ranges, South Australia. B.Sc. (Hons) thesis, The University of Melbourne Melbourne (unpubl.).
457600	Wertaloona Scarp	2	139.348	-30.694	32.0	15	0			40.00	C	0.09713244676	0	2.35	7.0	3 arc-second Shuttle Radar Tomography Mission DEM	DEM profile	HARPER K. L. 2002. Geologic and geomorphic applications of aster satellite imagery, Northern Flinders Ranges, South Australia. B.Sc. (Hons) thesis, The University of Melbourne Melbourne (unpubl.).
457601	Wertaloona West Scarps	2	139.329	-30.600	17.0	10	0			15.00	C	0.09713244676	0	1.63	6.8	3 arc-second Shuttle Radar Tomography Mission DEM	DEM profile	
457842	Charleston Scarp	1	137.070	-33.478	17.0	88	0			30.00	C	0.19035940256	0	1.37	6.6	3 arc-second Shuttle Radar Tomography Mission DEM	DEM profile	WEATHERMAN M. 2006. Basement Control on Distribution of Active Faults on North-eastern Eyre Peninsula, and some Seismic Implications. B. Sc. (Hons) thesis, The University of Melbourne, Melbourne (unpubl.).
457843	Cowell Scarp	1	136.882	-33.581	48.0	42	0			30.00	C	0.21650875681	0	2.56	7.0	3 arc-second Shuttle Radar Tomography Mission DEM	DEM profile	WEATHERMAN M. 2006. Basement Control on Distribution of Active Faults on North-eastern Eyre Peninsula, and some Seismic Implications. B. Sc. (Hons) thesis, The University of Melbourne, Melbourne (unpubl.).
457847	Yorketown Scarp	1	137.628	-35.049	23.0	334	0			20.00	C	0.10051366405	0	1.64	6.7	3 arc-second Shuttle Radar Tomography Mission DEM	DEM profile	
457848	Coobowie Scarp	1	137.703	-34.982	13.0	343	0			10.00	C	0.10051366405	0	1.17	6.5	3 arc-second Shuttle Radar Tomography Mission DEM	DEM profile	
457849	Balgowan Scarp	1	137.524	-34.295	21.0	344	0			20.00	C	0.46681668993	0	1.55	6.7	3 arc-second Shuttle Radar Tomography Mission DEM	DEM profile	
457850	Wallaroo Scarp	1	137.785	-33.908	34.5	90	0			20.00	C	0.32069836751	0	2.09	6.9	3 arc-second Shuttle Radar Tomography Mission DEM	DEM profile	

database #	Feature_Name	Domain ID	Lat	Long	Length km	Avg Strike deg	Dip deg	Dip Direction	Movement	Vert Displ m	Confidence	Dist to Nearest Feature dec deg	Shmax Orientation	Max Single Event Slip m	Max Prob M	Arcs source	Height source	Main Reference
457851	Hummock Range (Pine Point) Fault	2	138.069	-34.059	111.0	19	0			40.00	C	0.32069836751	0	5.05	7.6	3 arc-second Shuttle Radar Tomography Mission DEM	DEM profile	Steve Hill (University of Adelaide) pers comm
463665	Boyanup Scarp	6	115.796	-33.418	31.0	27	0			1.00	C	0.00000000000	0	2.31	7.0	Land Monitor 10 m DEM	DEM profile	CLARK D. 2006. Field investigation of linear scarps south of Perth, Western Australia: relationships to faulting. Geoscience Australia, Earthquake Hazard Project unpublished report, 30p.
463666	Wagerup Scarp	6	115.903	-32.943	38.0	5	0			20.00	C	0.00000000000	0	2.60	7.1	Land Monitor 10 m DEM	DEM profile	CLARK D. 2006. Field investigation of linear scarps south of Perth, Western Australia: relationships to faulting. Geoscience Australia, Earthquake Hazard Project unpublished report, 30p.